



VNIVERSITAT E VALÈNCIA

**Synthesis of 2-alkyl benzopyran analogues of
polycerasoidol as PPAR agonists or agents against
triple negative breast cancer**

Doctoral thesis

Biomedicine and Pharmacy program

Ainhoa Natividad García Martín

Directors:

Diego M. Cortes Martínez

Nuria Cabedo Escrig

Faculty of Pharmacy

Department of Pharmacology

Valencia, January, 2024



VNIVERSITAT
DE VALÈNCIA

VNIVERSITAT
DE VALÈNCIA  Facultat de Farmàcia

Dr. Diego M. Cortes Martínez, Catedrático del Departamento de Farmacología de la Universitat de València, y Dra. Nuria Cabedo Escrig, Profesora Titular del Departamento de Farmacología de la Universitat de València,

CERTIFICAN

Que el trabajo realizado por **Ainhoa Natividad García Martín**, titulado: **Synthesis of 2-alkyl benzopyran analogues of polycerasoidol as PPAR agonists or agents against triple negative breast cancer**, ha sido realizado bajo su dirección y asesoramiento, y reúne todos los requisitos para su juicio y calificación.

Valencia, 16 de Octubre de 2023

Diego M. Cortes Martínez

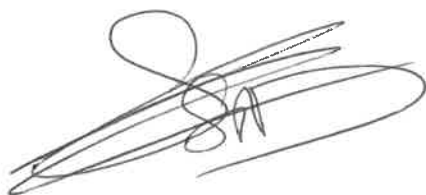
Nuria Cabedo Escrig

Unité 1011 : Récepteurs Nucléaires, Maladies Métaboliques et Cardiovasculaires

Bart STAELS
Tel : (33) 3 20 87 78 25
Fax : (33) 3 20 87 73 60
e.mail : Bart.Staels@pasteur-lille.fr

Lille, 23 may 2022

I, the undersigned Professor Bart Staels, director of the mixed research unit U1011 entitled: Nuclear Receptors, Metabolic and Cardiovascular Diseases, certify that I have hosted Ms. Ainhoa Garcia, doctorate student, in my laboratory located at the Pasteur Institute of Lille at 1 rue du professeur Calmette in Lille from February 1st, 2022 to April 30th, 2022.



Acknowledgments

This may have been the most difficult part of the thesis, but also the most important. During these years I have learned a lot and met some amazing people whom I would like to express my gratitude to.

Esta tesis se ha desarrollado en el grupo de investigación dirigido por Diego Cortes y Nuria Cabedo del Departamento de Farmacología de la Facultad de Farmacia de la Universidad de Valencia y bajo su dirección y tutela. A ellos les quiero dar las gracias, por acogerme, brindarme la oportunidad de formar parte del equipo, enseñarme que con trabajo todo se consigue y sobre todo por ayudarme y aconsejarme. Siempre os estaré muy agradecida.

A mis compañeros de laboratorio, por hacer más fácil y llevadera esta etapa. Laura, Carlos y Álvaro, vosotros habéis formado mi segunda familia. Gracias de corazón por vuestra ayuda siempre que la he necesitado.

A mes collègues de laboratoire pendant mon séjour à Lille, Doriane, Viktor et Audrey, qui m'ont ouvert leur cœur dès le premier instant et ont fait de mon séjour à Lille un vrai plaisir. Isabelle, pour son temps, son énergie et sa bonne humeur. Et à Nathalie, pour m'avoir enseigné et fait de la pharmacologie un plaisir. A tous pour avoir rendu mon séjour si beau, pour m'avoir fait sentir comme chez moi.

A mis amigos y amigas, los de siempre y los que he conocido por el camino. Cada persona me ha aportado su granito de arena que me ha permitido crecer tanto personal como profesionalmente. A mi peña de Villanueva y mis amigas de Calamocha. A mis amigas de la residencia y mis amigas de la universidad, que aparecieron en mi vida para quedarse siempre. A Amparo, mi amiga y compañera de laboratorio. A Cloe y Bea, por ser ese triángulo irrompible e incondicional. A Irina y Ana, por ser mis compañeras de carreras y darme siempre energía.

A mi familia, por ser mi apoyo incondicional. A mis abuelos, mis tíos y mis primos. Especialmente a mis padres y mi hermano, porque sin ellos, esto no habría sido posible. Gracias por comprenderme y ayudarme en cada paso que he dado. Sois un ejemplo a seguir y me habéis demostrado que, con esfuerzo, trabajo y constancia, todo es posible. Espero que estéis orgullosos de mí.

A Sergio, mi pilar fundamental, por tu apoyo y cariño, por soportar mis bajones cuando las cosas no salían bien y también celebrar los éxitos conmigo. Por enseñarme no solo a levantarme cuando caía sino a hacerlo con más fuerzas y ganas, gracias por estar ahí, siempre.

List of projects and grants

The present thesis has been helped by the following projects and grants:

- 1. Desarrollo de nuevos moduladores multidiana de receptores nucleares y biomarcadores lipídicos para el tratamiento del síndrome metabólico y las comorbilidades asociadas** (PI21/02045, Instituto de Salud Carlos III). 01/01/2022-31/12/2024
- 2. Diseño, síntesis y estudio farmacológico de nuevos medicamentos útiles para el tratamiento del síndrome metabólico, y las enfermedades cardiometabólicas asociadas** (CPI-22-265, Universitat de València, AICO/2021/081). 01/01/2021-31/12/2023
- 3. Beca Intramural INCLIVA para estancias formativas en centros de prestigio 2022** (INCLIVA). 01/02/2022-30/04/2022
- 4. Contrato como técnica media de soporte a la investigación** (CPI-22-265, Universitat de València, AICO/2021/081). 08/09/2022-30/07/2023

List of publications

The present thesis is based on the following manuscripts:

1. **Synthesis of 2-prenylated alkoxyated benzopyrans by Horner-Wadsworth–Emmons olefination with PPAR α / γ Agonist Activity**, A. García, L. Vila, P. Martín, Á. Bernabeu, C. Villarroel-Vicente, N. Hennuyer, B. Staels, X. Franck, B. Fidagère, N. Cabedo, D. Cortes, *ACS Medicinal Chemistry Letters*, 12 (2021) 1783-1786.
2. **Synthesis and biological studies of “Polycerasoidol” and “trans- δ -Tocotrienolic acid” derivatives as PPAR α and/or PPAR γ agonists**, L. Vila, N. Cabedo, C. Villarroel-Vicente, A. García, Á. Bernabeu, N. Hennuyer, B. Staels, X. Franck, B. Fidagère, M.J. Sanz, D. Cortes, *Bioorganic & Medicinal Chemistry*, 53 (2022) 116532.
3. **Benzopyran hydrazones with dual PPAR α / γ or PPAR α / δ agonism and an anti-inflammatory effect on human THP-1 macrophages**, A. García, L. Vila, I. Duplan, M.A. Schiel, N. Hennuyer, R.D. Enriz, B. Staels, N. Cabedo, D. Cortes, *European Journal of Medicinal Chemistry*, in press.
4. **Synthesis of 2-Aminopropyl benzopyran derivatives as potential agents against triple negative breast cancer**, A. García, S. Torres-Ruiz, L. Vila, C. Villarroel-Vicente, Á. Bernabeu, P. Eroles, N. Cabedo, D. Cortes, *RSC Medicinal Chemistry*, 14 (2023), 2327.

Lists of abbreviations

BC: Breast cancer

Bcl-2: B-cell lymphoma 2

BP: Benzopyran

BP-2: 2-(Ethyl-4'-methylpentanoate)-6-(*p*-fluorobenzyloxy)-2-(methyl)-benzodihydropyran

CCND2: G1/S-specific cyclin-D2

CCNE1: G1/S-specific cyclin-E1

COSY: Correlation spectroscopy

DCFDA: Dichlorodihydrofluorescein-diacetate

DIBAL-H: Diisobutylaluminium hydride

DNA: Deoxyribonucleic acid

DMAP: Dimethylaminopyridine

DMEM: Dulbecco's modified Eagle's medium

DMSO: Dimethylsulfoxide

EC₅₀: Half maximal effective concentration

ERs: Estrogen receptors

ESI-HRMS: Electrospray ionization high-resolution mass spectrometry

FA: Fatty acid

HER-2: Human epidermal growth factor receptor-2

HETE: Hydroxyeicosatetraenoic acid

HMBC: Heteronuclear multiple bond connectivity

HSQC: Heteronuclear single quantum coherence spectroscopy

HUVECs: Human umbilical vein endothelial cells

IC₅₀: Half maximal inhibitory concentration

IL6: Interleukin 6

LC/MS/MS: Liquid chromatography-tandem mass spectrometry

LDL: Low density lipoprotein

LPS: Lipopolysaccharide

NAFLD: Non-alcoholic fatty liver disease

NF- κ B: Nuclear factor kappa-light-chain-enhancer of activated B cells

NMR: Nuclear magnetic resonance

NR1C1: Nuclear receptor subfamily 1 - group C - member 1

NR1C2: Nuclear receptor subfamily 1 - group C - member 2

NR1C3: Nuclear receptor subfamily 1 - group C - member 3

MCP1: Monocyte chemoattractant protein 1

MD: Molecular dynamic

PDC: Pyridinium dichromate

PI: Propidium iodide

PMA: Forbol-12-myristate-13-acetate

PPAR: Peroxisome proliferator activated receptors

PPAR γ Ms: PPAR γ modulators

PPREs: DNA specific PPAR-response elements

PRs: Progesterone receptors

ROS: Reactive oxygen species

RPMI: Roswell park memorial institute medium

RXR: Retinoid X receptor

SAR: Structure-activity relationship

SI: Selectivity index

TNBC: Triple negative breast cancer

TZDs: Thiazolidinediones

UHPLC: Ultra-high performance liquid chromatography

WST-1: Water-soluble tetrazolium dye

Lists of figures and schemes

Figure 1	<hr/>	3
Figure 2	<hr/>	19
Figure 3	<hr/>	20
Figure 4	<hr/>	21
Figure 5	<hr/>	22
Figure 6	<hr/>	63
Figure 7	<hr/>	65

Scheme 1	<hr/>	3
Scheme 2	<hr/>	4
Scheme 3	<hr/>	5
Scheme 4	<hr/>	5
Scheme 5	<hr/>	6
Scheme 6	<hr/>	6
Scheme 7	<hr/>	6
Scheme 8	<hr/>	7
Scheme 9	<hr/>	7
Scheme 10	<hr/>	7
Scheme 11	<hr/>	7
Scheme 12	<hr/>	8
Scheme 13	<hr/>	8
Scheme 14	<hr/>	9
Scheme 15	<hr/>	9

Overview

This Doctoral Thesis, which focuses on the synthesis of bioactive polycerasoidol benzopyran (BP) analogues, aims to bring novel compounds that could emerge as new hits useful in the treatment of different pathologies. For this purpose, different BP derivatives containing a chromane nucleus have been synthesised based on previous structure-activity relationship (SAR) studies on other BP compounds, and evaluated. The work is divided into an introduction, two chapters and a section of conclusions, which are briefly explained below.

Introduction section tackles the concept of prenylated BP, localization, structure, biogenesis, activities and a review of the forms that authors have used for their synthesis. In this work, the synthesis of the BP nucleus starts from the condensation between hydroxyacetophenones and alkyl ketones.

In **Chapter 1**, a general introduction of peroxisome proliferator-activated receptors (PPARs) is undertaken, where each of the receptors, functions and ligands are discussed, highlighting those with a BP nucleus. The objective is the synthesis of new BPs with the aim of finding a potential PPAR agonist in the treatment of metabolic syndrome. Therefore, in a second part, we find the related **articles (1-3)**, where the synthesis of 2-prenylated derivatives (bearing an α -alkoxy- α,β -unsaturated ester moiety or some isoprenoid units) and 2-alkyl hydrazone derivatives is described. Synthesised compounds are evaluated in terms of their agonism activity and anti-inflammatory capacity.

In **Chapter 2**, a general introduction of cancer is presented, emphasizing one of its most aggressive types, triple negative breast cancer (TNBC), and outlining anticancer compounds containing a BP core. The objective is to find new compounds useful in the treatment of this type of cancer. Therefore, in a second part, we find the related **article 4**, where the synthesis of 2-aminopropyl derivatives is described. Synthesised compounds are evaluated against TNBC cells.

Conclusions section outlines:

1. 2-Prenylated alkoxyated benzopyrans synthesised in **article 1** were efficient as dual PPAR α/γ agonists.
2. 2-Prenylated benzopyrans synthesised in **article 2** displayed selectivity for hPPAR α or showed high efficacy to activate hPPAR γ .
3. 2-Alkyl hydrazone benzopyrans synthesised in **article 3** showed partial hPPAR α/γ or hPPAR α/β agonism activity and attenuated inflammatory markers such as *IL-6* and *MCP-1* in THP-1 cells via NF- κ B pathway activation.
4. 2-Aminopropyl benzopyrans synthesised in **article 4** promoted apoptosis or caused cell cycle arrest in TNBC cells by downregulating apoptotic *Bcl-2* or cyclins (*CCNE1* and *CCND2*), respectively.
5. Benzopyran derivatives analogues of polycerasoidol emerge as lead compounds for developing useful candidates to prevent cardiovascular diseases associate with metabolic disorders or useful agents against breast cancer.

Resumen

La presente Tesis Doctoral, centrada en la síntesis de benzopiranos (BPs) análogos bioactivos de polycerasoidol, pretende aportar compuestos novedosos que puedan surgir como nuevos hits útiles en el tratamiento de diferentes patologías. Para ello, se han sintetizado y evaluado diferentes derivados BP que contienen un núcleo cromano, basándose en estudios previos de relación estructura-actividad (SAR) de otros compuestos BP. El trabajo se divide en una introducción, dos capítulos y una sección de conclusiones, que se explican brevemente a continuación.

En la **introducción** se aborda el concepto de BPs prenilados, localización, estructura, biogénesis, actividades y una revisión de las formas que los autores han utilizado para su síntesis. En este trabajo, la síntesis del núcleo BP parte de la condensación entre hidroxiacetofenonas y alquilcetonas.

En el **Capítulo 1**, se realiza una introducción general de los receptores activados por proliferadores de peroxisomas (PPARs), donde se discuten cada uno de los receptores, funciones y ligandos, destacando aquellos con un núcleo BP. El objetivo es la síntesis de nuevos BPs con el fin de encontrar un agonista potencial PPAR en el tratamiento del síndrome metabólico. Por lo tanto, en una segunda parte, encontramos los **artículos** relacionados **(1-3)**, donde se describe la síntesis de derivados 2-prenilados (con una cadena éster α -alkoxi- α,β -insaturada o con algunas unidades isoprenoides) y derivados 2-alquil hidrazona. Los compuestos sintetizados se evalúan en términos de su actividad agonista y capacidad anti-inflamatoria.

En el **Capítulo 2** se muestra una introducción general al cáncer, haciendo hincapié en uno de sus tipos más agresivos, el cáncer de mama triple negativo (TNBC), y se describen los compuestos anticancerígenos que contienen un núcleo BP. El objetivo es encontrar nuevos compuestos útiles en el tratamiento de este tipo de cáncer. Por lo tanto, en una segunda parte, encontramos el **artículo** relacionado **4**, donde se describe la síntesis de derivados 2-aminopropil. Los compuestos sintetizados se evalúan frente a células TNBC.

La sección de **conclusiones** destaca:

1. Los benzopiranos alcoxilados 2-prenilados sintetizados en el **artículo 1** fueron eficientes como PPAR α/γ agonistas.
2. Los benzopiranos 2-prenilados sintetizados en el **artículo 2** mostraron selectividad para hPPAR α o presentaron alta eficacia para activar hPPAR γ .
3. Los benzopiranos 2-alkil hidrazona sintetizados en el **artículo 3** mostraron una actividad agonista parcial hPPAR α/γ o hPPAR α/β y disminuyeron marcadores inflamatorios como *IL-6* y *MCP-1* en células THP-1 mediante la activación de la vía NF- κ B.
4. Los benzopiranos 2-aminopropil sintetizados en el **artículo 4** favorecen la apoptosis o causan arresto del ciclo celular en células TNBC mediante la regulación a la baja de *Bcl-2* o ciclinas (*CCNE1* y *CCND2*), respectivamente.
5. Los derivados benzopirano análogos de polycerasoidol surgen como compuestos líderes para el desarrollo de candidatos útiles asociados con patologías del síndrome metabólico o agentes potenciales contra el cáncer de mama.

Table of Contents

<i>Introduction of prenylated benzopyrans.....</i>	<i>1</i>
◇ Structure and biogenesis.....	3
◇ Biologic activity.....	4
◇ Synthesis	4
▪ BP nucleus.....	4
▪ Prenylated chain elongation	9
<i>Objectives.....</i>	<i>11</i>
<i>Chapter 1.....</i>	<i>15</i>
1. Peroxisome proliferator activated receptors (PPARs)	19
2. Benzopyrans as PPAR agonists.....	21
3. Articles	23
Article 1.....	23
Article 2.....	29
Article 3.....	41
<i>Chapter 2.....</i>	<i>59</i>
1. Triple negative breast cancer (TNBC).....	63
2. Benzopyrans as antitumor agents	64
3. Article	67
Article 4.....	67
<i>References.....</i>	<i>85</i>
<i>Conclusions</i>	<i>95</i>
<i>Conclusiones.....</i>	<i>99</i>
<i>Annex.....</i>	<i>103</i>

Introduction of prenylated benzopyrans

◇ Structure and biogenesis

Secondary metabolites are bioactive molecules that are biosynthesized in nature from primary metabolites. They have been the main source of chemical diversity driving the discovery and development of new therapeutic agents in the past century. Prenylated benzopyrans (BPs) are secondary metabolites widely distributed in marine organisms such as brown algae of the genera *Cystoseira*, *Cystophora* and *Sargassum* [1,2], sponges of the genus *Irnicina* [3,4], and corals and tunicates of the genera *Alcyonium* and *Amaroucium* [5,6]. To a lesser extent, they have also been found in higher plants of the families Clusiaceae [7,8], Umbelliferae [9] and Myristicaceae [10]. In 1995 and 1996, our research group isolated two novel sesquiterpene BP metabolites from the stem bark of *Polyalthia cerasoides* (Annonaceae) [11,12] (**Figure 1**).

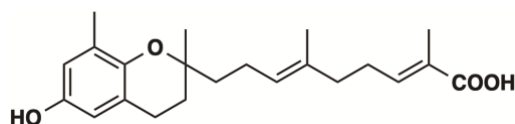
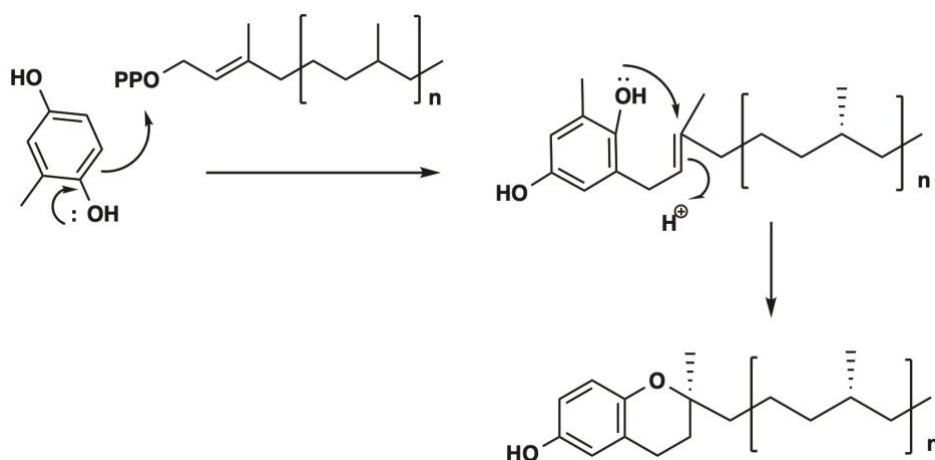


Figure 1. Prenylated benzopyran of *Polyalthia cerasoides*

Prenylated BPs are characterized by the combination of a phenolic system and a terpene subunit which can be linear or cyclic. They may contain one isoprene unit (monoterpenes), one and a half (sesquiterpenes), two units (diterpenes) or up to eight isoprene units (polyterpenes). They are probably formed from compounds consisting of a toluquinol, which are condensed with an isoprene chain by C-alkylation in phenolic OH *ortho*. Pyranic cycle formation is carried out by the nucleophilic attack of the electron pair of OH (**Scheme 1**).



Scheme 1. Biogenetic hypothesis of prenylated benzopyrans

◇ Biologic activity

Prenylated BPs exert prominent pharmacological and biological activities including antitumor [13-15], cytotoxic [12,15], anti-inflammatory [16], hypoglycemic [14,17,18], anticholesterolemic [19-21], antibacterial [22-24], antiparasitic [25,26], antiviral [27,28], antifungal [29,30] and antimalarial [31,32] activity. This work addresses two main research fields, reported in Chapters 1 and 2, respectively: BPs with PPAR agonism activity and BPs with antitumor and cytotoxic capacity.

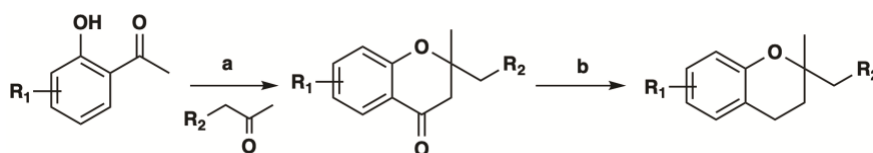
◇ Synthesis

▪ BP nucleus

There are different routes for the synthesis of the BP nucleus depending on the starting reagents used: a) synthesis from hydroxyacetophenones, b) synthesis from salicylic aldehydes or c) synthesis from hydroquinones, among others. In the present work, the methodology followed for the synthesis of the chromane nucleus starts from the condensation between hydroxyacetophenones and alkyl ketones, as explained below.

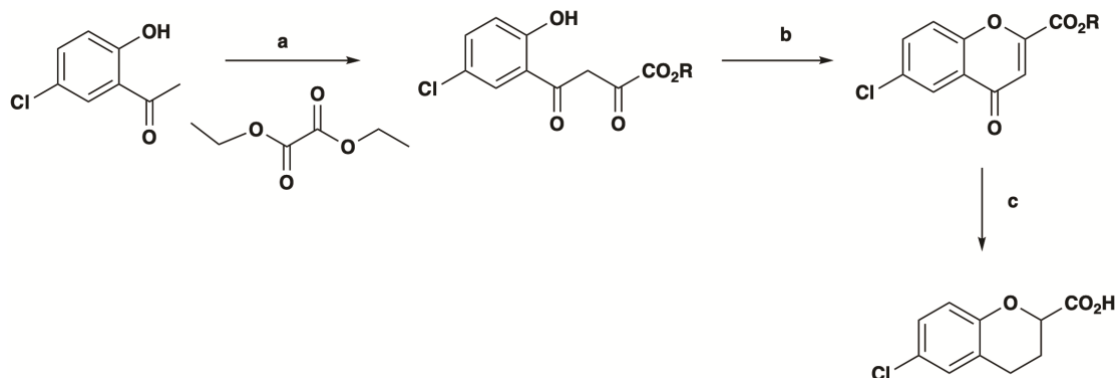
a) Synthesis from hydroxyacetophenones

This synthesis was proposed by Kabbe and Heitzer [33] and consists of a condensation between the appropriate hydroxyacetophenone and the corresponding alkyl ketone to generate the benzopyran-4-one skeleton. Pearce *et al.* [34] improved the yield for the condensation step using pyrrolidine as the base and ethanol as the solvent as well as incorporating new methylated ketones, different alkyl chains or the reduction of carbonyls (**Scheme 2**).



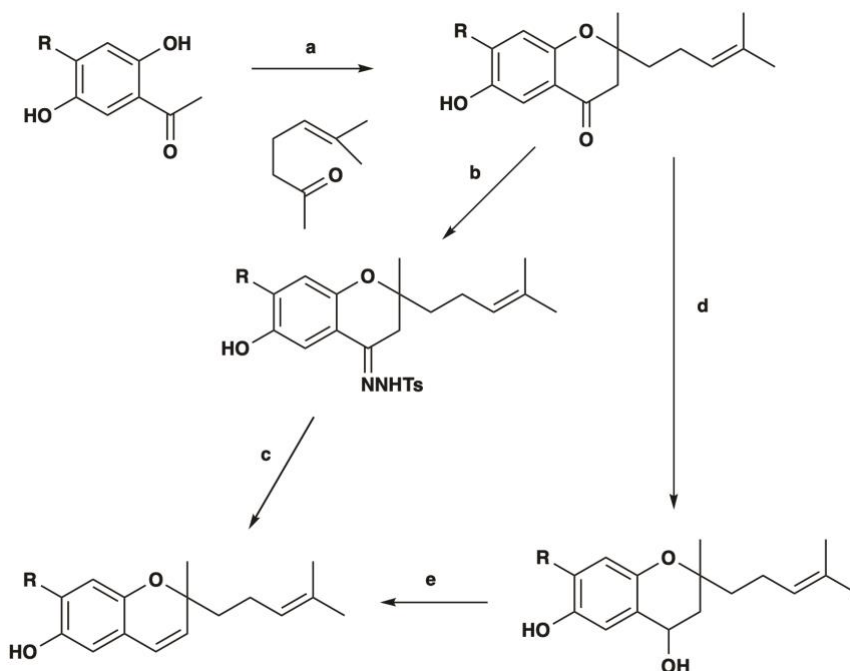
Scheme 2. a) Pyrrolidine, EtOH, 24-95%; b) AlCl₃/LiAlH₄ (2:1), Et₂O, 21-91%

Witiak *et al.* started from 2-hydroxy-5-chloroaceto-phenone as the hydroxyacetophenone and di-ethyloxalate as the alkyl ketone in the presence of NaOEt [35]. A cyclization was produced by heating in HCl-HOAc (1:4) and then, the reduction of the carbonyl group was obtained by hydrogenation in the presence of 5% Pd/C (**Scheme 3**).



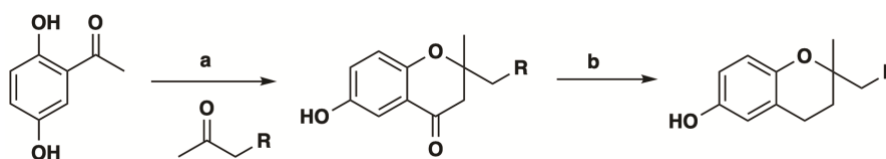
Scheme 3. a) NaOEt; b) HOAc, HCl, 60%; c) HOAc, 5% Pd/C, 75%

2,5-Dihydroxyacetophenones and 2-methyl-2-hepten-6-one were condensed to 4-chromanones in the presence of pyrrolidine by Sato *et al.* [36]. Synthesized chromanones were smoothly reduced to a diastereomeric mixture of corresponding 4-chromanols by two different methodologies (**Scheme 4**).

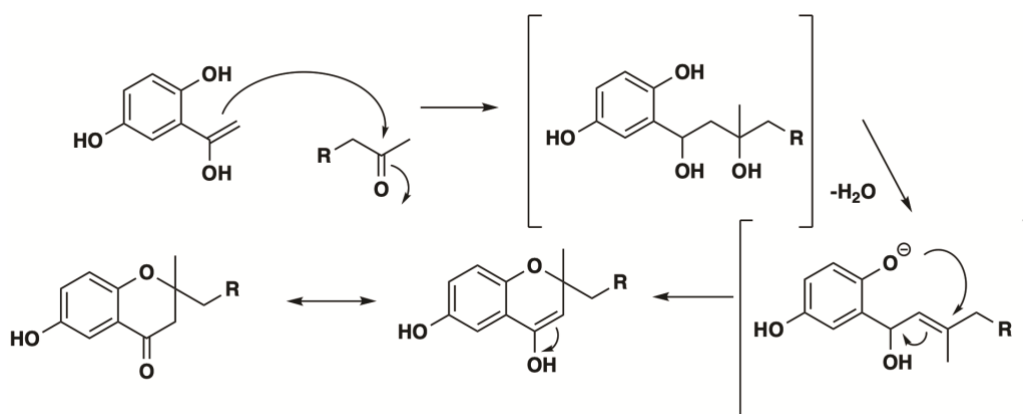


Scheme 4. a) Pyrrolidine/toluene, 63-66%; b) 60°/H₂NNTs/HOAc, 30%; (c) 120°/NaOCH₂CH₂OH, 25%; d) LiAlH₄/ THF, 90%; e) 180°/DMSO, 5% NaOH, 8-56%

Our research group obtained benzopyran-4-one nucleus similarly to the method described by Pearce *et al.* [34] but the reduction of the carbonyl group was achieved by treating zinc in hydrochloride under Clemmensen conditions (**Scheme 5**) [37]. The reaction mechanism consists of an aldol condensation between the enolate from an *ortho*-hydroxyacetophenone and the carbonyl group from an alkyl ketone. This is followed by an intramolecular cyclization via Michael addition (**Scheme 6**).



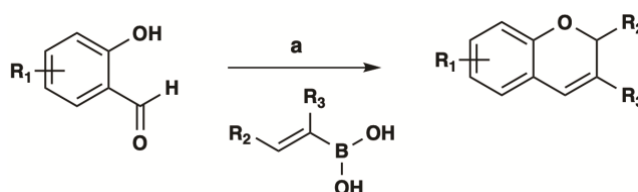
Scheme 5. a) Pyrrolidine, EtOH, 31-66%; b) Zn/HCl-AcOH, 30-46%



Scheme 6. Hypothetic mechanism of benzopyran-4-one nucleus formation

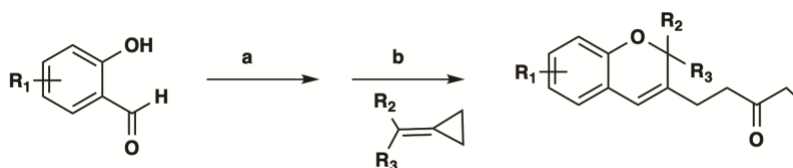
b) Synthesis from salicylic aldehydes

A catalytic preparation of 2H-chromenes using resin-bound amine was reported (**Scheme 7**) [38].



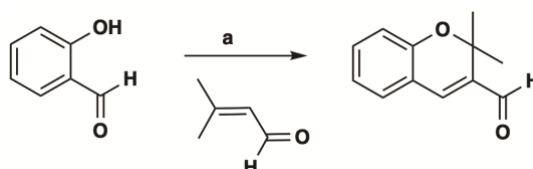
Scheme 7. a) R₂NH (cat.), dioxane, 75-99%

Lewis acid catalyzed cycloaddition of O-quinonemethides with methylenecyclopropanes produced novel benzopyran derivatives under mild conditions (**Scheme 8**) [39].



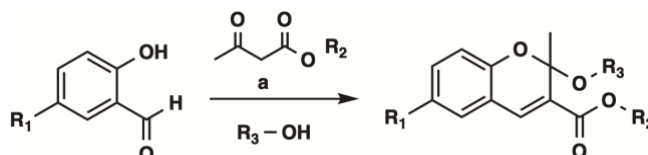
Scheme 8. a) $\text{CH}(\text{OEt})_3$, $\text{Sc}(\text{OTf})_2$, $\text{CH}_3\text{CH}_2\text{Cl}_2$, 61-82%

It has been reported the synthesis of regioselective 3-formyl-2H-chromenes from Michael/aldol condensation reactions in the presence of 1,5,7-Triazabicyclo[4.4.0]dec-5-ene (TBD) under solvent free condition (**Scheme 9**) [40].



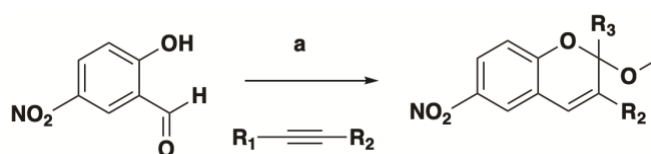
Scheme 9. a) TBD (10 mol%), 87%

Recently, an efficient and chemoselective Knoevenagel/Hemiketalization process for the synthesis of new 2H-chromenes in a one-pot three-component reaction was developed (**Scheme 10**) [41].



Scheme 10. a) L-proline, 64-81%

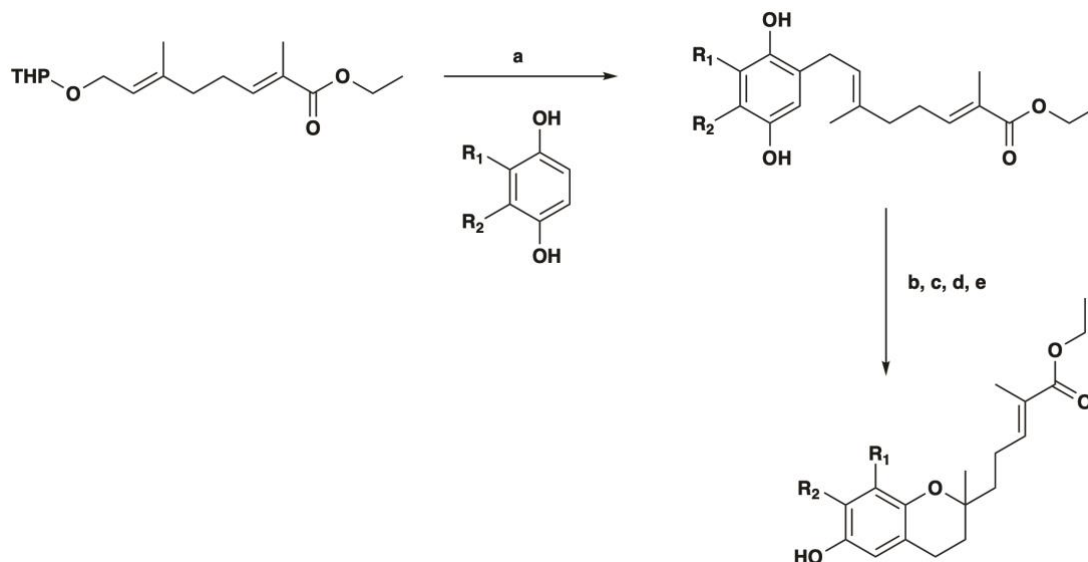
A highly regioselective one-pot synthesis of 2,3-disubstituted-2H-1-benzopyrans has been developed through Brønsted acid catalyzed [4+2] cycloaddition reaction with a variety of arylalkynes via orthoquinone methides (**Scheme 11**) [42].



Scheme 11. a) TfOH , $\text{CH}(\text{OMe})_3$, Toluene, MeOH, 37-99%

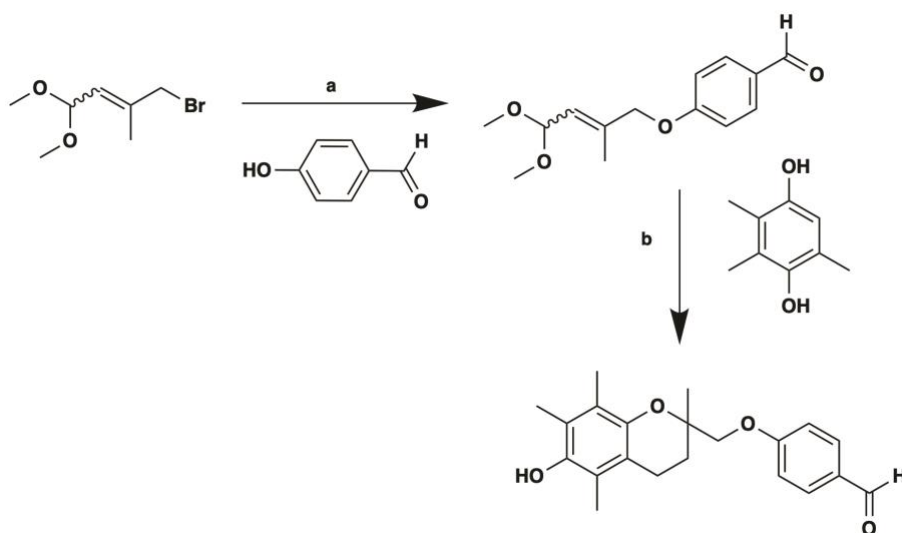
c) Synthesis of benzopyrans from hydroquinones

Pearce *et al.* designed their synthetic route [43] starting from an ester and reacting it with the corresponding hydroquinone (**Scheme 12**).



Scheme 12. a) BF₃, dioxane; b) p-toluenesulphonic acid, benzene; c) 2-methoxyethoxymethyl chloride, NaH, THF; d) AlH₃, Et₂O; e) thiozianate, Me₂S, CH₂Cl₂, 61-94%

In this synthetic section, it is noteworthy the synthesis realized by Cossy *et al.* [44] where an unsaturated acetal was reacted with trimethylhydroquinone (**Scheme 13**).

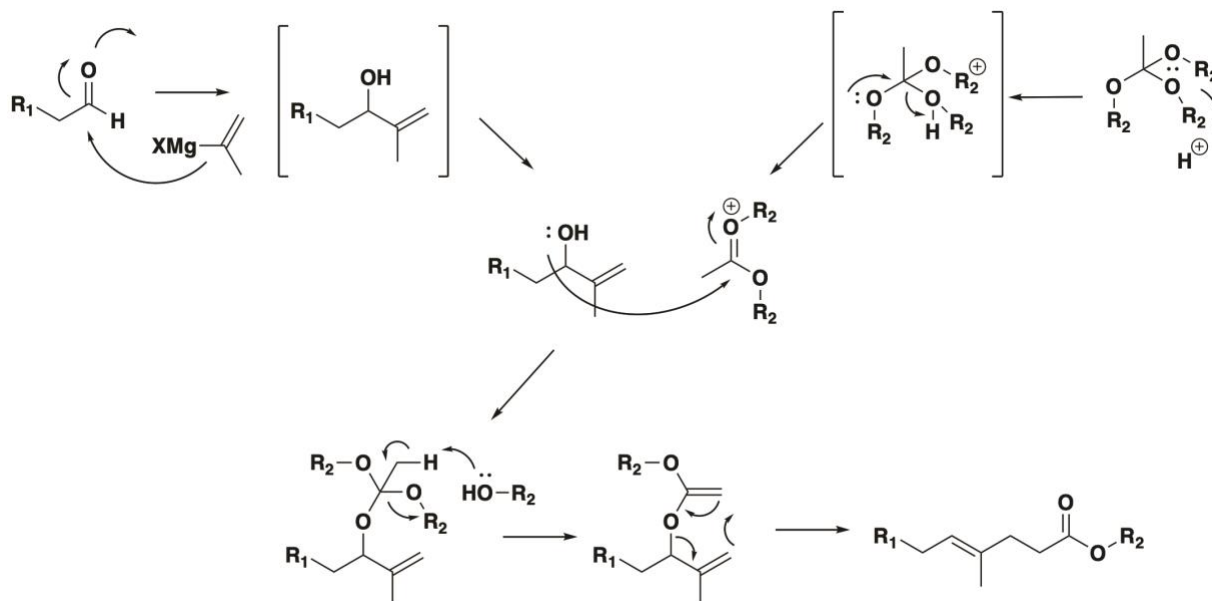


Scheme 13. a) K₂CO₃, NaI, acetone, 70%; b) HN(Tf)₂, CH₂Cl₂, 30%

▪ Prenylated chain elongation

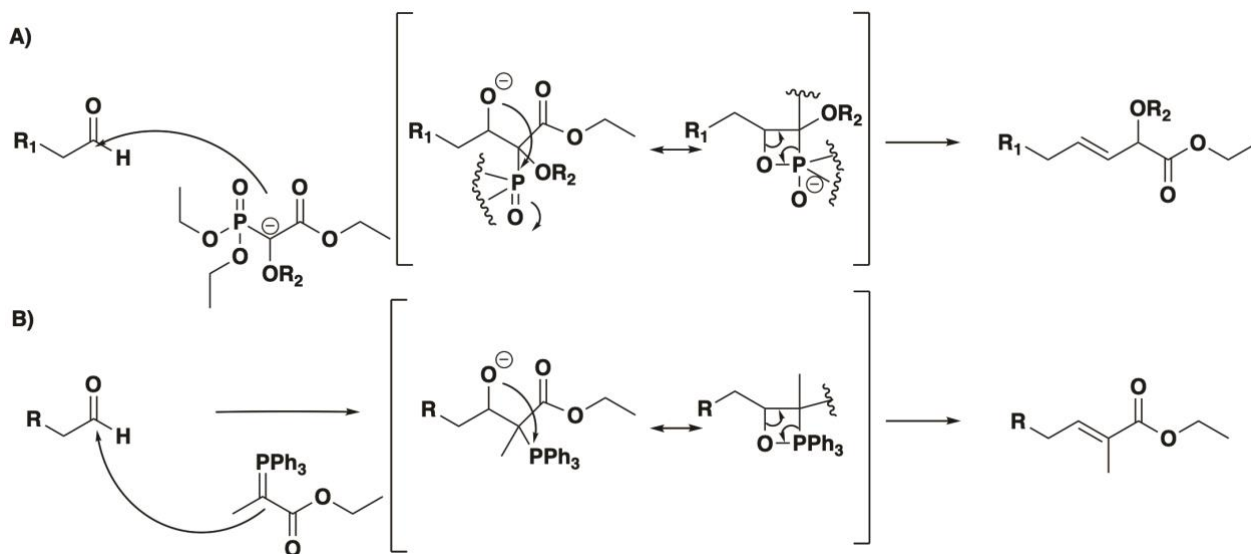
There are several mechanisms for forming and prolonging the prenylated chain. The different strategies used in this work are explained below.

The Grignard reaction consist of the addition of an organomagnesium halide (Grignard reagent) to a ketone or aldehyde to form the secondary or tertiary alcohol [45]. This reaction followed by a Johnson Claisen rearrangement allows to elongate the prenylated chain (**Scheme 14**).



Scheme 14. Chain elongation mechanism

Another synthetic strategy from aldehydes or ketones are the Horner-Wadsworth-Emmons and the Wittig reaction. These reactions are two of the most famous methods for the construction of carbon–carbon double bonds [46,47] (**Scheme 15**).



Scheme 15. Horner-Wadsworth-Emmons (A) and Wittig mechanism reactions (B)

Objectives

This work has the following objectives:

Chapter 1:

1- Design and synthesis of new benzopyran derivatives containing a 2-prenylated chain (with some isoprenoid units or an α -alkoxy- α,β -unsaturated ester moiety) or a 2-alkyl hydrazone group as potential PPAR agonists

2- *In vitro* pharmacological studies of the PPAR agonist activity and the anti-inflammatory effect

Chapter 2:

1- Design and synthesis of 2-aminopropyl benzopyran derivatives as potential agents for the treatment of triple negative breast cancer

2- *In vitro* pharmacological studies of the cytotoxic capacity and the cell death mechanism

Chapter 1

2-Prenylated and 2-alkyl hydrazone derivatives with dual PPAR α / γ or PPAR α / δ agonism

1. Peroxisome proliferator activated receptors (PPARs)

2. Benzopyrans as PPAR agonists

3. Articles

Article 1: Synthesis of 2-prenylated alkoxyated benzopyrans by Horner-Wadsworth–Emmons olefination with PPAR α / γ Agonist Activity, *ACS Medicinal Chemistry Letters*, 12 (2021) 1783-1786.

Article 2: Synthesis and biological studies of “Polycerasoidol” and “trans- δ -Tocotrienolic acid” derivatives as PPAR α and/or PPAR γ agonists, *Bioorganic & Medicinal Chemistry*, 53 (2022) 116532.

Article 3: Benzopyran hydrazones with dual PPAR α / γ or PPAR α / δ agonism and an anti-inflammatory effect on human THP-1 macrophages, *European Journal of Medicinal Chemistry*, in press.

1. Peroxisome proliferator activated receptors (PPARs)

Peroxisome proliferator-activated receptors (PPARs) are ligand-activated transcription factors of the nuclear hormone receptor superfamily. After the interaction with ligands, PPARs are translocated to the nucleus and heterodimerise with the retinoid X receptor (RXR) to form the PPAR-RXR complex. The PPAR-RXR heterodimer bind to DNA specific PPAR-response elements (PPREs) in the promoter region of the target genes activating the transcription of that genes involved in numerous cell functions including the control of lipid and carbohydrate metabolism and inflammation [48] (**Figure 2**). PPARs comprise three isotypes, PPAR α (NR1C1), PPAR β/δ (NR1C2) and PPAR γ (NR1C3), which have different tissue distribution, ligand specificities, and metabolic regulatory activities [49]. PPAR α is expressed mainly in the tissues involved in increased fatty acid oxidation, such as liver, skeletal muscle and heart, and it is implicated in lipid metabolism, glucose homeostasis and insulin resistance [50-52]. PPAR β/δ is ubiquitous, but is highly expressed in those tissues involved in fatty acid metabolism, such as skeletal and cardiac muscle, hepatocytes and adipocytes. Its activation improves insulin sensitivity and the plasma lipid profile [53]. PPAR γ is widely expressed in adipose tissue, and is related to adipogenesis, lipid storage, insulin sensitivity and glucose homeostasis. Its agonists have been used for treating type 2 diabetes [54].

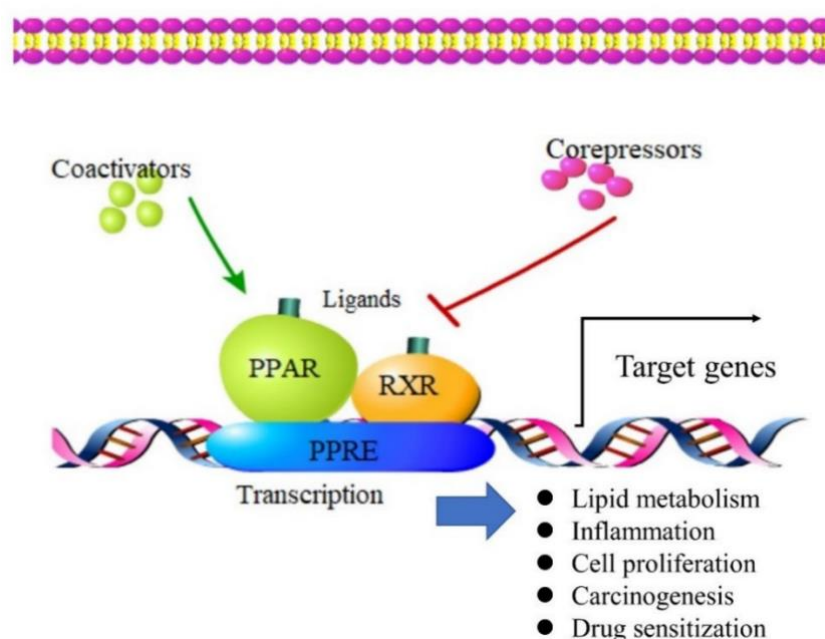


Figure 2. Transcriptional regulation of PPARs-RXR complex

Endogenous ligands include mainly saturated or unsaturated fatty acids (FA) and FA derived compounds, eicosanoids (e.g., leukotriene B4 and 8-HETE), phospholipids (e.g., azelaoyl phosphatidylcholine, 16:0/18:1 GPC) and certain prostaglandins (e.g., 15-deoxy-'12,14-prostaglandin-J2) (**Figure 3**) [55]. The most known synthetic ligands are fibrates and thiazolidinediones, which act as strong agonists for PPAR α and PPAR γ , respectively (**Figure 4**) [56]. However, full PPAR γ activators have shown negative effects, including weight gain, fluid retention, bone fracture and cardiac hypertrophy. Therefore, there is a great interest to identify new partial PPAR γ agonists or PPAR γ modulators (PPAR γ Ms) lacking of adverse effects associated to full activation [48]. In addition, the three isoforms (α , β/δ , γ) play a major role in regulating inflammatory processes, and have been recognised as the target for the management of metabolic syndrome, obesity, dyslipidaemia, type 2 diabetes, atherosclerosis, and non-alcoholic fatty liver disease (NAFLD) [57]. Infiltrate macrophages in tissues also release pro-inflammatory cytokines and chemokines, which contribute to an inflammation state. PPAR agonists have been reported to suppress the immunoreactive state of macrophages by the suppression of immune reactive cytokine and chemokines markers, including MCP-1 and IL-6 [48, 58, 59].

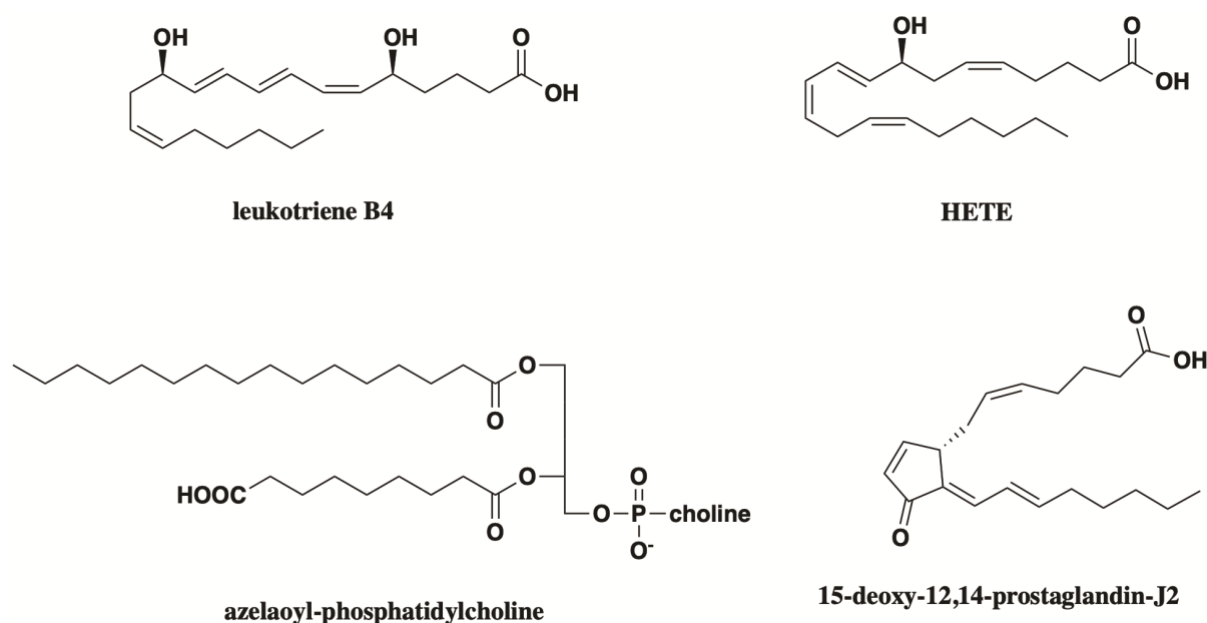


Figure 3. PPAR endogenous ligands

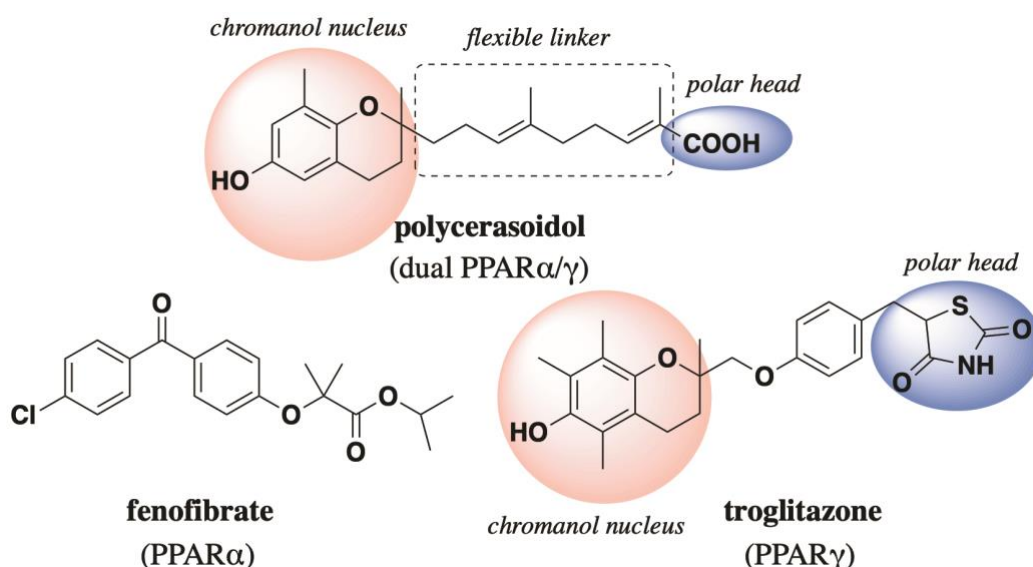


Figure 4. PPAR ligands

2. Benzopyrans as PPAR agonists

Some benzopyrans have been demonstrated to be PPAR agonists. Acacetin (**Figure 5**), an *O*-methylated flavone which can be isolated from several medicinal plants such as *Betula pendula*, *Carthamus tinctorius*, *Robinia pseudoacacia* and *Turnera diffusa*, acted as an essential PPAR α activator in high glucose-exposed cardiomyocytes [60]. The synthetic troglitazone (**Figure 4**), widely used as an antidiabetic and anti-inflammatory drug, contains a chromanol nucleus. Quercetin (**Figure 5**) is a flavonoid widely distributed in nature, with a benzopyran-4-one skeleton, which exerts anti-atherogenic effects by upregulating the gene expression of PPAR γ and LXR α [61]. Formononetin (**Figure 5**), an isoflavonoid identified from the Chinese herb *Astragalus membranaceus*, alleviates ox-LDL-induced endothelial injury in HUVECs by stimulating PPAR γ signaling [62]. Bavachinin (**Figure 5**), a flavonoid with a BP skeleton, is a novel natural pan-PPAR agonist which exhibits synergistic effects with synthetic PPAR γ and PPAR α agonists [63].

The 2-prenylated benzopyran polycerasoidol (**Figure 4**), which contains the chromanol nucleus like the PPAR γ agonist troglitazone, two isoprenoid units, and a terminal carboxylic group on the side chain, displayed potent dual PPAR α/γ agonism with potential anti-inflammatory effects [11,64]. A new prenylated benzopyran synthesised by our research group, 2-(ethyl-4'-methylpentanoate)-6-(*p*-fluorobenzyloxy)-2-(methyl)-benzodihydropyran (BP-2) (**Figure 5**), displays pan-PPAR agonism with a strong PPAR α , moderate PPAR β/δ and weak PPAR γ activity, and exerted anti-inflammatory effects [65].

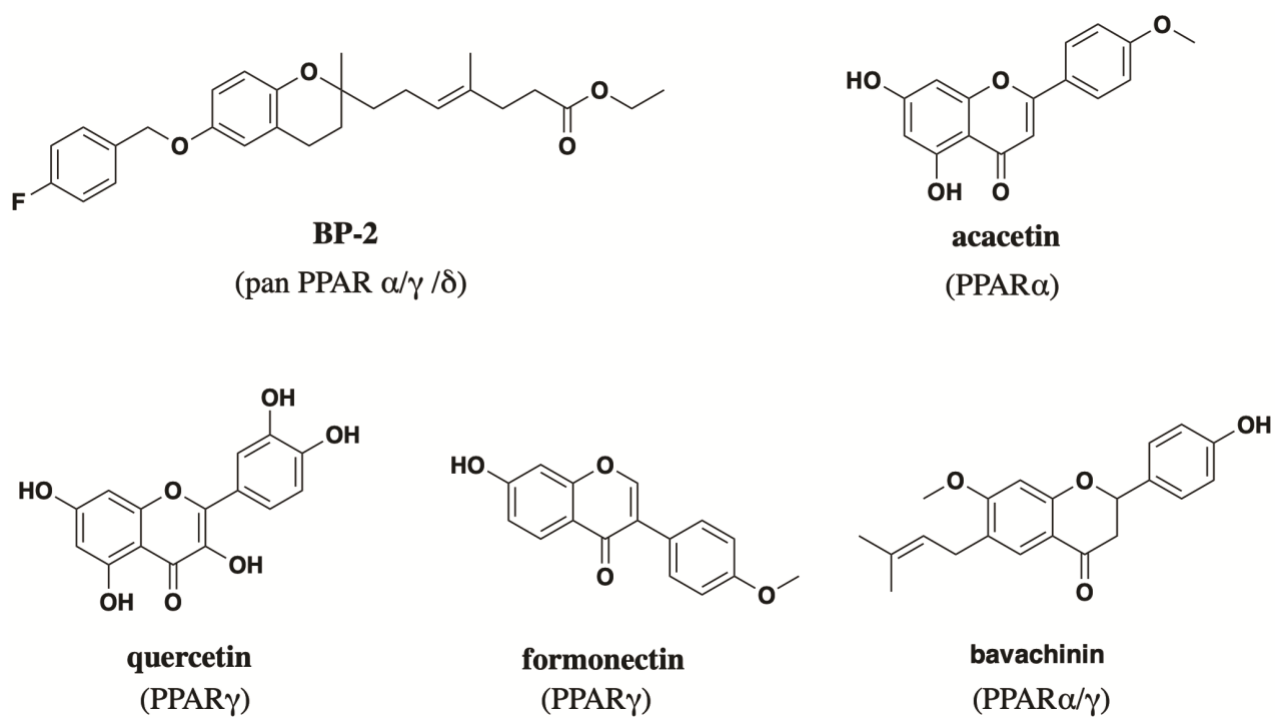


Figure 5. PPAR agonists with a benzopyran nucleus

3. Articles

Article 1: Synthesis of 2-prenylated alkoxyated benzopyrans by Horner-Wadsworth–Emmons olefination with PPAR α / γ Agonist Activity, *ACS Medicinal Chemistry Letters*, 12 (2021) 1783.

Synthesis of 2-Prenylated Alkoxyated Benzopyrans by Horner–Wadsworth–Emmons Olefination with PPAR α / γ Agonist Activity

Published as part of the ACS Medicinal Chemistry Letters virtual special issue “Medicinal Chemistry in Portugal and Spain: A Strong Iberian Alliance”.

Ainhoa García, Laura Vila, Paloma Marín, Álvaro Bernabeu, Carlos Villarroel-Vicente, Nathalie Hennuyer, Bart Staels, Xavier Franck, Bruno Figadère, Nuria Cabedo,* and Diego Cortes*



Cite This: *ACS Med. Chem. Lett.* 2021, 12, 1783–1786



Read Online

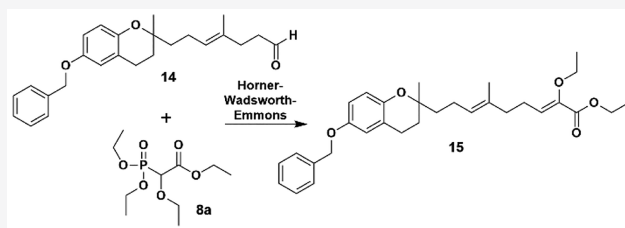
ACCESS |

Metrics & More

Article Recommendations

ABSTRACT: We have synthesized series of 2-prenylated benzopyrans as analogues of the natural polycerasoidol, a dual PPAR α / γ agonist with anti-inflammatory effects. The prenylated side chain consists of five or nine carbons with an α -alkoxy- α,β -unsaturated ester moiety. Prenylation was introduced via the Grignard reaction, followed by Johnson–Claisen rearrangement, and the α -alkoxy- α,β -unsaturated ester moiety was introduced by the Horner–Wadsworth–Emmons reaction. Synthetic derivatives showed high efficacy to activate both hPPAR α and hPPAR γ as dual PPAR α / γ agonists. These prenylated benzopyrans emerge as lead compounds potentially useful for preventing cardiometabolic diseases.

KEYWORDS: Prenylated benzopyrans, Horner–Wadsworth–Emmons reaction, PPAR α / γ activity



Among the nuclear receptor family, peroxisome proliferator activated receptors (PPARs) are transcription factors activated by ligands, which are implicated in numerous cell functions including glucose and lipid metabolism and inflammation.¹ Dual PPAR α / γ activators can improve atherogenic dyslipidemia and insulin resistance.¹ Polycerasoidol is a *trans*- δ -tocotrienolic acid analogue² isolated from *Polyalthia cerasoides* (Annonaceae).^{3,4} Polycerasoidol, containing a 6-chromanol nucleus and a 2-prenylated side chain, is biosynthesized from homogentisate and geranylgeranyl pyrophosphate via the shikimate pathway and the mevalonate pathway, respectively (Figure 1). Pharmacologically, it displays dual PPAR α / γ agonist activity and ameliorates inflammation of dysfunctional endothelium.⁵ In structural terms, this natural benzopyran possesses a benzopyran nucleus (lipophilic tail), a prenylated chain (flexible linker), and a carboxylic acid (polar head), as do other natural and synthetic PPAR α and/or

PPAR γ agonists.⁶ The structure–activity relationships (SARs) of polycerasoidol and semisynthetic analogues revealed that the 6-oxygenated dihydrobenzopyran core and the linker hydrocarbon chain of at least a five-carbon length are essential moieties to activate PPAR α and/or PPAR γ .⁷ It is noteworthy that the chroman-6-ol pharmacophore is present in troglitazone, the first PPAR γ agonist belonging to the class of thiazolidinediones, which was approved as an antidiabetic agent.^{8,9} Currently, rosiglitazone and pioglitazone are selective PPAR γ agonists used to manage hyperglycemia in type 2 diabetes, while saroglitazar and lobeglitazone are PPAR α / γ activators (agonists) approved against diabetes in India and South Korea, respectively.⁹ In order to find new active and safer PPAR activators, we describe the synthesis and PPAR activity of 2-prenylated benzopyrans that bear an α -alkoxy- α,β -unsaturated ester as a trioxxygenated polar head on the prenylated side chain.

We first prepared the benzopyran-4-one nucleus (γ -benzopyrone 3) by conventional methods.¹⁰ The reaction mechanism consists of an aldol condensation between the

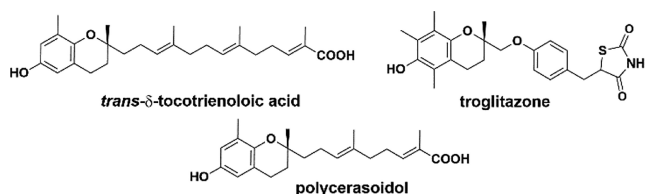
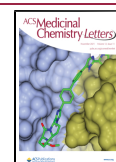


Figure 1. Bioactive prenylated benzopyrans.

Received: July 22, 2021

Accepted: October 4, 2021

Published: October 6, 2021



enolate from an *ortho*-hydroxyacetophenone and the carbonyl group from an alkyl ketone. This is followed by an intramolecular cyclization via Michael addition, which is promoted by the *ortho*-phenol group.¹¹ Thus, 2,5-dihydroxyacetophenone (**1**) and ethyl levulinate (**2**) in the presence of pyrrolidine gave the chroman-4-one **3** as a racemic mixture in a single step with a good yield (80%) (Figure 2).^{7,10} γ -

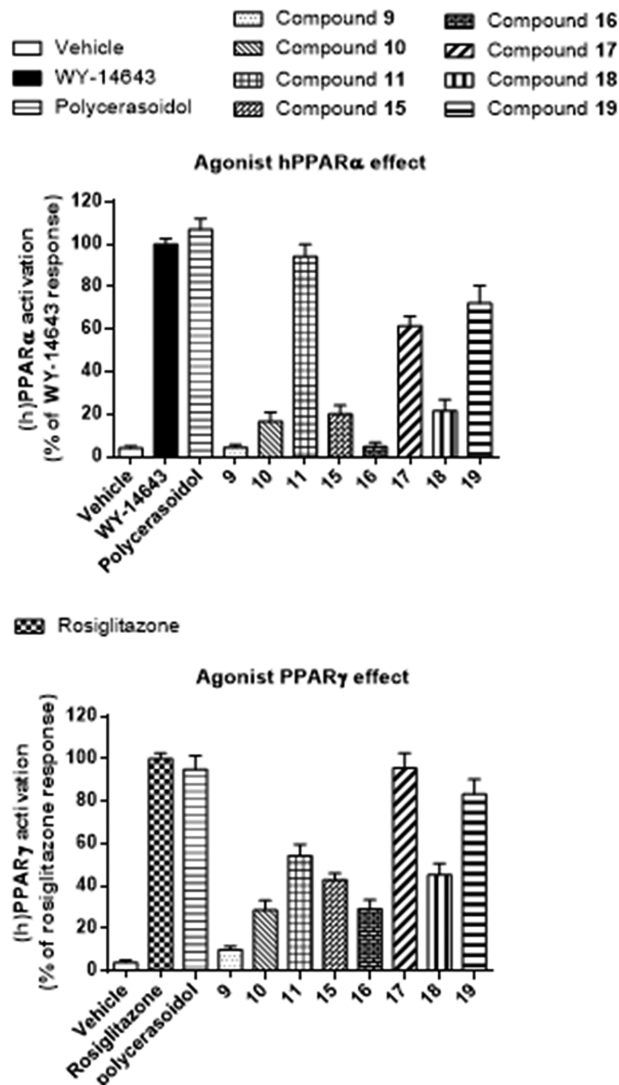
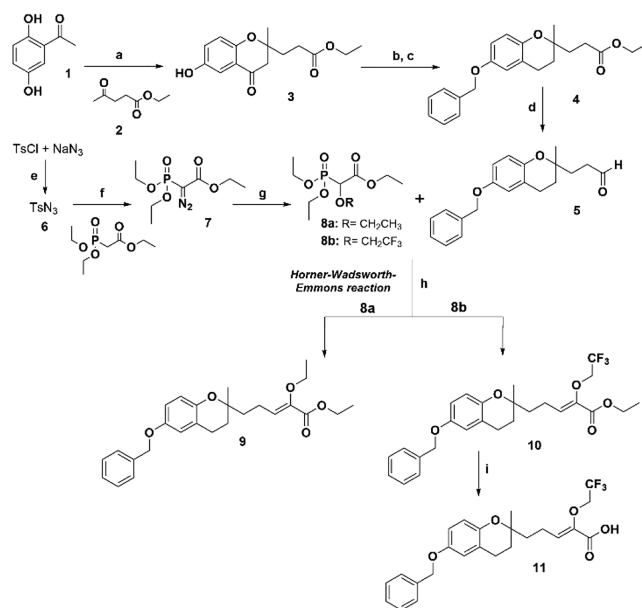


Figure 2. hPPAR α and hPPAR γ transactivation assays. Synthesized benzopyrans were tested at 10 μ M, and WY-14,643 (10 μ M) and rosiglitazone (1 μ M) are reference compounds for α and γ , respectively.

Benzopyrone **3** was reduced under Clemmensen conditions, and the phenol hydroxyl group at 6-position was protected by *O*-benzylation to give compound **4** with a good overall yield. The controlled reduction of the ester function by DIBAL-H at -78 °C gave the aldehyde **5** with a 92% yield. In a first approach, we synthesized five-carbon side chain alkoxyated prenylated benzopyrans (series 1) from aldehyde intermediate **5** by Horner–Wadsworth–Emmons olefination. For this purpose, appropriate alkylphosphonates, e.g., ethyl 2-(diethoxyphosphoryl)-2-ethoxyacetate (**8a**) and ethyl 2-(diethoxyphosphoryl)-2-(2,2,2-trifluoroethoxy)acetate (**8b**), were previously prepared from (ethoxyacetate) diethoxyphosphorane and

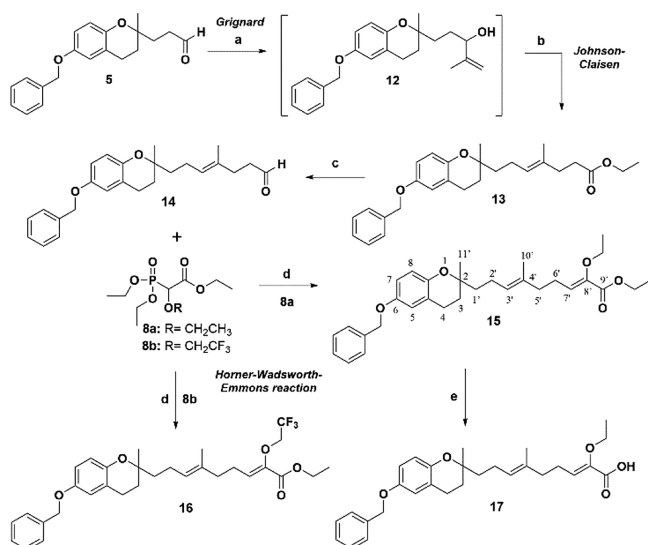
TsN₃ (**6**) in the presence of NaH.¹² Then, aldehyde intermediate **5** was reacted with phosphonate **8a** or **8b** to afford the α -alkoxy- α,β -unsaturated esters of prenylated benzopyrans **9** (20%, *Z/E* = 60:40) or **10** (84%, *Z/E* = 35:65), respectively. The saponification of ethyl ester (**10**) quantitatively afforded carboxylic acid (**11**, *Z/E* = 40:60) (Scheme 1).

Scheme 1. Synthesis of Prenylated Benzopyrans 9–11 (Series 1)^a



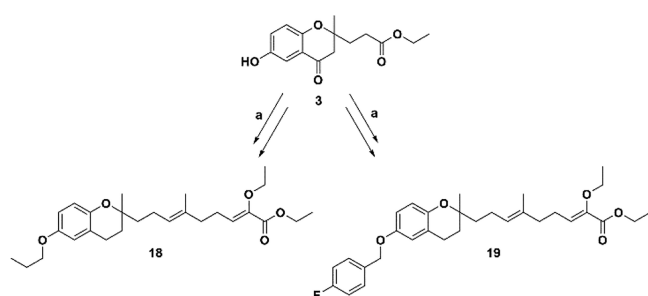
^aReaction conditions: (a) Pyrrolidine, EtOH, 60 °C, molecular sieve 3 Å, 24 h, 80%; (b) Zn/HCl, AcOH-H₂O, rt, 2 h; (c) ClCH₂C₆H₅, K₂CO₃, EtOH, 60 °C, 5 h, 90%; (d) DIBAL-H, CH₂Cl₂, -78 °C, N₂, 20 min, 92%; (e) 0 °C, acetone, 2 h, 81%; (f) 60% NaH, THF, 0 °C, N₂, 16 h, 65%; (g) EtOH, Rh(OAc)₂, toluene, 45 °C, overnight, **8a** (R = CH₂CH₃), 40.2% or **8b** (R = CH₂CF₃), 51%; (h) phosphonate **8a** or **8b**, THF, NaH, 0 °C, N₂, 1 h + S, THF, rt, overnight: **9**, 20% or **10**, 84%; (i) 20% KOH, reflux, 5 h, 99%.

In a second approach, we synthesized the nine-carbon side chain *O*-alkoxyated prenylated benzopyrans (series 2) **15**, **16**, and **17** from aldehyde intermediate **5**. The prenylated side chain at the 2-position of the dihydrobenzopyran nucleus was elongated with a sequence of Grignard reaction, Johnson–Claisen rearrangement and Horner–Wadsworth–Emmons olefination (Scheme 2). The aldehyde synthon **5** was treated with isoprenylmagnesium bromide as the vinyl Grignard reagent, followed by Johnson–Claisen rearrangement of allylic alcohol **12** using ethyl orthoacetate to produce unsaturated ester **13** with a 50% yield in the last two steps. Ester **13** was subjected to a controlled reduction using DIBAL-H at -78 °C to give the aldehyde intermediate **14** in 89% yield. The α -alkoxy- α,β -unsaturated ester on the prenylated side chain was introduced by a Horner–Wadsworth–Emmons reaction.¹³ Thus, aldehyde **14** was treated with phosphonates **8a** and **8b** to afford esters **15** (85%) and **16** (82%), respectively.¹⁴ It is noteworthy that ester **15** was obtained as a *Z*-alkene isomer exclusively. Once again, the saponification of ethyl ester **15** quantitatively yielded carboxylic acid **17** (Scheme 2). In addition to *O*-benzyloxy benzopyrans bearing a nine-carbon prenylated alkoxy side chain (series 2), we accomplished the

Scheme 2. Synthesis of Prenylated Benzopyrans 15–17 (Series 2)^a

^aReaction conditions: (a) $\text{CH}_3\text{C}(\text{MgBr})=\text{CH}_2$, THF, -78°C , N_2 , 1 h, 84%; (b) $\text{MeC}(\text{OEt})_3$, isobutyric acid, 140°C , 2 h, 50%; (c) DIBAL-H, CH_2Cl_2 , -78°C , N_2 , 20 min, 89%; (d) phosphonate 8a or 8b, THF, NaH, 0°C , N_2 , 1 h + 14 in THF, rt, overnight: 15 (R = CH_2CH_3), 85% or 16 (R = CH_2CF_3), 82%; (e) 20% KOH, reflux, 5 h, 99%.

synthesis of its *O*-propyloxy and *O*-*p*-fluorobenzyloxy benzopyran analogues. According to the second approach followed to prepare ester 15, but starting from the chroman-4-one 3, we synthesized *O*-propyloxy ester 18 and *O*-*p*-fluorobenzyloxy ester 19 (Scheme 3).

Scheme 3. Synthesis of Prenylated Benzopyrans 18 and 19^a

^aReaction conditions: (a) See reagents and conditions described in Scheme 1 for the synthesis of 5, and Scheme 2 for the synthesis of 15 and 16.

The transactivation studies¹⁵ of the synthesized benzopyrans were carried out and compared to the maximal efficacy of WY-14,643 (at $10\ \mu\text{M}$) or rosiglitazone (at $1\ \mu\text{M}$) as hPPAR α and hPPAR γ reference compounds, respectively. At the $10\ \mu\text{M}$ dose, compounds 10, 15, 16, and 18 were moderate hPPAR activators for both receptors while compounds 11, 17, and 19 showed high efficacy as dual hPPAR α/γ agonists. Indeed, compound 11 showed higher efficacy to activate hPPAR α than PPAR γ did (α/γ ratio = 1.73), and 17 displayed slight selectivity toward hPPAR γ (α/γ ratio = 0.64). Therefore, the elongation of the side chain from five to nine carbons is beneficial to activate hPPAR γ . In agreement with a previous docking analysis of polycerasoidol, the carboxylic moiety at the

C-9' position of 17 plays a key role as an anchoring point to bind the PPAR γ receptor.⁵

In conclusion, we efficiently prepared new series of the 2-prenylated *O*-alkoxylated benzopyrans possessing the α -alkoxy- α,β -unsaturated moiety on the prenylated chain by the Horner–Wadsworth–Emmons reaction. Synthetic derivatives were efficient in activating both hPPAR α and hPPAR γ as dual PPAR α/γ agonists. These prenylated benzopyrans emerge as lead compounds that might be potentially useful for preventing cardiometabolic diseases.

AUTHOR INFORMATION

Corresponding Authors

Diego Cortes – Departamento de Farmacología, Facultad de Farmacia, Universidad de Valencia, 46100 Burjassot, Valencia, Spain; Email: dcortes@uv.es

Nuria Cabedo – Departamento de Farmacología, Facultad de Farmacia, Universidad de Valencia, 46100 Burjassot, Valencia, Spain; Institute of Health Research-INCLIVA, University Clinic Hospital of Valencia, 46010 Valencia, Spain; orcid.org/0000-0001-6729-8057; Email: ncabedo@uv.es

Authors

Ainhoa García – Departamento de Farmacología, Facultad de Farmacia, Universidad de Valencia, 46100 Burjassot, Valencia, Spain

Laura Vila – Departamento de Farmacología, Facultad de Farmacia, Universidad de Valencia, 46100 Burjassot, Valencia, Spain; Institute of Health Research-INCLIVA, University Clinic Hospital of Valencia, 46010 Valencia, Spain

Paloma Marín – Departamento de Farmacología, Facultad de Farmacia, Universidad de Valencia, 46100 Burjassot, Valencia, Spain

Álvaro Bernabeu – Departamento de Farmacología, Facultad de Farmacia, Universidad de Valencia, 46100 Burjassot, Valencia, Spain

Carlos Villarroel-Vicente – Departamento de Farmacología, Facultad de Farmacia, Universidad de Valencia, 46100 Burjassot, Valencia, Spain; Institute of Health Research-INCLIVA, University Clinic Hospital of Valencia, 46010 Valencia, Spain

Nathalie Hennuyer – Université Lille, Inserm, CHU Lille, Institut Pasteur Lille, U1011-EGID, S9000 Lille, France

Bart Staels – Université Lille, Inserm, CHU Lille, Institut Pasteur Lille, U1011-EGID, S9000 Lille, France

Xavier Franck – Normandie Univ, CNRS, INSA Rouen, UNIROUEN, COBRA (UMR6014 & FR 3038), 76000 Rouen, France; orcid.org/0000-0002-5615-7504

Bruno Figadère – BioCIS, CNRS, Université Paris-Saclay, 92296 Châtenay-Malabry, France; orcid.org/0000-0003-4226-8489

Complete contact information is available at: <https://pubs.acs.org/10.1021/acsmmedchemlett.1c00400>

Notes

The authors declare no competing financial interest.

ACKNOWLEDGMENTS

We are grateful for the financial support from Generalitat Valencia (APOTIP/2020/011), Carlos III Health Institute (ISCIII), and the European Regional Development Fund

(CP15/00150 and PI18/01450) and from Agence Nationale pour la Recherche ANR-10 LABX-0046 and an ERC Advanced Grant (694717). N.C. is a "Miguel Servet" program researcher (CP15/00150, CPII20/00010) of the ISCIII cofunded by the European Social Fund. C.V.-V. is thankful for the PFIS grant (FI19/00153) of ISCIII.

■ ABBREVIATIONS

PPARs, peroxisome proliferator-activated receptors; SAR, structure–activity relationships; DIBAL-H, diisobutylaluminum hydride; TsN₃, tosyl azide

■ REFERENCES

- (1) Villarroel-Vicente, C.; Gutiérrez-Palomo, S.; Ferri, J.; Cortes, D.; Cabedo, N. Natural products and analogs as preventive agents for metabolic syndrome via peroxisome proliferator-activated receptors: An overview. *Eur. J. Med. Chem.* **2021**, *221*, 113535.
- (2) Azzí, A. Tocopherols, tocotrienols and tocomonoenols: Many similar molecules but only one vitamin E. *Redox Biol.* **2019**, *26*, 101259.
- (3) González, M. C.; Serrano, A.; Zafra-Polo, M. C.; Cortes, D.; Rao, K. S. Polycerasoidin and polycerasoidol, two new prenylated benzopyran derivatives from *Polyalthia cerasoides*. *J. Nat. Prod.* **1995**, *58*, 1278–1284.
- (4) Zafra-Polo, M. C.; González, M. C.; Tormo, J. R.; Estornell, E.; Cortes, D. Polyalthidin: new prenylated benzopyran inhibitor of the mammalian mitochondrial respiratory chain. *J. Nat. Prod.* **1996**, *59*, 913–916.
- (5) Bermejo, A.; Collado, A.; Barrachina, I.; Marques, P.; El Aouad, N.; Franck, X.; Garibotto, F.; Dacquet, C.; Caignard, D.-H.; Suvire, F.; Enriz, R. D.; Piqueras, L.; Figadère, B.; Sanz, M. J.; Cabedo, N.; Cortes, D. Polycerasoidol, a natural prenylated benzopyran with a dual PPAR α /PPAR γ agonist activity and anti-inflammatory effect. *J. Nat. Prod.* **2019**, *82*, 1802–1812.
- (6) Mirza, A. Z.; Althagafi, I. I.; Shamshad, H. Role of PPAR receptor in different diseases and their ligands: Physiological importance and clinical implications. *Eur. J. Med. Chem.* **2019**, *166*, 502–513.
- (7) Bermejo, A.; Barrachina, I.; El Aouad, N.; Franck, X.; Chahboune, N.; Andreu, I.; Figadère, B.; Vila, L.; Hennuyer, N.; Staels, B.; Dacquet, C.; Caignard, D.-H.; Sanz, D. M. J.; Cortes, D.; Cabedo, N. Synthesis of benzopyran derivatives as PPAR α and/or PPAR γ activators. *Bioorg. Med. Chem.* **2019**, *27*, 115162.
- (8) Tafazoli, S.; Wright, J. S.; O'Brien, P. J. Prooxidant and antioxidant activity of vitamin E analogues and troglitazone. *Chem. Res. Toxicol.* **2005**, *18*, 1567–1574.
- (9) Yasmin, S.; Jayaprakash, V. Thiazolidinediones and PPAR orchestra as antidiabetic agents: From past to present. *Eur. J. Med. Chem.* **2017**, *126*, 879–893.
- (10) Pearce, B. C.; Parker, R. A.; Deason, M. E.; Dischino, D. D.; Gillespie, E.; Qureshi, A. A.; Volk, K.; Wright, J. J. K. Inhibitors of cholesterol biosynthesis. 2. Hypocholesterolemic and antioxidant activities of benzopyran and tetrahydronaphthalene analogues of the tocotrienols. *J. Med. Chem.* **1994**, *37*, 526–541.
- (11) Xiong, W.; Wang, X.; Shen, X.; Hu, C.; Wang, X.; Wang, F.; Zhang, G.; Wang, C. Synthesis of flavonols via pyrrolidine catalysis: Origins of the selectivity for flavonol versus aurone. *J. Org. Chem.* **2020**, *85*, 13160–13176.
- (12) General procedure for the synthesis of alkylphosphonates: Synthesis of ethyl 2-(diethoxyphosphoryl)-2-ethoxyacetate (**8a**). Ethyl 2-diazo-2-(diethoxyphosphoryl) acetate (**7**, 379 mg, 1.503 mmol) in ethanol (900 μ L) was stirred, and rhodium acetate (II) (6.66 mg, 0.015 mmol) in toluene (8 mL) was added to this solution. The mixture was stirred at 45 °C overnight. Usual workup followed by column chromatography purification (ethyl ether/ EtOAc 98:2) gave 162 mg of **8a** (40.2%).
- (13) Wadsworth, W. S., Jr Synthetic Applications of Phosphoryl-Stabilized Anions. *Org. React.* **1977**, *25*, 73–253.
- (14) General procedure for Horner–Wadsworth–Emmons reaction. Synthesis of 6-benzyloxy-2-((8'-ethoxy-4'-methyl)ethylnona-3'E, 7'Z-dienoate)-2-methyl-dihydrobenzopyran (**15**): Ethyl 2-(diethoxyphosphoryl)-2-ethoxyacetate (**8a**) (0.156 mmol) in anhydrous THF (4 mL) at 0 °C under N₂ atmosphere was treated with 60% NaH (10.6 mg, 0.265 mmol), and the mixture was stirred for 1 h at 0 °C. Then, a solution of aldehyde (**59** mg, 0.156 mmol) in anhydrous THF (5 mL) was added and the mixture was stirred overnight at room temperature. Usual workup followed by column chromatography purification (hexane/ EtOAc 80:20) yielded 64.5 mg of **15** (85%) as a colorless oil: ¹H NMR (300 MHz, CDCl₃): δ 7.36 (m, 5H, H-2" to 6"), 6.75 (dd, J = 7.1, 2.3 Hz, 1H, H-7), 6.72 (d, J = 7.1 Hz, 1H, H-8), 6.69 (d, J = 2.3 Hz, 1H, H-5), 6.23 (t, J = 7.4 Hz, 1H, H-7'), 5.16 (m, 1H, H-3'), 4.99 (s, 2H, OCH₂Ar), 4.21 (q, J = 7 Hz, 2H, COOCH₂CH₃), 3.85 (q, J = 7 Hz, 2H, OCH₂CH₃), 2.73 (t, J = 6.8 Hz, 2H, CH₂-4), 2.34 (q, J = 7.4 Hz, 2H, CH₂-6'), 2.09 (m, 4H, CH₂-2', CH₂-5'), 1.81 (m, 2H, CH₂-3), 1.62 (m, 2H, CH₂-1'), 1.60 (s, 3H, CH₃-10'), 1.30, 132 (2t, J = 7 Hz, 3H, OCH₂CH₃, COOCH₂CH₃), 1.27 (s, 3H, CH₃-11'). ¹³C NMR (75 MHz, CDCl₃): δ 164.6 (CO), 152.5 (C-6), 148.5 (C-8a), 145.4 (C-8'), 137.9 (C-1"), 134.5 (C-4'), 129.1 (CH-7'), 128.9, 128.2, 127.9 (CH-2" to CH-6"), 125.4 (CH-3'), 122.0 (C-4a), 116.4 (CH-7), 115.5 (CH-5), 114.7 (CH-8), 76.0 (C-2), 71.0 (OCH₂Ar), 68.4 (OCH₂CH₃), 61.1, (COOCH₂CH₃), 40.3 (CH₂-5'), 39.7 (CH₂-1'), 31.1 (CH₂-3), 25.4 (CH₂-6'), 24.5 (CH₃-11'), 22.8 (CH₂-4), 22.6 (CH₂-2'), 16.2 (CH₃-10'), 15.8 (COOCH₂CH₃), 14.9 (OCH₂CH₃). HREIMS m/z 492.2869 [M]⁺ (492.2875 calcd. for C₃₁H₄₀O₅) (100%).
- (15) Amans, D.; Bellosta, V.; Dacquet, C.; Ktorza, A.; Hennuyer, N.; Staels, B.; Caignard, D.-H.; Cossy, J. Synthesis and evaluation of new polyenic compounds as potential PPARs modulators. *Org. Biomol. Chem.* **2012**, *10*, 6169–6185.

Article 2: Synthesis and biological studies of “Polycerasoidol” and “trans- δ -Tocotrienolic acid” derivatives as PPAR α and/or PPAR γ agonists, *Bioorganic & Medicinal Chemistry*, 53 (2022) 116532.



Synthesis and biological studies of “Polycerasoidol” and “*trans*- δ -Tocotrienolic acid” derivatives as PPAR α and/or PPAR γ agonists

Laura Vila^{a,b}, Nuria Cabedo^{a,b,*}, Carlos Villarroel-Vicente^{a,b}, Ainhoa García^a, Álvaro Bernabeu^a, Nathalie Hennuyer^c, Bart Staels^c, Xavier Franck^d, Bruno Figadère^e, María-Jesús Sanz^b, Diego Cortes^{a,*}

^a Departamento de Farmacología, Facultad de Farmacia, Facultad de Medicina, Universidad de Valencia, Valencia, Spain

^b Institute of Health Research-INCLIVA, University Clinic Hospital of Valencia, Valencia, Spain

^c Univ Lille, Inserm, CHU Lille, Institut Pasteur de Lille, U-1011-EGID, F-59000 Lille, France

^d Normandie Univ, CNRS, INSA Rouen, UNIRIOUEN, COBRA (UMR6014 & FR 3038), 76000 Rouen, France

^e BioCIS, Université Paris-Sud, CNRS, Université Paris-Saclay, 92290 Châtenay-Malabry, France

ARTICLE INFO

Keywords:

2-Prenylated benzopyrans
Polycerasoidol analogs
Tocotrienol analogs
Grignard/Johnson-Claisen rearrangement
Wittig olefination
hPPAR activity

ABSTRACT

2-Prenylated benzopyrans represent a class of natural and synthetic compounds showing a wide range of significant activities. Polycerasoidol is a natural prenylated benzopyran isolated from the stem bark of *Polyalthia cerasoides* (Annonaceae) that exhibits dual PPAR α / γ agonism and an anti-inflammatory effect by inhibiting mononuclear leukocyte adhesion to the dysfunctional endothelium. Herein, we report the synthesis of three new series of prenylated benzopyrans containing one (series 1), two (series 2, “polycerasoidol” analogs) and three (series 3, “*trans*- δ -tocotrienolic acid” analogs) isoprenoid units in the hydrocarbon side chain at the 2-position of the chroman-6-ol (6-hydroxy-dihydrobenzopyran) scaffold. Isoprenoid moieties were introduced through a Grignard reaction sequence, followed by Johnson-Claisen rearrangement and subsequent Wittig olefination. hPPAR transactivation activity and the structure activity relationships (SAR) of eleven novel synthesized 2-prenylated benzopyrans were explored. PPAR transactivation activity demonstrated that the seven-carbon side chain analogs (series 1) displayed selectivity for hPPAR α , while the nine-carbon side chain analogs (polycerasoidol analogs, series 2) did so for hPPAR γ . The side chain elongation to 11 or 13 carbons (series 3) resulted in weak dual PPAR α / γ activation. Therefore, 2-prenylated benzopyrans of seven- and nine-carbon side chain (polycerasoidol analogs) are good lead compounds for developing useful candidates to prevent cardiovascular diseases associated with metabolic disorders.

1. Introduction

2-Prenylated benzopyrans represent a class of natural and synthetic compounds with significant biological activity, including hypocholesterolemic,^[1] antioxidant,^[1–3] anti-HIV,^[4] cytotoxic,^[5–7] antibacterial,^[7] and neuroprotective^[8] properties. The 2-prenylated benzopyran moiety, consisting in a chroman-6-ol ring linked with an isoprenoid side chain at the C-2 position, is limited to a few natural products.^[9] In 1995, we isolated the first members of a new class of 2-prenylated benzopyrans with a terminal carboxylic group, polycerasoidol and polycerasoidin, from the stem bark of *Polyalthia cerasoides* (Annonaceae) (Roxb.) Benth. & Hook.f. ex Bedd. and *P. sclerophylla* Hook.f. ex Thomson (Annonaceae) (Figure 1).^[10–11] We

have reported that polycerasoidol and its analogs are dual peroxisome proliferator-activated receptors (PPAR) α and γ agonists that displayed a potent anti-inflammatory effect by inhibiting mononuclear leukocyte adhesion to the dysfunctional endothelium.^[12] Structure-activity relationship (SAR) studies, together with a docking analysis of the polycerasoidol and semisynthetic analogs, revealed that the oxygenated atom at the C-6 position on the chromanol nucleus and the carboxylic acid at C-9' of the side chain act as key groups/atoms to optimally interact with PPAR α - and PPAR γ -binding domains.^[12] It is noticeable that the chroman-6-ol core is also present in the synthetic troglitazone, which is a dual PPAR α / γ agonist with a thiazolidinedione moiety capable of regulating lipid metabolism, insulin sensitivity, glucose homeostasis and atherosclerosis (Figure 1).^[13–14] Recently, we have also

* Corresponding authors at: Departamento de Farmacología, Facultad de Farmacia, Universidad de Valencia, 46100 Burjassot, Valencia, Spain (N. Cabedo).

E-mail addresses: ncabedo@uv.es (N. Cabedo), dcortes@uv.es (D. Cortes).

<https://doi.org/10.1016/j.bmc.2021.116532>

Received 29 September 2021; Received in revised form 9 November 2021; Accepted 23 November 2021

Available online 27 November 2021

0968-0896/© 2021 Elsevier Ltd. All rights reserved.

described the synthesis and hPPAR α/γ agonist activity of 2-prenylated benzopyrans bearing an original α -alkoxy- α,β -unsaturated ester instead of the carboxylic acid on the side chain [ACS Med Chem Lett 2021].

PPARs are ligand-activated transcription factors of the nuclear hormone receptor superfamily. Upon ligand activation, the PPAR-RXR heterodimer activate the transcription of the target genes involved in the control of lipid and carbohydrate metabolism.^[15] Consequently, PPARs have attracted much attention to be able to manage metabolic diseases, including metabolic syndrome, type 2 diabetes, atherogenic dyslipemia and non-alcoholic fat liver disease (NAFLD).^[15–16] PPARs are activated by a wide range of naturally occurring or metabolized lipids that derive from diet and/or result from metabolic pathways of fatty acids. Endogenous ligands include mainly saturated or unsaturated FA and FA-derived compounds, eicosanoids (e.g., leukotriene B4 and 8 (S)-HETE), phospholipids (e.g., azelaoyl phosphatidylcholine, 16:0/18:1 GPC) and certain prostaglandins (e.g., 15-deoxy- Δ 12,14-prostaglandin-J₂, prostaglandin PGJ₂).^[17] Fibrates, which are the most representative synthetic PPAR α agonists, are clinically used to treat dyslipidemia. They reduce triglycerides, increase plasma HDL-cholesterol (HDL-C) and can improve glucose homeostasis in prediabetic patients.^[16,18] Glitazones, also called thiazolidinediones (TZDs), are oral anti-diabetic PPAR γ agonists with beneficial effects on glucose homeostasis as they enhance insulin sensitivity.^[16,18] Both PPAR isotypes (α , γ) may have synergistic therapeutic effects to improve both glucose and lipid metabolism in patients with metabolic syndrome and/or type 2 diabetes.^[18–19] However, full PPAR γ activators have shown negative effects, including such as weight gain, fluid retention, bone fracture and cardiac hypertrophy. Therefore, there is a great interest to identify new partial PPAR γ agonists or PPAR γ modulators (PPAR γ Ms) lacking of adverse effects associated to full activation.^[15]

Given the structural similarity between the benzopyran core and the dual PPAR α/γ agonist troglitazone, we were encouraged to explore the PPAR activity of polycerasoidol and its analogs.^[12,20,21] Polycerasoidol contains a flexible linker which is a prenylated chain formed by two isoprenoid units connecting the polar head (carboxylic acid) and the hydrophobic tail (benzopyran nucleus) like most PPAR ligands, including endogenous ligands, fibrates and TZDs.^[17] *Trans*- δ -tocotrienolic acid (garcinoic acid) from *Garcinia kola* is structurally related to polycerasoidol, and a bioactive metabolite with anti-inflammatory properties that contains farnesyl isoprenoid moiety as an unsaturated hydrocarbon chain (Figure 1).^[22–23]

In order to expand the arsenal of PPAR agonists, we describe herein the synthesis and hPPAR transactivation activity of novel polycerasoidol analogs characterized by a variable linker length containing one (series 1), two (series 2) or three (series 3) isoprenoid units. We perform SAR studies between the prenylated benzopyrans bearing a side chain of seven-carbons (the shortest ones, series 1), nine-carbons (“polycerasoidol” analogs, series 2) and thirteen-carbons (“*trans*- δ -tocotrienolic acid”, series 3). Further modifications are also explored by varying the substituents in the phenolic group at the C-6 position (lipophilic tail), such as alkyloxy or aryloxy groups, as well as the carboxylic function on the isoprenoid side chain (polar head), such as ester and amide bioisosteres.

2. Results and discussion

2.1. Synthesis of 2-prenylated benzopyrans

2-Alkyl chromans (dihydrobenzopyrans) were prepared via a chroman-4-one scaffold, which is usually obtained by the aldol condensation between *ortho*-hydroxyacetophenones and ketones or aldehydes in the presence of a secondary amine (e.g., pyrrolidine, piperidine or morpholine) via enamino intermediate followed by oxa-Michael addition.^[1,20,21] Thus, the chroman-4-one or γ -benzopyrone skeleton was prepared in accordance with Pearce^[1] and Kabbe's method^[24] as briefly described in our previous report.^[20–21] The first key step involves a single condensation between the commercially available 2,5-dihydroxyacetophenone and an appropriate methyl ketone, the ethyl levulinate in the presence of pyrrolidine (Scheme 1). The obtained γ -benzopyrone **1** was reduced in one step to give the chroman-6-ol ring of the dihydrobenzopyran ester by Clemmensen conditions using dust zinc in acid medium. Subsequently, the phenolic hydroxyl group of dihydrobenzopyran was protected using propyl bromide in the presence of an appropriate base to afford *O*-propyloxy-dihydrobenzopyran **2** with a good yield.^[20–21] The aldehyde **4** intermediate was prepared by the controlled reduction of the ester function to give a good yield by using DIBAL-H reagent^[21] along with small amounts of the corresponding alcohol **3** which after pyridinium dichromate (PDC) oxidation could turn into aldehyde **4**.

By elongating the hydrocarbon side chain from aldehyde **4**, we achieved the synthesis of a series 1 of benzopyrans containing a flexible hydrocarbon linker length of seven-carbons. This elongation was

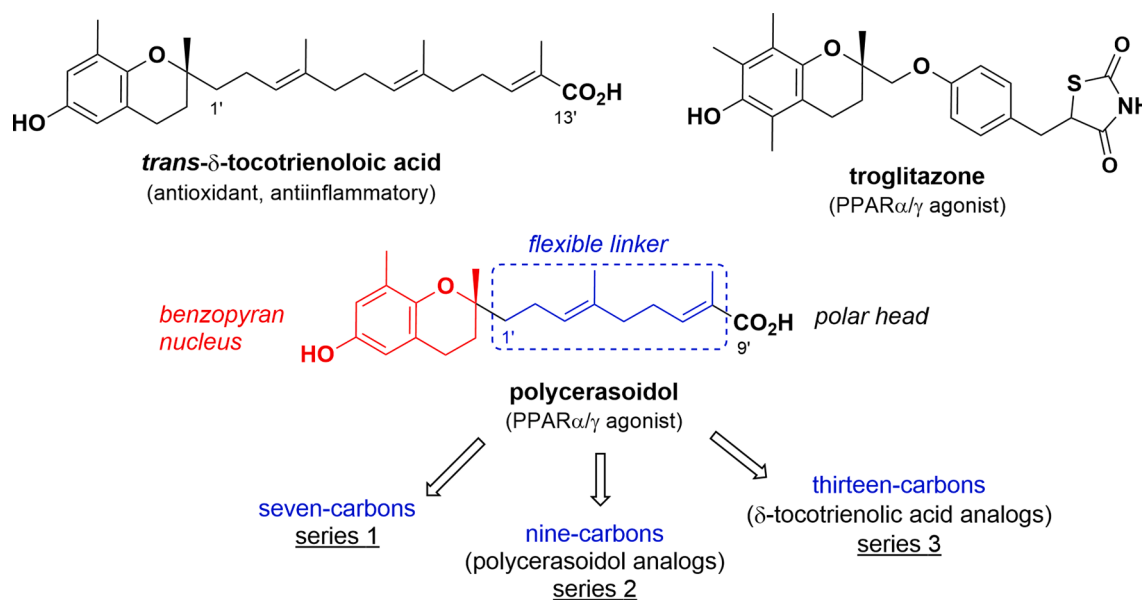
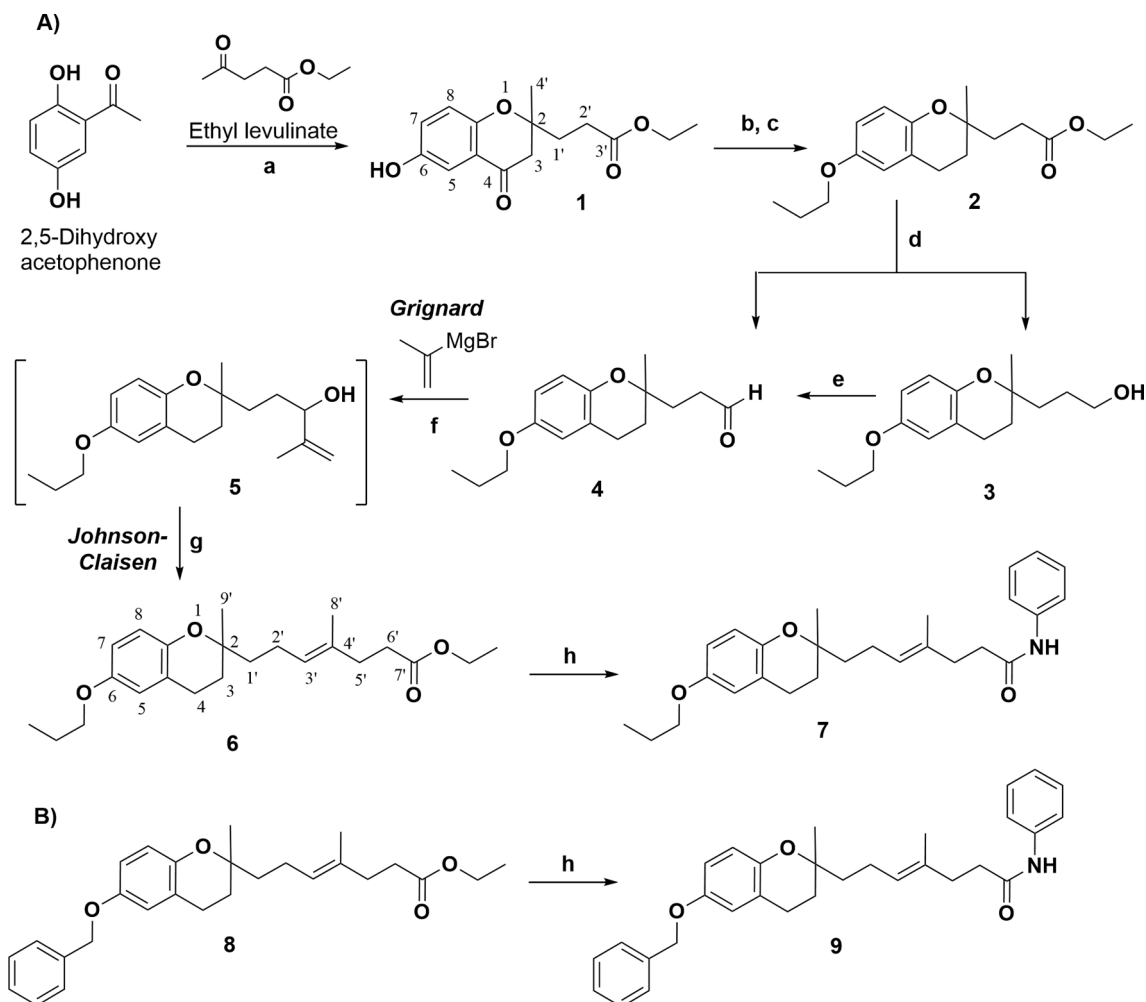


Figure 1. Bioactive prenylated benzopyrans.



Scheme 1. Synthesis of prenylated benzopyrans with seven-carbon side chain (6–9): Series 1. **Reagents and conditions:** (a) Pyrrolidine, EtOH, 60 °C, molecular sieve 3A, 24 h; (b) Zn / HCl, AcOH-H₂O, rt, 2 h; (c) PrBr, K₂CO₃, CH₃CN, reflux, 5 h; (d) DIBAL-H, CH₂Cl₂, –78 °C, N₂, 20 min; (e) PDC, CH₂Cl₂, reflux, 2 h; (f) THF, –78 °C, N₂, 60 min; (g) MeC(OEt)₃, isobutyric acid, 140 °C, 2 h; (h) KOH 20 %, MeOH, reflux, 2 h; SOCl₂ / CH₂Cl₂, reflux, 3 h; aniline, 4-DMAP, Et₃N, N₂, rt, overnight.

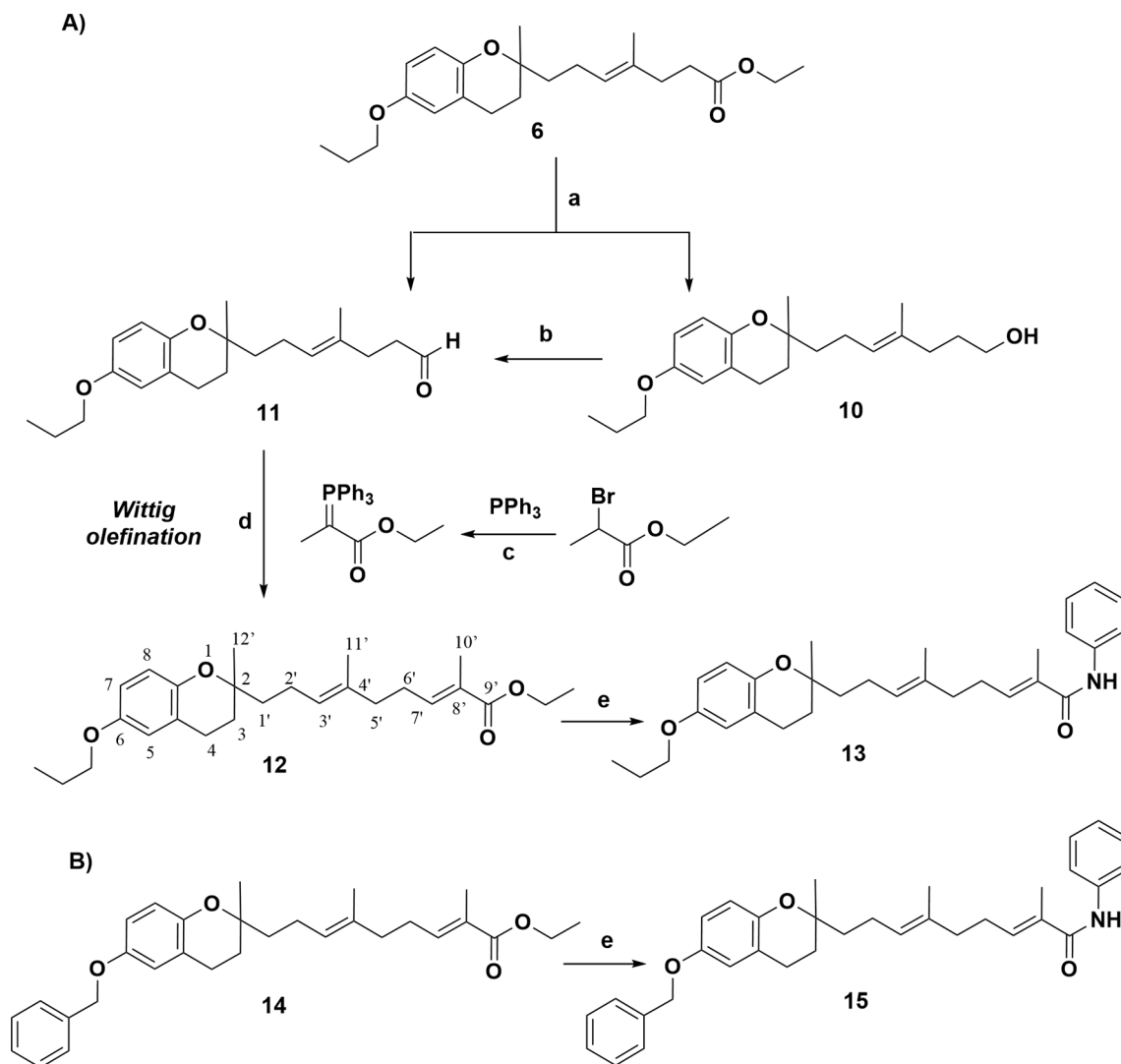
performed by an efficient Grignard reaction, followed by Johnson-Claisen rearrangement to obtain the desired 2-prenylated benzopyran 6.^[25] The Grignard reaction consisted in the nucleophilic attack of propenyl magnesium bromide to the electrophilic carbon of aldehyde intermediate 4 to form a carbon–carbon bond. Prenylated benzopyran ester 6 was prepared by Johnson-Claisen rearrangement, using allylic alcohol intermediate 5, which quickly reacted with 1,1,1-triethoxyethane and catalytic amounts of isobutyric acid (Scheme 1).

After saponification of ethyl ester 6 with basic conditions, the residue was treated with SOCl₂ at reflux to obtain the corresponding acid chloride intermediate, which was added dropwise to a solution of aniline in the presence of catalytic amounts of 4-DMAP and Et₃N to give amide 7. In order to explore the benzyloxy group *versus* the propyloxy substituent at the C-6 position on the chromanol ring, we prepared the corresponding 6-benzyloxybenzopyran homologs, ester 8 and amide 9, following the same procedure as described above for 6 and 7 (Scheme 1).

We designed the synthesis of a series 2 of benzopyrans containing a flexible hydrocarbon linker length of nine-carbons like polycerasoidol (Figure 1). Starting from *O*-propyloxy-benzopyran ester 6, we performed an initial controlled reduction using DIBAL-H^[21] to provide the key aldehyde 11, which was also provided by the oxidation of alcohol 10. The side chain of seven-carbons was elongated to synthesize 12 through Wittig olefination^[26] between aldehyde 11 and the ylide. For this

purpose, (carbethoxyethylidene) triphenylphosphorane was freshly prepared from 2-bromoethyl propanoate and triphenylphosphine. Then, aldehyde 11 was treated with the ylide to obtain the desired vinyl ester 12 (Scheme 2). By following the same procedure starting from *O*-benzyloxy ester 8, we prepared its homolog *O*-benzyloxy-benzopyran ester 14. Both polycerasoidol analogs 12 and 14 were reacted with aniline under the same conditions as those described above for compound 7 to obtain amide 13 and amide 15, respectively (Scheme 2).

The synthesis of series 3 was achieved from the benzopyrans containing a flexible hydrocarbon linker length of thirteen-carbons like *trans*- δ -tocotrienolic acid (Figure 1). As described above, aldehyde 11 was prepared by either a controlled reduction of ester 6 or the oxidation of alcohol 10. Aldehyde 11 was subjected to Grignard reaction by adding organomagnesium reagent, followed by Johnson-Claisen rearrangement using 1,1,1-triethoxyethane to provide the benzopyran ester 17 bearing an eleven-carbon side chain. A controlled reduction of 17 with DIBAL-H resulted in aldehyde intermediate 19, which was also obtained by the oxidation of alcohol 18. The side chain was elongated via Wittig olefination between aldehyde 19 and the (carbethoxyethylidene)triphenylphosphorane to give the desired vinyl ester 20 as the “*trans*- δ -tocotrienolic acid” analog (Scheme 3). Saponification of 20 with KOH, followed by the preparation of acid chloride by SOCl₂ and its treatment with aniline, gave *O*-propyloxy benzopyran amide 21 according to the same procedure reported for the synthesis of compound 7



Scheme 2. Synthesis of prenylated benzopyrans as “polycerasoidol” analogs (12–15): Series 2. **Reagents and conditions:** (a) DIBAL-H, CH_2Cl_2 , -78°C , N_2 , 20 min; (b) PDC, CH_2Cl_2 , reflux, 2 h; (c) AcOEt, reflux, 5 h; NaOH, EtOH, 20 min; (d) THF, rt, N_2 , 24 h; (e) KOH 20 %, reflux, 2 h; $\text{SOCl}_2/\text{CH}_2\text{Cl}_2$, reflux, 3 h; aniline, 4-DMAP, Et_3N , N_2 , rt, overnight.

(Scheme 3).

2.2. PPAR α and PPAR γ agonist activity

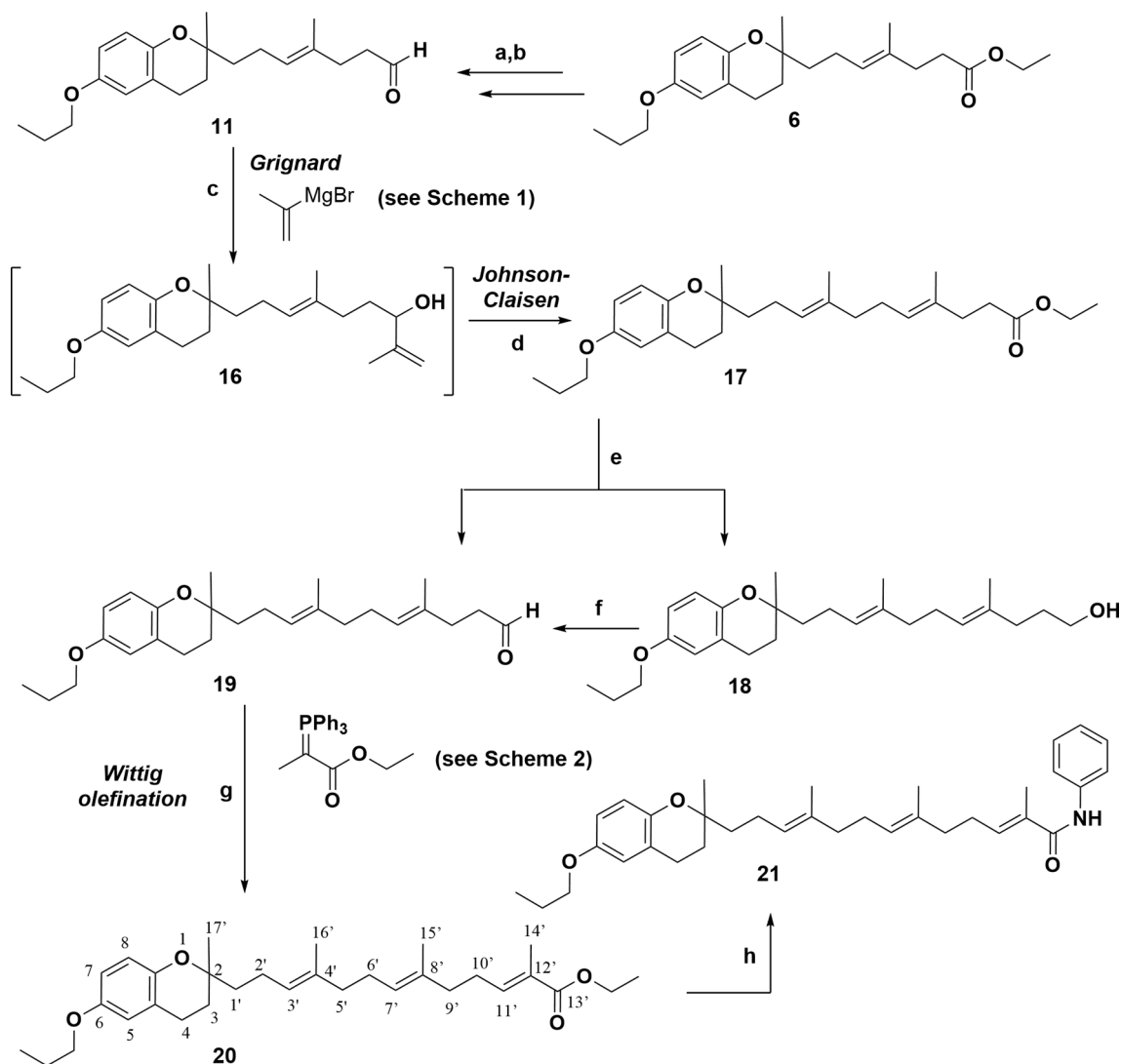
All the synthesized compounds were assayed *in vitro* for hPPAR α and hPPAR γ transactivation activity by means of an established cell-based transcription assay in Cos-7 cells transiently transfected with a luciferase-reported plasmid in the presence of expression vectors pGAL4hPPAR α and pGAL4hPPAR γ .^[12,20,21,27] The synthesized compounds were tested at the 10 μM dose and compared to the reference compounds such as WY-14,643 at 10 μM and rosiglitazone at 1 μM for hPPAR α and hPPAR γ , respectively. The activating efficacy of compounds was calculated as the maximal transactivation response, expressed as a percentage of the maximum activity of the reference compounds for each receptor subtype (Figure 2). Natural polycerasoidol showed full agonist activity for both hPPAR α and hPPAR γ , exhibiting the maximal transactivation percentage (107% and 95% for hPPAR α and hPPAR γ , respectively).^[13] The benzopyrans containing a shorter side chain of seven-carbons (series 1: 6–9) (series 1, Scheme 1) were able to activate both hPPAR α and γ isotypes. It is noteworthy that the *O*-benzyloxy-ester **8** displayed a full agonism for hPPAR α with high selectivity (123 % and 38% for α and γ , respectively). By contrast, the

polycerasoidol analogs (series 2, Scheme 2) containing a side chain of nine-carbons, ester **12** (61 %, ester) and principally amide **15** (73 %), showed the highest efficacy for PPAR γ . Finally, long-chain derivatives, such as the *trans*- δ -tocotrienolic acid analogs (series 3, Scheme 3) containing a side chain of eleven- or thirteen-carbons, showed weak dual PPAR α/γ agonism (Figure 2).

In order to provide a structural understanding of how benzopyran **15** and **8** activate PPAR γ and PPAR α , respectively, we carried out molecular docking analysis. Compound **15**/PPAR γ complex showed a nearby spatial location to the natural polycerasoidol, which was previously reported.^[12] Compound **15** showed a hydrogen bond between nitrogen of amide group and Cys285, and also strong interactions with Tyr473, Tyr327, Leu330 and Ile 341 of PPAR γ (Figure 3A). Benzopyran **8**/PPAR α complex exhibited strong interactions with Ala333, Ser280, Thr283, Tyr314 and His440. This analysis indicated that molecule **8** adopted a spatial ordering slightly different than polycerasoidol for PPAR α (Figure 3B).^[12]

3. Conclusion

Herein, we efficiently prepared three series of prenylated benzopyrans with a sequence of reactions, including Grignard reaction



Scheme 3. Synthesis of prenylated benzopyrans as “*trans*- δ -tocotrienoloic acid” analogs (**20**, **21**): Series 3. **Reagents and conditions:** (a) DIBAL-H, CH_2Cl_2 , -78°C , N_2 , 20 min; (b) PDC, CH_2Cl_2 , reflux, 2 h; (c) THF, -78°C , N_2 , 60 min.; (d) $\text{MeC}(\text{OEt})_3$, isobutyric acid, 140°C , 2 h; (e) DIBAL-H, CH_2Cl_2 , -78°C , N_2 , 20 min; (f) PDC, CH_2Cl_2 , reflux, 2 h; (g) THF, rt, N_2 , 24 h; (h) KOH 20 %, reflux, 2 h; $\text{SOCl}_2/\text{CH}_2\text{Cl}_2$, reflux, 3 h; aniline, 4-DMAP, Et_3N , N_2 , rt, overnight.

followed by Johnson-Claisen rearrangement, as well as Wittig olefination with (carbethoxyethylidene) triphenylphosphorane to introduce one, two or three prenylated moieties in the side chain. Seven-carbon side chain analogs like **8** (series 1), displayed selectivity for hPPAR α . By contrast, nine-carbon side chain analogs, like **15** (series 2), showed high efficacy to activate hPPAR γ without raising a full agonism and probably avoiding adverse effects. Therefore, these novel molecules are good lead compounds for developing useful candidates to prevent cardiovascular diseases associated with metabolic disorders.

4. Experimental section

4.1. General instrumentation

EIMS and HREIMS, were recorded on a VG Auto Spec Fisons spectrometer instruments. Liquid chromatography with mass spectrometry detection (LC-MSD) with API (atmospheric pressure ionization) source configured as APIES (electrospray ionisation) in positive or negative mode were determined on a Hewlett-Packard (HP-1100). Liquid chromatography-mass spectrometry detection was performed on a liquid chromatography UHPLC apparatus (Shimadzu, LCMS-8040) coupled to a tandem mass spectrometry (MS/MS) triple quadrupole

equipped with electrospray ionization (ESI) ion source (Shimadzu, Kyoto, Japan). ^1H NMR and ^{13}C NMR spectra were recorded with CDCl_3 as solvent on a Bruker AC-300, AC-400 or AC-500. Multiplicities of ^{13}C NMR resonances were assigned by DEPT experiments. The assignments in proton and carbon NMR were made by COSY 45, HSQC and HMBC correlations recorded at 400 or 500 MHz. All reactions were monitored by analytical TLC with silica gel 60 F254 (Merck 5554). The residues were purified through 60H silica gel column (5–40 μm , Merck 7736) and by flash chromatography (230–400 μm , Merck 9385). Solvents and reagents were used as purchased from commercial sources. Quoted yields are of purified material.

4.2. General procedure for synthesis of prenylated benzopyrans **1** and **2**

2-(Ethylpropanoate)-6-hydroxy-2-methyldihydrobenzopyran-4-one (**1**) and 2-(ethylpropanoate)-2-methyl-6-propoxydihydrobenzopyran (**2**) were prepared from 2,5-dihydroxy acetophenone and ethyl levulinate as previously described.^[20–21]

4.3. General procedure for synthesis of alcohol **3** and aldehyde **4**

A solution of (250 mg, 0.816 mmol) of **2** in anhydrous CH_2Cl_2 (10

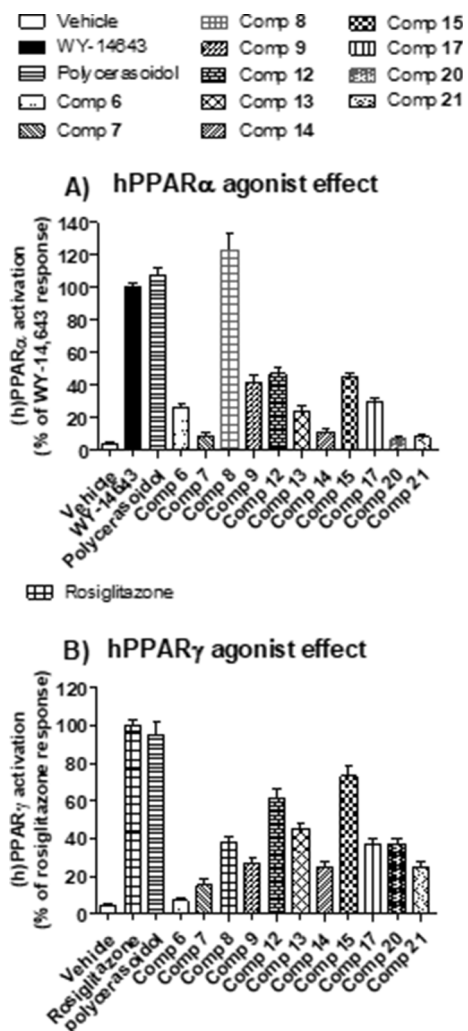


Figure 2. *In vitro* hPPAR α (A) and hPPAR γ activation (B) for active benzopyrans at 10 μ M. Results refer to the maximal PPAR fold activation of each compound relative to the maximum activation of reference compounds, WY-14,643 (10 μ M) and rosiglitazone (1 μ M), which corresponded to 100% in GAL4 chimeric hPPAR α and hPPAR γ system.

mL) at -78°C under nitrogen atmosphere was stirred for 10 min. To this solution was added dropwise 4.4 mL of 1.0 M DIBAL-H solution in THF. After 20 min, the mixture was quenched by addition of 5 mL of MeOH and 10 mL of halfsat aqueous NH_4Cl solution. The reaction mixture was stirred for additional 10 min at room temperature and concentrated in vacuo. Then, water was added and extracted with EtOAc. The combined organic layers were washed with water, dried over anhydrous Na_2SO_4 and evaporated to dryness. The residue was purified by silica gel column chromatography (hexane/EtOAc, 90:10) to afford 80 mg of the corresponding alcohol **3** (35%) and 120 mg of the aldehyde **4** (53%).^[21] Alcohol **3** (80 mg, 0.303 mmol) in anhydrous CH_2Cl_2 (4 mL) was treated with pyridinium dichromate (PDC) (230 mg, 0.611 mmol). The reaction mixture was stirred under reflux for 2 h. The mixture was diluted with diethyl ether and filtered through a pad of silica gel. The filtrate was concentrated under reduced pressure, and the crude purified as above described to give 71 mg of aldehyde **4** (89%) as a colorless oil.

2-Methyl-2-propanol-6-propoxydihydrobenzopyran (3): ^1H NMR (300 MHz, CDCl_3): δ_{H} 6.63 (m, 3H, H-5, 7, 8), 3.83 (t, $J = 6.6$ Hz, 2H, $\text{OCH}_2\text{CH}_2\text{CH}_3$), 3.65 (m, 2H, CH_2 -3'), 2.74 (m, 2H, CH_2 -4), 1.72 (m, 8H, CH_2 -1', CH_2 -2', CH_2 -3, $\text{OCH}_2\text{CH}_2\text{CH}_3$), 1.27 (s, 3H, CH_3 -4'), 1.01 (t, $J = 7.3$ Hz, 3H, CH_3); ^{13}C NMR (75 MHz, CDCl_3): δ_{C} 152.4 (C-6), 147.8 (C-8a), 121.5 (C-4a), 117.5 (CH-7), 114.7 (CH-5), 114.0 (CH-8), 75.5 (C-2),

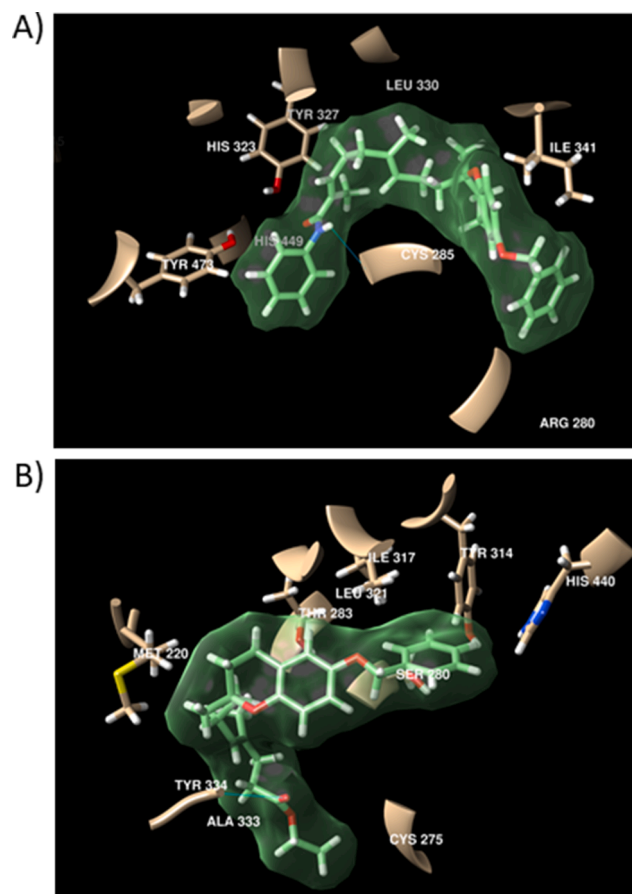


Figure 3. Spatial view obtained for the benzopyran **15**/PPAR γ complex (A) and **8**/PPAR α complex (B). Molecules **15** and **8** are depicted in green, and the hydrogen bonds established with the different amino acids in these conformations are also shown. Benzopyran **15** establishes strong hydrogen bond interactions with Cys285, Tyr473, Tyr327, Leu330 and Ile 341 of PPAR γ , while benzopyran **8** establishes strong hydrogen bond interactions with Ala333, Ser280, Thr283, Tyr314 and His440 of PPAR α . (For interpretation of the references to colour in this figure legend, the reader is referred to the web version of this article.)

70.0 ($\text{OCH}_2\text{CH}_2\text{CH}_3$), 63.1 (CH_2 -3'), 35.8 (CH_2 -2'), 31.2 (CH_2 -3), 26.8 (CH_2 -1'), 24.3 (CH_3 -4'), 22.6 ($\text{OCH}_2\text{CH}_2\text{CH}_3$), 22.3 (CH_2 -4), 10.9 ($\text{OCH}_2\text{CH}_2\text{CH}_3$). MS (ESI) m/z : 265 [$\text{M} + \text{H}$] $^+$.

2-Methyl-2-propanal-6-propoxydihydrobenzopyran (4): ^1H NMR (300 MHz, CDCl_3): δ_{H} 9.73 (s, CHO), 6.67 (m, 3H, H-5, H-7, H-8), 3.84 (t, $J = 6.6$ Hz, 2H, $\text{OCH}_2\text{CH}_2\text{CH}_3$), 2.76 (m, 2H, CH_2 -4), 2.60 (m, 2H, CH_2 -2'), 2.02, 1.89 (m, 2H, CH_2 -1'), 1.77 (m, 4H, CH_2 -3, $\text{OCH}_2\text{CH}_2\text{CH}_3$), 1.25 (s, 3H, CH_3 -4'), 1.01 (t, $J = 7.3$ Hz, 3H, CH_3); ^{13}C NMR (75 MHz, CDCl_3): δ_{C} 202.3 (CHO), 152.6 (C-6), 147.2 (C-8a), 121.2 (C-4a), 117.6 (CH-7), 114.7 (CH-5), 114.2 (CH-8), 74.5 (C-2), 70.0 ($\text{OCH}_2\text{CH}_2\text{CH}_3$), 38.4 (CH_2 -2'), 31.7 (CH_2 -1'), 31.2 (CH_2 -3), 23.7 (CH_3 -4'), 22.6 ($\text{OCH}_2\text{CH}_2\text{CH}_3$), 22.2 (CH_2 -4), 10.5 ($\text{OCH}_2\text{CH}_2\text{CH}_3$); MS (ESI) m/z : 263 [$\text{M} + \text{H}$] $^+$.

5. General procedure for synthesis of Seven-Carbons side chain prenylated Benzopyrans: Compounds 6–9 (series 1)

A mixture of aldehyde **4** (300 mg, 1.14 mmol) and 13.7 mL of 0.5 M isopropenylmagnesium bromide solution (6.84 mmol) in THF (30 mL) at -78°C was stirred for 1 h under nitrogen atmosphere. The resulting mixture reaction was quenched by addition of halfsat aqueous NH_4Cl solution. The reaction was stirred for 15 min at room temperature. Then, water was added and extracted with ethyl acetate. The combined

organic layers were washed with water, dried with anhydrous Na_2SO_4 and evaporated to dryness. The residue obtained, 174 mg of **5** (not isolated), was directly treated with 10 mL of triethylorthoacetate and a catalytic amount of isobutyric acid. The mixture was stirred at 140 °C for 2 h, and then, cooled and concentrated under reduced pressure to remove the excess of ethylorthoacetate. The residue diluted with hexane, and successively washed with water, dried over anhydrous Na_2SO_4 and concentrated in vacuo. The residue was purified by silica gel column chromatography (hexane/EtOAc, 80:20) to afford 135 mg of benzopyran **6** (31.6 %). Amide **7** was obtained from **6** (100 mg, 0.27 mmol) by KOH 20% solution at reflux for 2 h and SOCl_2 (0.15 mL, 2.06 mmol) in anhydrous CH_2Cl_2 refluxed for 3 h. Then, the solvent was removed to obtain quantitatively the acid chloride which was used in the next step without further purification. The crude of acid chloride in dry CH_2Cl_2 (1 mL) was added dropwise to a solution of aniline (32 μL , 0.35 mmol), 4-DMAP (2.4 mg, 0.02 mmol) and Et_3N (19 μL , 0.14 mmol) under N_2 atmosphere and in a cooling ice bath. After stirring at room temperature for 1 h, 5% aq HCl (1.5 mL) solution was added and extracted with CH_2Cl_2 . The organic layer was washed with 5% aq NaHCO_3 solution, brine, water, dried and the solvent was removed under reduced pressure to give 23 mg of amide **7** (37.5 %) as a colorless oil. The 6-benzylated homologs of type **6**, compounds **8** and **9** were prepared according to the procedure for the synthesis of **6** and **7**.

2-Methyl-2-((4'-methyl)ethylhept-3'-enoate)-6-propoxydihydrobenzopyran (6). ^1H NMR (300 MHz, CDCl_3): δ_{H} 6.67 (m, 3H, H-5, 7, 8), 5.15 (t, J = 7 Hz, 1H, CH-3'), 4.11 (q, J = 7.2 Hz, 2H, OCH_2CH_3), 3.84 (t, J = 6.6 Hz, 2H, $\text{OCH}_2\text{CH}_2\text{CH}_3$), 2.72 (t, J = 6.6 Hz, 2H, CH₂-4), 2.32 (m, 4H, CH₂-5', CH₂-6'), 2.09 (q, J = 7.8 Hz, 2H, CH₂-2'), 1.68 (m, 6H, CH₂-3, $\text{OCH}_2\text{CH}_2\text{CH}_3$, CH₂-1'), 1.61 (s, 3H, CH₃-8'), 1.26 (s, 3H, CH₃-9'), 1.24 (t, J = 7.2 Hz, 3H, OCH_2CH_3), 1.01 (t, J = 7.3 Hz, 3H, $\text{OCH}_2\text{CH}_2\text{CH}_3$); ^{13}C NMR (75 MHz, CDCl_3): δ_{C} 173.3 (CO), 152.3 (C-6), 147.7 (C-8a), 133.4 (C-4'), 124.9 (CH-3'), 121.4 (C-4a), 117.6 (CH-7), 114.7 (CH-5), 114.0 (CH-8), 75.3 (C-2), 70.0 ($\text{OCH}_2\text{CH}_2\text{CH}_3$), 60.1 (OCH_2CH_3), 39.1 (CH₂-1'), 34.6 (CH₂-5'), 34.5 (CH₂-6'), 33.1 (CH₂-3), 24.0 (CH₃-9'), 22.6 (CH₂-4), 22.3 ($\text{OCH}_2\text{CH}_2\text{CH}_3$, CH₂-2'), 15.7 (CH₃-8'), 14.1 (OCH_2CH_3), 10.4 ($\text{OCH}_2\text{CH}_2\text{CH}_3$); HREIMS m/z 375.5233 [$\text{M} + \text{H}$]⁺ (375. 5216, calcd. for $\text{C}_{23}\text{H}_{35}\text{O}_4$).

2-Methyl-2-((4'-methyl)-N-phenylhept-3'-enamide)-6-propoxydihydrobenzopyran (7). ^1H NMR (300 MHz, CDCl_3): δ_{H} 7.47 (d, J = 7.8 Hz, 2H, H-2'', 6''), 7.30 (t, J = 7.8 Hz, 2H, H-3'', 5''), 7.09 (t, J = 7.4 Hz, 1H, H-4''), 6.70 (m, 3H, H-5, H-7, H-8), 5.25 (t, J = 7 Hz, 1H, CH-3'), 3.84 (t, J = 6.6 Hz, 2H, $\text{OCH}_2\text{CH}_2\text{CH}_3$), 2.73 (t, J = 6.6 Hz, 2H, CH₂-4), 2.38 (m, 4H, CH₂-5', CH₂-6'), 2.12 (q, J = 7.8 Hz, 2H, CH₂-2'), 1.75 (m, 4H, CH₂-3, $\text{OCH}_2\text{CH}_2\text{CH}_3$), 1.65 (s, 3H, CH₃-8'), 1.58 (m, 2H, CH₂-1'), 1.27 (s, 3H, CH₃-9'), 1.01 (t, J = 7.3 Hz, 3H, $\text{OCH}_2\text{CH}_2\text{CH}_3$); ^{13}C NMR (75 MHz, CDCl_3): δ_{C} 173.7 (CO), 152.4 (C-6), 147.7 (C-8a), 137.8 (C-1'), 133.7 (C-4'), 129.3 (C-3', 5'), 129.0 (C-4'), 125.8 (C-3'), 121.6 (C-4a), 117.6 (CH-7), 115.1 (CH-5), 114.8 (CH-8), 75.4 (C-2), 70.1 ($\text{OCH}_2\text{CH}_2\text{CH}_3$), 39.1 (CH₂-1'), 36.2 (CH₂-6'), 35.1 (CH₂-5'), 31.1 (CH₂-3), 24.1 (CH₃-9'), 22.7 (CH₂-4), 22.2, 22.4 ($\text{OCH}_2\text{CH}_2\text{CH}_3$) and (CH₂-2'), 15.9 (CH₃-8'), 10.5 ($\text{OCH}_2\text{CH}_2\text{CH}_3$); HREIMS m/z 421.2620 [M]⁺ (421.2457 calcd. for $\text{C}_{27}\text{H}_{35}\text{NO}_3$).

6-Benzylxy-2-methyl-2-((4'-methyl)ethylhept-3'-enoate)-dihydrobenzopyran (8). ^1H NMR (400 MHz, CDCl_3): δ_{H} 7.35 (m, 5H, H-2' to H-6'), 6.72 (m, 3H, H-5, H-7, H-8), 5.20 (t, J = 7 Hz, 1H, CH-3'), 4.99 (s, 2H, OCH_2Ar), 4.11 (q, J = 7.4 Hz, 2H, OCH_2CH_3), 2.75 (t, J = 6.7 Hz, 2H, CH₂-4), 2.38 (m, 4H, CH₂-6', CH₂-5'), 2.09 (m, 2H, CH₂-2'), 1.68 (m, 4H, CH₂-3, CH₂-1'), 1.61 (s, 3H, CH₃-8'), 1.27 (s, 3H, CH₃-9'), 1.23 (t, J = 7.3 Hz, 3H, OCH_2CH_3); ^{13}C NMR (100 MHz, CDCl_3): δ_{C} 173.4 (CO), 152.1 (C-6), 148.1 (C-8a), 137.5 (C-1''), 133.5 (C-4'), 128.5, 127.8, 127.4 (CH-2'' to CH-6''), 125.0 (CH-3'), 121.6 (C-4a), 117.7 (CH-7), 115.1 (CH-5), 114.4 (CH-8), 75.5 (C-2), 70.6 (OCH_2Ar), 60.2 (OCH_2CH_3), 39.2 (CH₂-1'), 34.6 (CH₂-6'), 33.2 (CH₂-5'), 30.9 (CH₂-3), 24.1 (CH₃-9'), 22.3 (CH₂-4), 22.1 (CH₂-2'), 15.8 (CH₃-8'), 14.2 (OCH_2CH_3); HREIMS m/z 422.2473 [M]⁺ (422.2457 calcd. for $\text{C}_{27}\text{H}_{34}\text{O}_4$).

6-Benzylxy-2-methyl-2-((N-phenyl(4'-methyl)hept-3'-enamide)-dihydrobenzopyran (9). ^1H NMR (400 MHz, CDCl_3): δ_{H} 7.47 (d, J = 7.8 Hz, 2H, H-2'', 6''), 7.36 (m, 8H, H-3'' to H-5'' and H-2' to H-6'), 6.72 (m, 3H, H-5, H-7, H-8), 5.26 (t, J = 6.8 Hz, 1H, CH-3'), 4.96 (s, 2H, OCH_2Ar), 2.73 (t, J = 6.8 Hz, 2H, CH₂-4), 2.42 (m, 4H, CH₂-5', 6'), 2.14 (m, 2H, CH₂-2'), 1.70 (m, 4H, CH₂-3, CH₂-1'), 1.65 (s, 3H, CH₃-8'), 1.27 (s, 3H, CH₃-9'); ^{13}C NMR (100 MHz, CDCl_3): δ_{C} 170.9 (CO), 152.1 (C-6), 148.0 (C-8a), 137.9, 137.5 (C-1'', C-1'''), 133.7 (C-4'), 128.9–125.7 (CH-Ar), 124.2 (CH-3'), 121.7 (C-4a), 119.7 (CH-2'', 6''), 117.7 (CH-7), 115.2 (CH-5), 114.4 (CH-8), 75.5 (C-2), 70.6 (OCH_2Ar), 39.2 (CH₂-1'), 36.2 (CH₂-6'), 35.0 (CH₂-5'), 31.0 (CH₂-3), 24.2 (CH₃-9'), 22.5 (CH₂-4), 22.2 (CH₂-2'), 15.9 (CH₃-8'); HREIMS m/z 469.2596 [M]⁺ (469.2616 calcd. for $\text{C}_{31}\text{H}_{35}\text{NO}_3$).

5.0.1. General procedure for synthesis of nine-carbon side chain prenylated benzopyrans: "polycerasoidol" analogs **12–15** (series 2)

Alcohol **10** and aldehyde **11**, obtained by controlled reduction from ethyl-ester **6**, were prepared according to the procedure for the synthesis of **3** and **4**. For Wittig olefination the carbethoxyethylidene triphenylphosphorane was previously prepared. For this purpose, triphenylphosphine dissolved was dissolved in ethyl acetate, and then splashed into 2-bromoethyl propanoate under room temperature at reflux for 5 h. The obtained white solid was dissolved in EtOH and treated with 20% NaOH during 20 min, to obtain carbethoxyethylidene triphenylphosphorane. The aldehyde **11** (200 mg, 0.60 mmol) was added to a solution of the ylide (350 mg, 0.97 mmol) in THF under N_2 atmosphere. The reaction was stirred for 24 h at room temperature. Then, water was added and extracted with ethyl acetate. The organic layer was washed with 5% aq NaHCO_3 solution, brine, water, dried and the solvent was removed under reduced pressure. The residue was purified via silica gel column chromatography (hexane/EtOAc, 85:15) to afford 237 mg of ethyl-ester polycerasoidol analog **12** (54.5%) as a colorless oil. The 6-benzylated homolog **14** was prepared according to the same procedure for the synthesis of **12** above. The corresponding amides **13** and **15** were prepared according to the procedure for the synthesis of **7** (Scheme 2).

2-Methyl-2-((4'-methyl)hept-3'-enol)-6-propoxydihydrobenzopyran (10). ^1H NMR (500 MHz, CDCl_3): δ_{H} 6.63 (m, 3H, H-5, 7, 8), 5.14 (t, J = 6.5 Hz, 1H, H-3'), 3.82 (t, J = 6.4 Hz, 2H, $\text{OCH}_2\text{CH}_2\text{CH}_3$), 3.59 (t, J = 6.5 Hz, 2H, CH₂-7'), 2.70 (t, J = 6.8 Hz, 2H, CH₂-4), 2.07 (m, 2H, CH₂-2'), 2.02 (t, J = 7.4 Hz, 2H, CH₂-5'), 1.75 (m, 4H, CH₂-3, $\text{OCH}_2\text{CH}_2\text{CH}_3$), 1.63 (m, 4H, CH₂-1, CH₂-6), 1.58 (s, 3H, CH₃-8'), 1.25 (s, 3H, CH₃-9'), 0.99 (t, J = 7.4 Hz, 3H, $\text{OCH}_2\text{CH}_2\text{CH}_3$); ^{13}C NMR (125 MHz, CDCl_3): δ_{C} 152.4 (C-6), 147.8 (C-8a), 133.4 (C-4'), 124.6 (CH-3'), 121.5 (C-4a), 117.6 (CH-7), 114.7 (CH-5), 114.0 (CH-8), 75.5 (C-2), 70.1 ($\text{OCH}_2\text{CH}_2\text{CH}_3$), 62.7 (CH₂-7'), 39.2 (CH₂-1'), 35.8 (CH₂-6'), 30.9 (CH₂-3), 30.6 (CH₂-5'), 24.0 (CH₃-9'), 22.6 (CH₂-4), 22.3 ($\text{OCH}_2\text{CH}_2\text{CH}_3$), 22.0 (CH₂-2'), 15.7 (CH₃-8'), 10.4 ($\text{OCH}_2\text{CH}_2\text{CH}_3$); MS (ESI) m/z 333 [$\text{M} + \text{H}$]⁺.

2-Methyl-2-((4'-methyl)hept-3'-enal)-6-propoxydihydrobenzopyran (11). ^1H NMR (400 MHz, CDCl_3): δ_{H} 6.65 (m, 3H, H-5, 7, 8), 5.15 (t, J = 6.5 Hz, 1H, H-3'), 3.84 (dd, J = 6.6 Hz, 2H, $\text{OCH}_2\text{CH}_2\text{CH}_3$), 2.73 (t, J = 6.8 Hz, 2H, CH₂-4), 2.50 (t, J = 6.5 Hz, 2H, CH₂-6'), 2.30 (t, J = 7.4 Hz, 2H, CH₂-5'), 2.10 (dq, J = 7.4 Hz, 1.6 Hz, 2H, CH₂-2'), 1.78 (m, 6H, CH₂-3, $\text{OCH}_2\text{CH}_2\text{CH}_3$, CH₂-1'), 1.57 (s, 3H, CH₃-8'), 1.27 (s, 3H, CH₃-9'), 1.01 (t, J = 7.4 Hz, 3H, CH₃); ^{13}C NMR (100 MHz, CDCl_3): δ_{C} 202.5 (CHO), 152.4 (C-6), 147.8 (C-8a), 133.1 (C-4'), 125.3 (CH-3'), 121.6 (C-4a), 117.7 (CH-7), 114.8 (CH-5), 114.1 (CH-8), 75.4 (C-2), 70.1 ($\text{OCH}_2\text{CH}_2\text{CH}_3$), 42.1 (CH₂-6'), 39.2 (CH₂-1'), 31.7 (CH₂-5'), 31.1 (CH₂-3), 24.1 (CH₃-9'), 22.7 (CH₂-4), 22.4 ($\text{OCH}_2\text{CH}_2\text{CH}_3$), 22.2 (CH₂-2'), 16.0 (CH₃-8'), 10.5 ($\text{OCH}_2\text{CH}_2\text{CH}_3$); HREIMS m/z 330.2247 [M]⁺ (330.2194 calcd. for $\text{C}_{21}\text{H}_{30}\text{O}_3$).

2-((4',8'-Dimethyl)ethylnonan-3',7'-dienoate)-2-methyl-6-propoxydihydrobenzopyran (12). ^1H NMR (400 MHz, CDCl_3): δ_{H} 6.70 (m, 1H, H-7'), 6.65 (m, 3H, H-7, 8), 6.60 (m, 3H, H-5), 5.15 (t, J = 7.2 Hz, 1H, H-3'),

4.17 (q, $J = 7.1$ Hz, 2H, OCH_2CH_3), 3.84 (t, $J = 6.6$ Hz, 2H, $\text{OCH}_2\text{CH}_2\text{CH}_3$), 2.73 (t, $J = 6.8$ Hz, 2H, CH_2 -4), 2.25 (q, $J = 7.5$ Hz, 2H, CH_2 -6'), 2.09 (m, 4H, CH_2 -2', 5'), 1.81 (d, $J = 1.2$ Hz, 3H, CH_3 -10'), 1.74 (m, 6H, CH_2 -3, $\text{OCH}_2\text{CH}_2\text{CH}_3$, CH_2 -1'), 1.60 (s, 3H, CH_3 -11'), 1.28 (t, $J = 7.2$ Hz, 3H, $\text{OCH}_2\text{CH}_2\text{CH}_3$), 1.27 (s, 3H, CH_3 -12'), 1.01 (t, $J = 7.4$ Hz, 3H, $\text{OCH}_2\text{CH}_2\text{CH}_3$); ^{13}C NMR (100 MHz, CDCl_3): δ_{C} 168.2 (CO), 152.4 (C-6), 147.8 (C-8a), 141.8 (CH-7'), 134.1 (C-4'), 127.8 (C-8'), 124.3 (CH-3'), 121.6 (C-4a), 117.7 (CH-7), 114.8 (CH-5), 114.1 (CH-8), 75.5 (C-2), 70.1 ($\text{OCH}_2\text{CH}_2\text{CH}_3$), 60.4 (OCH_2CH_3), 39.2 (CH_2 -1'), 38.2 (CH_2 -5'), 31.1 (CH_2 -3), 27.3 (CH_2 -6'), 24.2 (CH_3 -12'), 22.7 (CH_2 -4), 22.5 ($\text{OCH}_2\text{CH}_2\text{CH}_3$), 22.2 (CH_2 -2'), 15.9 (CH_3 -11'), 14.3 (OCH_2CH_3), 12.4 (CH_3 -10'), 10.6 ($\text{OCH}_2\text{CH}_2\text{CH}_3$); HREIMS m/z 414.2768 $[\text{M}]^+$ (414.2770 calcd. for $\text{C}_{26}\text{H}_{38}\text{O}_4$).

2-Methyl-2-((4',8'-dimethyl)-N-phenylnona-3',7'-dienamide)-6-propoxy-dihydro-benzopyran (13): ^1H NMR (300 MHz, CDCl_3): δ_{H} 7.52 (d, $J = 8.2$ Hz, 2H, H-2'', 6''), 7.36 (t, 2H, $J = 8.2$ Hz, H-3'', 5''), 7.12 (t, $J = 8.2$ Hz, 1H, H-4''), 6.72 (m, 3H, H-5, H-7, H-8), 6.38 (dt, $J = 7.1$ Hz, 1.3 Hz, 1H, H-7'), 5.18 (t, $J = 7$ Hz, 1H, CH-3'), 3.83 (t, $J = 6.6$ Hz, 2H, $\text{OCH}_2\text{CH}_2\text{CH}_3$), 2.73 (t, $J = 6.7$ Hz, 2H, CH_2 -4), 2.28 (m, 2H, CH_2 -6'), 2.13 (m, 4H, CH_2 -2', 5'), 1.95 (s, 3H, CH_3 -10'), 1.76 (m, 6H, CH_2 -3, $\text{OCH}_2\text{CH}_2\text{CH}_3$, CH_2 -1'), 1.62 (s, 3H, CH_3 -11'), 1.27 (s, 3H, CH_3 -12') 1.01 (t, $J = 7.4$ Hz, 3H, $\text{OCH}_2\text{CH}_2\text{CH}_3$); ^{13}C NMR (75 MHz, CDCl_3): δ_{C} 167.7 (CO), 152.4 (C-6), 147.7 (C-8a), 138.1 (C-1'), 136.2 (CH-7'), 134.0 (C-4'), 132.0 (C-8'), 129.0 (CH-3', 5'), 125.2 (CH-4'), 124.1 (CH-3'), 121.6 (C-4a), 120.0 (CH-2', 6''), 117.7 (CH-7), 114.8 (CH-5), 114.1 (CH-8), 75.5 (C-2), 70.1 ($\text{OCH}_2\text{CH}_2\text{CH}_3$), 39.2 (CH_2 -1'), 38.4 (CH_2 -5'), 31.0 (CH_2 -3), 26.9 (CH_2 -6'), 24.1 (CH_3 -12'), 22.7 (CH_2 -4), 22.4 ($\text{OCH}_2\text{CH}_2\text{CH}_3$), 22.2 (CH_2 -2'), 15.9 (CH_3 -11'), 12.9 (CH_3 -10'), 10.6 ($\text{OCH}_2\text{CH}_2\text{CH}_3$); HREIMS m/z 461.2625 $[\text{M}]^+$ (461.2520 calcd. for $\text{C}_{30}\text{H}_{39}\text{NO}_3$).

6-Benzoyloxy-2-((4',8'-dimethyl)ethylnona-3',7'-dienoate)-2-methyl-dihydro-benzopyran (14): ^1H NMR (300 MHz, CDCl_3): δ_{H} 7.33 (m, 5H, H-2'' to H-6''), 6.70 (m, 1H, H-7'), 6.68 (m, 3H, H-5, 7, 8), 5.14 (t, $J = 6$ Hz, 1H, H-3'), 4.98 (s, 2H, OCH_2Ar), 4.18 (q, $J = 7.1$ Hz, 2H, OCH_2CH_3), 2.73 (t, $J = 6.8$ Hz, 2H, CH_2 -4), 2.26 (q, $J = 7.5$ Hz, 2H, CH_2 -6'), 2.10 (m, 4H, CH_2 -2', 5'), 1.82 (s, 3H, CH_3 -10'), 1.76 (q, $J = 6.8$ Hz, 2H, CH_2 -3), 1.63 (m, 2H, CH_2 -1'), 1.60 (s, 3H, CH_3 -11'), 1.28 (s, 3H, CH_3 -12'), 1.26 (t, $J = 7.1$ Hz, 3H, OCH_2CH_3); ^{13}C NMR (75 MHz, CDCl_3): δ_{C} 168.2 (CO), 152.1 (C-6), 148.1 (C-8a), 141.8 (CH-7'), 137.5 (C-1'), 134.1 (C-4'), 128.5 (CH-2'', 6''), 127.8 (C-8'), 127.7 (CH-4'), 127.5 (CH-3', CH-5'), 125.0 (CH-3'), 121.7 (C-4a), 117.7 (CH-7), 115.1 (CH-5), 114.3 (CH-8), 75.6 (C-2), 70.6 (OCH_2Ar), 60.3 (OCH_2CH_3), 39.2 (CH_2 -1'), 38.2 (CH_2 -5'), 30.9 (CH_2 -3), 27.2 (CH_2 -6'), 24.1 (CH_3 -12'), 22.4 (CH_2 -4), 22.1 (CH_2 -2'), 15.9 (CH_3 -11'), 14.3 (OCH_2CH_3), 12.4 (CH_3 -10'); HREIMS m/z 462.2729 $[\text{M}]^+$ (462.2770 calcd. for $\text{C}_{30}\text{H}_{38}\text{O}_4$).

6-Benzoyloxy-2-methyl-2-((4',8'-dimethyl)-N-phenylnona-3',7'-dienamide)-dihydro-benzopyran (15): ^1H NMR (300 MHz, CDCl_3): δ_{H} 7.54 (d, $J = 8.7$ Hz, 2H, H-2'', 6''), 7.36 (m, 7H, H-3'', 5'' and H-2' to H-6'), 7.14 (m, 1H, H-4''), 6.72 (m, 3H, H-5, H-7, H-8), 6.37 (dt, $J = 7.1$ Hz, 1.3 Hz, 1H, H-7'), 5.18 (t, $J = 7$ Hz, 1H, CH-3'), 4.98 (s, 2H, OCH_2Ar), 2.73 (t, $J = 6.7$ Hz, 2H, CH_2 -4), 2.28 (m, 2H, CH_2 -6'), 2.12 (m, 4H, CH_2 -2', 5'), 1.93 (s, 3H, CH_3 -10'), 1.78 (m, 2H, CH_2 -3), 1.64 (m, 2H, CH_2 -1'), 1.62 (s, 3H, CH_3 -11'), 1.27 (s, 3H, CH_3 -12'); ^{13}C NMR (75 MHz, CDCl_3): δ_{C} 167.6 (CO), 152.1 (C-6), 148.0 (C-8a), 138.1, 137.5 (C-1'', C-1'), 136.1 (CH-7'), 134.0 (C-4'), 132.0 (C-8'), 129.0, 128.5, 127.8, 127.5 and 125.2 (CH-Ar), 124.2 (CH-3'), 121.7 (C-4a), 120.0 (CH-2'', 6''), 117.1 (CH-7), 115.2 (CH-5), 114.4 (CH-8), 75.6 (C-2), 70.7 (OCH_2Ar), 39.2 (CH_2 -1'), 38.4 (CH_2 -5'), 31.1 (CH_2 -3), 26.9 (CH_2 -6'), 24.1 (CH_3 -12'), 22.7 (CH_2 -4), 22.5 (CH_2 -2'), 15.8 (CH_3 -11'), 12.9 (CH_3 -10'); HREIMS m/z 509.2953 $[\text{M}]^+$ (509.2930 calcd. for $\text{C}_{34}\text{H}_{39}\text{NO}_3$).

5.0.2. General procedure for synthesis of eleven- and thirteen-carbon side chain prenylated benzopyrans: “trans- δ -tocotrienolic acid” analogs 17–21 (series 3)

Following the same methodology described to synthesize compound

6, the prenylated benzopyran **17** was prepared by reacting aldehyde **11** with a solution of isopropenylmagnesium bromide. Intermediate **16** was treated directly with triethylorthoacetate, to give compound **17** (50%) as a colorless oil. For the preparation of compounds **20**, prenylated benzopyran “trans- δ -tocotrienolic acid” type, the same procedure was followed as that used for the synthesis of compound **12** (63%) as a colorless oil. The amidation from compound **20** to give compound **21** (23 %) as a colorless oil was carried out following the procedure described to synthesize compound **7** (Schemes 2, 3 and 4).

2-((4',8'-Dimethyl)ethylundeca-3',7'-dienoate)-2-methyl-6-propoxy-dihydro-benzopyran (17): ^1H NMR (300 MHz, CDCl_3): δ_{H} 6.75 (m, 3H, H-5, 7, 8), 5.10 (m, 2H, H-3', 7'), 4.11 (q, $J = 7.1$ Hz, 2H, OCH_2CH_3), 3.84 (t, $J = 6.6$ Hz, 2H, $\text{OCH}_2\text{CH}_2\text{CH}_3$), 2.73 (t, $J = 6.8$ Hz, 2H, CH_2 -4), 2.30 (m, $J = 4$ Hz, CH_2 -9', 10'), 2.10 (m, 6H, CH_2 -2', 5', 6'), 1.80 (m, 6H, CH_2 -3, $\text{OCH}_2\text{CH}_2\text{CH}_3$, CH_2 -1'), 1.59 (s, 6H, CH_3 -12', 13'), 1.27 (t, $J = 7.2$ Hz, 3H, OCH_2CH_3), 1.24 (s, 3H, CH_3 -14'), 1.00 (t, $J = 7.4$ Hz, 3H, $\text{OCH}_2\text{CH}_2\text{CH}_3$); ^{13}C NMR (75 MHz, CDCl_3): δ_{C} 173.5 (CO), 152.3 (C-6), 147.8 (C-8a), 135.0 (C-8'), 133.3 (C-4'), 125.0 (CH-7'), 124.2 (CH-3'), 121.6 (C-4a), 117.7 (CH-7), 114.8 (CH-5), 114.0 (CH-8), 75.6 (C-2), 70.1 ($\text{OCH}_2\text{CH}_2\text{CH}_3$), 60.2 (OCH_2CH_3), 39.5 (CH_2 -1'), 39.3 (CH_2 -5'), 34.7 (CH_2 -10'), 33.3 (CH_2 -9'), 31.0 (CH_2 -3), 26.5 (CH_2 -6'), 24.1 (CH_3 -14'), 22.7 (CH_2 -4), 22.4 ($\text{OCH}_2\text{CH}_2\text{CH}_3$), 22.1 (CH_2 -2'), 15.9, 15.8 (CH_3 -12', 13'), 12.4 (OCH₂CH₃), 10.5 ($\text{OCH}_2\text{CH}_2\text{CH}_3$); HREIMS m/z 442.3123 $[\text{M}]^+$ (442.3083 calcd. for $\text{C}_{28}\text{H}_{42}\text{O}_4$).

2-((4',8'-Dimethyl)undeca-3',7'-dien-11'-ol)-2-methyl-6-propoxydihydrobenzopyran (18): ^1H NMR (500 MHz, CDCl_3): δ_{H} 6.70 (m, 3H, H-5, 7, 8), 5.12 (m, 2H, H-3', 7'), 3.84 (t, $J = 6.6$ Hz, 2H, $\text{OCH}_2\text{CH}_2\text{CH}_3$), 3.61 (t, $J = 6.4$ Hz, 2H, CH_2 -11), 2.73 (t, $J = 6.7$ Hz, 2H, CH_2 -4), 2.30 (m, 4H, CH_2 -9', 10'), 2.10 (m, 6H, CH_2 -2', 5', 6'), 1.80 (m, 6H, CH_2 -3, $\text{OCH}_2\text{CH}_2\text{CH}_3$, CH_2 -1'), 1.59 (s, 6H, CH_3 -12', 13'), 1.28 (s, 3H, CH_3 -14'), 1.01 (t, $J = 7.4$ Hz, 3H, $\text{OCH}_2\text{CH}_2\text{CH}_3$); ^{13}C NMR (125 MHz, CDCl_3): δ_{C} 152.3 (C-6), 147.8 (C-8a), 135.0 (C-8'), 133.3 (C-4'), 124.7 (CH-7'), 124.3 (CH-3'), 121.6 (C-4a), 117.7 (CH-7), 114.8 (CH-5), 114.1 (CH-8), 75.6 (C-2), 70.1 ($\text{OCH}_2\text{CH}_2\text{CH}_3$), 62.8 (CH_2 -11'), 39.5 (CH_2 -1'), 39.3 (CH_2 -5'), 36.0 (CH_2 -9'), 31.0 (CH_2 -3), 30.7 (CH_2 -10'), 26.4 (CH_2 -6'), 24.2 (CH_3 -14'), 22.7 (CH_2 -4), 22.4 ($\text{OCH}_2\text{CH}_2\text{CH}_3$), 22.2 (CH_2 -2'), 15.9 (CH_3 -12', 13'), 10.6 ($\text{OCH}_2\text{CH}_2\text{CH}_3$); HREIMS m/z 400.3048 $[\text{M}]^+$ (400.2977 calcd. for $\text{C}_{26}\text{H}_{40}\text{O}_3$).

2-((4',8'-Dimethyl)undeca-3',7'-dienal)-2-methyl-6-propoxydihydrobenzopyran (19): ^1H NMR (500 MHz, CDCl_3): δ_{H} 9.8 (d, $J = 1.6$ Hz, CHO-11'), 6.68 (m, 3H, H-5, 7, 8), 5.14 (m, 2H, H-3', 7'), 3.84 (t, $J = 6.6$ Hz, 2H, $\text{OCH}_2\text{CH}_2\text{CH}_3$), 2.73 (t, $J = 6.8$ Hz, 2H, CH_2 -4), 2.50 (dt, $J = 7.6$ Hz, 1.6 Hz, 2H, CH_2 -10'), 2.30 (t, $J = 7.5$ Hz, 2H, CH_2 -9'), 2.10 (m, 6H, CH_2 -2', 5', 6'), 1.80 (m, 6H, CH_2 -3, $\text{OCH}_2\text{CH}_2\text{CH}_3$, CH_2 -1'), 1.60 (s, 3H, CH_3 -12'), 1.57 (s, 3H, CH_3 -13'), 1.27 (s, 3H, CH_3 -14'), 1.01 (t, $J = 7.4$ Hz, 3H, $\text{OCH}_2\text{CH}_2\text{CH}_3$); ^{13}C NMR (125 MHz, CDCl_3): δ_{C} 202.6 (CO), 152.4 (C-6), 147.7 (C-8a), 133.1 (C-8' and C-4'), 125.3 (CH-7' and CH-3'), 121.6 (C-4a), 117.6 (CH-7), 114.8 (CH-5), 114.1 (CH-8), 75.5 (C-2), 70.1 ($\text{OCH}_2\text{CH}_2\text{CH}_3$), 42.1 (CH_2 -10'), 39.1 (CH_2 -1', 5'), 31.7 (CH_2 -9'), 31.0 (CH_2 -3), 30.7 (CH_2 -10'), 26.4 (CH_2 -6'), 24.2 (CH_3 -14'), 22.7 (CH_2 -4), 22.4 ($\text{OCH}_2\text{CH}_2\text{CH}_3$), 22.2 (CH_2 -2'), 16.0 (CH_3 -12', 13'), 10.5 ($\text{OCH}_2\text{CH}_2\text{CH}_3$); HREIMS m/z 398.2913 $[\text{M}]^+$ (398.2821 calcd. for $\text{C}_{26}\text{H}_{38}\text{O}_3$).

2-Methyl-6-propoxy-2-((4',8',12'-trimethyl)ethyltrideca-3',7',11'-trienoate)-dihydro-benzopyran (20): ^1H NMR (400 MHz, CDCl_3): δ_{H} 6.72 (dt, $J = 7.3$ Hz, 1.4 Hz, H-11'), 6.65 (m, 3H, H-5, 7, 8), 5.15 (dt, $J = 5.7$ Hz, 1.2 Hz, 2H, H-7', H-3'), 4.18 (q, $J = 7.1$ Hz, 2H, OCH_2CH_3), 3.84 (t, $J = 6.6$ Hz, 2H, $\text{OCH}_2\text{CH}_2\text{CH}_3$), 2.73 (t, $J = 6.8$ Hz, 2H, CH_2 -4), 2.25 (q, $J = 7.5$ Hz, 2H, CH_2 -10'), 2.08 (m, 8H, CH_2 -2', 5', 6', 9'), 1.83 (s, 3H, CH_3 -14'), 1.77 (m, 6H, CH_2 -3, $\text{OCH}_2\text{CH}_2\text{CH}_3$, CH_2 -1'), 1.60 (s, 6H, CH_3 -15', 16'), 1.30 (t, $J = 7.2$ Hz, 3H, OCH_2CH_3), 1.27 (s, 3H, CH_3 -17'), 1.02 (t, $J = 7.4$ Hz, 3H, $\text{OCH}_2\text{CH}_2\text{CH}_3$); ^{13}C NMR (100 MHz, CDCl_3): δ_{C} 168.1 (CO), 152.3 (C-6), 147.7 (C-8a), 141.8 (CH-11'), 134.9 (C-8'), 133.8 (C-4'), 127.6 (C-12'), 125.0 (CH-7'), 124.2 (CH-3'), 121.5 (C-4a), 117.7 (CH-7), 114.8 (CH-5), 114.0 (CH-8), 75.5 (C-2), 70.0 ($\text{OCH}_2\text{CH}_2\text{CH}_3$), 60.3 (OCH_2CH_3), 39.5 (CH_2 -1'), 39.3 (CH_2 -5'), 38.2 (CH_2 -9'), 31.0 (CH_2 -

3), 27.3 (CH₂-10'), 26.5 (CH₂-6'), 24.1 (CH₃-17'), 22.7 (CH₂-4), 22.5 (OCH₂CH₂CH₃), 22.1 (CH₂-2'), 15.9 (CH₃-15', 16'), 14.2 (OCH₂CH₃), 12.3 (CH₃-14'), 10.5 (OCH₂CH₂CH₃); HREIMS *m/z* 482.2538 [M]⁺ (482.2402 calcd. for C₃₁H₄₆O₄).

2-Methyl-2-(N-phenyl(4',8',12'-trimethyl)trideca-3',7',11'-trienamide)-6-propyloxy-dihydrobenzopyran (21). ¹H NMR (300 MHz, CDCl₃): δ_H 7.42 (m, 5H, H-2' to 6'), 6.65 (m, 3H, H-5, 7, 8), 6.37 (dt, *J* = 7.1 Hz, 1.3 Hz, 1H, H-11'), 5.15 (t, *J* = 7.2 Hz, 2H, H-3', H-7'), 3.83 (t, *J* = 6.6 Hz, 2H, OCH₂CH₂CH₃), 2.73 (t, *J* = 6.8 Hz, 2H, CH₂-4), 2.25 (q, *J* = 7.5 Hz, 2H, CH₂-10'), 2.08 (m, 8H, CH₂-2', 5', 6', 9'), 1.83 (s, 3H, CH₃-14'), 1.77 (m, 6H, CH₂-3, OCH₂CH₂CH₃, CH₂-1'), 1.60 (s, 3H, CH₃-15'), 1.59 (s, 3H, CH₃-16'), 1.27 (s, 3H, CH₃-17'), 1.00 (t, *J* = 7.4 Hz, 3H, OCH₂CH₂CH₃); ¹³C NMR (75 MHz, CDCl₃): δ_C 168.2 (CO), 152.4 (C-6), 147.8 (C-8a), 141.8 (CH-11'), 134.9 (C-8'), 133.8 (C-4'), 129.0, 127.8 and 125.2 (CH-Ar), 127.6 (C-12'), 125.0 (CH-7'), 124.2 (CH-3'), 121.5 (C-4a), 117.7 (CH-7), 114.8 (CH-5), 114.0 (CH-8), 75.5 (C-2), 70.0 (OCH₂CH₂CH₃), 39.5 (CH₂-1'), 39.3 (CH₂-5'), 38.2 (CH₂-9'), 31.0 (CH₂-3), 27.3 (CH₂-10'), 26.5 (CH₂-6'), 24.1 (CH₃-12'), 22.7 (CH₂-4), 22.5 (OCH₂CH₂CH₃), 22.1 (CH₂-2'), 15.9 (CH₃-15', 16'), 12.3 (CH₃-17'), 10.5 (OCH₂CH₂CH₃); HREIMS *m/z* 529.2416 [M]⁺ (529.2230 calcd. for C₃₅H₄₇NO₃).

5.1. Evaluation of PPAR activity by transactivation assays

PPAR transcriptional activity of synthesized compounds was performed using a human chimera PPAR/Gal4 gene reporter luciferase system to obtain the maximal transactivation response for each compound at 10 μM dose and compared with WY-14,643 (pirinixic acid, Sigma-Aldrich, St. Louis, MO) at 10 μM for PPARα or rosiglitazone (Sigma-Aldrich) at 1 μM for PPARγ. Cos-7 cells (CRL-1651, ATCC, Manassas, VA) were maintained under standard culture conditions (Dulbecco's modified Eagle's minimal essential medium: DMEM supplemented with 10% fetal calf serum [FCS], Thermo Fisher Scientific, Waltham, MA) at 37 °C in a humidified atmosphere of 5% CO₂. The medium was changed every 2 days. Cells (5.5 × 10⁵ cells/mL) were seeded in 60-mm dishes in DMEM supplemented with 10% FCS and incubated at 37 °C for 16 h prior to transfection. Cells were transfected in DMEM with the jetPEI transfection reagent (Polyplus-Transfection S. A., Strasbourg, France) using the reporter plasmid pG5-TK-pGL3 in combination with one of the expression plasmids, pGal4hPPARα or pGal4hPPARγ. The pCMV-β-galactosidase expression plasmid was included as a control of transfection efficiency. The transfection was stopped after 16 h by the addition of DMEM supplemented with 10% FCS, and cells were detached with trypsin and re-seeded in 96-well plates and incubated for 6 h in DMEM containing 10% FCS. Cells were then incubated for 24 h in DMEM containing 0.2% FCS and increasing concentrations of the compound tested or vehicle (dimethylsulfoxide, DMSO, 0.1% final concentration). At the end of the experiment, cells were washed once with ice-cold phosphate-buffered saline (PBS) and lysed, and luciferase and β-galactosidase activity was measured. Each experiment was achieved in triplicate, and mean ± standard error (SEM) values were calculated using GraphPad Prism 5 Software.

6. Molecular modeling

Molecular docking simulation was performed to localize the ligand 15 in the binding pocket of PPARγ and molecular interactions. The 3D crystal structure of PPARγ in complex with rosiglitazone (PDB code: 4EMA) and PPARα in complex with WY-14,643 (PDB code: 4BCR) were retrieved from RCSB Protein Data Bank (PDB, <https://www.rcsb.org>). USCF Chimera software^[28] was used for ligand and protein preparation. Solvent molecules were removed, while hydrogens and Gasteiger charges were added.^[29] Docking simulations were performed with AutoDock Vina tool, and the results obtained were analyzed with USCF Chimera. The ligand/protein complex was considered stable when the values of the binding free energy (ΔG_{ligand-residue}) were lower than −5 Kcal/mol.

Declaration of Competing Interest

The authors declare that they have no known competing financial interests or personal relationships that could have appeared to influence the work reported in this paper.

Acknowledgements

We are grateful for the financial support from Carlos III Health Institute (ISCIII) and the European Regional Development Fund (FEDER) (grants: PI18/01450 and CP15/00150), the Spanish Ministry of Science and Innovation (SAF2017-89714-R), Generalitat Valenciana (APOTIP/2020/011, PROMETEO/2019/032 and AICO2021/081) and from Agence Nationale pour la Recherche (ANR-10 LABX-0046), and an ERC Advanced Grant (694717). N.C. was an investigator in the 'Miguel Servet' programme (CP15/00150 and CPII20/00010) of the ISCIII and the European Social Fund. C.V. thanks ISCIII for a PFIS grant (FI19/00153).

Appendix A. Supplementary data

Supplementary data to this article can be found online at <https://doi.org/10.1016/j.bmc.2021.116532>.

References

- [1] Pearce BC, Parker RA, Deason ME, et al. Inhibitors of cholesterol biosynthesis. 2. Hypocholesterolemic and antioxidant activities of benzopyran and tetrahydronaphthalene analogues of the tocotrienols. *J. Med. Chem.* 1994;37: 526–541. <https://doi.org/10.1021/jm00030a012>.
- [2] Jang KH, Lee BH, Choi BW, Lee H-S, Shin J. Chromenes from brown alga *Sargassum siliquastrum*. *J. Nat. Prod.* 2005;68:716–723. <https://doi.org/10.1021/np058003i>.
- [3] Kruk J, Szymańska R, Cela J, Munne-Bosch S. Plastochromanol-8: Fifty years of research. *Phytochemistry*. 2014;108:9–16. <https://doi.org/10.1016/j.phytochem.2014.09.011>.
- [4] Kashiwada Y, Yamazaki K, Ikeshiro Y, et al. Isolation of rhododaurichromanic acid B and the anti-HIV principles rhododaurichromanic acid A and rhododaurichromenic acid from *Rhododendron dauricum*. *Tetrahedron*. 2001;57(8): 1559–1563. [https://doi.org/10.1016/S0040-4020\(00\)01144-3](https://doi.org/10.1016/S0040-4020(00)01144-3).
- [5] Basabe P, de Román M, Marcos IS, et al. Prenylflavonoids and prenyl/alkyl-phloracetophenones: Synthesis and antitumor biological evaluation. *Eur. J. Med. Chem.* 2010;45(9):4258–4269. <https://doi.org/10.1016/j.ejmech.2010.06.025>.
- [6] Taha H, Looi CY, Arya A, et al. (6E,10E) Isopolycerasoidol and (6E,10E) isopolycerasoidol methyl ester, prenylated benzopyran derivatives from *Pseuduvaria monticola* induce mitochondrial-mediated apoptosis in human breast adenocarcinoma cells. *PLoS ONE*. 2015;10(5):e0126126. <https://doi.org/10.1371/journal.pone.0126126>.
- [7] Winkelmann K, San M, Kypriotakis Z, Skaltsa H, Bosilij B, Heilmann J. Antibacterial and cytotoxic activity of prenylated bicyclic acylphloroglucinol derivatives from *Hypericum amblycalyx*. *Z. Naturforsch.* 2003;58c:527–532. <https://doi.org/10.1515/znc-2003-7-814>.
- [8] Frank J, Chin XWD, Schrader C, Eckert GP, Rimbach G. Do tocotrienols have potential as neuroprotective dietary factors? *Ageing Res. Rev.* 2012;11(1):163–180. <https://doi.org/10.1016/j.arr.2011.06.006>.
- [9] Birringer M, Siems K, Maxones A, Frank J, Lorkowski S. Natural 6-hydroxy-chromenols and -chromenols: structural diversity, biosynthetic pathways and health implications. *RSC Adv.* 2018;8(9):4803–4841. <https://doi.org/10.1039/C7RA11819H>.
- [10] Gonzalez MC, Serrano A, Zafra-Polo MC, Cortes D, Rao KS. Polycerasoidin and polycerasoidol, two new prenylated benzopyran derivatives from *Polyalthia cerasoides*. *J. Nat. Prod.* 1995;58(8):1278–1284. <https://doi.org/10.1021/np50122a022>.
- [11] Carmen González M, Sentandreu MA, Sundar Rao K, Carmen Zafra-Polo M, Cortes D. Prenylated benzopyran derivatives from two *Polyalthia* species. *Phytochemistry*. 1996;43(6):1361–1364. [https://doi.org/10.1016/S0031-9422\(96\)00450-5](https://doi.org/10.1016/S0031-9422(96)00450-5).
- [12] Bermejo A, Collado A, Barrachina I, et al. Polycerasoidol, a natural prenylated benzopyran with a dual PPARα/PPARγ agonist activity and anti-inflammatory effect. *J. Nat. Prod.* 2019;82(7):1802–1812. <https://doi.org/10.1021/acs.jnatprod.9b00003>.
- [13] Consoli A, Formoso G. Do thiazolidinediones still have a role in treatment of type 2 diabetes mellitus? *Diabetes Obes Metab.* 2013;15(11):967–977. <https://doi.org/10.1111/dom.12101>.
- [14] Yasmin S, Jayaprakash V. Thiazolidinediones and PPAR orchestra as antidiabetic agents: From past to present. *Eur. J. Med. Chem.* 2017;126:879–893. <https://doi.org/10.1016/j.ejmech.2016.12.020>.
- [15] Villarroel-Vicente C, Gutiérrez-Palomo S, Ferri J, Cortes D, Cabedo N. Natural products and analogs as preventive agents for metabolic syndrome via peroxisome

- proliferator-activated receptors: An overview. *Eur. J. Med. Chem.* 2021;221: 113535. <https://doi.org/10.1016/j.ejmech.2021.113535>.
- [16] Mirza AZ, Althagafi II, Shamshad H. Role of PPAR receptor in different diseases and their ligands: Physiological importance and clinical implications. *Eur. J. Med. Chem.* 2019;166:502–513. <https://doi.org/10.1016/j.ejmech.2019.01.067>.
- [17] Schupp M, Lazar MA. Endogenous ligands for nuclear receptors: Digging deeper. *J. Biol. Chem.* 2010;285(52):40409–40415. <https://doi.org/10.1074/jbc.R110.182451>.
- [18] Dubois, V.; Eeckhoutte, J.; Lefebvre, P.; Staels, B. Distinct but complementary contributions of PPAR isotypes to energy homeostasis. *J. Clin. Invest.* 2017, 127, 1202–1214; DOI: 10.1172/JCI88894.
- [19] Jain N, Bhansali S, Kurpad AV, et al. Effect of a dual PPAR α/γ agonist on insulin sensitivity in patients of type 2 diabetes with hypertriglyceridemia-randomized double-blind placebo-controlled trial. *Sci. Rep.* 2019;9(1). <https://doi.org/10.1038/s41598-019-55466-3>.
- [20] Bermejo A, Barrachina I, El Aouad N, et al. Synthesis of benzopyran derivatives as PPAR α and/or PPAR γ activators. *Bioorg. Med. Chem.* 2019;27(24):115162. <https://doi.org/10.1016/j.bmc.2019.115162>.
- [21] García, A.; Vila, L.; Marín, P.; Bernabeu, A.; Villarroel-Vicente, C.; Hennuyer, N.; Staels, B.; Franck, X.; Figadère, B.; Cabedo, N.; Cortes, D. Synthesis of 2-prenylated alkoxyated benzopyrans by Horner–Wadsworth–Emmons olefination with PPAR α/γ agonist activity. *ACS Med. Chem. Lett.* 2021 (in press); DOI: 10.1021/acsmchemlett.1c00400.
- [22] Wallert M, Kluge S, Schubert M, et al. Diversity of chromanol and chromenol structures and functions: An emerging class of anti-inflammatory and anti-carcinogenic agents. *Front. Pharmacol.* 2020;11. <https://doi.org/10.3389/fphar.2020.00362>.
- [23] Bartolini D, De Franco F, Torquato P, et al. Garcinoic acid is a natural and selective agonist of pregnane X receptor. *J. Med. Chem.* 2020;63(7):3701–3712. <https://doi.org/10.1021/acs.jmedchem.0c00012>.
- [24] Kabbe H-J, Widdig A. Synthesis and reactions of 4-chromanones. *Angew. Chem. Int. Ed. Engl.* 1982;21(4):247–256. [https://doi.org/10.1002/\(ISSN\)1521-377310.1002/anie.v21:410.1002/anie.198202471](https://doi.org/10.1002/(ISSN)1521-377310.1002/anie.v21:410.1002/anie.198202471).
- [25] Sun D-Y, Han G-Y, Yang N-N, Lan L-F, Li X-W, Guo Y-W. Racemic trinosesquiterpenoids from the Beihai sponge *Spongia officinalis*: structure and biomimetic total synthesis. *Org. Chem. Front.* 2018;5(6):1022–1027. <https://doi.org/10.1039/C7QO01091E>.
- [26] Bruckner S, Weise M, Schobert R. Synthesis of the entomopathogenic fungus metabolites militarinone C and fumosorinone A. *J. Org. Chem.* 2018;83(18): 10805–10812. <https://doi.org/10.1021/acs.joc.8b01530>.
- [27] Le Naour M, Leclerc V, Farce A, et al. Effect of oxime ether incorporation in acyl indole derivatives on PPAR subtype selectivity. *ChemMedChem.* 2012;7(12): 2179–2193. <https://doi.org/10.1002/cmdc.v7.1210.1002/cmdc.201200316>.
- [28] Pettersen EF, Goddard TD, Huang CC, et al. UCSF Chimera—A visualization system for exploratory research and analysis. *J. Comput. Chem.* 2004;25(13):1605–1612. [https://doi.org/10.1002/\(ISSN\)1096-987X10.1002/jcc.v25:1310.1002/jcc.20084](https://doi.org/10.1002/(ISSN)1096-987X10.1002/jcc.v25:1310.1002/jcc.20084).
- [29] Wang J, Wang W, Kollman PA, Case DA. Automatic atom type and bond type perception in molecular mechanical calculations. *J. Mol. Graph. Model.* 2006;25(2): 247–260. <https://doi.org/10.1016/j.jmglm.2005.12.005>.

Article 3: Benzopyran hydrazones with dual PPAR α / γ or PPAR α / δ agonism and an anti-inflammatory effect on human THP-1 macrophages, *European Journal of Medicinal Chemistry*, in press.



Research paper

Benzopyran hydrazones with dual PPAR α / γ or PPAR α / δ agonism and an anti-inflammatory effect on human THP-1 macrophagesAinhoa García ^{a, b}, Laura Vila ^b, Isabelle Duplan ^c, María Ayelén Schiel ^d, Ricardo D. Enriz ^d, Nathalie Hennuyer ^{c, **}, Bart Staels ^c, Nuria Cabedo ^{a, b, *}, Diego Cortes ^a^a Department of Pharmacology, University of Valencia, 46100, Valencia, Spain^b Institute of Health Research-INCLIVA, University Clinic Hospital of Valencia, 46010, Valencia, Spain^c Univ. Lille, Inserm, CHU Lille, Institut Pasteur de Lille, U-1011-EGID, F-59000, Lille, France^d Faculty of Chemistry, Biochemistry and Pharmacy, National University of San Luis-IMIBIO-SL-CONICET, Chacabuco, 917-5700, San Luis, Argentina

ARTICLE INFO

Keywords:

Benzopyran hydrazones

Synthesis

Molecular modelling

PPAR agonists

Anti-inflammatory activity

Cytotoxicity

ABSTRACT

Peroxisome proliferator-activated receptors (PPARs) play a major role in regulating inflammatory processes, and dual or pan-PPAR agonists with PPAR γ partial activation have been recognised to be useful to manage both metabolic syndrome and metabolic dysfunction-associated fatty liver disease (MAFLD). Previous works have demonstrated the capacity of 2-prenylated benzopyrans as PPAR ligands. Herein, we have replaced the isoprenoid bond by hydrazone, a highly attractive functional group in medicinal chemistry. In an attempt to discover novel and safety PPAR activators, we efficiently prepared benzopyran hydrazone/hydrazine derivatives containing benzothiazole (*series 1*) or 5-chloro-3-(trifluoromethyl)-2-pyridine moiety (*series 2*) with a 3- or 7-carbon side chain at the 2-position of the benzopyran nucleus. Benzopyran hydrazones **4** and **5** showed dual hPPAR α / γ agonism, while hydrazone **14** exerted dual hPPAR α / δ agonism. These three hydrazones greatly attenuated inflammatory markers such as IL-6 and MCP-1 on the THP-1 macrophages via NF- κ B activation. Therefore, we have discovered novel hits (**4**, **5** and **14**), containing a hydrazone framework with dual PPAR α / γ or PPAR α / δ partial agonism, depending on the length of the side chain. Benzopyran hydrazones emerge as potential lead compounds which could be useful for treating metabolic diseases.

1. Introduction

Peroxisome proliferator-activated receptors (PPARs) are members of the nuclear receptor superfamily of transcription factors, comprising three isotypes [PPAR α (NR1C1), PPAR β / δ (NR1C2) and PPAR γ (NR1C3)] which have different tissue distribution, ligand specificities, and metabolic regulatory activities [1,2]. In structural terms, PPARs contain a DNA-binding domain (DBD) in the N-terminus and a ligand-binding domain (LBD) in the C-terminus. The DBD sets the binding with PPAR response elements (PPREs) in specific regions of the target genes and the LBD forms the pocket for direct interaction with specific ligands. After the interaction with ligands, PPARs are translocated to the nucleus and heterodimerise with the retinoid X receptor (RXR) to form the PPAR-RXR complex. PPAR-RXR binding by agonists induces the recruitment of coactivators (e.g., CBP or p300) and the release of corepressors (e.g., NCoR or SMRT) by stimulating the gene transcription of

the target genes [3–5]. The three PPAR isoforms are involved in fatty acid oxidation, glucose metabolism, and lipid metabolism. PPAR α is expressed mainly in the tissues involved in increased fatty acid oxidation, such as liver, skeletal muscle and heart, and controls lipid metabolism. PPAR α activation decreases triglyceride levels in plasma and increases HDL-c to play a significant role in the treatment of dyslipidaemia [6]. PPAR α is also implicated in glucose homeostasis and insulin resistance [7,8]. PPAR β / δ is ubiquitous, but is highly expressed in those tissues involved in fatty acid metabolism, such as skeletal and cardiac muscle, hepatocytes and adipocytes. Its activation improves insulin sensitivity and the plasma lipid profile, which may manage both dyslipidaemia and type 2 diabetes, although no PPAR β / δ agonist has yet been approved for clinical use [9]. PPAR γ is widely expressed in adipose tissue and its activation is related to adipogenesis, lipid storage, insulin sensitivity and glucose homeostasis. Its agonists have been widely used for treating type 2 diabetes. However, much evidence indicates that potent

* Corresponding author. Department of Pharmacology, University of Valencia, 46100, Valencia, Spain.

** Corresponding author.

E-mail addresses: nathalie.hennuyer@pasteur-lille.fr (N. Hennuyer), ncabedo@uv.es (N. Cabedo), dcortes@uv.es (D. Cortes).<https://doi.org/10.1016/j.ejmech.2024.116125>Received 13 July 2023; Received in revised form 2 January 2024; Accepted 3 January 2024
0223-5234/© 20XX

and full PPAR γ activators are related with serious adverse effects, and a partial agonism would lead to safer drugs [2]. The endogenous ligands for PPARs are fatty acids, cyclooxygenase-derived eicosanoids and prostaglandins, as well as their metabolites. The most known synthetic ligands are fibrates and WY-14,643, GW501516 or rosiglitazone (thiazolidinedione) (Fig. 1), which act as strong agonists for PPAR α , PPAR β/δ or PPAR γ , respectively [10]. In addition, the three isoforms (α , β/δ , γ) play a major role in regulating inflammatory processes, and have been recognised as the target for the management of metabolic syndrome, obesity, dyslipidaemia, type 2 diabetes, atherosclerosis [2,4], and metabolic dysfunction-associated fatty liver disease (MAFLD). They are all accompanying with a persistent chronic, low-grade inflammation state in several tissues, including adipose tissue, pancreatic islets and liver [11]. Macrophages are phagocytic innate immune cells involved in immunity, tissue remodelling and lipid homeostasis. These immune cells are present in all tissues and play a crucial role during the development of metabolic disorders [11–13] and associated inflammation. The three PPAR isoforms are highly expressed in human macrophages [13], whose function can be regulated by PPAR agonists to prevent metabolic diseases. Infiltrate macrophages in tissues

also release pro-inflammatory cytokines and chemokines, which contribute to an inflammation state. Of them, monocyte chemoattractant protein-1 (MCP-1/CCL2) is an important chemokine that is implicated in both the recruitment and activation of monocytes [14], and its down-regulation has been found to occur with improvement of metabolic disorders [15,16]. Interleukin 6 (IL-6) is an inflammatory cytokine IL-6 whose overproduction is directly related to obesity, diabetes and progression to metabolic and cardiovascular disorders [17]. PPAR agonists have been reported to suppress the immunoreactive state of macrophages by the suppression of immune reactive cytokine and chemokines markers, including MCP-1 and IL-6 [2,18].

In 1995, our research group isolated polycerasoidol from the stem bark of *Polyalthia cerasoides* (Annonaceae) [19] (Fig. 1). This 2-prenylated benzopyran contains the chroman-6-ol nucleus like the PPAR γ agonist troglitazone (Fig. 1), two isoprenoid units and a terminal carboxylic group on the side chain at 2-position. Polycerasoidol displayed potent dual PPAR α/γ agonism and anti-inflammatory effects by inhibiting mononuclear cell-endothelium interactions in a dysfunctional endothelium [20]. Polycerasoidol became the first-in-class with potential to manage several of the risk factors involved in the develop-

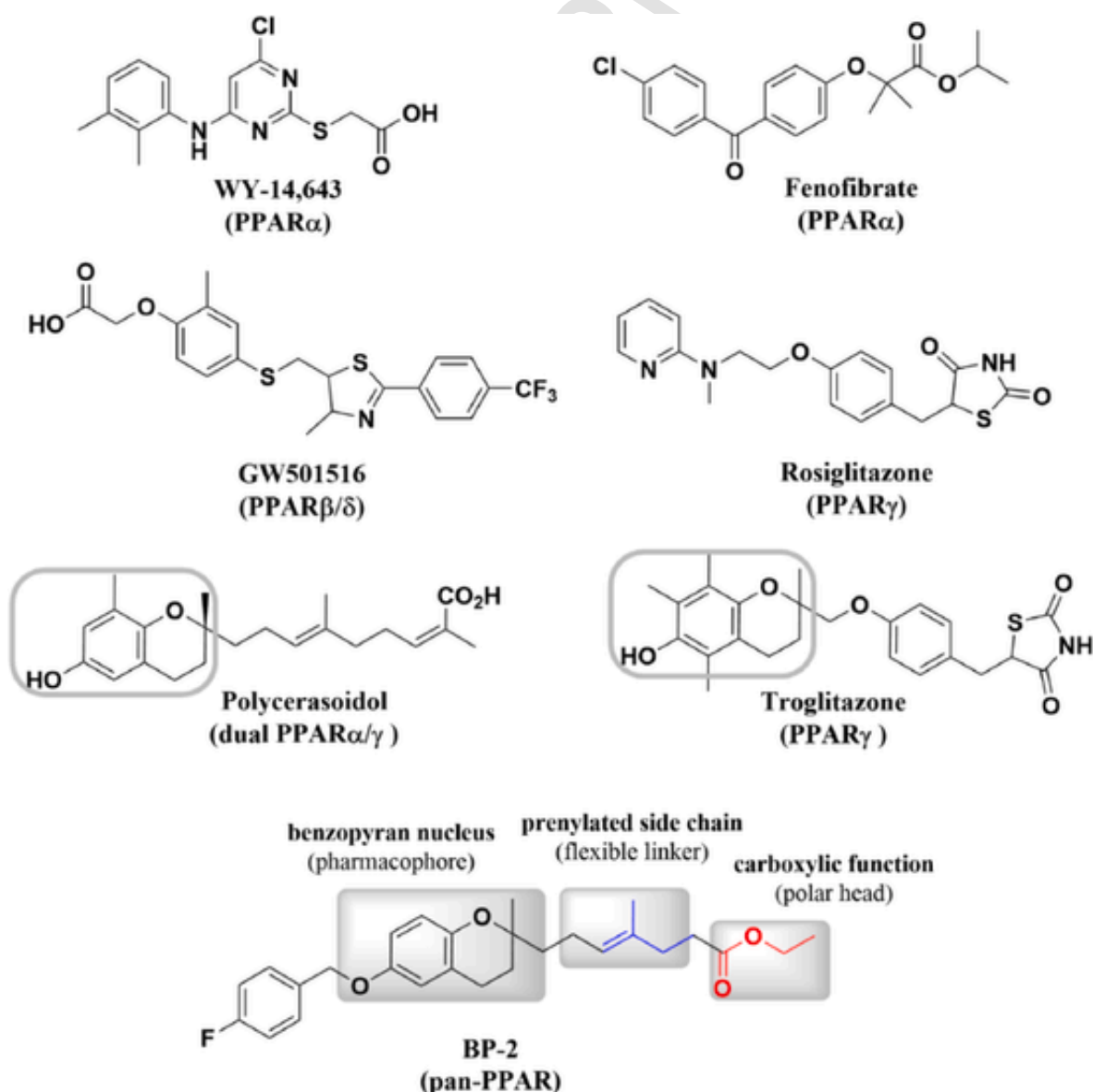


Fig. 1. Synthetic ligands, and natural or synthetic benzopyrans as PPAR agonists.

ment of metabolic syndrome. Next, we carried out structure-activity relationship (SAR) studies of synthetic polycerasoidol analogues and molecular modelling study analyses to explore those key structural features implicated in the modulation of PPARs [21–23]. These studies have indicated that: i) the oxygen atom at 6-position in the benzopyran nucleus (pharmacophore); ii) the length of the prenylated side chain (flexible linker) from 5- to 11-carbons; iii) ester, amide and *O*-alkoxylated bioisosters in the carboxylic function (polar head) can improve hPPAR α and hPPAR γ interactions. A recent hit-to-lead strategy identified 2-(ethyl-4'-methylhept-4'-enoate)-6-(*p*-fluorobenzyloxy)-2-(methyl)-benzodihydropyran (BP-2) (Fig. 1) as a pan-PPAR with PPAR γ partial activation, and capable of ameliorating metabolic alterations in an obese and diabetic mouse model (*ob/ob* mice) [24].

On the other hand, hydrazone ($-\text{CH}=\text{N}-\text{NH}-$) and hydrazine ($-\text{CH}_2-\text{NH}-\text{NH}_2$) functions are present in many bioactive natural and synthetic compounds [25–29], attracting the interest as privilege moieties in medicinal chemistry. Among them, the antibiotic rifampicin and the antiparasitic nifurtimox (anti-parasitic drug for Chagas disease) contain the hydrazone moiety, while the hydrazine group is found in the anti-hypertensive hydralazine (vasodilator), the antidepressant phenelzine (monoamine oxidase inhibitor) and the anticancer procarbazine, all of which are clinically used drugs (Fig. 2). Synthesised hydrazones were also reported to display antidiabetic and antilipidemic activities by different mechanisms [30,31]. In addition, heterocyclic systems are valuable scaffolds to design new therapeutic derivatives. Benzo[d]thiazole moiety is found in lanifibranor (Fig. 3), a pan-PPAR agonist and the first drug clinically approved for MAFLD, whereas pyridyl fragment is present in rosiglitazone (Fig. 1) and pioglitazone (Fig. 3), two thiazolidinediones with full PPAR γ agonism and used as anti-diabetic agents.

Based on our previous works on 2-prenylated benzopyrans, and in a view of discovering novel chemical entities with dual- or pan-PPAR agonism, but with PPAR γ partial agonism to avoid adverse effects associated to a full and selective PPAR γ activation, we have explored the possibility to replace both the isoprenyl (flexible linker) and the ethyl carboxylate (polar head) moieties by potential bioisosters. Herein, we have synthesised and evaluated the PPAR activity of novel benzopyrans (pharmacophore) containing in the hydrocarbon side chain at 2-

position a hydrazone or hydrazine (its reduced form) function linked to a heterocyclic system such as benzothiazole or 5-chloro-3-(trifluoromethyl)-2-pyridine, two attractive templates for PPAR target (Fig. 3). The anti-inflammatory potential of synthesised compounds was also evaluated *in vitro* in terms of modulating the expression of MCP-1 and IL-6 in human THP-1 macrophages under inflammatory conditions. Accordingly, we have identified novel hits as potential drugs to develop lead candidates which could be useful for metabolic syndrome, type 2 diabetes, dyslipidaemia, MAFLD or inflammation, which can further progress to microvascular problems and cardiovascular events, primary causes of morbidity and death worldwide [32].

2. Results and discussion

2.1. Synthesis of benzopyran hydrazones

We prepared two series of benzopyran hydrazones/hydrazines containing benzothiazole moiety (*series 1*) or 1-[5-chloro-3-(trifluoromethyl)-2-pyridyl] (*series 2*). The benzopyran nucleus was synthesised *via* a chroman-4-one scaffold, which was obtained by the aldol condensation between an *ortho*-hydroxyacetophenone and a ketone in the presence of a secondary amine by Michael addition as previously reported [21–23]. The reaction started with the condensation between 2,5-dihydroxyacetophenone and ethyl levulinate as the proper ketone in the presence of pyrrolidine (Scheme 1). Then, the γ -benzopyrone was reduced under Clemmensen conditions using dust zinc in acid medium to afford the benzodihydropyran **1**, and its phenolic group was protected utilising *p*-fluorobenzyl chloride in the presence of potassium carbonate to give the *p*-fluorobenzyloxy benzodihydropyran **2**. The controlled reduction of the ester function of benzopyran **2** using DIBAL-H reagent allowed us to obtain the aldehyde intermediate **3**.

In a first approach, we prepared benzopyran hydrazones with a 3-carbon side chain. For this purpose, aldehyde intermediate **3** condensed with the available hydrazines such as 2-hydrazinobenzothiazole and 1-[5-chloro-3-(trifluoromethyl)-2-pyridyl]hydrazine in anhydrous dichloroethane gave imines (Schiff bases) with hydrazone moieties **4** (*series 1*) and **5** (*series 2*), respectively [33]. Deprotection of compounds

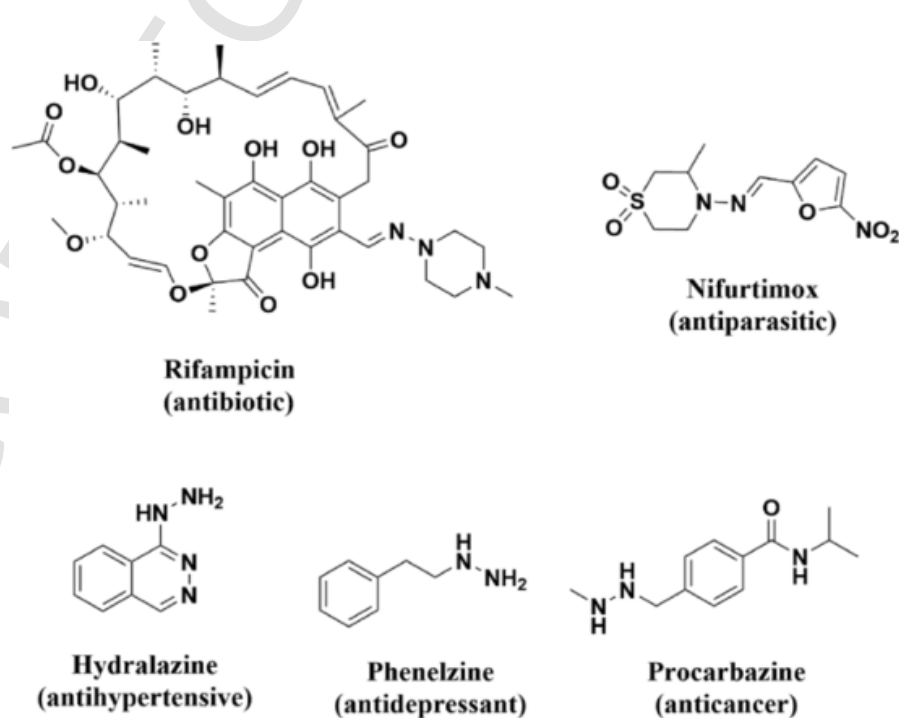


Fig. 2. Clinical drugs containing hydrazone ($\text{C}=\text{N}-\text{NH}$) or hydrazine ($\text{NH}-\text{NH}$) moiety.

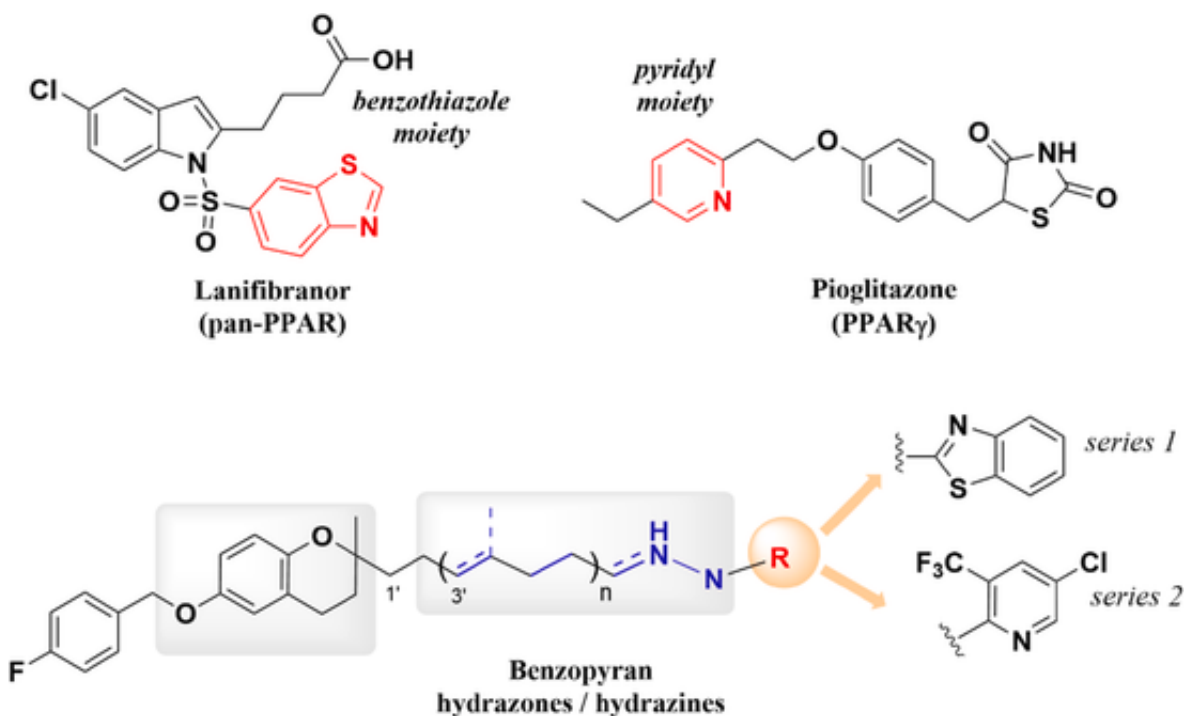
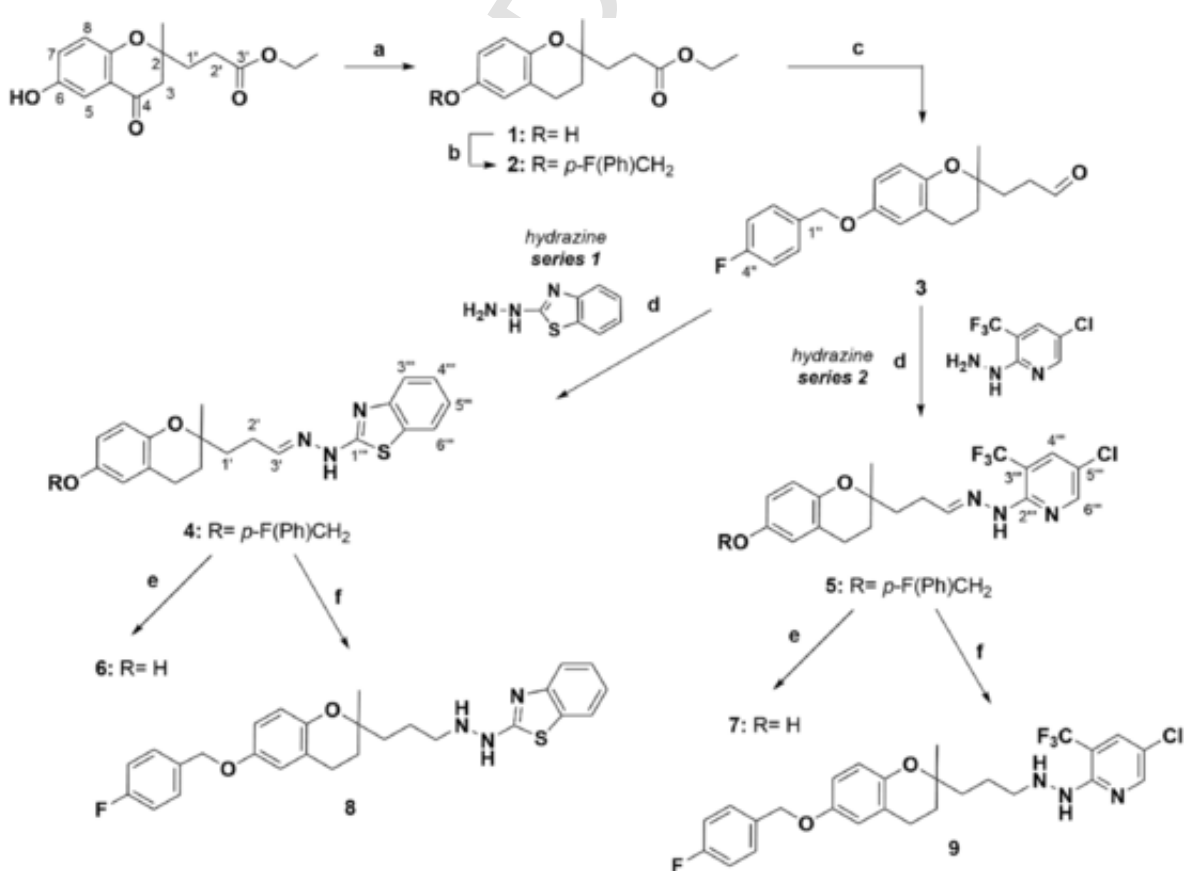


Fig. 3. Clinical drugs and designed benzopyran hydrazones/hydrazines containing benzothiazole or pyridinyl moiety.



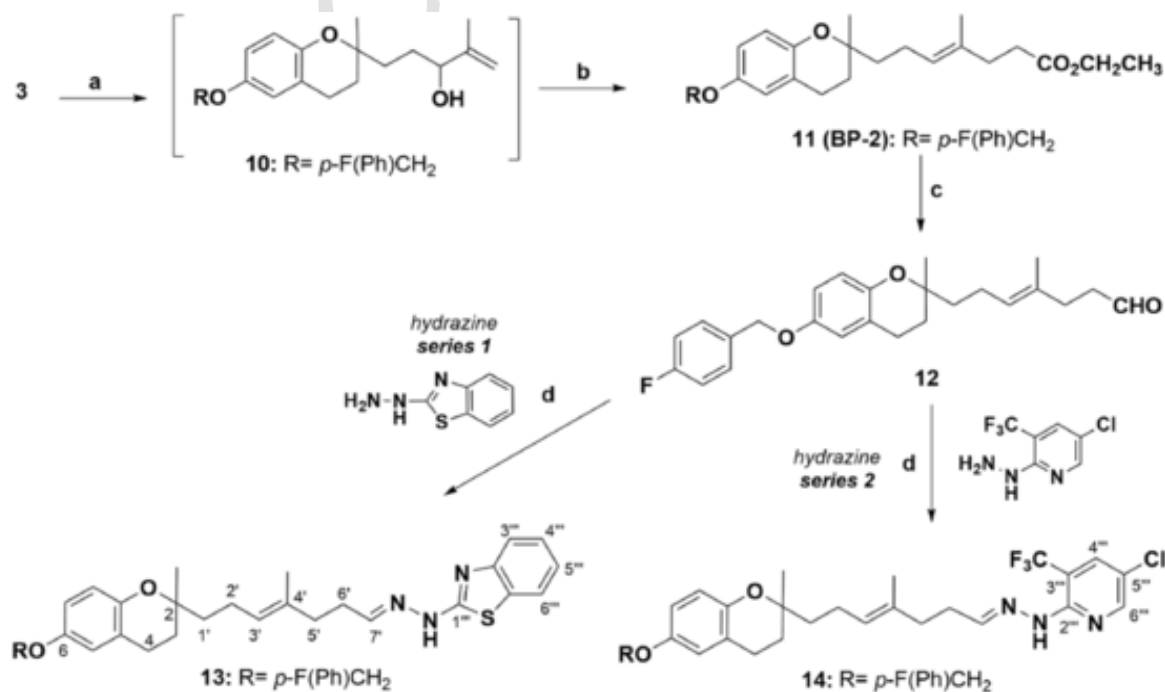
Scheme 1. Synthesis of 2-substituted benzopyrans containing hydrazone/hydrazine moiety. *Reagents and conditions:* (a) Zn dust/conc HCl, AcOH-H₂O (2:1, v/v), r.t., 1 h 30 min (58%); (b) *p*-fluorobenzyl chloride, K₂CO₃, EtOH, reflux, 4 h (79%); (c) 1 M DIBAL-H in THF, CH₂Cl₂, -78 °C, N₂, 15 min (92%); (d) hydrazines: 2-hydrazinobenzothiazole or 1-[5-Cl-3-(CF₃-2-pyridyl)]NHNH₂, (CH₂)₂Cl₂, r.t., N₂, 1 h (80% for 4; 89% for 5); (e) BBr₃, CH₂Cl₂, r.t., N₂, 1 h (91% for 6; 92% for 7); (f) NaBH₄CN, BF₃OEt, MeOH, N₂, reflux, 1 h (96% for 8; 75% for 9).

4 and 5 with boron tribromide afforded compounds 6 (series 1) and 7 (series 2), respectively, bearing both a hydrazone moiety and a free phenolic group (Scheme 1) [34]. The reduction of the imine double bond in hydrazones ($-C=N-NH-$) to attain hydrazines ($-CH_2-NH-NH-$) has been reported by catalytic hydrogenation under high pressure or hydride reductions, including lithium aluminium hydride [35], sodium borohydride in Raney nickel [36], sodium cyanoborohydride [37], the borane trimethylamine complex in hydrochloric acid [38] and magnesium in methanol [39], which are usually tedious or inefficient procedures. In our approach, hydrazones were reduced using a methodology previously reported to reduce quinolines to tetrahydroquinolines [40]. Thus, benzopyran hydrazines 8 (series 1) and 9 (series 2) were easily and efficiently prepared from their hydrazones 4 and 5, respectively, by sodium cyanoborohydride and boron trifluoride etherate as catalyst to generate diborane *in situ* (Scheme 1).

In a second approach, we synthesised two series of benzopyran hydrazones with a 7-carbon side chain (C-1' to C-7') instead of 3-carbons (C-1' to C-3'). The elongation of the hydrocarbon side chain from aldehyde 3 was performed by an efficient Grignard reaction, followed by Johnson-Claisen rearrangement to obtain benzopyran ester 11 [21,22,24]. The Grignard reaction consisted in the nucleophilic attack of propenyl magnesium bromide to the electrophilic carbon of aldehyde 3 to form a carbon-carbon bond. The Johnson-Claisen rearrangement of allylic alcohol intermediate 10 was carried out using 1,1,1-triethoxyethane and catalytic amounts of isobutyric acid. Then benzopyran ester 11 was subjected to controlled reduction with DIBAL-H reagent to give aldehyde 12. The condensation of aldehyde 12 with the corresponding hydrazines, such as 2-hydrazinobenzothiazole and 1-[5-chloro-3-(trifluoromethyl)-2-pyridyl]hydrazine in anhydrous dichloroethane gave benzopyran hydrazones 13 (series 1) and 14 (series 2), respectively (Scheme 2).

2.2. PPAR α , PPAR β/δ and PPAR γ agonist activity

All the synthesized compounds were assayed *in vitro* for hPPAR α , hPPAR β/δ or hPPAR γ transcriptional activity by a cell-based transactivation assay in Cos-7 cells properly transfected with a luciferase-reported plasmid in the presence of expression vectors pGAL4hPPAR α , pGAL4hPPAR β/δ and pGAL4hPPAR γ [24]. The activity of each compound was expressed as each compound' percentage of efficacy at 10 μ M by comparing to the maximal efficacy of the reference compounds: WY-14,643 (at 10 μ M), rosiglitazone (at 1 μ M) or GW501516 (at 1 μ M) as hPPAR α , hPPAR γ or hPPAR β/δ respectively. Half maximal effective concentration EC₅₀ was calculated by using the Prism software (Table 1). The results showed that benzopyran hydrazones 4 (series 1) and 5 (series 2) at 10 μ M displayed dual hPPAR α/γ partial activation. It was noteworthy that hydrazone framework, instead of the isoprenyl, also exerts a PPAR activity providing a new class of benzopyran agonists. Benzopyran hydrazone 14 (series 2), bearing an elongated 7-carbon side chain with an isoprenoid unit and 1-[5-chloro-3-(trifluoromethyl)-2-pyridyl]hydrazine moiety, displayed dual hPPAR α/δ activation with a full PPAR α agonism. SAR studies established that: i) the free phenol group was detrimental for PPAR activation and afforded non-active analogues 8 and 9, compared to *p*-fluorobenzylbenzopyran hydrazones 4 and 5, respectively; ii) the reduction of the imine bond of hydrazones 4 and 5 led to non-active hydrazines 6 and 7, which indicated that the C(sp²) = N-NH- function that contains a C=N bond conjugated with a lone pair of electrons of the amine nitrogen atom ($-NH-$) plays a key role in the interaction with the binding pocket of hPPARs; iii) the elongation of the isoprenyl side chain at 2-position to 7-carbons to give benzopyran 14 (series 2) drastically increased the activation for hPPAR α , and moderately for hPPAR β/δ instead of hPPAR γ moiety, but not in benzopyran 13 (series 1). Therefore, we have discovered novel hits (4, 5 and 14), containing a hydrazone framework which exhibited dual PPAR α/γ or PPAR α/δ partial agonism, depending on the length of the side chain. Hydrazones ($C=N^1-N^2$) have been reported to possess great intrinsic hydrolytic stability due to the participation of



Scheme 2. Synthesis of benzopyran hydrazones with a 7-carbon length side chain. *Reagents and conditions:* (a) $CH_3C(MgBr)=CH_2$, THF, $-78^\circ C$, N_2 , 3 h; (b) $MeC(OEt)_3$, isobutyric acid, $140^\circ C$, 2 h (48%); (c) 1 M DIBAL-H in THF, CH_2Cl_2 , $-78^\circ C$, 15 min (89%); (d) hydrazines: 2-hydrazinobenzothiazole or 1-[5-Cl-3-(CF₃-2-pyridyl)]NHNH₂, dry $(CH_2)_2Cl_2$, r.t, N_2 , 1 h (70% for 13; 60% for 14).

Table 1

Evaluation of agonist activity in a cell-based transactivation assays for human PPAR/Gal₄ receptors. EC₅₀ values against human PPARα/Gal₄, PPARβ/δ/Gal₄ and PPARγ/Gal₄ receptors.

	Efficacy (%) at 10 μmol/L			EC ₅₀ (nmol/L)		
	PPARα	PPARβ/δ	PPARγ	PPARα	PPARβ/δ	PPARγ
4	47	NA	39	493	NA	3,270
5	48	NA	42	226	NA	5,540
6	22	NA	14	NA	NA	NA
7	1	NA	8	NA	NA	NA
8	24	NA	15	NA	NA	NA
9	11	NA	16	NA	NA	NA
13	28	NA	13	NA	NA	NA
14	121	43	11	3,255	1,475	NA
WY-14,643	100	NA	NA	4,193	NA	NA
GW501516	NA	100	NA	NA	4	NA
Rosiglitazone	NA	NA	100	NA	NA	60

Efficacy: Emax was the maximal PPAR fold-activation relative to maximum activation obtained with WY14,643 (10 μM), GW501516 (1 μM) and rosiglitazone (1 μM) corresponded to 100% in GAL4 chimeric hPPARα, hPPARβ/δ and hPPARγ system. NA: not active.

N² in electron delocalization [41]. We previously demonstrated the importance of bioisosteric replacement in carboxylic function (polar head) of polycerasoidol by ester, amide and O-alkoxylated bioisosters to modulate hPPARα and hPPARγ interactions [20–23]. In addition, given the potential metabolic instability and toxicity associated to an acid functionality, the use of bioisosters could counter such issues and improve drug-like properties of the new PPAR agonists [42]. In this work, both benzothiazole and pyridyl groups have also shown ability to replace carboxylic moiety to activate hPPAR isoforms. Furthermore, these groups, which appear in many clinically approved drugs, have been reported to provide a good solubility range and stability in polar solvents and human plasma [43,44].

2.3. Molecular Modelling studies

At the molecular level, to understand the dual PPARα/γ agonism for hydrazones 4 and 5, as well as the dual PPARα/δ agonism for hydrazone 14, we carried out a combined analysis by means of a docking study and MD simulations. These studies predict how compounds 4, 5 and 14 bind in the same region of the active site of PPARα as that reported for WY-14,643 [45,46] (Fig. 4A–C). These results can be observed in the per residue analysis, which was performed on the different ligand-receptor complexes (Fig. S1, Supporting Information). MD simulations indicate that these molecules are arranged spatially in a slightly different way. In agreement with the results obtained for WY-14643, the simulations obtained for the complexes showed the relevance of His440, Leu321 and Ser280 for ligand binding [45,46]. The other residues with significant interactions to stabilise these complexes are Cys276, Thr464, Lys358 and Ile317. In accordance with our experimental data, the interactions obtained for compounds 4 and 5 were generally weaker than those observed for WY-14,643 (Fig. S1), while the interactions obtained for hydrazone 14 were closely related to those observed for the reference compound (Fig. S1). With the PPARγ receptor, our simulations indicated that hydrazones 4 and 5 bound to the active site in a closely related way to that reported for rosiglitazone [47,48] (Fig. 3D and E). Indeed, hydrazones 4 and 5 interacted mainly with Cys285, Arg288, Tyr324, Leu330, Ile342, Phe366, Met364, His449 and Tyr473, although they generally displayed weaker interactions compared to rosiglitazone (Fig. S1). In contrast, the complex of hydrazone 14 with PPARδ (Fig. 4F) showed this hydrazone with a 7-carbon side chain to be spatially arranged in a similar way to reference compound GW501516 [49]. The analysis per residues of 14 (Fig. S1) showed that its interactions with PPARδ were significantly weaker to those formed by GW501516, which falls in line with our experimental results.

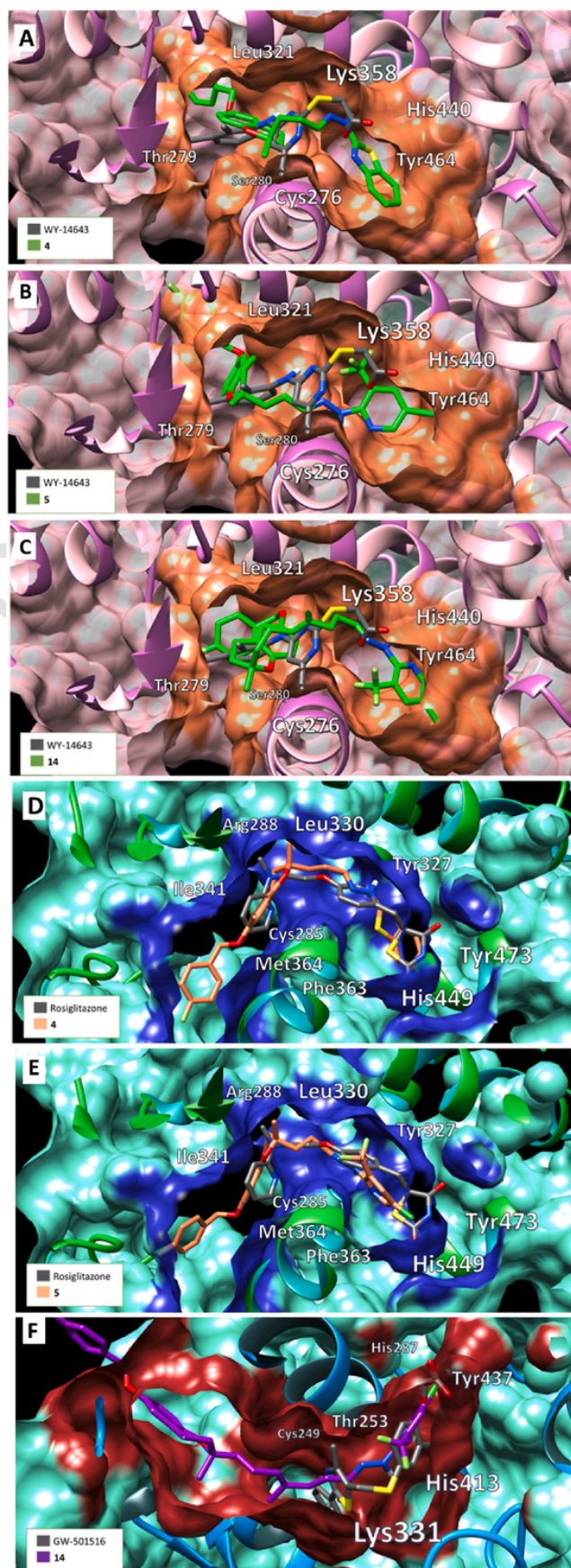


Fig. 4. Spatial view of interactions for WY-14,643, rosiglitazone or GW501516, and active benzopyran hydrazones bonded in the binding pocket of PPAR α , PPAR γ or PPAR δ by docking experiments. Spatial view of (A) WY-14,643 (grey) and **4** (green)/PPAR α interaction, (B) WY-14,643 (grey) and **5** (green)/PPAR α , (C) WY-14,643 (grey) and **14** (green)/PPAR α , (D) rosiglitazone (grey) and **4** (pink)/PPAR γ interaction, (E) rosiglitazone (grey) and hydrazone **5** (purple)/PPAR γ , (F) GW501516 (grey) and **14** (pink)/PPAR δ . The orange, blue or burgundy zone represent the binding site for PPAR α , PPAR γ or PPAR δ , respectively, and the rest is shown in pink color or light green. The names of the residues stabilizing the complex are remarked in the figure.

2.4. Anti-inflammatory effects of benzopyran hydrazones **4**, **5** and **14**

In order to evaluate the anti-inflammatory effect of the dual PPAR α / γ and PPAR α / δ agonists on macrophages, the PMA-differentiated THP-1 cells were treated with benzopyran hydrazones **4**, **5** and **14** at 10 μ M prior to the LPS stimulation. The mRNA expression and secretion of the pro-inflammatory markers, such as chemokine MCP-1 and cytokine IL-6, were determined in the LPS-stimulated THP-1 macrophages for 4 h and 24 h. The results at 4 h showed that benzopyran **4**, with a 3-carbon side chain and benzothiazole moiety, decreased the gene expression of MCP-1 and IL-6 by 67% and 71%, respectively. Its pyridyl analogues **5** and **14**, respectively bearing a 3-carbon and 7-carbon side chain, showed a moderate activity. The results at 24 h revealed that benzopyran **4** inhibited the gene expression of MCP-1 and IL-6 by 71% and 93%, respectively, but also the chemo- and cytokine secretion by 85% and 79%, respectively. Its pyridyl analogue **5** moderately reduced the gene expression of MCP-1 (54%) and IL-6 (63%), and did not inhibit their secretion in the LPS-stimulated THP-1 macrophages. Finally, dual PPAR δ / γ agonist **14** lowered the IL-6 gene expression levels by 88% at 24 h and reduced the secretion of both MCP-1 and IL-6 by 70–80% in the LPS-stimulated THP-1 macrophages (Fig. 5). Therefore, **4**, **5** and **14** may ameliorate the inflammation state associated with the progression of metabolic disorders.

2.5. Anti-inflammatory effects of benzopyran hydrazones **4**, **5** and **14** via NF- κ B

In order to investigate the intracellular signalling pathways underlying the anti-inflammatory effect of hydrazones **4**, **5** and **14**, the THP-1 cells were stimulated with LPS for 1 h in the presence or absence of compounds (10 μ M, 24 h) prior to the pathway analysis. The results showed that the three hydrazones significantly blunted the TNF α -induced phosphorylation of NF- κ B by 34% for **4**, 35% for **5** and 36% for **14** (Figs. 6 and 7).

2.6. Cytotoxicity study of compounds **4**, **5** and **15**

Apoptosis cell death was studied by an Annexin V-FITC/PI dual staining assay on THP-1 cells. None of the three compounds showed toxicity at doses 10 μ M and 30 μ M, and only hydrazone **5** displayed slight toxicity at the highest concentration of 100 μ M (Figs. 8 and 9).

3. Conclusions

We herein efficiently prepared two series of benzopyran hydrazones and hydrazines as *polycerasoidol* analogues containing the hydrazone function in the 3-carbon or 7-carbon side chain at 2-position of the benzopyran nucleus. Benzopyran hydrazones **4** and **5** with a 3-carbon side chain, showed dual hPPAR α / γ partial agonism, and hydrazone **14**, with 1-[5-chloro-3-(trifluoromethyl)-2-pyridyl]hydrazone moiety on the prenylated 7-carbon side chain, exerted dual PPAR α / δ partial agonism. However, the direct reduction of hydrazones **4** and **5** effectively provided hydrazine derivatives **8** and **9**, respectively, which were inactive in any PPAR isoform. The SAR studies indicated that the side chain at

the 2-position in the benzopyran nucleus required the C=N double bond in the hydrazone function to activate the PPAR isoforms. Structurally speaking, the hydrazone function alongside the presence or absence of a prenylated moiety on the elongated side chain can modulate the activation of the PPAR isoforms. In addition, hydrazones **4**, **5** and **14** greatly attenuated inflammatory markers such as IL-6 and MCP-1, on the THP-1 cells via NF- κ B activation, which are associated with obesity, type 2 diabetes and the progression of metabolic disorders. Therefore, benzopyran hydrazones emerge as novel dual PPAR α / γ or dual PPAR α / δ agonists with the potential for treat metabolic diseases.

4. Experimental section

4.1. Chemistry methods

High-resolution electrospray ionization mass spectrometry (HRMS (ESI)) was performed on a TripleTOFTM 5600 LC/MS/MS System (AB SCIEX) (Toronto, Canada). Liquid chromatography-mass spectrometry detection was performed on a liquid chromatography UHPLC apparatus (Shimadzu, LCMS-8040) coupled to a tandem mass spectrometry (MS/MS) triple quadrupole equipped with electrospray ionization (ESI) ion source (Shimadzu, Kyoto, Japan). ¹H and ¹³C NMR spectra were recorded on a Bruker AC-300 or AC-500 (Bruker Instruments, Kennewick, WA). The assignments in ¹H and ¹³C NMR were made by COSY 45, HSQC and HMBC correlations. Chemical shifts (δ) are reported in ppm relative to an internal deuterated solvent reference, with multiplicities indicated as s (singlet), br (broad singlet), d (doublet), t (triplet), q (quartet) m (multiplet) or dd (doublet). All reactions were monitored by analytical TLC with silica gel 60 F254 (Merck 5554). All reactions were monitored by analytical thin-layer chromatography with silica gel 60 F₂₅₄ (Merck 5554; Merck Group, Darmstadt, Germany). Residues were purified by silica gel column chromatography (40–63 μ m, Merck Group). Solvents and reagents were purchased from the commercial sources Scharlab S.L. (Barcelona, Spain) and Sigma-Aldrich (St. Louis, MO), respectively, and used without further purification unless otherwise noted. Dry and freshly distilled solvents were used in those reactions performed under N₂. Quoted yields are of purified material. Final compounds were purified to \geq 95% as assessed by ¹H NMR and LC-MS/MS analysis.

4.2. Ethyl 3-(6-(*p*-fluorobenzyloxy)-2-methyldihydrobenzopyran-2-yl)propanoate (**2**)

Ethyl 3-(6-(hydroxy-2-methylbenzopyran-4-one-2-yl)propanoate (1.2 g, 4.32 mmol) was dissolved in a mixture of AcOH-H₂O (2:1, v/v) (14 mL). Then, Zn dust (5.07 g, 76.45 mmol) followed by concentrated HCl (9 mL) was added slowly in small portions for 30 min. After stirring for an additional 1 h at room temperature, water (15 mL) was added and the mixture was extracted with AcOEt (3 \times 15 mL). The organic layers were combined, dried over anhydrous Na₂SO₄, and evaporated under reduced pressure. The residue was purified by column chromatography (hexane/EtOAc, 85:15) to yield the ethyl 3-(6-(hydroxy-2-methyldihydrobenzopyran-2-yl)propanoate (**1**, 0.66 g, 2.50 mmol, 58%) as a colorless oil [24]. A solution of benzopyran ester **1** (500 g, 1.89 mmol), *p*-fluorobenzyl chloride (0.3 mL, 2.46 mmol), anhydrous K₂CO₃ (0.4 g, 2.83 mmol) in absolute EtOH (20 mL) was refluxed under N₂ for 4 h. The mixture was evaporated, water was added (20 mL) and the mixture was extracted with dichloromethane (3 \times 15 mL). The organic layers were combined, washed with 1 M HCl and brine, dried over anhydrous Na₂SO₄, and evaporated under reduced pressure. The residue was purified by column chromatography (hexane/EtOAc, 90:10) to yield the O-protected benzopyran ester (**2**) (556 mg, 1.49 mmol, 79%) as a colorless oil. ¹H NMR (300 MHz, CDCl₃) δ 7.41–7.36 (m, 2H, CH-2", CH-6"), 7.09–7.03 (m, 2H, CH-3", CH-5"), 6.72–6.67 (m, 3H, CH-5, CH-7, CH-8), 4.94 (s, 2H, OCH₂Ph-*p*-F), 4.13

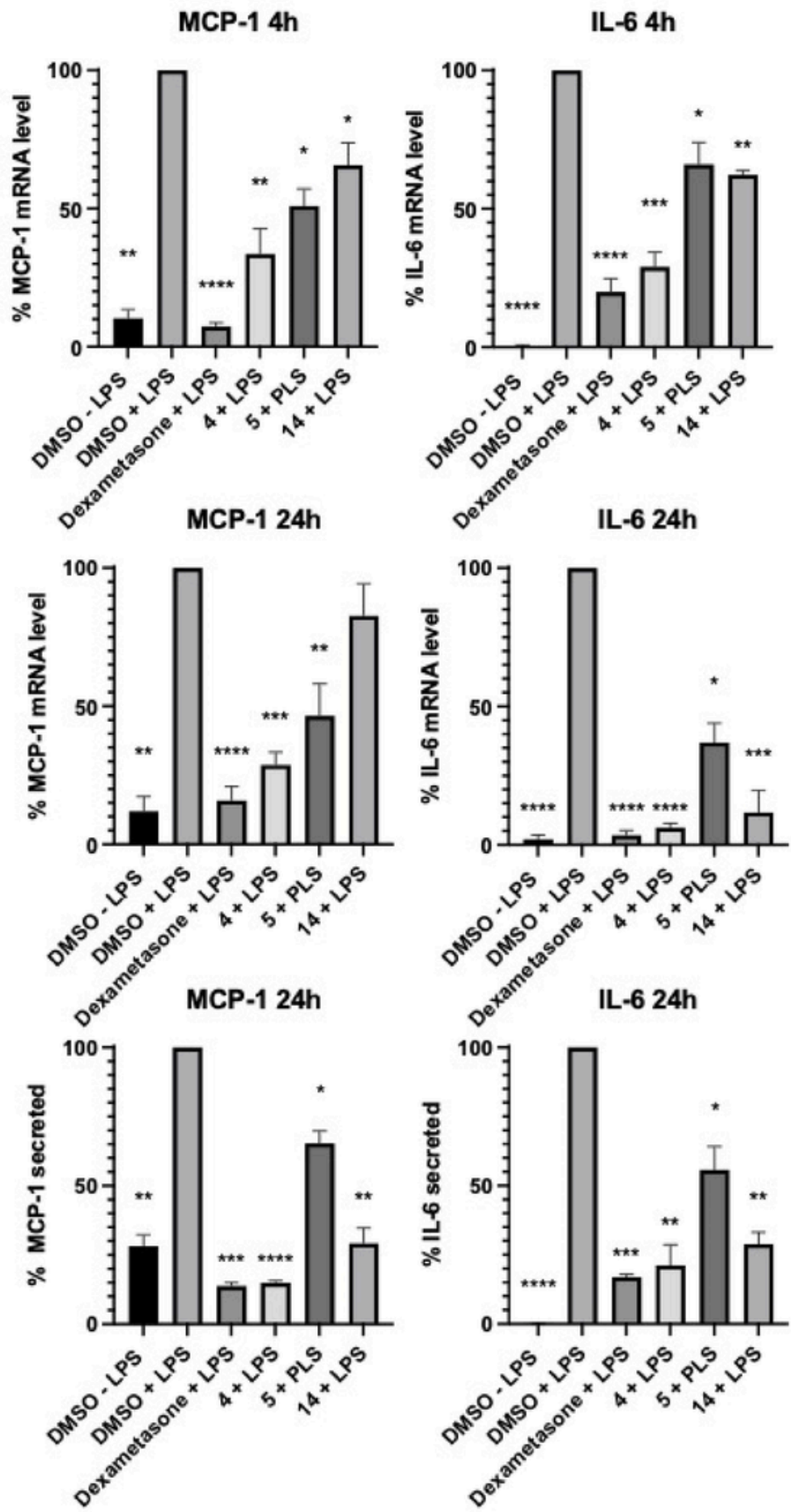


Fig. 5. Anti-inflammatory effects of hydrazones **4**, **5**, **14**, and dexamethasone by inhibition of pro-inflammatory cytokine IL-6 and chemokine MCP-1 production in LPS-induced THP-1 cells. THP-1 cells were pretreated with benzopyran hydrazones **4**, **5** and **14** (10 μ M) or dexamethasone (Dexa) (positive control at 10^{-8} μ M) for 1 h before stimulation with LPS (100 ng/mL) for 4 h and 24 h. The levels of IL-6 and MCP-1 were measured using qPCR (A, B, C, D) or ELISA (E, F). The data are expressed as % of LPS stimulated condition and presented as means \pm SD of three independent experiments performed in triplicate. *P < 0.05, **P < 0.01, ***P < 0.001, ****P < 0.0001 vs. LPS-induced group.

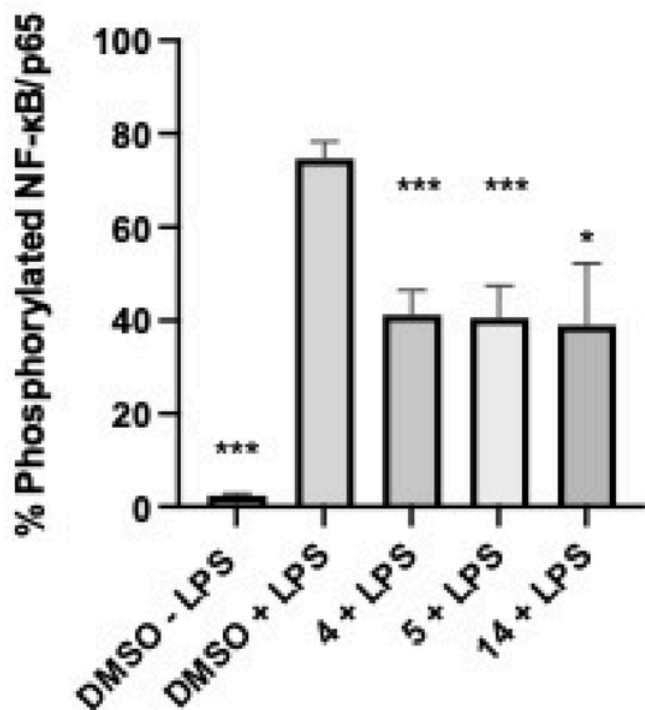


Fig. 6. Phosphorylated NF-κB/p65% of hydrazones **4**, **5**, **14** at 10 μ M. on the THP-1 cells. The data are presented as means \pm SD of three independent experiments performed in triplicate. *P < 0.05, ***P < 0.001 vs. LPS-induced group.

(q, J = 7.1 Hz, 2H, CO₂CH₂CH₃), 2.76 (t, J = 6.7 Hz, 2H, CH₂-4), 2.48 (t, J = 7.7 Hz, 2H, CH₂-2'), 2.0–1.75 (m, 4H, CH₂-3, CH₂-1'), 1.24 (t, J = 7.2 Hz, 3H, CO₂CH₂CH₃), 1.23 (s, 3H, CH₃-2); ¹³C NMR (75 MHz, CDCl₃) δ 173.6 (COOCH₂CH₃), 162.3 (d, J_{CF} = 244 Hz, C-4'), 152.0 (C-6), 147.9 (C-8a), 133.1 (d, J_{CF} = 3 Hz, C-1'), 129.1 (d, J_{CF} = 8 Hz, CH-2'), 121.4 (C-4a), 117.7 (CH-5), 115.2 (d, J_{CF} = 25 Hz, CH-3'), 115.1 (CH-7), 114.4 (CH-8), 74.6 (C-2), 69.9 (OCH₂Ph-p-F), 60.3 (CO₂CH₂CH₃), 34.3 (CH₂-1'), 31.0 (CH₂-3), 28.7 (CH₂-2'), 23.6 (CH₃-2), 22.2 (CH₂-4), 14.1 (CO₂CH₂CH₃); HREIMS m/z calcd for C₂₂H₂₅O₄F [M] + 372.1737, found: 372.1730.

4.3. 3-(6-((p-Fluorobenzyl)oxy)-2-methyldihydrobenzopyran-2-yl)propanal (**3**)

A solution of **2** (250 mg, 0.67 mmol) in anhydrous dichloromethane (10 mL) at -78 °C under N₂ atmosphere was stirred for 10 min. To this solution was added dropwise 4.4 mL of 1.0 M DIBAL-H solution in THF. After 15 min, the mixture was quenched by addition of 5 mL of MeOH and 10 mL of half-saturated aqueous NH₄Cl solution. The reaction mixture was stirred for additional 10 min at room temperature and concentrated in vacuo. Then, water was added and extracted with EtOAc (3 x 15 mL). The combined organic layers were washed with water, dried over anhydrous Na₂SO₄ and evaporated to dryness. The residue was purified by silica gel column chromatography (hexane/EtOAc, 90:10) to afford the corresponding aldehyde **3** (203 mg, 0.62 mmol, 92%) as a colorless oil. ¹H NMR (300 MHz, CDCl₃) δ 9.78 (t, J = 1.6 Hz, 1H, CHO), 7.39–7.37 (m, 2H, CH-2', CH-6'), 7.08–7.04 (m, 2H, CH-3', CH-5'), 6.74–6.67

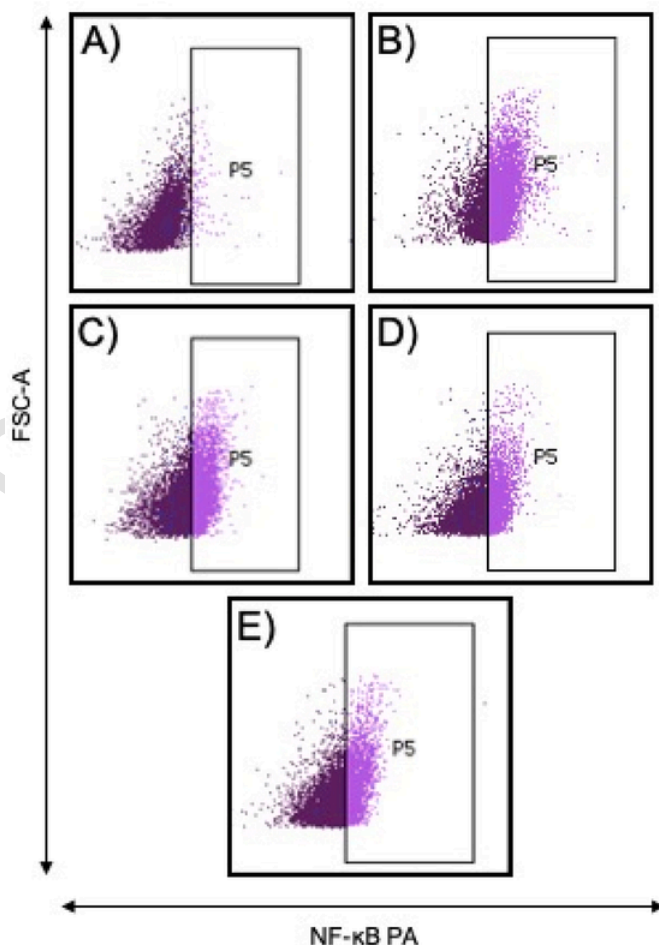


Fig. 7. Representative images of one of the flow cytometry analyses for **4**, **5** and **14** at 10 μ M of activated NF-κB on the THP-1 macrophages. A) DMSO, B) **4**, C) **5**, D) **14**.

(m, 3H, CH-5, CH-7, CH-8), 4.94 (s, 2H, OCH₂Ph-p-F), 2.77–2.74 (m, 2H, CH₂-4), 2.62–2.59 (m, 2H, CH₂-2'), 2.03–1.75 (m, 4H, CH₂-3, CH₂-1'), 1.26 (s, 3H, CH₃-2); ¹³C NMR (75 MHz, CDCl₃) δ 202.2 (CHO), 162.4 (d, J_{CF} = 244 Hz, C-4'), 152.1 (C-6), 147.7 (C-8a), 133.1 (d, J_{CF} = 3 Hz, C-1'), 129.3 (d, J_{CF} = 8 Hz, CH-2', CH-6'), 121.4 (C-4a), 117.7 (CH-5), 115.2 (d, J_{CF} = 25 Hz, CH-3', CH-5'), 115.2 (CH-7), 114.5 (CH-8), 74.6 (C-2), 69.9 (OCH₂Ph-p-F), 38.4 (CH₂-2'), 31.8 (CH₂-1'), 31.2 (CH₂-3), 23.7 (CH₃-2), 22.3 (CH₂-4); HRMS (ESI) m/z calcd for C₂₀H₂₁O₃F [M + H] + 329.1547, found: 329.1552.

4.4. General procedure for synthesis of hydrazone benzopyrans (**4**, **5**)

A mixture of aldehyde **3** (58.1 mg, 0.18 mmol) and 2-hydrazinobenzothiazole (48.6 mg, 0.294 mmol) or 1-[5-chloro-3-(trifluoromethyl)-2-pyridyl]hydrazine (62.2 mg, 0.29 mmol) in anhydrous dichloroethane (3 mL) was stirred for 1 h under N₂. The resulting mixture was basified with 5% aq NH₃ and then, water was added and extracted EtOAc (3 x 5 mL). The combined organic layers were dried over anhydrous Na₂SO₄ and evaporated to dryness. The residues obtained were purified by silica gel column chromatography (hexane/

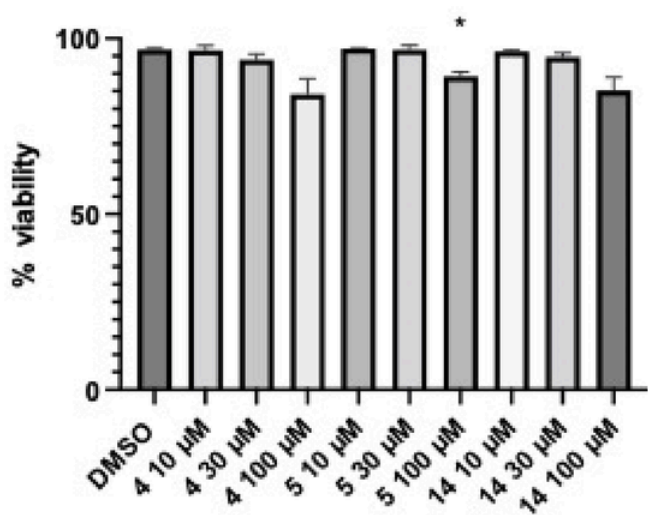


Fig. 8. Cytotoxic effects of hydrazones 4, 5, 14 on the THP-1 cells. The data are presented as means \pm SD of three independent experiments performed in triplicate. *P < 0.05 vs. LPS-induced group.

EtOAc, 80:20) to afford hydrazone 4 (68.6 mg, 0.14 mmol, 80 %) as a reddish oil or 5 (82.3 mg, 0.16 mmol, 89 %) as a yellowish oil.

4.4.1. 2-(2-(3-(6-((p-Fluorobenzyl)oxy)-2-methylbenzodihydropyran-2-yl)propylidene)hydrazineyl)benzo[d]thiazole (4)

^1H NMR (300 MHz, CDCl_3) δ 8.96 (1H, brs, NH), 7.62 (dd, J = 7.8 Hz, 1.3 Hz, 1H, CH-3'''), 7.42–7.35 (m, 3H, CH-2'', CH-6'', CH-6'''), 7.29–7.25 (m, 2H, CH-4''', CH-3'), 7.11–7.03 (m, 3H, CH-3'', CH-5'', CH-5'''), 6.72–6.67 (m, 3H, CH-5, CH-7, CH-8), 4.92 (s, 2H, $\text{OCH}_2\text{Ph-p-F}$), 2.77–2.75 (m, 2H, CH_2 -4), 2.36–2.31 (m, 2H, CH_2 -2'), 1.78–1.74 (m, 4H, CH_2 -1', CH_2 -3), 1.27 (s, 3H, CH_3 -2); ^{13}C NMR (75 MHz, CDCl_3): δ 168.9

(C-1'''), 162.4 (d, J_{CF} = 244 Hz, C-4''), 152.0 (C-6), 149.9 (C-2a'''), 147.9 (CH-3', C-8a), 133.1 (d, J_{CF} = 3 Hz, C-1''), 129.8 (C-6a'''), 129.2 (d, J_{CF} = 8 Hz, CH-2'', CH-6''), 125.9 (CH-4'''), 121.7 (CH-5'''), 121.5 (C-4a), 121.3 (CH-3'''), 117.7 (CH-5), 117.6 (CH-6'''), 115.3 (d, J_{CF} = 21 Hz, CH-3'', CH-5''), 115.2 (CH-7), 114.4 (CH-8), 75.1 (C-2), 69.9 ($\text{OCH}_2\text{Ph-p-F}$), 35.7 (CH_2 -1'), 31.1 (CH_2 -3), 26.7 (CH_2 -2'), 23.9 (CH_3 -2), 22.3 (CH_2 -4); HRMS (ESI) m/z calcd for $\text{C}_{27}\text{H}_{26}\text{FN}_3\text{O}_2\text{S}$ [M+H] $^+$ + 476.1803, found: 476.1808.

4.4.2. 5-Chloro-2-(2-(3-(6-((p-fluorobenzyl)oxy)-2-methylbenzodihydropyran-2-yl)propylidene)hydrazineyl)-3-(trifluoromethyl)pyridine (5)

^1H NMR (300 MHz, CDCl_3) δ 8.47–8.44 (m, 1H, CH-6'''), 8.36–8.33 (brs, 1H, NH), 7.72 (d, J = 2 Hz, 1H, CH-4'''), 7.42–7.36 (m, 3H, CH-2'', CH-6'', CH-3'), 7.07–7.01 (m, 2H, CH-3'', CH-5''), 6.75–6.64 (m, 3H, CH-5, CH-7, CH-8), 4.92 (s, 2H, $\text{OCH}_2\text{Ph-p-F}$), 2.78–2.71 (m, 2H, CH_2 -4), 2.66–2.57 (m, 2H, CH_2 -2'), 1.96–1.72 (m, 4H, CH_2 -3, CH_2 -1'), 1.29 (s, 3H, CH_3 -2); ^{13}C NMR (75 MHz, CDCl_3): δ 162.4 (d, J_{CF} = 244 Hz, C-4''), 152.3 (q, J_{CF} = 4 Hz, C-2''), 152.0 (C-6), 149.6 (CH-3'), 147.8 (C-8a), 144.5 (CH-6''), 133.8 (q, J_{CF} = 3 Hz, CH-4'''), 133.1 (d, J_{CF} = 3 Hz, C-1'''), 129.2 (d, J_{CF} = 8 Hz, CH-2'', CH-6''), 123.2 (q, J_{CF} = 270 Hz, CF_3), 121.6 (C-4a), 118.5 (q, J_{CF} = 33 Hz, C-3''), 117.8 (CH-5), 115.3 (d, J_{CF} = 21 Hz, CH-3'', CH-5''), 114.6 (CH-7), 114.3 (C-5''), 113.8 (CH-8), 75.2 (C-2), 70.0 ($\text{OCH}_2\text{Ph-p-F}$), 36.4 (CH_2 -1'), 31.2 (CH_2 -3), 26.9 (CH_2 -2'), 23.9 (CH_3 -2), 22.3 (CH_2 -4); HRMS (ESI) m/z calcd for $\text{C}_{26}\text{H}_{24}\text{ClF}_4\text{N}_3\text{O}_2$ [M+H] $^+$ + 522.1566, found: 522.1567.

4.5. General procedure for O-deprotection to prepare compounds 6 and 7

A solution of compound 4 (30 mg, 0.063 mmol) or 5 (33 mg, 0.063 mmol) in anhydrous dichloromethane (1 mL) was added BBr_3 (0.25 mL, 0.25 mmol) at -78°C , and stirred for 15 min under N_2 atmosphere. Then, the reaction mixture was stirred under N_2 and at room temperature for an additional 45 min. The resulting mixture was basi-

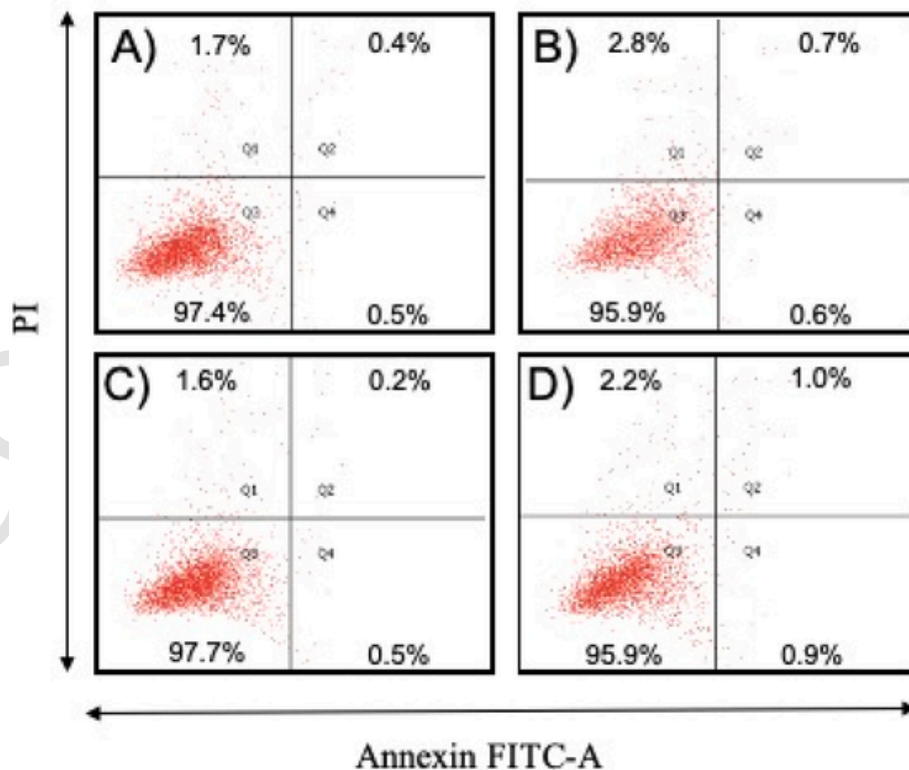


Fig. 9. Representative images of one of the apoptosis/necrosis analyses for 4, 5 and 14 at 30 μM on the THP-1 macrophages. A) DMSO, B) 4, C) 5, D) 14.

fied with 5% NH_3 and then, water was added and extracted with EtOAc (3 x 5 mL). The combined organic layers were dried over anhydrous Na_2SO_4 and evaporated to dryness. The residue obtained was purified by silica gel column chromatography ($\text{CH}_2\text{Cl}_2/\text{MeOH}$, 98:2) to afford compound **6** (21 mg, 0.06 mmol, 91 %) as a greenish oil and compound **7** (24 mg, 0.06 mmol, 92 %) as a yellowish oil, respectively.

4.5.1. 2-(3-(2-(Benzo[d]thiazol-2-yl)hydrazineylidene)propyl)-2-methylbenzodihydropyran-6-ol (**6**)

^1H NMR (300 MHz, CDCl_3 + 1 drop CD_3OD) δ 7.59 (dd, J = 7.8 Hz, 1.3 Hz, 1H, CH-3''), 7.45–7.42 (m, 1H, CH-6''), 7.37–7.23 (m, 2H, CH-4'', CH-3'), 7.16–7.06 (m, 1H, CH-5''), 6.67–6.43 (m, 3H, CH-5, CH-7, CH-8), 2.75–2.65 (m, 2H, CH_2 -4), 2.51–2.37 (m, 2H, CH_2 -2'), 1.91–1.64 (m, 4H, CH_2 -1', CH_2 -3), 1.27 (s, 3H, CH_3 -2); ^{13}C NMR (75 MHz, CDCl_3 + 1 drop CD_3OD): δ 168.0 (C-1''), 149.9 (C-2a''), 149.4 (C-6), 147.7 (C-8a), 146.9 (CH-3'), 128.9 (C-6a''), 126.3 (CH-4''), 122.4 (CH-5''), 121.6 (C-4a), 121.3 (CH-3''), 117.7 (CH-5), 117.4 (CH-6''), 115.3 (CH-7), 114.5 (CH-8), 74.9 (C-2), 35.5 (CH_2 -1'), 31.2 (CH_2 -3), 26.9 (CH_2 -2'), 23.9 (CH $_3$ -2), 22.1 (CH $_2$ -4); HRMS (ESI) m/z calcd for $\text{C}_{20}\text{H}_{22}\text{N}_3\text{O}_2\text{S}$ [M + H] $^+$ + 368.1433, found: 368.1417.

4.5.2. 2-(3-(2-(5-chloro-3-(trifluoromethyl)pyridin-2-yl)hydrazineylidene)propyl)-2-methylbenzodihydropyran-6-ol (**7**)

^1H NMR (300 MHz, CDCl_3 + 1 drop CD_3OD) δ 8.39–8.38 (m, 1H, CH-6''), 7.90 (brs, 1H, NH), 7.74–7.73 (m, 1H, CH-4''), 7.31 (t, J = 3 Hz, 1H, CH-3'), 6.64–6.52 (m, 3H, CH-5, CH-7, CH-8), 2.77–2.69 (m, 2H, CH_2 -4), 2.62–2.55 (m, 2H, CH_2 -2'), 1.92–1.72 (m, 4H, CH_2 -3, CH_2 -1'), 1.28 (s, 3H, CH_3 -2); ^{13}C NMR (75 MHz, CDCl_3 + 1 drop CD_3OD) δ 150.8 (CH-6''), 149.6 (q, J_{CF} = 4 Hz, C-2''), 148.8 (C-8a, C-6), 147.4 (CH-3'), 135.4 (q, J_{CF} = 4 Hz, CH-4''), 123.2 (q, J_{CF} = 270 Hz, CF $_3$), 121.7 (C-4a), 118.5 (q, J_{CF} = 33 Hz, C-3''), 117.7 (CH-5), 115.4 (CH-7), 114.6 (CH-8), 108.8 (C-5''), 75.0 (C-2), 36.2 (CH_2 -1'), 31.1 (CH_2 -3), 26.8 (CH $_2$ -2'), 23.9 (CH $_3$ -2), 22.1 (CH $_2$ -4); HRMS (ESI) m/z calcd for $\text{C}_{19}\text{H}_{17}\text{ClF}_3\text{N}_3\text{O}_2$ [M + H] $^+$ + 412.1034, found: 412.1028.

4.6. General procedure for synthesis of hydrazine benzopyrans (**8**, **9**)

A solution of compound **4** (37.9 mg, 0.08 mmol) or **5** (41.4 mg, 0.08 mmol) in anhydrous MeOH (4 mL) was added NaBH_4CN (15 mg, 0.238 mmol) and two drops of BF_3OEt . The reaction was refluxed for 1 h under N_2 atmosphere. The resulting mixture was basified with 5% NH_3 and then, water was added and extracted ethyl acetate (3 x 5 mL). The combined organic layers were washed with water, dried over anhydrous Na_2SO_4 and evaporated to dryness. The residue obtained was purified by silica gel column chromatography (hexane/EtOAc, 60:40 or hexane/EtOAc, 85:15) to afford compound **8** (37 mg, 0.08 mmol, 96%) as a bluish grey oil and compound **9** (31 mg, 0.06 mmol, 75%) as a red-dish yellow oil.

4.6.1. 2-(2-(3-(6-((p-Fluorobenzyl)oxy)-2-methylbenzodihydropyran-2-yl)propyl)hydrazineyl) benzo[d]thiazole (**8**)

^1H NMR (300 MHz, CDCl_3) δ 7.64 (dd, J = 8 Hz, 1.2 Hz, 1H, CH-3''), 7.48 (dd, J = 8 Hz, 1.2 Hz, 1H, CH-6''), 7.43–7.37 (m, 2H, CH-2'', CH-6''), 7.29 (td, J = 8 Hz, 1.2 Hz, 1H, CH-4''), 7.13–7.03 (m, 3H, CH-3'', CH-5'', CH-5''), 6.75–6.65 (m, 3H, CH-5, CH-7, CH-8), 4.94 (s, 2H, $\text{OCH}_2\text{Ph-p-F}$), 3.07–2.92 (m, 2H, CH_2 -3'), 2.71 (t, J = 7 Hz, 2H, CH_2 -4), 1.82–1.61 (m, 6H, CH_2 -1', CH_2 -2', CH_2 -3), 1.24 (s, 3H, CH_3 -2); ^{13}C NMR (75 MHz, CDCl_3): δ 174.0 (C-1''), 162.3 (d, J_{CF} = 244 Hz, C-4''), 152.3 (C-6), 151.9 (C-2a''), 148.0 (C-8a), 133.1 (d, J_{CF} = 3 Hz, C-1''), 130.6 (C-6a''), 129.2 (d, J_{CF} = 8 Hz, CH-2'', CH-6''), 125.6 (CH-4''), 121.6 (C-4a), 121.2 (CH-3''), 121.0 (CH-5''), 118.3 (CH-6''), 117.7 (CH-5), 115.3 (d, J_{CF} = 21 Hz, CH-3'', CH-5''), 115.1 (CH-7), 114.3 (CH-8), 75.4 (C-2), 69.9 ($\text{OCH}_2\text{Ph-p-F}$), 52.6 (CH_2 -3'), 36.9 (CH_2 -1'), 30.8 (CH_2 -3), 23.8 (CH $_3$ -2), 22.3 (CH_2 -2'), 22.0 (CH_2 -4); HRMS (ESI) m/z calcd for $\text{C}_{27}\text{H}_{26}\text{FN}_3\text{O}_2\text{S}$ [M + H] $^+$ + 476.1803, found: 476.1802.

4.6.2. 5-Chloro-2-(2-(3-(6-((p-fluorobenzyl)oxy)-2-methylbenzodihydropyran-2-yl)propyl)hydrazineyl)-3-(trifluoromethyl)pyridine (**9**)

^1H NMR (300 MHz, CDCl_3) δ 8.32–8.28 (m, 1H, CH-6''), 7.72 (d, J = 2.0 Hz, 1H, CH-4''), 7.42–7.33 (m, 2H, CH-2'', CH-6''), 7.11–7.01 (m, 2H, CH-3'', CH-5''), 6.77–6.61 (m, 3H, CH-5, CH-7, CH-8), 4.94 (s, 2H, $\text{OCH}_2\text{Ph-p-F}$), 2.98–2.89 (m, 2H, CH_2 -3'), 2.80–2.71 (m, 2H, CH_2 -4), 1.88–1.61 (m, 6H, CH_2 -3, CH_2 -1', CH_2 -2'), 1.27 (s, 3H, CH_3 -2); ^{13}C NMR (75 MHz, CDCl_3): δ 162.4 (d, J_{CF} = 244 Hz, C-4''), 153.3 (q, J_{CF} = 4 Hz, CH-4''), 152.0 (C-6), 149.6 (CH-6''), 148.2 (C-8a), 135.2 (q, J_{CF} = 4 Hz, CH-4''), 133.3 (d, J_{CF} = 3 Hz, C-1''), 129.2 (d, J_{CF} = 8 Hz, CH-2'', CH-6''), 123.2 (q, J_{CF} = 270 Hz, CF $_3$), 121.7 (C-4a), 119.9 (q, J_{CF} = 33 Hz, C-3''), 117.8 (CH-5), 115.4 (d, J_{CF} = 21 Hz, CH-3'', CH-5''), 115.2 (CH-7), 114.4 (CH-8), 109.3 (C-5''), 75.6 (C-2), 70.0 ($\text{OCH}_2\text{Ph-p-F}$), 51.7 (CH_2 -3'), 36.9 (CH_2 -1'), 31.0 (CH_2 -3), 24.0 (CH_2 -2'), 22.4 (CH $_3$ -2), 22.0 (CH $_2$ -4); HRMS (ESI) m/z calcd for $\text{C}_{26}\text{H}_{27}\text{ClF}_4\text{N}_3\text{O}_2$ [M + H] $^+$ + 524.1728, found: 524.1683.

4.7. General procedure for the synthesis of hydrazone benzopyrans (**13**, **14**)

A solution of compound aldehyde (**3**) (130 mg, 0.40 mmol) in anhydrous THF (5 mL) was stirred at -78°C under N_2 for 15 min and treated with 0.5 M isopropenylmagnesium bromide solution (4.8 mL, 1.35 mmol). The mixture was stirred at -78°C for 3 h. The resulting mixture reaction was quenched by the addition of a half-saturated aqueous NH_4Cl solution. The reaction was stirred for 15 min at room temperature. Subsequently, water was added, and the mixture was extracted with ethyl acetate (3 x 15 mL). The combined organic layers were washed with brine, dried over anhydrous Na_2SO_4 and evaporated to dryness under reduced pressure. The residue obtained (162 mg) was treated without further purification with 10 mL of triethylorthoacetate and a catalytic amount of isobutyric acid (3 drops). The mixture was stirred at 140°C for 2 h. After cooling, the mixture was concentrated under reduced pressure to remove the excess triethylorthoacetate. Then, water was added and extracted with dichloromethane (3 x 15 mL), dried over anhydrous Na_2SO_4 and concentrated under reduced pressure. The residue was purified by silica gel column chromatography (hexane/EtOAc, 98:2) to yield benzopyran ester **11** (84 mg, 0.2 mmol, 48 %) as a white solid.

4.7.1. Ethyl 7-(6-((p-fluorobenzyl)oxy)-2-methyldihydrobenzopyran-2-yl)-4-methylhept-4-enoate (**11**)

^1H NMR (500 MHz, CDCl_3) δ 7.41–7.36 (m, 2H, CH-2'', CH-6''), 7.09–7.06 (m, 2H, CH-3'', CH-5''), 6.72–6.66 (m, 3H, CH-5, CH-7, CH-8), 5.14 (t, J = 7.0 Hz, 1H, CH-3'), 4.94 (s, 2H, $\text{OCH}_2\text{Ph-p-F}$), 4.11 (q, J = 7.4 Hz, 2H, $\text{CO}_2\text{CH}_2\text{CH}_3$), 2.72 (t, J = 6.8 Hz, 2H, CH_2 -4), 2.41–2.35 (m, 2H, CH_2 -6'), 2.29–2.27 (m, 2H, CH_2 -5'), 2.09–2.05 (m, 2H, CH_2 -2'), 1.84–1.72 (m, 2H, CH_2 -3), 1.66–1.60 (m, 2H, CH_2 -1'), 1.60 (s, 3H, CH_3 -4'), 1.27 (s, 3H, CH_3 -2'), 1.23 (t, J = 7.3 Hz, 3H, $\text{CO}_2\text{CH}_2\text{CH}_3$); ^{13}C NMR (125 MHz, CDCl_3) δ 173.4 (CO), 162.4 (d, J_{CF} = 244 Hz, C-4''), 151.9 (C-6), 148.2 (C-8a), 133.5 (C-4'), 133.3 (d, J_{CF} = 3 Hz, C-1''), 129.2 (d, J_{CF} = 8.3 Hz, CH-2'', CH-6''), 124.9 (C-3'), 121.7 (C-4a), 117.8 (CH-5), 115.3 (d, J_{CF} = 24.8 Hz, CH-3'', CH-5''), 115.2 (CH-7), 114.4 (CH-8), 75.6 (C-2), 70.1 ($\text{OCH}_2\text{Ph-p-F}$), 60.2 ($\text{CO}_2\text{CH}_2\text{CH}_3$), 39.2 (CH_2 -6'), 34.6 (CH_2 -1'), 33.2 (CH_2 -5'), 30.9 (CH $_2$ -3), 24.1 (CH $_3$ -2), 22.4 (CH_2 -2'), 22.2 (CH $_2$ -4), 15.8 (CH $_3$ -4'), 14.2 ($\text{CO}_2\text{CH}_2\text{CH}_3$); HREIMS m/z calcd for $\text{C}_{27}\text{H}_{33}\text{FO}_4$ [M] $^+$ + 441.2436, found: 441.2441.

4.7.2. 7-(6-((p-Fluorobenzyl)oxy)-2-methyldihydrobenzopyran-2-yl)-4-methylhept-4-enal (**12**)

The title compound was prepared from benzopyran ester **11** (80 mg, 0.18 mmol) following the general procedure for the synthesis of aldehyde **3** to afford compound **12** (63 mg, 0.16 mmol, 89%) as a colorless oil. ^1H NMR (300 MHz, CDCl_3) δ 9.74 (t, J = 2 Hz, 1H, CHO), 7.42–7.36

(m, 2H, CH-2", CH-6"), 7.09–7.03 (m, 2H, CH-3", CH-5"), 6.73–6.67 (m, 3H, CH-5, CH-7, CH-8), 5.14 (t, $J = 7$ Hz, 1H, CH-3'), 4.94 (s, 2H, OCH₂Ph-p-F), 2.74 (t, $J = 7$ Hz, 2H, CH₂-4), 2.50–2.47 (m, 2H, CH₂-6'), 2.33–2.30 (m, 2H, CH₂-5'), 2.15–2.08 (m, 2H, CH₂-2'), 1.86–1.73 (m, 2H, CH₂-3), 1.71–1.54 (m, 5H, CH₂-1', CH₃-4'), 1.27 (s, 3H, CH₃-2); ¹³C NMR (75 MHz, CDCl₃) δ 202.6 (CHO), 162.4 (d, $J_{CF} = 244$ Hz, C-4"), 151.9 (C-6), 148.2 (C-8a), 133.4 (C-4'), 133.3 (d, $J_{CF} = 3$ Hz, C-1"), 129.2 (d, $J_{CF} = 8$ Hz, CH-2", CH-6"), 124.9 (C-3'), 121.7 (C-4a), 117.8 (CH-5), 115.3 (d, $J_{CF} = 25$ Hz, CH-3", CH-5"), 115.2 (CH-7) 114.4 (CH-8), 75.6 (C-2), 70.1 (OCH₂Ph-p-F), 42.1 (CH₂-6'), 39.2 (CH₂-1'), 31.8 (CH₂-5'), 31.0 (CH₂-3), 24.1 (CH₃-2), 22.4 (CH₂-2'), 22.2 (CH₂-4), 16.0 (CH₃-4'); EIMS m/z (%) 396.50 [M]⁺.

4.7.3. 2-(2-(7-(6-((p-Fluorobenzyl)oxy)-2-methylbenzodihydropyran-2-yl)-4-methylhept-4-en-1-ylidene)hydrazineyl)benzo[d]thiazole (**13**)

The title compound was prepared from aldehyde **12** (26.50 mg, 0.07 mmol) and 2-hydrazinobenzothiazole (18.4 mg, 0.11 mmol) following the general procedure for the synthesis of compound **4**. The residue obtained was purified by silica gel column chromatography (CH₂Cl₂/MeOH, 98:2) to afford compound **13** (26.5 mg, 69.5%) as a reddish oil. ¹H NMR (300 MHz, CDCl₃) δ 7.64 (dd, $J = 8$ Hz, 1.2 Hz, 1H, CH-3"), 7.45 (dd, $J = 8$ Hz, 1.2 Hz, 1H, CH-6"), 7.42–7.35 (m, 2H, CH-2", CH-6"), 7.34–7.24 (m, 2H, CH-7', CH-4"), 7.16–7.01 (m, 3H, CH-5", CH-3", CH-5'), 6.74–6.63 (m, 3H, CH-5, CH-7, CH-8), 5.22–5.08 (m, 1H, CH-3'), 4.93 (s, 2H, OCH₂Ph-p-F), 2.70 (t, 2H, $J = 7.0$ Hz, CH₂-4), 2.42–2.38 (m, 2H, CH₂-5'), 2.21 (t, 2H, $J = 7.7$ Hz, CH₂-6'), 2.17–2.05 (m, 2H, CH₂-2'), 1.89–1.67 (m, 2H, CH₂-3), 1.63 (s, 3H, CH₃-4'), 1.61–1.53 (m, 2H, CH₂-1'), 1.26 (s, 3H, CH₃-2); ¹³C NMR (75 MHz, CDCl₃) δ 168.5 (C-1"), 162.4 (d, $J_{CF} = 244$ Hz, C-4"), 151.9 (C-6), 150.3 (C-2a"), 148.2 (CH-7'), 147.6 (C-8a), 133.6 (C-4'), 133.2 (d, $J_{CF} = 3$ Hz, C-1"), 130.1 (C-6a"), 129.3 (d, $J_{CF} = 8$ Hz, CH-2", CH-6"), 125.9 (CH-4"), 125.4 (CH-3'), 121.8 (CH-5"), 121.7 (C-4a), 121.3 (CH-3"), 119.0 (CH-6"), 117.7 (CH-5), 115.3 (d, $J_{CF} = 21$ Hz, CH-5", CH-3"), 115.2 (CH-7), 114.3 (CH-8), 75.6 (C-2), 70.0 (OCH₂Ph-p-F), 39.2 (CH₂-1'), 36.3 (CH₂-6'), 31.0 (CH₂-3), 30.7 (CH₂-5'), 24.1 (CH₃-2), 22.4 (CH₂-2'), 22.1 (CH₂-4), 15.9 (CH₃-4'); HRMS (ESI) m/z calcd for C₃₂H₃₅FN₃O₂S [M + H]⁺ + 544.2429, found: 544.2409.

4.7.4. 5-Chloro-2-(2-(7-(6-((p-fluorobenzyl)oxy)-2-methylbenzodihydropyran-2-yl)-4-methylhept-4-en-1-ylidene)hydrazineyl)-3-(trifluoromethyl)pyridine (**14**)

The title compound was prepared from aldehyde **12** (26.50 mg, 0.07 mmol) and 1-[5-chloro-3-(trifluoromethyl)-2-pyridyl]hydrazine (23.6 mg, 0.114 mmol) following the general procedure for the synthesis of compound **5**. The residue obtained was purified by silica gel column chromatography (CH₂Cl₂/MeOH, 98:2) to afford compound **14** (24.5 mg, 0.04 mmol, 59.5%) as a yellowish oil. ¹H NMR (300 MHz, CDCl₃) δ 8.42–8.40 (m, 1H, CH-6"), 7.96 (brs, 1H, NH), 7.74–7.72 (m, 1H, CH-4"), 7.40–7.36 (m, 2H, CH-2", CH-6"), 7.28–7.26 (m, 1H, CH-7'), 7.08–7.02 (m, 2H, CH-3", CH-5"), 6.72–6.65 (m, 3H, CH-5, CH-7, CH-8), 5.21–5.16 (m, 1H, CH-3'), 4.93 (s, 2H, OCH₂Ph-p-F), 2.74–2.70 (m, 2H, CH₂-4), 2.57–2.40 (m, 2H, CH₂-5'), 2.33–2.09 (m, 4H, CH₂-6', CH₂-2'), 1.84–1.76 (m, 2H, CH₂-3), 1.74 (s, 3H, CH₃-4'), 1.73–1.56 (m, 2H, CH₂-1'), 1.27 (s, 3H, CH₃-2); ¹³C NMR (75 MHz, CDCl₃) δ 162.4 (d, $J_{CF} = 244$ Hz, C-4"), 151.9 (C-6), 150.9 (q, $J_{CF} = 4$ Hz, CH-2"), 148.4 (CH-7'), 148.2 (C-8a), 146.9 (CH-6"), 135.2 (q, $J = 4$ Hz, CH-4"), 135.5 (C-4'), 133.2 (d, $J_{CF} = 3$ Hz, C-1"), 129.2 (d, $J_{CF} = 8$ Hz, CH-2", CH-6"), 125.4 (CH-3'), 123.4 (q, $J_{CF} = 270$ Hz, CF₃), 121.6 (C-4a), 121.2 (C-5"), 117.7 (CH-5), 115.3 (d, $J_{CF} = 21$ Hz, CH-3", CH-5"), 115.2 (CH-7), 114.3 (CH-8), 108.5 (q, $J_{CF} = 33$ Hz, C-3"), 75.5 (C-2), 70.0 (OCH₂Ph-p-F), 39.1 (CH₂-1'), 36.7 (CH₂-6'), 31.0 (CH₂-3), 30.6 (CH₂-5'), 24.0 (CH₃-2), 22.4 (CH₂-2'), 22.1 (CH₂-4), 15.8 (CH₃-4'); HRMS (ESI) m/z calcd for C₃₁H₃₁ClF₄N₃O₂ [M – H]⁺ + 588.2040, found: 588.2017.

4.8. Evaluation of PPAR activity by transactivation assays

PPAR transcriptional activity of synthesized compounds was performed using a human chimera PPAR/Gal4 gene reporter luciferase system for each compound and compared with WY-14,643 (pirinixic acid, Sigma-Aldrich, St. Louis, MO) at 10 μ M for PPAR α , rosiglitazone (Sigma-Aldrich) at 1 μ M for PPAR γ and GW501516 (Sigma-Aldrich) at 1 μ M for PPAR β/δ . Cos-7 cells (CRL-1651, ATCC, Manassas, VA) were maintained under standard culture conditions (Dulbecco's modified Eagle's minimal essential medium: DMEM supplemented with 10% fetal calf serum [FCS], Thermo Fisher Scientific, Waltham, MA) at 37 °C in a humidified atmosphere of 5% CO₂. The medium was changed every 2 days. Cells (5.5 \times 10⁵ cells/mL) were seeded in 60-mm dishes in DMEM supplemented with 10% FCS and incubated at 37 °C for 16 h prior to transfection. Cells were transfected in DMEM with the jetPEI transfection reagent (Polyplus-Transfection S.A., Strasbourg, France) using the reporter plasmid pG5-TK-pGL3 in combination with one of the expression plasmids, pGal4hPPAR α , pGal4hPPAR γ or pGal4hPPAR β/δ . The pCMV- β -galactosidase expression plasmid was included as a control of transfection efficiency. The transfection was stopped after 16 h by the addition of DMEM supplemented with 0.2% FCS, and cells were detached with trypsin and re-seeded in 96-well plates and incubated for 6 h in DMEM containing 0.2% FCS. Cells were then incubated for 24 h in DMEM containing 0.2% FCS and increasing concentrations of the compound tested or vehicle (DMSO, 0.1% final concentration). At the end of the experiment, cells were washed once with ice-cold phosphate buffered saline (PBS) and lysed, and luciferase and β -galactosidase activity were measured. Each experiment was achieved in triplicate, and mean \pm standard error (SEM) values were calculated using GraphPad Prism 5 Software.

4.9. Molecular modelling

In molecular simulations for PPAR α PPAR γ and PPAR δ receptors, we have used the same methodology as previously reported [20,24]. Docking calculations were carried out by using the Autodock 4.2 program [50] to localize the different ligands in the binding pocket; such complexes were used as starting structures for MD simulations. We used a molecular mechanics generalized born surface area (MM-GBSA) free energy decomposition analysis to determine the molecular interactions between the different ligands with PPAR α PPAR γ and PPAR δ receptors. The 3D crystal structure of PPAR γ in complex with rosiglitazone (PDB code: 4eMA) of PPAR α in complex with WY-14643 (PDB code: 4BcR), and of PPAR δ in complex with GW501516 (PDB code: 5U46) were used for MD simulations. The missing loop (261–275) in the PPAR γ was modeled based on the 3D structure (PPAR γ IPRG model) [51] using the Swiss-Model server [52]. Geometries of the complexes obtained from docking were soaked in boxes of explicit water using the TIP3P model and subjected to MD simulation. MD simulations were performed with the Amber 22 software package [52]. The geometry of the system went through a two-step energy minimization process: in the first step, the backbone atoms of the complex were constrained with 10.0 kcal/(mol Å²) force constants; in the second step, all solute and solvent atoms were allowed to move with no constraint to obtain the final relaxed geometry. The nonbonded interaction cutoff was kept at its default value, and the particle mesh Ewald method was also used. Simulations were performed with a total of 90 ns for each complex (three runs of 30 ns). The cluster process was carried out in the following manner: using the 90 ns obtained from three runs, 15 ns were discarded (the first 5 ns of each individual run). The remaining 75 ns were submitted to the cluster process, from which 10 different families of complexes were obtained. The free energy decomposition by residue was calculated using the *mm.pbsa* program in Amber22 [52]. Each ligand–residue pair includes four energy terms: van der Waals contribution (ΔE_{vdw}), electrostatic contribution (ΔE_{ele}), polar desolvation term (ΔG_{GB}), and

nonpolar desolvation term (ΔG_{SA}), which are summarized in the following equation: $\Delta G_{ligand-residue} = \Delta E_{vdW} + \Delta E_{ele} + \Delta G_{GB} + \Delta G_{SA}$. MD trajectories and the explicit water molecules were removed from the snapshots.

4.10. Study of anti-inflammatory activity

THP-1 human monocytes (ATCC, TIB-202™, Manassas, VA) were cultured in RPMI-1640 medium containing gentamycin (40 mg/mL), 1% (v/v) glutamine and 10% (v/v) fetal calf serum and maintained in a 37 °C, 5% CO₂ incubator. Cells (2×10^6 cells/mL) were seeded in 6-well plates and were differentiated into macrophages by the addition of phorbol-12-myristate-13-acetate at 5 ng/mL (PMA, Promega). After 48 h, the cells were washed with PBS and replaced with 0% SVF medium for 1 h. After 1 h the depravation medium was replaced with stimulation medium containing hydrazones (**4**, **5** and **14** at 10 μ M) or vehicle (<0.02% DMSO). The following hour, THP-1 macrophages were stimulated with LPS (100 ng/mL) in presence or not of PPAR activators hydrazones **4**, **5** and **14** at 10 μ M, and secreted cytokine levels were measured 24 h later with ELISA kits according to the manufacturer's instructions (R&D System, Minneapolis, MN, USA). Cytokine mRNA levels were determined by quantitative PCR analysis.

4.11. Flow cytometry analysis of activated NF- κ B

The effect of hydrazones **4** and **5** on LPS-induced NF- κ B activation was determined in THP-1 cells by flow cytometry. THP-1 cells were incubated for 24 h with compounds (10 μ M) or vehicle (0.02% DMSO) and then stimulated for 1 h with LPS 100 ng/mL.

Cells were then fixed and permeabilized using a commercial kit (Transcription Factor Phospho Buffer Set, 563239, BD Biosciences). Cells were then incubated with saturated amounts of a PE-conjugated monoclonal antibody against human NF- κ B p65 (clone K10-895.12.50, IgG2B, BD Biosciences), for 45 min at 4 °C in the dark. Samples were run in a flow cytometer (BD LSRFortessa™ X-20, BD Biosciences). Results are presented as the mean fluorescence intensity of p65-NF- κ B-expressing (PE fluorescence) THP-1.

4.12. Study of cytotoxic activity

THP-1 human monocytes (ATCC, TIB-202™, Manassas, VA) were cultured in RPMI-1640 medium containing gentamycin (40 mg/mL), 1% (v/v) glutamine and 10% (v/v) fetal calf serum and maintained in a 37 °C, 5% CO₂ incubator. Cells (1×10^5 cells/mL) were seeded in 24-well plates and were differentiated into macrophages by the addition of phorbol-12-myristate-13-acetate at 5 ng/mL (PMA, Promega). After 48 h, the cells were washed with PBS and replaced with the different compounds at 10 μ M, 30 μ M and 100 μ M in complete medium or vehicle (<0.2% DMSO). Then, all cells were processes with Annexin V-assay kit (ANXCKF7, Immunoestep, Salamanca, Spain) according to the manufacturer's instructions. BD LSR Fortessa cytometer (BD Biosciences, New Jersey, USA) was used for samples and cell analyses were performed by using BD FACSDiva X20 Software).

4.13. Statistical analysis

Data are presented as mean \pm SEM. Statistical analyses were carried out by one-way or two-way ANOVA, followed by Tukey's or Dunnett's multiple comparisons test (GraphPad Prism 9). Paired analysis was performed by Wilcoxon matched-pairs signed rank test (GraphPad Prism 9). Differences with a p-value < 0.05 were considered statistically different.

CRediT authorship contribution statement

Ainhoa García: Writing – original draft, Investigation, Formal analysis. **Laura Vila:** Methodology, Investigation, Formal analysis. **Isabelle Duplan:** Software, Methodology, Investigation, Formal analysis. **María Ayelén Schiel:** Software, Methodology, Investigation, Formal analysis. **Ricardo D. Enriz:** Validation, Supervision. **Nathalie Hennuyer:** Visualization, Validation, Supervision, Investigation. **Bart Staels:** Visualization, Supervision. **Nuria Cabedo:** Writing – review & editing, Writing – original draft, Supervision, Project administration, Funding acquisition, Data curation, Conceptualization. **Diego Cortes:** Validation, Supervision, Conceptualization.

Declaration of competing interest

The authors declare that they have no known competing financial interests or personal relationships that could have appeared to influence the work reported in this paper.

Data availability

No data was used for the research described in the article.

Acknowledgment

We are grateful for the financial support from Carlos III Health Institute (ISCIII) and the European Regional Development Fund (FEDER) (grants: PI18/01450 and PI21/0245), as well as Generalitat Valencia (APOTIP/2020/011 and AICO/2021/081). N.C. is an investigator in the 'Miguel Servet' programme (CPII20/00010) funded by the ISCIII and the European Social Fund. C.V. was funded by pre-doctoral PFIS grant from the ISCIII (FI19/00153).

Appendix A. Supplementary data

Supplementary data to this article can be found online at <https://doi.org/10.1016/j.ejmech.2024.116125>.

References

- [1] B. Gross, M. Pawlak, P. Lefebvre, B. Staels, PPARs in obesity-induced T2DM, dyslipidaemia and NAFLD, *Nat. Rev. Endocrinol.* 13 (1) (2017) 36–49, <https://doi.org/10.1038/nrendo.2016.135>.
- [2] C. Villarreal-Vicente, S. Gutiérrez-Palomo, J. Ferri, D. Cortes, N. Cabedo, Natural products and analogs as preventive agents for metabolic syndrome via peroxisome proliferator-activated receptors: an overview, *Eur. J. Med. Chem.* 221 (2021) 113535, <https://doi.org/10.1016/j.ejmech.2021.113535>.
- [3] M. Dominguez, S. Alvarez, A.R. de Lera, Natural and structure-based RXR Ligand scaffolds and their functions, *Curr. Top. Med. Chem.* 17 (6) (2017) 631–662, <https://doi.org/10.2174/1568026616666160617072521>.
- [4] T.M. Willson, P.J. Brown, D.D. Sternbach, B.R. Henke, The PPARs: from orphan receptors to drug discovery, *J. Med. Chem.* 43 (4) (2000) 527–550, <https://doi.org/10.1021/jm990554g>.
- [5] O. Ziouzenkova, J. Plutzky, Retinoid metabolism and nuclear receptor responses: new insights into coordinated regulation of the PPAR-RXR complex, *FEBS Lett.* 582 (1) (2008) 32–38, <https://doi.org/10.1016/j.febslet.2007.11.081>.
- [6] M. Pawlak, P. Lefebvre, B. Staels, Molecular mechanism of PPAR α action and its impact on lipid metabolism, inflammation and fibrosis in non-alcoholic fatty liver disease, *J. Hepatol.* 62 (3) (2015) 720–733, <https://doi.org/10.1016/j.jhep.2014.10.039>.
- [7] S.K. Ramakrishnan, L. Russo, S.S. Ghanem, P.R. Patel, A.M. Oyarce, G. Heinrich, S.M. Najjar, Fenofibrate decreases insulin clearance and insulin secretion to maintain insulin sensitivity, *J. Biol. Chem.* 291 (46) (2016) 23915–23924, <https://doi.org/10.1074/jbc.M116.745778>.
- [8] F. Lalloyer, B. Vandewalle, F. Percevault, G. Torpier, J. Kerr-Conte, M. Oosterveer, R. Paumelle, J.C. Fruchart, F. Kuipers, F. Pattou, C. Fiévet, B. Staels, B. Peroxisome proliferator-activated receptor alpha improves pancreatic adaptation to insulin resistance in obese mice and reduces lipotoxicity in human islets, *Diabetes* 55 (6) (2006) 1605–1613, <https://doi.org/10.2337/db06-0016>.
- [9] X. Palomer, E. Barroso, J. Pizarro-Delgado, L. Peña, G. Botteri, M. Zarei, D. Aguilar, M. Montori-Grau, M. Vázquez-Carrera, Ppar β /8: a key therapeutic target in metabolic disorders, *Int. J. Mol. Sci.* 19 (3) (2018) 913, <https://doi.org/10.3390/ijms19030913>.
- [10] L. Wang, B. Waltenberger, E.M. Pferschy-Wenzig, M. Blunder, X. Liu, C.

- Malainer, T. Blazevic, S. Schwaiger, J.M. Rollinger, E.H. Heiss, D. Schuster, B. Kopp, R. Bauer, H. Stuppner, V.M. Dirsch, A.G. Atanasov, Natural product agonists of peroxisome proliferator-activated receptor gamma (PPAR γ): a review, *Biochem. Pharmacol.* 92 (1) (2014) 73–89, <https://doi.org/10.1016/j.bcp.2014.07.018>.
- [11] S. Russo, M. Kwiatkowski, N. Govorukhina, R. Bischoff, B.N. Melgert, Meta-inflammation and metabolic reprogramming of macrophages in diabetes and obesity: the importance of metabolites, *Front. Immunol.* 12 (2021) 746151, <https://doi.org/10.3389/fimmu.2021.746151>.
- [12] A.E. Boniakowski, A.S. Kimball, B.N. Jacobs, S.L. Kunkel, K.A. Gallagher, Macrophage-mediated inflammation in normal and diabetic wound healing, *J. Immunol.* 199 (1) (2017) 17–24, <https://doi.org/10.4049/jimmunol.1700223>.
- [13] A. Chawla, Control of macrophage activation and function by PPARs, *Circ. Res.* 106 (10) (2010) 1559–1569, <https://doi.org/10.1161/CIRCRESAHA.110.216523>.
- [14] T.L. Cranford, R.T. Enos, K.T. Velázquez, J.L. McClellan, J.M. Davis, U.P. Singh, M. Nagarkatti, P.S. Nagarkatti, C.M. Robinson, E.A. Murphy, Role of MCP-1 on inflammatory processes and metabolic dysfunction following high-fat feedings in the FVB/N strain, *Int. J. Obes.* 40 (5) (2016) 844–851, <https://doi.org/10.1038/ijo.2015.244>.
- [15] J. Pánee, Monocyte chemoattractant protein 1 (MCP-1) in obesity and diabetes, *Cytokine* 60 (1) (2012) 1–12, <https://doi.org/10.1016/j.cyt.2012.06.018>.
- [16] H. Kanda, S. Tateya, Y. Tamori, K. Kotani, K. Hiasa, R. Kitazawa, S. Kitazawa, H. Miyachi, S. Maeda, M. Egashira, M. Kasuga, MCP-1 contributes to macrophage infiltration into adipose tissue, insulin resistance, and hepatic steatosis in obesity, *J. Clin. Invest.* 116 (6) (2016) 1494–1505, <https://doi.org/10.1172/JCI26498>.
- [17] D. Qu, J. Liu, C.W. Lau, Y. Huang, IL-6 in diabetes and cardiovascular complications, *Br. J. Pharmacol.* 171 (15) (2014) 3595–3603, <https://doi.org/10.1111/bph.12713>.
- [18] D. Toobian, P. Ghosh, G.D. Katkar, Parsing the role of PPARs in macrophage processes, *Front. Immunol.* 12 (2021) 783780, <https://doi.org/10.3389/fimmu.2021.783780>.
- [19] M.C. Gonzalez, A. Serrano, M.C. Zafra-Polo, D. Cortes, K.S. Rao, Polycerasoidin and polycerasoidol, two new prenylated benzopyran derivatives from *Polyalthia cerasoides*, *J. Nat. Prod.* 58 (8) (1995) 1278–1284, <https://doi.org/10.1021/np50122a022>.
- [20] A. Bermejo, A. Collado, I. Barrachina, P. Marqués, N. El Aouad, X. Franck, F. Garibotto, C. Dacquet, D.H. Caignard, F.D. Suvire, R.D. Enriz, L. Piqueras, B. Figadère, M.J. Sanz, N. Cabedo, D. Cortes, Polycerasoidol, a natural prenylated benzopyran with a dual PPAR α /PPAR γ agonist activity and anti-inflammatory effect, *J. Nat. Prod.* 82 (7) (2019) 1802–1812, <https://doi.org/10.1021/acs.jnatprod.9b00003>.
- [21] A. García, L. Vila, P. Marín, Á. Bernabeu, C. Villarroel-Vicente, N. Hennuyer, B. Staels, X. Franck, B. Figadère, N. Cabedo, D. Cortes, Synthesis of 2-prenylated alkoxyalkylated benzopyrans by horner-wadsworth-emmons olefination with PPAR α / γ agonist activity, *ACS Med. Chem. Lett.* 12 (11) (2021) 1783–1786, <https://doi.org/10.1021/acsmmedchemlett.1c00400>.
- [22] L. Vila, N. Cabedo, C. Villarroel-Vicente, A. García, Á. Bernabeu, N. Hennuyer, B. Staels, X. Franck, B. Figadère, M.J. Sanz, D. Cortes, Synthesis and biological studies of “Polycerasoidol” and “trans- δ -Tocotrienolic acid” derivatives as PPAR α and/or PPAR γ agonists, *Bioorg. Med. Chem.* 53 (2022) 116532, <https://doi.org/10.1016/j.bmc.2021.116532>.
- [23] A. Bermejo, I. Barrachina, N. El Aouad, X. Franck, N. Chahboune, I. Andreu, B. Figadère, L. Vila, N. Hennuyer, B. Staels, C. Dacquet, D.H. Caignard, M.J. Sanz, D. Cortes, N. Cabedo, Synthesis of benzopyran derivatives as PPAR α and/or PPAR γ activators, *Bioorg. Med. Chem.* 27 (24) (2019) 115162, <https://doi.org/10.1016/j.bmc.2019.115162>.
- [24] P. Marques, C. Villarroel-Vicente, A. Collado, A. García, L. Vila, I. Duplan, N. Hennuyer, F. Garibotto, R.D. Enriz, C. Dacquet, B. Staels, L. Piqueras, D. Cortes, M.J. Sanz, N. Cabedo, Anti-inflammatory effects and improved metabolic derangements in ob/ob mice by a newly synthesized prenylated benzopyran with pan-PPAR activity, *Pharmacol. Res.* 187 (2023) 106638, <https://doi.org/10.1016/j.phrs.2022.106638>.
- [25] L.M. Blair, J. Sperry, Natural products containing a nitrogen-nitrogen bond, *J. Nat. Prod.* 76 (4) (2013) 794–812, <https://doi.org/10.1021/np400124n>.
- [26] M.A. El-Sayed, N.I. Abdel-Aziz, A.A. Abdel-Aziz, A.S. El-Azab, Y.A. Asiri, K.E. Eltahir, Design, synthesis, and biological evaluation of substituted hydrazones and pyrazole derivatives as selective COX-2 inhibitors: molecular docking study, *Bioorg. Med. Chem.* 19 (11) (2011) 3416–3424, <https://doi.org/10.1016/j.bmc.2011.04.027>.
- [27] K. Pyta, A. Janas, M. Szukowska, P. Pecyna, M. Jaworska, M. Gajęcka, F. Bartl, P. Przybylski, Synthesis, docking and antibacterial studies of more potent amine and hydrazone rifamycin congeners than rifampicin, *Eur. J. Med. Chem.* 167 (2019) 96–104, <https://doi.org/10.1016/j.ejmech.2019.02.009>.
- [28] E.S. Coimbra, M.V. Nora de Souza, M.S. Terror, A.C. Pinheiro, J. da Trindade Granato, Synthesis, Biological activity, and mechanism of action of new 2-pyrimidinyl hydrazone and N-acylhydrazone derivatives, a potent and new classes of antileishmanial agents, *Eur. J. Med. Chem.* 184 (2019) 111742, <https://doi.org/10.1016/j.ejmech.2019.111742>.
- [29] H. Lei, C. Li, Y. Yang, F. Jia, M. Guo, M. Zhu, N. Jiang, X. Zhai, Structure guided design of potent indole-based ATX inhibitors bearing hydrazone moiety with tumor suppression effects, *Eur. J. Med. Chem.* 201 (2020) 112456, <https://doi.org/10.1016/j.ejmech.2020.112456>.
- [30] G. Pooja, S.R. Ravindra, R. Harshil, K. Sanjit, R.R. Sabbasani, Recent developments in the synthesis of N-heterocyclic compounds as α -amylase inhibitors via in-vitro and in-silico analysis: future drugs for treating diabetes, *ChemistrySelect* 7 (28) (2022), <https://doi.org/10.1002/slct.202201706>.
- [31] J. Dowarah, V.P. Singh, Anti-diabetic drugs recent approaches and advancements, *Bioorg. Med. Chem.* 28 (5) (2020) 115263, <https://doi.org/10.1016/j.bmc.2019.115263>.
- [32] D. Montaigne, L. Butruille, B. Staels, PPAR control of metabolism and cardiovascular functions, *Nat. Rev. Cardiol.* 18 (12) (2021) 809–823, <https://doi.org/10.1038/s41569-021-00569-6>.
- [33] E.B. Lindgren, M.A. de Brito, T.R. Vasconcelos, M.O. de Moraes, R.C. Montenegro, J.D. Yoneda, K.Z. Synthesis and anticancer activity of (E)-2-benzothiazole hydrazones, *Eur. J. Med. Chem.* 86 (2014) 12–16, <https://doi.org/10.1016/j.ejmech.2014.08.039>.
- [34] J. Párraga, L. Moreno, A. Díaz, N. El Aouad, A. Galán, M.J. Sanz, D.H. Caignard, B. Figadère, N. Cabedo, D. Cortes, Efficient synthesis of hexahydroindenopyridines and their potential as melatonergic ligands, *Eur. J. Med. Chem.* 86 (2014) 700–709, <https://doi.org/10.1016/j.ejmech.2014.09.038>.
- [35] Q.P. Peterson, D.C. Hsu, D.R. Goode, C.J. Novotny, R.K. Totten, P.J. Hergenrother, Procaspase-3 activation as an anti-cancer strategy: structure-activity relationship of procaspase-activating compound 1 (PAC-1) and its cellular colocalization with caspase-3, *J. Med. Chem.* 52 (18) (2009) 5721–5731, <https://doi.org/10.1021/jm900722z>.
- [36] Y. Yang, L. Shouxin, L. Junzhang, T. Xia, Z. Xiaoli, H. Jianrong, Convenient method for reduction of C-N double bonds in oximes, imines, and hydrazones using sodium borohydride-raney Ni system, *Synth. Commun.* 42 (17) (2012) 2540–2554, <https://doi.org/10.1080/00397911.2011.562063>.
- [37] M. Krátýř, Š. Štěpánková, K. Konečná, K. Svrčková, J. Maixnerová, M. Švarcová, O. Janďourek, F. Trejtnar, J. Vinšová, Novel aminoguanidine hydrazone analogues: from potential antimicrobial agents to potent cholinesterase inhibitors, *Pharmaceuticals* 14 (12) (2021) 1229, <https://doi.org/10.3390/ph14121229>.
- [38] D. Perdicchia, L. Emanuela, M. Estefano, B. Clara, G. Clelia, A new ‘one-pot’ synthesis of hydrazides by reduction of hydrazones, *Tetrahedron* 59 (39) (2003) 7733–7742, [https://doi.org/10.1016/S0040-4020\(03\)01208-0](https://doi.org/10.1016/S0040-4020(03)01208-0).
- [39] J.M. Khurana, B.M. Kandpal, P. Sharma, M. Gupta, A novel method of reduction of C=N-group in hydrazones, phenylhydrazones, azines, and tosylhydrazones by Mg-methanol, *Monatshfte für Chemie - Chemical Monthly* 146 (1) (2015) 187–190, <https://doi.org/10.1007/s00706-014-1306-6>.
- [40] A. Srikrishna, T.J. Reddy, R. Viswanjanani, Reduction of quinolines to 1,2,3,4-tetrahydro derivatives employing a combination of NaCNBH $_3$ and BF $_3$ ·OEt $_2$, *Tetrahedron* 52 (5) (1996) 1631–1636, [https://doi.org/10.1016/0040-4020\(95\)00991-4](https://doi.org/10.1016/0040-4020(95)00991-4).
- [41] J. Kalita, R.T. Raines, Hydrolytic stability of hydrazones and oximes, *Angew. Chem. Int. Ed. Engl.* 47 (39) (2008) 7523–7526, <https://doi.org/10.1002/anie.200802651>.
- [42] R. R. Kshirsagar, P.K. Gadekar, V.M. Khedkar, V. Vijayakumar, Design, synthesis, and the Effects of (E)-9-oxooctadec-10-en-12-ynoic acid analogues to promote glucose uptake, *ACS Omega* 6 (37) (2021) 24118–24127, <https://doi.org/10.1021/acsomega.1c03600>.
- [43] T. Kato, K. Fukao, T. Ohara, N. Naya, R. Tokuyama, S. Muto, H. Fukasawa, A. Imai, K.I. Matsumura, Design, synthesis, and anti-inflammatory evaluation of a novel PPAR δ agonist with a 4-(1-pyrrolidinyl)piperidine Structure, *J. Med. Chem.* 66 (16) (2023) 11428–11446, <https://doi.org/10.1021/acs.jmedchem.3c00932>.
- [44] M. Di Stefano, S. Masoni, G. Bononi, G. Poli, S. Galati, F. Gado, S. Manzi, C. Vagaggini, A. Brai, I. Caligiuri, K. Asif, F. Rizzolio, M. Macchia, A. Chicca, A. Sodi, V. Di Bussolo, F. Minutolo, P. Meier, J. Gertsch, C. Granchi, E. Dreassi, T. Tuccinardi, Design, synthesis, ADME and biological evaluation of benzylpiperidine and benzylpiperazine derivatives as novel reversible monoacylglycerol lipase (MAGL) inhibitors, *Eur. J. Med. Chem.* 263 (2023), 115916 <https://doi.org/10.1016/j.ejmech.2023.115916>, Advance online publication.
- [45] A. Bernardes, P.C. Souza, J.R. Muniz, C.G. Ricci, S.D. Ayers, N.M. Parekh, A.S. Godoy, D.B. Trivella, P. Reinach, P. Webb, M.S. Skaf, I. Polikarpov, Molecular mechanism of peroxisome proliferator-activated receptor α activation by WY14643: a new mode of ligand recognition and receptor stabilization, *J. Mol. Biol.* 425 (16) (2013) 2878–2893, <https://doi.org/10.1016/j.jmb.2013.05.010>.
- [46] H.E. Xu, T.B. Stanley, V.G. Montana, M.H. Lambert, B.G. Shearer, J.E. Cobb, D.D. McKee, C.M. Galdari, K.D. Plunket, R.T. Nolte, D.J. Parks, J.T. Moore, S.A. Klierer, T.M. Willson, J.B. Stimmel, Structural basis for antagonist-mediated recruitment of nuclear co-repressors by PPAR α , *Nature* 415 (6873) (2002) 813–817, <https://doi.org/10.1038/415813a>.
- [47] I. Kouskoumvekaki, R.K. Petersen, F. Fratev, O. Taboureaux, T.E. Nielsen, T.L. Oprea, S.B. Sonne, E.N. Flindt, S.Ó. Jónsdóttir, K. Kristiansen, Discovery of a novel selective PPAR γ ligand with partial agonist binding properties by integrated in silico/in vitro workflow, *J. Chem. Inf. Model.* 53 (4) (2013) 923–937, <https://doi.org/10.1021/ci3006148>.
- [48] M.V. Liberato, A.S. Nascimento, S.D. Ayers, J.Z. Lin, A. Cvor, R.L. Silveira, L. Martínez, P.C. Souza, D. Saidenberg, T. Deng, A.A. Amato, M. Togashi, W.A. Hsueh, K. Phillips, M.S. Palma, F.A. Neves, M.S. Skaf, P. Webb, I. Polikarpov, Medium chain fatty acids are selective peroxisome proliferator activated receptor (PPAR) γ activators and pan-PPAR partial agonists, *PLoS One* 7 (5) (2012) e36297, <https://doi.org/10.1371/journal.pone.0036297>.
- [49] C.C. Wu, T.J. Baiga, M. Downes, J.J. La Clair, A.R. Atkins, S.B. Richard, W. Fan, T.A. Stockley-Noel, M.E. Bowman, J.P. Noel, R.M. Evans, Structural basis for specific ligand of the peroxisome proliferator-activated receptor δ , *Proc. Natl. Acad. Sci. U S A* 114 (13) (2017) E2563–E2570, <https://doi.org/10.1073/pnas.1621513114>.
- [50] G.M. Morris, R. Huey, W. Lindstrom, M.F. Sanner, R.K. Belew, D.S. Goodsell, A.J. Olson, AutoDock4 and AutoDockTools4: automated docking with selective receptor flexibility, *J. Comput. Chem.* 30 (16) (2009) 2785–2791, <https://doi.org/10.1002/jcc.21256>.
- [51] R.T. Nolte, G.B. Wisely, S. Westin, J.E. Cobb, M.H. Lambert, R. Kurokawa, M.G.

- Rosenfeld, T.M. Willson, C.K. Glass, M.V. Milburn, Ligand binding and co-activator assembly of the peroxisome proliferator-activated receptor-gamma, *Nature* 395 (6698) (1998) 137–143, <https://doi.org/10.1038/25931>.
- [52] D.A. Case, H.M. Aktulga, K. Belfon, I.Y. Ben-Shalom, J.T. Berryman, S.R. Brozell, D.S. Cerutti, T.E. Cheatham III, G.A. Cisneros, V.W.D. Cruzeiro, T.A. Darden, N. Forouzes, G. Giambasu, T. Giese, M.K. Gilson, H. Gohlke, A.W. Goetz, J. Harris, S. Izadi, S.A. Izmailov, K. Kasavajhala, M.C. Kaymak, E. King, A. Kovalenko, T. Kurtzman, T.S. Lee, P. Li, C. Lin, J. Liu, T. Luchko, R. Luo, M. Machado, V. Man, M. Manathunga, K.M. Merz, Y. Miao, O. Mikhailovskii, G. Monard, H. Nguyen, K.A. O' Hearn, A. Onufriev, F. Pan, S. Pantano, R. Qi, A. Rahnamoun, D.R. Roe, A. Roitberg, C. Sagui, S. Schott-Verdugo, A. Shajan, J. Shen, C.L. Simmerling, N.R. Skrynnikov, J. Smith, J. Swails, R.C. Walker, J. Wang, J. Wang, H. Wei, X. Wu, Y. Wu, Y. Xiong, Y. Xue, D.M. York, S. Zhao, Q. Zhu, P.A. Kollman, Amber, University of California, San Francisco, 2023.

Chapter 2

2-Aminopropyl benzopyran derivatives as potential agents against triple negative breast cancer

1. Triple negative breast cancer (TNBC)

2. Benzopyrans as antitumor agents

3. Article

Article 4: Synthesis of 2-Aminopropyl benzopyran derivatives as potential agents against triple negative breast cancer, *RSC Medicinal Chemistry*, 14 (2023) 2327.

1. Triple negative breast cancer (TNBC)

Cancer is a group of diseases characterized by uncontrolled growth processes of mutated cells. Cell cycle is the process through cells multiply and proliferate including two different periods, interphase (G1, S and G2 phases) and cell division (M phase) (**Figure 6**). During interphase, the cell grows and makes a copy of its DNA meanwhile during mitotic phase, the cell separates its DNA into two groups and divides its cytoplasm to form two new cells [66]. Throughout the cell cycle, there are checkpoints that regulate cell proliferation, growth and DNA division. The G1 phase is an important revision point where proteins such as cyclins and cyclin-dependent kinases are relevant, since by binding, they are able to promote cell cycle progression [67]. The activation of cyclin D and cyclin E can promote the transition of cells from G1 phase to S phase, while the activation of CDC2 can promote the transformation of cells from S phase to G2/M phase. Overexpression of cell cycle-enhancing factors allows pathological proliferation responsible for cell growth. Apoptosis consists of a highly regulated death process where specific cells are sacrificed to obtain a benefit for the organism. In cancer, there is a loss of balance between cell division and cell death and cells that should have died did not receive the signals to do so [68]. Reactive oxygen species (ROS) plays a critical role in cell death including apoptosis. An excess of ROS targets biomembranes, propagates lipid peroxidation chain reactions and subsequently induces different cell death [69].

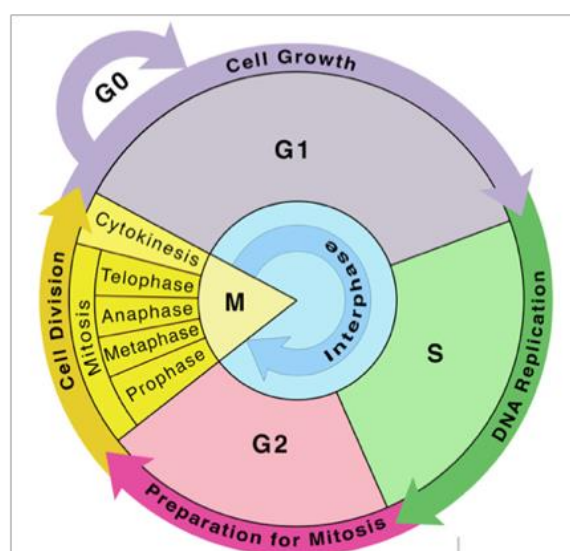


Figure 6. Cell cycle scheme

Breast cancer (BC) is a complex and heterogeneous disease, being the most frequent diagnosed and the leading cause of cancer-related deaths among women, with increasing mortality rates affecting to more than 1 million women worldwide [70-73]. The selection of drug therapy for patients depends on cancer subtype: hormone receptor-positive, human epidermal growth factor receptor 2 (HER-2) and triple-negative BC (TNBC). The TNBC is characterized by lacking estrogen receptor (ER), progesterone receptor (PR) and HER-2 [74-76]. Consequently, TNBC patients do not respond to hormonal and anti-HER2 monoclonal antibody trastuzumab-based targeted therapies. TNBC is characterized by a high level of cell invasiveness and visceral metastasis to organs, usually the brain, lungs, and liver. The affordable therapeutic strategy includes cytotoxic chemotherapy with taxane- and tetracycline-based combination treatment and platinum-based agents, but drug resistance constitutes one of the major challenges that TNBC research faces. Multifactorial resistance mechanisms include genetic alterations, microenvironmental changes, and cancer stem cells [77]. The discovery of new compounds that impact the survival of tumor cells in this particular subtype of breast cancer is highly significant for enhancing its treatment [78].

2. Benzopyrans as antitumor agents

Several natural products containing a BP skeleton have exhibited anti-tumor properties against BC. Genistein (**Figure 7**), an estrogenic soy-derived compound belonging to the isoflavone class, induces apoptosis in TNBC cells [79-82]. Wogonin (**Figure 7**), a natural flavone isolated from the roots of *Scutellaria baicalensis*, has proven to be able to suppress tumor angiogenesis in BC [83,84]. Moreover, hesperitin derivatives (**Figure 7**) also present anti-tumor activity against BC [85,86]. Therefore, the synthesis of BP nucleus has attracted the interest of numerous medicinal chemistry groups to search for new anti-tumors agents [87,88]. Our research group isolated polycerasoidol and polyalthidin (**Figure 7**) [11, 12] in the past. Polycerasoidol and synthetic analogs displayed PPAR-activating properties, anti-inflammatory effects and ameliorated metabolic derangements [64,65], while polyalthidin has shown to be an inhibitor of the mammalian mitochondrial respiratory chain [12]. In addition, isopolycerasoidol (**Figure 7**) has been reported to induce mitochondrial-mediated apoptosis in human BC cell lines [89].

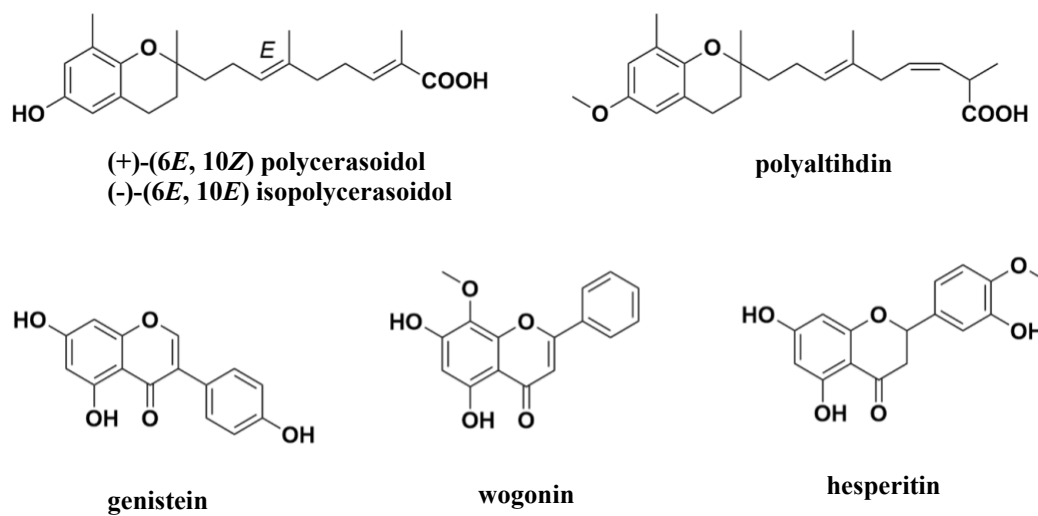


Figure 7. Benzopyrans as antitumor agents

3. Article

Article 4: Synthesis of 2-Aminopropyl benzopyran derivatives as potential agents against triple negative breast cancer, *RSC Medicinal Chemistry*, 14 (2023) 2327.

RESEARCH ARTICLE

View Article Online
View Journal | View IssueCite this: *RSC Med. Chem.*, 2023, 14, 2327

Synthesis of 2-aminopropyl benzopyran derivatives as potential agents against triple-negative breast cancer†

Ainhoa García, ^{ab} Sandra Torres-Ruiz, ^b Laura Vila, ^{ab} Carlos Villarroel-Vicente, ^{ab} Álvaro Bernabeu, ^a Pilar Eroles, ^{*bcd} Nuria Cabedo ^{id} ^{*ab} and Diego Cortes ^{id} ^a

Synthesis of three series of 2-aminopropyl derivatives containing a benzopyran nucleus was performed to evaluate their performance against triple-negative breast cancer cell lines (MDA-MB-231 and MDA-MB-436) and normal breast epithelial cells (MCF10A). For the three series, the cytotoxic activity was as follows: *N*-methylated derivatives (tertiary amines) **5b**, **6b**, and **7b** > secondary amine benzopyrans **5**, **6**, and **7** > quaternary amine salts **5c**, **6c**, and **7c** > free phenolic derivatives **5a**, **6a**, and **7a**. The structure–activity relationship showed the importance of the presence of an amine group and a *p*-fluorobenzyloxy substituent in the chromanol ring (IC₅₀ values from 1.5 μM to 58.4 μM). In addition, **5a**, **5b**, **6a**, and **7b** displayed slight selectivity towards tumor cells. Compounds **5**, **5a**, **5b**, **6**, **6a**, **6c**, **7**, and **7b** showed apoptotic/necrotic effects due to, at least in part, an increase in reactive oxygen species generation, whereas **5b**, **5c**, **6b**, **7a**, and **7c** caused cell cycle arrest in the G1 phase. Further cell-based mechanistic studies revealed that **5a**, **6a**, and **7b**, which were the most promising compounds, downregulated the expression of *Bcl-2*, while **5b** downregulated the expression of cyclins *CCND1* and *CCND2*. Therefore, 2-aminopropyl benzopyran derivatives emerge as new hits and potential leads for developing useful agents against breast cancer.

Received 2nd August 2023,
Accepted 5th September 2023

DOI: 10.1039/d3md00385j

rsc.li/medchem

1. Introduction

Breast cancer (BC) is a complex and heterogeneous disease, and the most frequently diagnosed and leading cause of cancer-related deaths in women, with increasing mortality rates affecting more than 1 million women worldwide.^{1–4} The selection of drug therapy for patients depends on the cancer subtype: hormone receptor-positive, human epidermal growth factor receptor 2 (HER-2), and triple-negative BC (TNBC).

TNBC is characterized as lacking estrogen receptors (ERs), progesterone receptors (PRs), and HER-2.^{5–9} This is the most aggressive subtype, and represents 15% of all breast cancers.¹⁰ Consequently, TNBC patients do not respond to hormonal and anti-HER2 monoclonal antibody trastuzumab-based targeted therapies. An affordable therapeutic strategy includes cytotoxic chemotherapy with taxane- and

tetracycline-based combination treatment and platinum-based agents, but drug resistance is one of the major challenges that is currently being addressed by TNBC research.^{10,11} The discovery of new compounds that decrease the survival of tumor cells in this particular subtype of breast cancer is highly significant for enhancing treatment of this disease.¹⁰

Several natural products containing a benzopyran skeleton (Fig. 1) have exhibited anti-tumor properties against BC through pleiotropic mechanisms involving apoptosis and cell cycle arrest, among others. Genistein, an estrogenic soy-derived compound belonging to the isoflavone class, induces apoptosis in TNBC cells.^{12–15} Wogonin, a natural flavone isolated from the roots of *Scutellaria baicalensis* Georgi, suppresses tumor angiogenesis

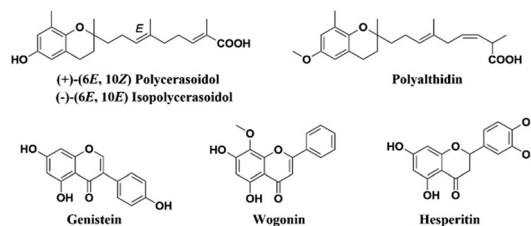


Fig. 1 Natural products containing a benzopyran skeleton.

^a Department of Pharmacology, University of Valencia, 46100 Valencia, Spain.
E-mail: ncabedo@uv.es^b Institute of Health Research-INCLIVA, University Clinic Hospital of Valencia, 46010 Valencia, Spain^c Department of Physiology, University of Valencia, 46010 Valencia, Spain.
E-mail: pilar.eroles@uv.es^d Center for Biomedical Network Research on Cancer (CIBERONC), 28019 Madrid, Spain† Electronic supplementary information (ESI) available. See DOI: <https://doi.org/10.1039/d3md00385j>

in BC.^{16,17} Moreover, hesperitin derivatives also present anti-tumor activity against BC.^{18,19} Therefore, the synthesis of the benzopyran nucleus has been performed by numerous medicinal chemistry groups in their search for new anti-tumor agents.^{20,21}

Our research group previously isolated polycerasoidol and polyalthidin (Fig. 1) from the stem bark of *Polyalthia cerasoides* (Annonaceae).^{22,23} Polycerasoidol and synthetic analogs displayed PPAR-activating properties, anti-inflammatory effects, and ameliorated metabolic derangements,^{24,25} while it has been shown that polyalthidin is an inhibitor of the mammalian mitochondrial respiratory chain.²³ In addition, it has been reported that isopolycerasoidol induces mitochondrial-mediated apoptosis in human BC cell lines.²⁶

Based on these pieces of evidence, our goal was to discover new molecules for future TNBC treatment. Therefore, we synthesised 2-aminopropyl benzopyran derivatives bearing a *p*-methoxyphenylethylamine (series 1), diphenylethylamine (series 2), or isoquinoline moiety (series 3) (Scheme 1). The 15 new compounds were tested against human TNBC cell lines (MDA-MB-231 and MDA-MB-436) and normal breast epithelial cells (MCF10A) for cytotoxic activity. Then, we studied their impact on the apoptosis/necrosis effect or cell cycle arrest, as well as their reactive oxygen species (ROS) production and the gene expression of some promising compounds.

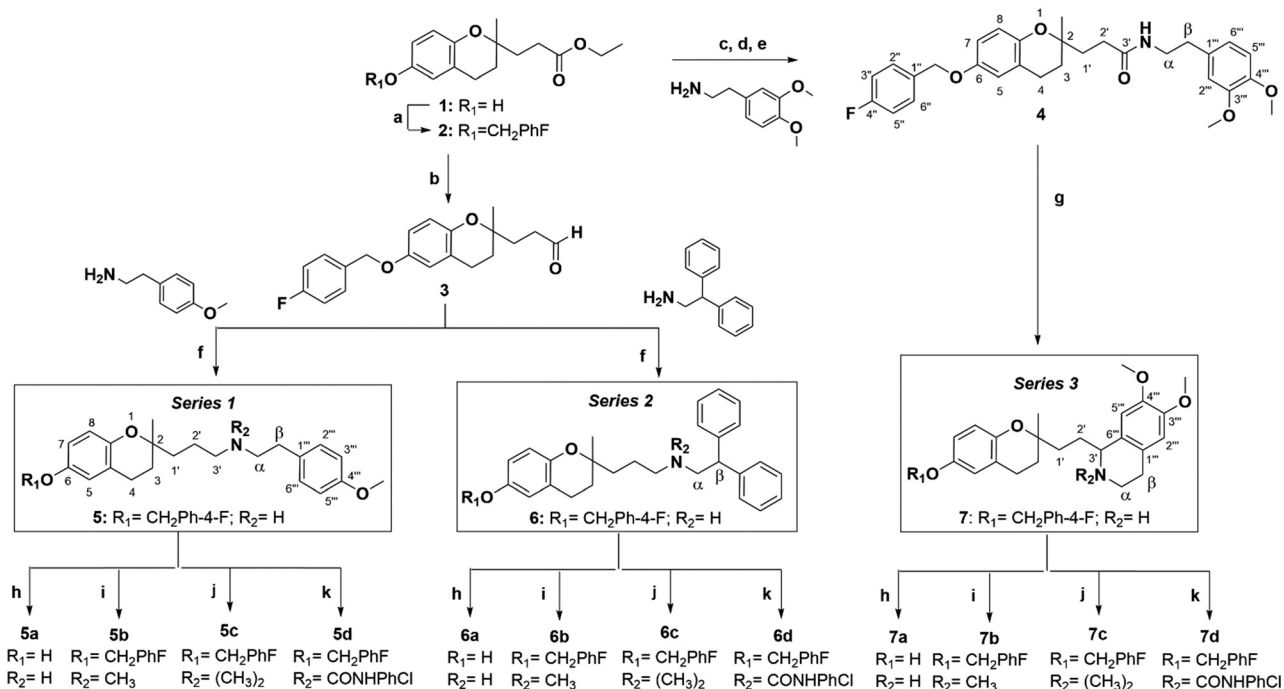
2. Results and discussion

2.1. Chemistry

Using different methodologies, we synthesized three series of compounds with a benzopyran skeleton. 2-Aminopropyl benzopyran derivatives were synthesised *via* a chroman-4-one scaffold. These derivatives were obtained by aldol condensation between *o*-hydroxyacetophenones and methylketones in the presence of a secondary amine by Michael addition, as previously reported.^{27–30} The free phenolic group of precursor benzopyran **1** was protected using *p*-fluorobenzyl chloride in the presence of potassium carbonate to afford benzopyran ester **2** (Scheme 1).

To obtain 2-aminopropyl benzopyran derivatives, two different synthetic pathways were followed from benzopyran ester **2**. The first was to synthesise *p*-methoxyphenylethylamine derivatives (series 1) and diphenylethylamine derivatives (series 2), and the second was used to synthesise isoquinoline derivatives (series 3). For the first pathway, controlled reduction by diisobutylaluminum hydride (DIBAL-H) of the ester group was carried out to obtain aldehyde intermediate **3**, from which compounds **5** (series 1) and **6** (series 2) were obtained by reductive amination.

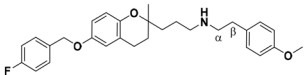
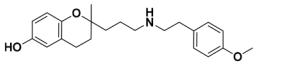
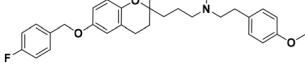
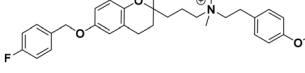
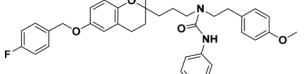
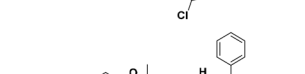
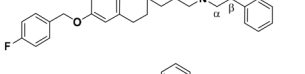
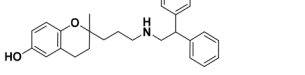
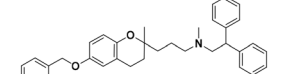
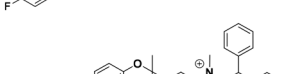
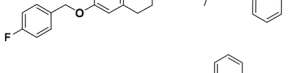
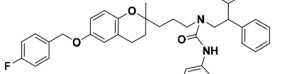
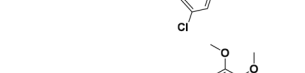
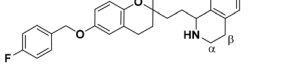
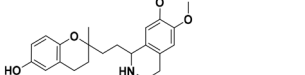
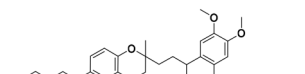
The condensation of **3** with 4-methoxyphenethylamine and 2,2-diphenylethylamine resulted in secondary amines **5** and **6**, respectively, *via* a Schiff base, followed by reduction with sodium triacetoxyborohydride under acid conditions.



Scheme 1 Reagents and conditions: (a) *p*-fluorobenzyl chloride, K₂CO₃, EtOH, reflux, N₂, 4 h, 79%, (b) DIBAL-H, DCM, −78 °C, N₂, 15 min, 92%, (c) MeOH, KOH 20%, reflux, N₂, 4 h, (d) SOCl₂, DCM, reflux, N₂, 3 h, (e) 4-DMAP, Et₃N, DCM, rt., N₂, overnight, 63%, (f) NaBH(OAc)₃, AcOH, (CH₂Cl)₂, rt., N₂, 1 h, 72% for **5** and 54% for **6**, (g) POCl₃, CH₂Cl₂, reflux, N₂, overnight, NaBH₄, MeOH, rt., N₂, 2 h, 53%, (h) HCl:EtOH 1:1, reflux, N₂, 3 h, 92–96%, (i) HCHO, HCO₂H, MeOH, reflux, N₂, 1 h, NaBH₄, rt., N₂, 45 min, 76–86%, (j) MeI, DMF, reflux, N₂, 30 min–1 h, 79–96%, (k) 4-chlorophenyl isocyanate, Et₃N, DCM, rt., N₂, overnight, 68–92%.



Table 1 IC₅₀ values in TNBC and normal breast epithelial cells, and selectivity index (SI)

Structure	MDA-MB-231 (μM)	MDA-MB-436 (μM)	MCF10A (μM)	SI MCF10A/MDA-MB-231	SI MCF10A/MDA-MB-436
	13.2 ± 1.6 ^a	13.0 ± 2.0	6.3 ± 0.9	0.48	0.48
	51.0 ± 5.8 ^a	30.9 ± 3.5 ^a	76.8 ± 0.5 ^b	1.51	2.50
	7.3 ± 0.7	12.6 ± 1.5	12.1 ± 2.8	1.65	0.96
	25.0 ± 1.1 ^c	24.0 ± 1.2 ^b	25.0 ± 2.0 ^a	1.0	1.0
	>100	>100	>100	—	—
	11.0 ± 2.6 ^a	19.3 ± 0.8 ^b	12.9 ± 1.8 ^a	1.17	0.67
	48.3 ± 4.2 ^a	31.1 ± 5.5 ^c	46.6 ± 3.6 ^b	0.96	1.5
	1.5 ± 0.1	2.0 ± 1.7	1.4 ± 0.7	0.94	0.70
	19.2 ± 2.9 ^b	24.6 ± 1.1 ^b	20.8 ± 4.0	1.09	0.84
	>100	>100	>100	—	—
	22.2 ± 1.8 ^a	22.0 ± 0.8	21.9 ± 3.8	0.98	0.99
	58.4 ± 4.0 ^a	55.2 ± 5.6 ^a	54.2 ± 3.7 ^b	0.93	0.98
	14.0 ± 0.8	21.8 ± 0.6	20.1 ± 1.9	1.44	0.92
	42.2 ± 4.9 ^a	53.5 ± 1.1 ^c	41.4 ± 2.1 ^b	0.98	0.77
	>100	>100	>100	—	—
	25.9 ± 0.1	15.80 ± 0.7	26.8 ± 0.5	1.03	1.70

The data are presented as the mean ± SD of three independent experiments performed in triplicate. ^a $P < 0.05$. ^b $P < 0.01$. ^c $P < 0.001$ vs. **5b**, **6b**, and **7b** for each family. Selectivity index (SI): ratio of cytotoxicity in MCF10A cells compared to that in cancer cells.



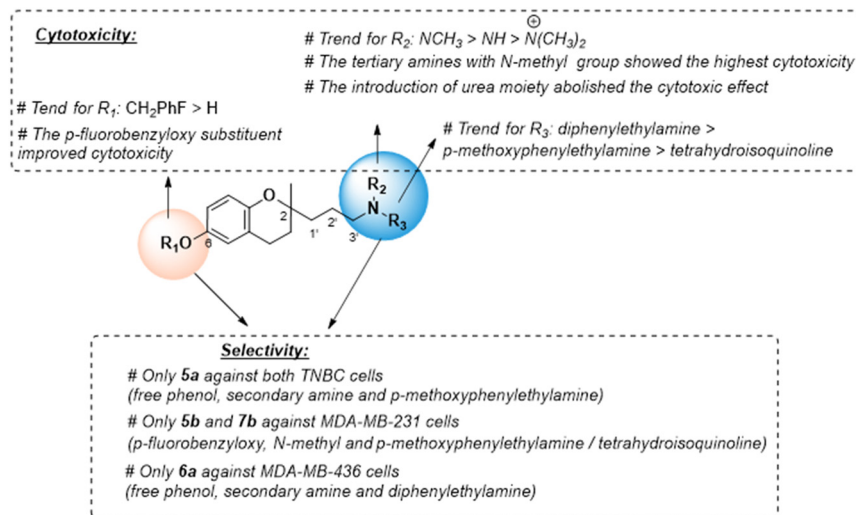


Fig. 2 SAR study of 2-aminopropyl benzopyran derivatives as potential anti-TNBC agents.

The second pathway was based on the formation of the amide intermediate **4** from an acid chloride. The ester group of **2** was submitted to basic hydrolysis, followed by a reaction with thionyl chloride. Then, acid chloride was reacted with 3,4-dimethoxyphenethylamine to yield amide **4**, from which compound **7** was obtained by Bischler–Napieralski cyclodehydration.

In each series, four derivatives were obtained from amines **5**, **6**, and **7**. The subsequent acid hydrolysis of the *p*-fluorobenzyl group yielded amines **5a**, **6a**, and **7a**. *N*-Methylated derivatives **5b**, **6b**, and **7b** were obtained with formic acid and formaldehyde, followed by reduction with sodium borohydride, while *N*-dimethylated salts **5c**, **6c**, and **7c** were obtained with methyl iodide. The functionalization of the amine group in the urea group was achieved by reacting it with 4-chlorophenyl isocyanate to obtain urea derivatives **5d**, **6d**, and **7d** (Scheme 1).

2.2. Pharmacology

2.2.1. Cytotoxicity evaluation and structure–activity relationships (SAR) study. The cytotoxicity of all the synthesised compounds against human breast MDA-MB-231 and MDA-MB-436 cell lines, and MCF10A cells was evaluated by the WST-1 assay. A dose–response curve analysis was performed to determine the drug concentrations required to inhibit cancer cell growth by 50% (IC_{50}) after 48 hours of incubation (Table 1).

For the three series, it was observed that the compounds were equally cytotoxic to cancer and normal cells. In the MDA-MB-231 cell line, the cytotoxic activity of the *N*-methylated compounds **5b**, **6b**, and **7b** (IC_{50} = 1.5–14.0 μM) was more potent than that of secondary amines **5**, **6**, and **7** (IC_{50} = 11.0–22.0 μM), followed by *N*-dimethylated derivatives as quaternary ammonium salts **5c**, **6c**, and **7c** (IC_{50} = 19.2–42.2 μM), as well as secondary amines with a free phenolic group **5a**, **6a**, and **7a** (IC_{50} = 58.4–48.3 μM).

In the MDA-MB-436 cells, the *N*-methylated compounds **5b**, **6b**, and **7b** (IC_{50} = 2.0–21.8 μM) were also more potent than secondary amines **5**, **6**, and **7** (IC_{50} = 13.0–22.0 μM), followed by *N*-dimethylated derivatives **5c**, **6c**, and **7c** (IC_{50} = 24.0–53.5 μM), and secondary amines with a free phenolic group **5a**, **6a**, and **7a** (IC_{50} = 30.9–55.2 μM).

In the MCF10A cells, *N*-methylated compounds were more potent than secondary amines, followed by *N*-dimethylated derivatives, and secondary amines with a free phenolic group. However, urea derivatives (**5d**, **6d**, and **7d**) did not produce any cellular cytotoxicity in either cell line.

For the three series, the structure–activity relationships (SAR) indicated that the nitrogen atom in the 2-propyl chain and the phenolic group in the benzopyran nucleus play a key role in cytotoxicity (Fig. 2). The tertiary or secondary amine function led to the most potent cytotoxic compounds, especially those bearing the *N*-(2,2-diphenylethyl) moiety (series 2), while its quaternization giving a ‘permanent cation’ decreased the cytotoxicity, which was most likely due to the difficulty in diffusing across cell membranes.

Urea-based derivatives are of growing interest for drug design and development, including anticancer drugs.³¹ However, the introduction in the 2-aminopropyl benzopyran of the *p*-chlorophenyl urea moiety increased the steric hindrance, which was detrimental for cytotoxic activity. The presence of the lipophilic *p*-fluorobenzoyloxy substituent in the chromanol ring favored cytotoxic activity, and its removal to a free phenolic group diminished the antitumor effect.

We also examined the selectivity of each compound against non-tumorigenic MCF10A cells. The selectivity index (SI) was calculated as the IC_{50} ratio of normal cells to cancer cells, $\text{SI} = \text{IC}_{50} (\text{MCF-10A}) / \text{IC}_{50} (\text{MDA-MB-231 or MDA-MB-436})$ (Table 1). Four compounds showed slight selectivity against malignant cells. Of those, compound **5a** (secondary amine and free phenolic group) bearing the *p*-methoxyethylamine moiety (series 1) suppressed the growth



of both cancer cell lines with higher SI, and **5b** (tertiary amine and *p*-fluorobenzyloxy) displayed selectivity against MDA-MB-231 cells. Similarly, compound **6a** (secondary amine and free phenolic group) bearing the diphenylethylamine moiety (series 2) and compound **7b** (tertiary amine and *p*-fluorobenzyloxy) with the isoquinoline moiety (series 3) were selective against MDA-MB-436 or MDA-MB-231 cells, respectively. However, the most cytotoxic compound, **6b**, did not exhibit selectivity against cancer cells (Fig. 2).

Compounds **5a**, **5b**, **6a**, and **7b** with higher SI values were selected to carry out further mechanistic studies.

2.2.2. Studies of apoptosis and necrosis. To determine the cause of cell death, we evaluated the apoptotic and necrotic effects of cytotoxic compounds. For this purpose, TNBC cells were treated with each compound at concentrations equal to their respective IC₅₀ values (Table 1), followed by Annexin V-FITC and propidium iodide (PI) staining. Representative flow cytometry dot plots showing the effects in MDA-MB-231

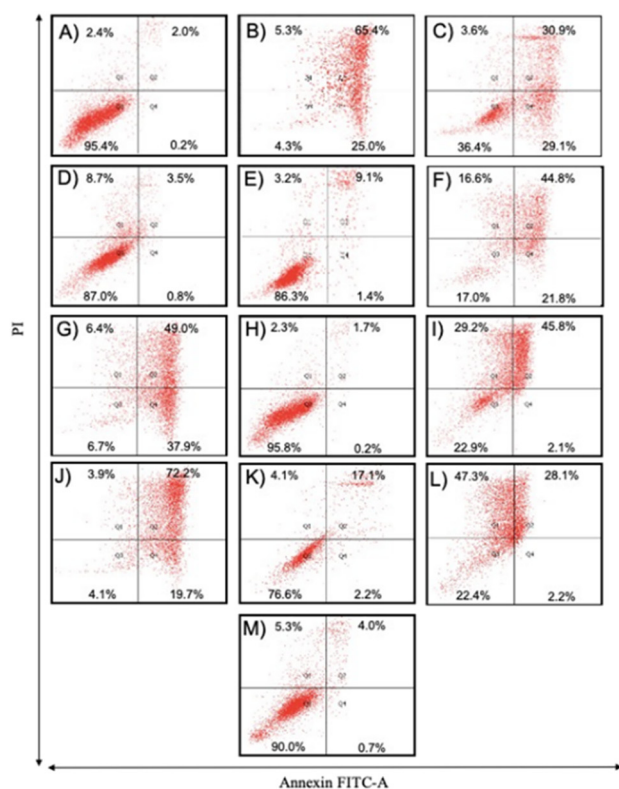


Fig. 3 Apoptosis/necrosis analyses of TNBC cells treated with compounds at their respective IC₅₀ values of cytotoxicity after Annexin V-FITC/PI staining. (A–M) Representative flow cytometry dot plots showing the effects of vehicle or compounds on MDA-MB-231 cell apoptosis/necrosis/survival have been included: (A) 0.1% DMSO, (B) **5** at 13.2 μ M, (C) **5a** at 51.0 μ M, (D) **5b** at 7.3 μ M, (E) **5c** at 25.0 μ M, (F) **6** at 11.0 μ M, (G) **6a** at 48.3 μ M, (H) **6b** at 1.5 μ M, (I) **6c** at 19.2 μ M, (J) **7** at 22.2 μ M, (K) **7a** at 58.4 μ M, (L) **7b** at 14.0 μ M, (M) **7c** at 42.2 μ M. (N) Histograms show the percentage of apoptotic and necrotic cell distribution. The data are expressed as the mean \pm SD of three independent experiments performed in triplicate. ** P < 0.01, *** P < 0.001, **** P < 0.0001 vs. DMSO group.

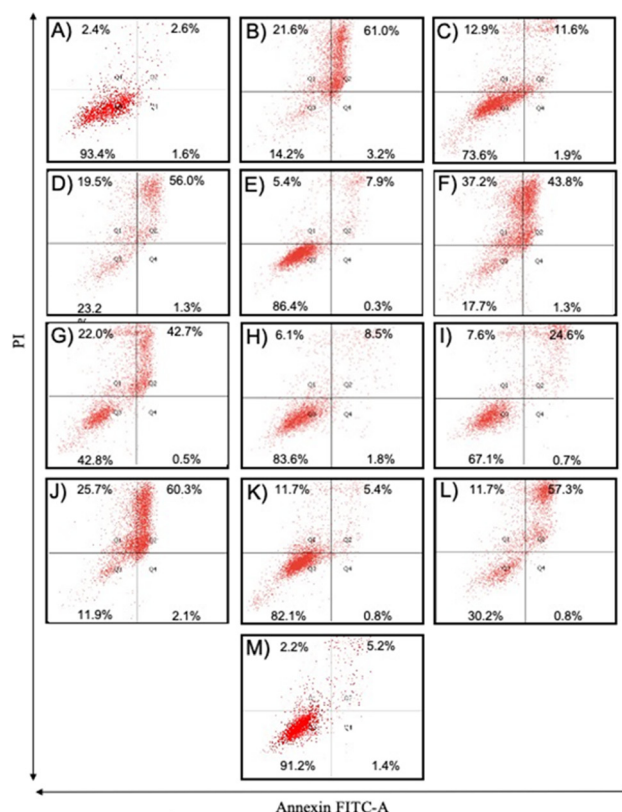


Fig. 4 Apoptosis/necrosis analyses of TNBC cells treated with compounds at their respective IC₅₀ values of cytotoxicity after Annexin V-FITC/PI staining. (A–M) Representative flow cytometry dot plots showing the effects of vehicle or compounds on MDA-MB-436 cell apoptosis/necrosis/survival have been included: (A) 0.1% DMSO, (B) **5** at 13.0 μ M, (C) **5a** at 30.9 μ M, (D) **5b** at 12.6 μ M, (E) **5c** at 24.0 μ M, (F) **6** at 19.3 μ M, (G) **6a** at 31.1 μ M, (H) **6b** at 2.0 μ M, (I) **6c** at 24.6 μ M, (J) **7** at 22.0 μ M, (K) **7a** at 55.2 μ M, (L) **7b** at 21.8 μ M, and (M) **7c** at 53.5 μ M. (N) Histograms show the percentage of apoptotic/necrotic cell distribution. The data are expressed as the mean \pm SD of three independent experiments performed in triplicate. * P < 0.05, ** P < 0.01, *** P < 0.001 vs. DMSO group.



and MDA-MB-436 cells are included in Fig. 3A–M and 4A–M, and histograms show the percentage of apoptotic and necrotic cell distribution in Fig. 3N and 4N, respectively. We observed that most cytotoxic compounds triggered apoptosis and necrosis. For both cancer cell lines, secondary amines **5**, **6**, and **7** significantly induced cell apoptosis and necrosis (83–96.5%), as did **6a** and **7b** (65–93%).

Compounds **5a** and **6c** induced a significant percentage of apoptotic and necrotic cells in the MDA-MB-231 line (64% and 75%, respectively), and to a lesser extent in the MDA-MB-436 line (30% and 32%, respectively). Significant apoptosis and necrosis were elicited by compound **5b**, but only in the MDA-MB-436 cell line (74%). In addition, ROS are crucial in inducing apoptosis through several pathways. Therefore, the

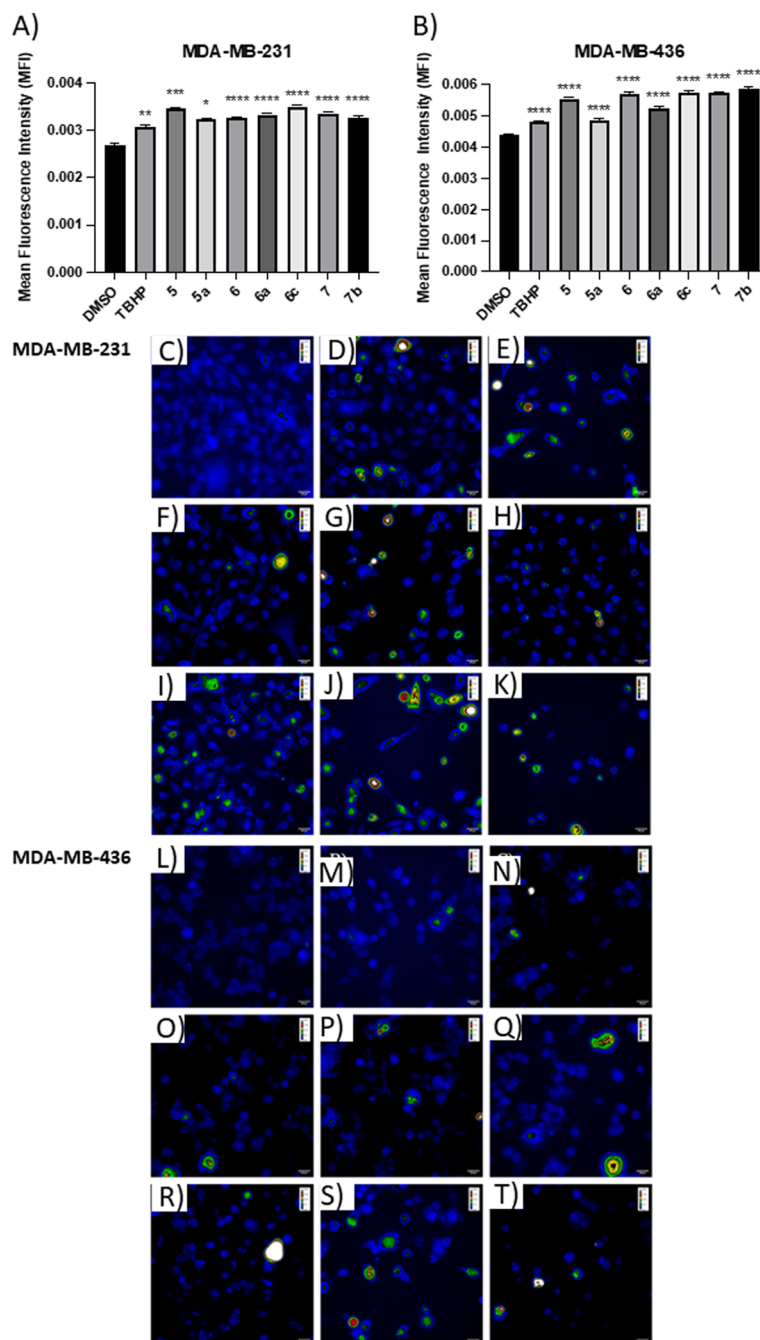


Fig. 5 Effect of compounds on intracellular ROS levels. Histograms display the quantification of mean fluorescence intensity (MFI) for vehicle or compounds in (A) MDA-MB-231 cells and (B) MDA-MB-436 cells. Representative confocal fluorescence microscopy images of ROS production in (C–K) MDA-MB-231 cells and (L–T) MDA-MB-436 cells. (C and L) 0.05% DMSO, (D and M) TBHP at 100 μ M, (E) **5** at 6.6 μ M, (F) **5a** at 25.5 μ M, (G) **6** at 5.5 μ M, (H) **6a** at 24.2 μ M, (I) **6c** at 9.6 μ M, (J) **7** at 11.1 μ M, (K) **7b** at 7.0 μ M, (N) **5** at 6.5 μ M, (O) **5a** at 15.5 μ M, (P) **6** at 9.7 μ M, (Q) **6a** at 15.6 μ M, (R) **6c** at 12.3 μ M, (S) **7** at 11.0 μ M, and (T) **7b** at 10.9 μ M. The data are expressed as the mean \pm SEM of three independent experiments performed in triplicate. * P < 0.05, ** P < 0.01, *** P < 0.001, **** P < 0.0001 vs. DMSO group.



capacity of the apoptotic and necrotic compounds (**5**, **6**, **6a**, **7**, and **7b**) to trigger oxidative stress was further studied in both cancer cell lines, whereas non-apoptotic but cytotoxic compounds (**5c**, **6b**, **7a**, and **7c** for both cancer cell lines, and **5b** for MDA-MB-231 cells) were studied to evaluate their influence on cell cycle distribution.

2.2.3. Measurement of reactive oxygen species (ROS) levels. At low or moderate doses, ROS are considered essential for the regulation of normal physiological cell conditions. However, high ROS levels cause damage to proteins, nucleic acids, lipids, membranes, and organelles, which can lead to the activation of cell death processes such as cell apoptosis.³² Because oxidative stress promotes apoptotic mechanisms, the effect of apoptotic benzopyrans in ROS production was evaluated. To that end, cell lines MDA-MB-231 and MDA-MB-436 were treated with selected representative apoptotic compounds at their respective IC₂₅ values. Then, fluorescence microscopy was employed to detect intracellular ROS levels by the dichlorodihydrofluorescein-diacetate (DCFDA) method.

The positive control, *tert*-butyl hydroperoxide (TBHP), significantly increased the mean fluorescence level, thus confirming its action mechanism. The results demonstrated that the apoptotic compounds **5**, **5a**, **6**, **6a**, **6c**, **7**, and **7b** significantly increased the level of ROS production in both TNBC cell lines (Fig. 5), as compared to control cells. The results suggested that these compounds can induce apoptosis by the generation of ROS in TNBC cells.

2.2.4. Cell cycle analysis. Because the cell growth inhibition observed in the cytotoxicity assay could be due to cell death *via* apoptosis/necrosis or cell cycle arrest, flow cytometry analysis was carried out to examine the arrest effects of non-apoptotic benzopyrans (**5b**, **5c**, **6b**, **7a**, and **7c**) on the cell cycle of both TNBC cell lines. For that purpose, cell lines MDA-MB-231 and MDA-MB-436 were treated with each compound at concentrations equal to their respective IC₅₀ values (Table 1), and then stained with PI.

The results showed that all non-apoptotic compounds significantly increased the percentage of the cells in the G1 phase, and lowered the percentage of the cells in the S phase. Regarding the MDA-MB-231 cell line, the percentage of the cells in the G1 phase increased from 49.81% for the control group to 63.02%, 63.73%, 56.12%, 62.18%, and 60.36% for compounds **5b**, **5c**, **6b**, **7a**, and **7c**, respectively (Fig. 6A and C–H). In the MDA-MB-436 cell line, the percentage of the cells in the G1 phase rose from 41.01% for the control group to 57.87%, 45.81%, 43.89%, and 55.78% for compounds **5c**, **6b**, **7a**, and **7c**, respectively (Fig. 6B and I–M). The percentage of the cells in the S phase in the MDA-MB-231 cell line decreased from 42.68% for the control group to 24.84%, 18.38%, 29.33%, 22.81%, and 23.05% for compounds **5b**, **5c**, **6b**, **7a**, and **7c**, respectively (Fig. 6A and C–H), and in MDA-MB-436 cells, decreased from 40.08% for the control group to 24.25%, 34.56%, 36.58%, and 30.13% for compounds **5c**, **6b**, **7a**, and **7c**, respectively (Fig. 6B and I–M). These results suggest that

non-apoptotic 2-aminopropyl benzopyrans **5b**, **5c**, **6b**, **7a**, and **7c** caused cell cycle arrest at the G1 phase.

2.2.5. Gene expression. Apoptosis is regulated by complex interactions between pro- and anti-apoptotic members of the B cell lymphoma-2 (Bcl-2) protein family.³³ Among the Bcl-2 family proteins, Bcl-2 promotes cell survival, while others can induce cell death.^{34–36} The cell cycle is regulated by a group of proteins known as cyclins, such as cyclin D1 (CCND1) or cyclin E2 (CCNE2), which regulate the progression from G1 to S phase.^{37–41} To explore the apoptosis and cell cycle arrest mechanism involved in the most promising compounds (those with a more appropriate SI value), we evaluated the gene expression of anti-apoptotic *Bcl-2* as well as *CCND1* and *CCNE2* in TNBC cells. The results showed that apoptotic compounds **5a**, **6a**, and **7b** downregulated *Bcl-2* (Fig. 7A and B), whereas compound **5b** downregulated the expression of the *CCND1* and *CCNE2* genes (Fig. 7C and D).

3. Conclusions

Three series of 2-aminopropyl benzopyran derivatives were synthesised (Scheme 1) and evaluated for their antitumor activity against the MDA-MB-231 and MDA-MB-436 TNBC cell lines. The SAR studies showed that the presence of an amino group (secondary, tertiary, or quaternary) in the structure seems to be essential for cytotoxicity in both TNBC cell lines, and its modification to a urea function renders the derivatives devoid of an anti-tumor effect. For the three series, the cytotoxic activity was as follows: *N*-methylated derivatives (tertiary amines) **5b**, **6b**, and **7b** > secondary amines **5**, **6**, and **7** > quaternary amine salts **5c**, **6c**, and **7c** > free phenolic derivatives **5a**, **6a**, and **7a**. In addition, **5a**, **5b**, **6a**, and **7b** displayed slight selectivity for tumor cells.

An apoptotic and necrotic effect was observed for benzopyrans **5**, **5a**, **5b**, **6**, **6a**, **6c**, **7**, and **7b** due to, at least in part, an increase in ROS generation, while **5b**, **5c**, **6b**, **7a**, and **7c** caused cell cycle arrest in the G1 phase. Further cell-based mechanistic studies revealed that the most promising compounds, **5a**, **6a**, and **7b**, downregulated the expression of *Bcl-2*, and **5b** downregulated the expression of cyclins *CCND1* and *CCND2*. Therefore, 2-aminopropyl benzopyrans emerge as new hits and can be used for designing new potential lead compounds in the development of useful agents against TNBC.

4. Experimental section

4.1. Chemistry

Electrospray ionization high-resolution mass spectrometry (ESI-HRMS) was performed using a TripleTOF™ 5600 liquid chromatography-tandem mass spectrometry (LC/MS/MS) System (AB SCIEX) (Toronto, Canada). LC-MS detection was performed using an ultra-high performance liquid chromatography (UHPLC) apparatus (Shimadzu, LCMS-8040)



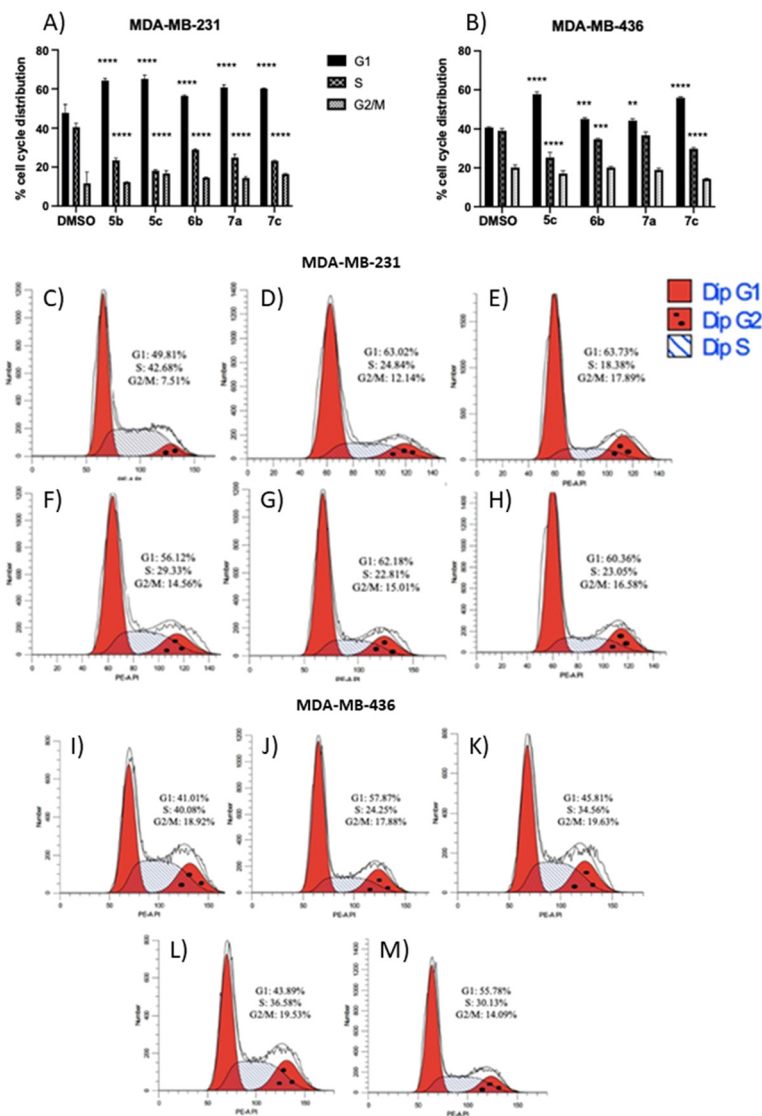


Fig. 6 Effect of non-apoptotic/necrotic compounds on cell cycle progression. The analysis of cell cycle distribution was performed by flow cytometry using PI staining. Histograms display the percentage of cell cycle distribution for (A) MDA-MB-231 cells and (B) MDA-MB-436 cells. Representative flow cytometry plots of cell cycle progression experiments with vehicle or non-apoptotic compounds for the (C–H) MDA-MB-231 cell line and (I–M) MDA-MB-436 cell line. (C and I) 0.1% DMSO, (D) **5b** at 7.3 μ M, (E) **5c** at 25.0 μ M, (F) **6b** at 1.5 μ M, (G) **7a** at 58.4 μ M, (H) **7c** at 42.2 μ M, (J) **5c** at 24.0 μ M, (K) **6b** at 2.0 μ M, (L) **7a** at 55.2 μ M, and (M) **7c** at 53.5 μ M. The data are expressed as the mean \pm SD of three independent experiments performed in triplicate. ** $P < 0.01$, *** $P < 0.001$, **** $P < 0.0001$ vs. DMSO group.

coupled to a tandem mass spectrometry (MS/MS) triple quadrupole equipped with an ESI ion source (Shimadzu, Kyoto, Japan).

^1H NMR and ^{13}C NMR spectra were recorded on a Bruker AC-300 (Bruker Instruments, Kennewick, WA). The assignments in ^1H and ^{13}C NMR were made by correlation spectroscopy (COSY) 45, heteronuclear single quantum correlation (HSQC), and heteronuclear multiple bond correlation (HMBC) recorded at 300 MHz. Chemical shifts (δ) are reported in ppm relative to an internal deuterated solvent reference, with multiplicities indicated as s (singlet), d (doublet), t (triplet), q (quartet), m (multiplet), or dd (double doublet). All reactions were monitored by analytical thin-layer chromatography (TLC) with silica gel 60 F254 (Merck 5554).

Residues were purified by silica gel column chromatography (40–63 μ m, Merck Group).

Solvents and reagents were purchased from the commercial sources Scharlab S.L. (Barcelona, Spain) and Sigma-Aldrich (St. Louis, MO, USA), respectively, and used without further purification unless otherwise noted. Dry and freshly distilled solvents were used in those reactions performed under N_2 . Quoted yields are of purified material. Final compounds were purified to $\geq 95\%$ as assessed by ^1H NMR and LC-MS/MS analysis.

Ethyl 3-(6-hydroxy-2-methyldihydrobenzopyran-2-yl)propanoate (1). Benzopyran ester **1** was synthesised as previously described^{27–30} from 2-(ethyl propanoate)-6-(hydroxyl)-2-(methyl)-dihydrobenzopyran-4-one. ^1H NMR (300 MHz,



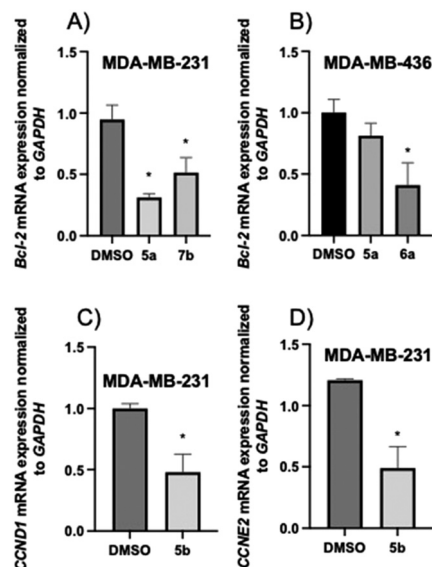


Fig. 7 Gene expression in TNBC cells treated with 2-aminopropyl benzopyrans **5a**, **5b**, **6a**, and **7b** at their respective IC_{25} values: (A) **5a** at 25.5 μ M and **7b** at 7.0 μ M, (B) **5a** at 15.5 μ M and **6a** at 15.6 μ M, and (C and D) **5b** at 3.7 μ M. The data are expressed as the mean \pm SD of three independent experiments performed in triplicate. * $P < 0.05$ vs. DMSO group.

$CDCl_3$) δ 6.59–6.53 (m, 3H, CH-5, CH-7, CH-8), 4.12 (q, $J = 7.1$ Hz, 2H, $CO_2CH_2CH_3$), 2.70 (m, 2H, CH_2-4), 2.44 (t, $J = 7.7$ Hz, 2H, CH_2-2'), 2.05–1.70 (m, 4H, CH_2-3 , CH_2-1'), 1.24 (t, $J = 7.1$ Hz, 3H, $CO_2CH_2CH_3$), 1.23 (s, 3H, CH_3-2); ^{13}C NMR (75 MHz, $CDCl_3$) δ 174.1 ($CO_2CH_2CH_3$), 148.8 (C-6), 147.4 (C-8a), 121.6 (C-4a), 117.8 (CH-5), 115.4 (CH-7), 114.6 (CH-8), 74.6 (C-2), 60.5 ($CO_2CH_2CH_3$), 34.3 (CH_2-1'), 31.1 (CH_2-3), 28.8 (CH_2-2'), 23.7 (CH_3-2), 22.1 (CH_2-4), 14.1 ($CO_2CH_2CH_3$); HREIMS m/z calculated for $C_{15}H_{20}O_4$ $[M]^+$ 264.1362, found: 264.1356.

Ethyl 3-(6-(*p*-fluorobenzoyloxy)-2-methyldihydrobenzopyran-2-yl)propanoate (2). A solution of benzopyran ester **1** (1.5 g, 5.68 mmol), *p*-fluorobenzyl chloride (0.9 mL, 7.38 mmol), and anhydrous K_2CO_3 (1.2 g, 8.49 mmol) in absolute EtOH (20 mL) was refluxed under N_2 for 4 hours. The mixture was evaporated, water was added (20 mL), and extraction proceeded with dichloromethane (3×15 mL). The organic layers were washed with 1 M HCl and brine, dried over anhydrous Na_2SO_4 , and evaporated under reduced pressure. The residue was purified by column chromatography (hexane/EtOAc, 90:10) to yield the *O*-protected benzopyran ester (**2**) (1.7 g, 79%) as a colorless oil. 1H NMR (300 MHz, $CDCl_3$) δ 7.41–7.36 (m, 2H, CH-2'', CH-6''), 7.09–7.03 (m, 2H, CH-3'', CH-5''), 6.72–6.67 (m, 3H, CH-5, CH-7, CH-8), 4.94 (s, 2H, $OCH_2Ph-p-F$), 4.13 (q, $J = 7.1$ Hz, 2H, $CO_2CH_2CH_3$), 2.76 (t, $J = 6.7$ Hz, 2H, CH_2-4), 2.48 (t, $J = 7.7$ Hz, 2H, CH_2-2'), 2.0–1.75 (m, 4H, CH_2-3 , CH_2-1'), 1.24 (t, $J = 7.2$ Hz, 3H, $CO_2CH_2CH_3$), 1.23 (s, 3H, CH_3-2); ^{13}C NMR (75 MHz, $CDCl_3$) δ 173.6 ($CO_2CH_2CH_3$), 162.3 (d, $J_{CF} = 244$ Hz, C-4''), 152.0 (C-6), 147.9 (C-8a), 133.1 (d, $J_{CF} = 3$ Hz, C-1''), 129.1 (d, $J_{CF} = 8$ Hz, CH-2'', CH-6''), 121.4 (C-4a), 117.7 (CH-5), 115.2 (d, $J_{CF} = 25$ Hz, CH-3'', CH-5''), 115.1 (CH-7), 114.4

(CH-8), 74.6 (C-2), 69.9 ($OCH_2Ph-p-F$), 60.3 ($CO_2CH_2CH_3$), 34.3 (CH_2-1'), 31.0 (CH_2-3), 28.7 (CH_2-2'), 23.6 (CH_3-2), 22.2 (CH_2-4), 14.1 ($CO_2CH_2CH_3$); HREIMS m/z calculated for $C_{22}H_{25}O_4F$ $[M]^+$ 372.1737, found: 372.1730.

3-(6-(*p*-Fluorobenzoyloxy)-2-methyldihydrobenzopyran-2-yl)propanal (3). A solution of **2** (500 mg, 1.34 mmol) in dry dichloromethane (10 mL) at $-78^\circ C$ under nitrogen atmosphere was stirred for 10 minutes. To this solution was added dropwise 8.8 mL of 1.0 M DIBAL-H solution in tetrahydrofuran (THF). After 15 minutes, the mixture was quenched by addition of 5 mL of MeOH and 10 mL of half sat aqueous NH_4Cl solution. The reaction mixture was stirred for an additional 10 minutes at room temperature, and then was concentrated *in vacuo*. Then, water was added (15 mL), and extraction proceeded with EtOAc (3×15 mL). The organic layers were washed with brine, dried over anhydrous Na_2SO_4 , and evaporated under reduced pressure. The residue was purified by silica gel column chromatography (hexane/EtOAc, 90:10) to afford 492 mg of the corresponding aldehyde **3** (406 mg, 92%) as a colorless oil. 1H NMR (300 MHz, $CDCl_3$) δ 9.78 (t, $J = 1.6$ Hz, 1H, CHO), 7.39–7.37 (m, 2H, H-2'', H-6''), 7.08–7.04 (m, 2H, H-3'', H-5''), 6.74–6.67 (m, 3H, H-5, H-7, H-8), 4.94 (s, 2H, $OCH_2Ph-p-F$), 2.77–2.74 (m, 2H, CH_2-4), 2.62–2.59 (m, 2H, CH_2-2'), 2.03–1.75 (m, 4H, CH_2-3 , CH_2-1'), 1.26 (s, 3H, CH_3-2); ^{13}C NMR (75 MHz, $CDCl_3$) δ 202.2 (CHO), 162.4 (d, $J_{CF} = 244$ Hz, C-4''), 152.1 (C-6), 147.7 (C-8a), 133.1 (d, $J_{CF} = 3$ Hz, C-1''), 129.3 (d, $J_{CF} = 8$ Hz, C-2'', C-6''), 121.4 (C-4a), 117.7 (CH-5), 115.2 (d, $J_{CF} = 25$ Hz, CH-3'', CH-5''), 115.2 (CH-7), 114.5 (CH-8), 74.6 (C-2), 69.9 ($OCH_2Ph-p-F$), 38.4 (CH_2-2'), 31.8 (CH_2-1'), 31.2 (CH_2-3), 23.7 (CH_3-2), 22.3 (CH_2-4); HRMS (ESI) m/z calculated for $C_{20}H_{21}O_3F$ $[M + H]^+$ 329.1547, found: 329.1552.

(*N*-3,4-Dimethoxyphenethyl)-3-(6-(*p*-fluorobenzoyloxy)-2-methyldihydrobenzopyran-2-yl)propanamide (4). A solution of ester **2** (1 g, 3.05 mmol) was dissolved in dry MeOH (10 mL) and KOH 20% (5 mL), and was refluxed under N_2 for 4 hours. The mixture was evaporated, water was added (20 mL), and extraction proceeded with dichloromethane (3×15 mL). The organic layers were washed with 1 M HCl and brine, dried over anhydrous Na_2SO_4 , and evaporated under reduced pressure to obtain 980 mg of carboxylic acid. To a solution of the carboxylic acid (980 mg, 2.85 mmol), dry dichloromethane and $SOCl_2$ (1.6 mL, 22.8 mmol) were added, and the solution was then reacted under reflux and N_2 for 3 hours. After stirring for an additional 30 minutes at room temperature, water was added (20 mL), and extraction proceeded with dichloromethane (3×15 mL). The organic layers were washed with brine, dried over anhydrous Na_2SO_4 , and evaporated under reduced pressure to obtain 1.3 g of chloride acid. A mixture of 3,4-dimethoxyphenethylamine (1.2 mL, 6.9 mmol), 4-DMAP (200 mg, 1.64 mmol), and Et_3N (0.06 mL, 0.45 mmol) was dissolved in 1 mL of dry dichloromethane under N_2 . To this mixture, a solution of the acid chloride (1 g, 2.6 mmol) in dry dichloromethane was added dropwise. This reaction remained at room temperature and under N_2 overnight. Dichloromethane (3×15 mL) was



added to the reaction mixture, and the organic layer was washed with HCl 1 M and brine, dried with anhydrous Na₂SO₄, filtered, and then evaporated to dryness. The residue obtained was subjected to silica gel column chromatography (hexane/EtOAc, 60:40) to afford compound 4 (976 mg, 63% yield) as a white oil. ¹H NMR (300 MHz, CDCl₃) δ 7.41–7.33 (m, 2H, CH-2'', CH-6''), 7.08–7.02 (m, 2H, CH-3'', CH-5''), 6.80–6.62 (m, 6H, CH-5, CH-7, CH-8, CH-2'', CH-5'', CH-6''), 5.69 (s, NH), 4.92 (s, 2H, OCH₂Ph-*p*-F), 3.85 (s, 6H, 2xOCH₃), 3.48–3.45 (m, 2H, CH₂-α), 2.81–2.67 (m, 4H, CH₂-4, CH₂-β), 2.32–2.27 (CH₂-2'), 2.03–1.83 (m, 2H, CH₂-1'), 1.80–1.67 (m, 2H, CH₂-3), 1.25 (s, 3H, CH₃-2). ¹³C NMR (75 MHz, CDCl₃) δ 172.9 (C=O), 162.0 (d, *J*_{CF} = 244 Hz, C-4''), 158.3 (C-3'', C-4''), 152.1 (C-6), 147.9 (C-8a), 133.2 (d, *J*_{CF} = 3 Hz, C-1''), 130.9 (C-1''), 129.7 (CH-6''), 129.3 (d, *J*_{CF} = 8 Hz, CH-2'', CH-6''), 121.6 (C-4a), 117.5 (CH-5), 115.4 (d, *J*_{CF} = 21 Hz, CH-3'', CH-5''), 115.2 (CH-7), 114.5 (CH-8), 114.1 (CH-2'', CH-5''), 75.0 (C-2), 70.0 (OCH₂Ph-*p*-F), 55.3 (2xOCH₃), 40.8 (CH₂-α), 35.2 (CH₂-1'), 34.8 (CH₂-β), 31.2 (CH₂-3), 30.8 (CH₂-2'), 23.7 (CH₃-2), 22.3 (CH₂-4). HRMS (ESI) *m/z* calculated for C₃₀H₃₅FNO₅ [M + H]⁺ 508.2494, found: 508.2481.

General procedure for synthesis of amine benzopyrans 5 and 6. A mixture of aldehyde 3 (240 mg, 0.73 mmol) and 4-methoxy-phenethylamine (0.25 mL, 1.4 mmol) or 2,2-diphenylethylamine (237 mg, 1.2 mmol) was dissolved in 5 mL of dry dichloroethane. The mixture was stirred at room temperature for 15 minutes and then added to a solution of sodium triacetoxymethylborohydride (360 mg, 1.7 mmol) and a drop of acetic acid in 1 mL of dry dichloroethane. The mixtures were stirred at room temperature under N₂ for 1 hour. Reaction mixtures were extracted with EtOAc (3 × 10 mL). The organic layer was washed with water and brine, dried with anhydrous Na₂SO₄, filtered, and then evaporated to dryness. The residue obtained was subjected to silica gel column chromatography (CH₂Cl₂/MeOH, 98:2) to afford compound 5 (244 mg, 72% yield) or 6 (201 mg, 54% yield) as colorless oils.

3-(6-(*p*-Fluorobenzyloxy)-2-methyldihydrobenzopyran-2-yl)-*N*-(*p*-methoxyphenethyl)propanamine (5). ¹H NMR (300 MHz, CDCl₃) δ 7.36–7.32 (m, 2H, CH-2'', CH-6''), 7.08–6.98 (m, 4H, CH-3'', CH-5'', CH-2'', CH-6''), 6.82–6.78 (m, 2H, CH-3'', CH-5''), 6.68–6.60 (m, 3H, CH-5, CH-7, CH-8), 4.89 (s, 2H, OCH₂-Ph-*p*-F), 3.74 (s, 3H, OCH₃), 3.03–2.57 (m, 8H, CH₂-4, CH₂-3', CH₂-α, CH₂-β), 1.78–1.66 (m, 2H, CH₂-3), 1.59–1.50 (m, 4H, CH₂-1', CH₂-2'), 1.20 (s, 3H, CH₃-2). ¹³C NMR (75 MHz, CD₃-OD) δ 162.0 (d, *J*_{CF} = 244 Hz, C-4''), 159.0 (C-4''), 152.2 (C-6), 147.7 (C-8a), 133.7 (CH-1''), 129.4 (CH-2'', CH-6''), 129.2 (d, *J*_{CF} = 8 Hz, CH-2'', CH-6''), 128.1 (C-1''), 121.6 (C-4a), 117.3 (CH-5), 115.0 (CH-7), 114.9 (CH-3'', CH-5''), 114.5 (d, *J*_{CF} = 13 Hz, CH-3'', CH-5''), 114.0 (CH-8), 74.9 (C-2), 69.6 (OCH₂Ph-*p*-F), 54.4 (OCH₃), 48.7 (CH₂-3', CH₂-α), 35.7 (CH₂-1'), 31.1 (CH₂-3), 30.8 (CH₂-β), 22.6 (CH₃-2), 21.8 (CH₂-4), 20.2 (CH₂-2'). HRMS (ESI) *m/z* calculated for C₂₉H₃₄FNO₃ [M + H]⁺ 464.2595, found: 464.2581.

***N*-(2,2-Diphenylethyl)-3-(6-(*p*-fluorobenzyloxy)-2-methyldihydrobenzopyran-2-yl)propanamine (6).** ¹H NMR

(300 MHz, CDCl₃) δ 7.44–7.40 (m, 2H, CH-2'', CH-6''), 7.36–7.22 (m, 10H, 2xPh), 7.15–7.08 (m, 2H, CH-3'', CH-5''), 6.80–6.71 (m, 3H, CH-5, CH-7, CH-8), 4.99 (s, 2H, OCH₂Ph-*p*-F), 4.28 (t, 1H, *J* = 7.8 Hz, CH-β), 3.30 (d, 2H, *J* = 7.8 Hz, CH₂-α), 2.76–2.70 (m, 4H, CH₂-4, CH₂-3'), 1.80–1.73 (m, 2H, CH₂-3), 1.65–1.54 (m, 4H, CH₂-1', CH₂-2'), 1.26 (s, 3H, CH₃-2). ¹³C NMR (75 MHz, CDCl₃) δ 162.5 (d, *J*_{CF} = 244 Hz, C-4''), 151.9 (C-6), 148.0 (C-8a), 142.5 (C-Ph), 133.2 (d, *J*_{CF} = 3 Hz, C-1''), 129.2 (d, *J*_{CF} = 8 Hz, CH-2'', CH-6''), 128.7 and 128.0 (CH-Ph), 121.6 (C-4a), 117.7 (CH-5), 115.3 (d, *J*_{CF} = 22 Hz, CH-3'', CH-5''), 115.2 (CH-7), 114.4 (CH-8), 75.3 (C-2), 70.0 (OCH₂Ph-*p*-F), 53.9 (CH₂-α), 50.7 (CH-β), 49.8 (CH₂-3'), 36.9 (CH₂-1'), 30.9 (CH₂-3), 23.9 (CH₃-2), 23.5 (CH₂-2'), 22.3 (CH₂-4). HRMS (ESI) *m/z* calculated for C₃₄H₃₆FNO₂ [M + H]⁺ 510.2803, found: 510.2801.

General procedure for synthesis of amine benzopyran 7. A mixture of amide 4 (880 mg, 1.72 mmol) and phosphoryl chloride (2.4 mL, 26 mmol) was dissolved in dry dichloromethane (10 mL) and refluxed under N₂ overnight. The reaction mixture was evaporated to dryness and dissolved in dry MeOH (7 mL) in an ice bath at –78 °C. Sodium borohydride (600 mg, 15.9 mmol) was added, and the reaction remained at room temperature and under N₂ for 2 hours. Then, the reaction mixture was alkalized with ammonia 5% and extracted with EtOAc (3 × 15 mL). The organic layer was washed with water and brine, dried with anhydrous Na₂SO₄, filtered, and evaporated to dryness. The residue obtained was subjected to silica gel column chromatography (CH₂Cl₂/MeOH, 98:2) to afford compound 7 (443.8 mg, 53% yield) as a colorless oil.

1-(2-(6-((4-Fluorobenzyl)oxy)-2-methyldihydrobenzopyran-2-yl)ethyl)-6,7-dimethoxy-1,2,3,4-tetrahydroisoquinoline (7). ¹H NMR (300 MHz, CDCl₃) δ 7.41–7.35 (m, 2H, CH-2'', CH-6''), 7.10–7.02 (m, 2H, CH-3'', CH-5''), 6.74–6.58 (m, 3H, CH-5, CH-7, CH-8), 6.56 and 6.55 (2 s, 2H, CH-2'', CH-5''), 4.93 (s, 2H, OCH₂Ph-*p*-F), 3.99–3.95 (m, 1H, CH-3'), 3.84 and 3.77 (2 s, 6H, 2xOCH₃), 3.25–3.18 and 2.99–2.94 (2 m, 2H, CH₂-α), 2.93–2.65 (m, 4H, CH₂-4, CH₂-β), 1.99–1.67 (m, 6H, CH₂-3, CH₂-1', CH₂-2'), 1.28 (s, 3H, CH₃-2). ¹³C NMR (75 MHz, CDCl₃) δ 162.0 (d, *J*_{CF} = 244 Hz, C-4''), 152.0 (C-6), 148.2 (C-8a), 147.5 and 147.3 (C-3'', C-4''), 133.2 (d, *J*_{CF} = 3 Hz, C-1''), 129.3 (d, *J*_{CF} = 8 Hz, CH-2'', CH-6''), 127.0 (C-1'', C-6''), 121.7 (C-4a), 117.7 (CH-5), 115.5 (d, *J*_{CF} = 21 Hz, CH-3'', CH-5''), 115.2 (CH-7), 114.4 (CH-8), 111.8 (CH-2''), 109.2 (CH-5''), 75.7 (C-2), 70.0 (OCH₂Ph-*p*-F), 56.0 and 55.8 (2xOCH₃), 55.9 (CH-3'), 41.1 (CH₂-α), 35.5 (CH₂-1'), 31.4 (CH₂-3), 30.9 (CH₂-2'), 29.6 (CH₂-β), 24.2 (CH₃-2), 22.5 (CH₂-4). HRMS (ESI) *m/z* calculated for C₃₀H₃₄FNO₄ [M + H]⁺ 492.2545, found: 492.2523.

General procedure for O-deprotection to prepare compounds 5a, 6a, and 7a. Amine 5 (50 mg, 0.11 mmol), 6 (56 mg, 0.11 mmol), and 7 (54 mg, 0.11 mmol) was dissolved in 1 M HCl:EtOH in a 1:1 ratio, and refluxed under N₂ for 3 hours. Reaction mixtures were stirred for an additional 30 minutes at room temperature, and ammonia 15% was added for alkalization. Mixtures were concentrated *in vacuo*, and then, water was added, and extraction proceeded with EtOAc (3 × 15 mL). The combined organic layers were dried over



anhydrous Na₂SO₄ and evaporated to dryness. The residue was purified by C18 column chromatography to afford 36.1 mg, 42.5 mg, and 40.6 mg of the corresponding compound **5a**, **6a**, and **7a** (92–96%) as colorless oils.

3-(6-Hydroxy-2-methyldihydrobenzopyran-2-yl)-N-(p-methoxyphenethyl)propanamine (5a). ¹H NMR (300 MHz, CD₃OD) δ 7.20 (d, 2H, *J* = 8.6 Hz, CH-2'', CH-6''), 6.90 (d, 2H, *J* = 8.6 Hz, CH-3'', CH-5''), 6.53–6.50 (m, 3H, CH-5, CH-7, CH-8), 3.78 (s, 3H, OCH₃), 3.22–2.89 (m, 6H, CH₂-3', CH₂- α , CH₂- β), 2.77–2.71 (m, 2H, CH₂-4), 1.92–1.56 (m, 6H, CH₂-3, CH₂-1', CH₂-2'), 1.27 (s, 3H, CH₃-2). ¹³C NMR (75 MHz, CD₃OD) δ 160.6 (C-4''), 151.7 (C-6), 148.0 (C-8a), 131.0 (CH-2'', CH-6''), 129.7 (C-1''), 123.1 (C-4a), 118.7 (CH-5), 116.4 (CH-3'', CH-5''), 115.7 (CH-7), 115.6 (CH-8), 76.1 (C-2), 55.9 (OCH₃), 50.6 (CH₂-3', CH₂- α), 37.2 (CH₂-1'), 32.8 (CH₂-3), 32.6 (CH₂- β), 24.2 (CH₃-2), 23.3 (CH₂-4), 21.9 (CH₂-2'). HRMS (ESI) *m/z* calculated for C₂₂H₂₉NO₃ [M + H]⁺ 356.2220, found: 356.2217.

2-(3-((2,2-Diphenylethyl)amino)propyl)-2-methyldihydrobenzopyran-6-ol (6a). ¹H NMR (300 MHz, CDCl₃) δ 7.30–7.20 (m, 10H, 2xPh), 6.55–6.47 (m, 3H, CH-5, CH-7, CH-8), 4.23 (t, *J* = 7.7 Hz, 1H, CH- β), 3.24 (d, *J* = 7.7 Hz, 2H, CH₂- α), 2.68–2.56 (m, 4H, CH₂-4, CH₂-3'), 1.70–1.45 (m, 6H, CH₂-3, CH₂-1', CH₂-2'), 1.19 (s, 3H, CH₃-2). ¹³C NMR (75 MHz, CDCl₃) δ 149.2 (C-6), 147.2 (C-8a), 142.4 (C-Ph), 128.7, 128.0 and 126.7 (2XCH-Ph), 121.7 (C-4a), 117.7 (CH-5), 115.6 (CH-7), 114.8 (CH-8), 75.3 (C-2), 54.0 (CH₂- α), 50.6 (CH- β), 49.8 (CH₂-3'), 36.7 (CH₂-1'), 30.9 (CH₂-3), 24.0 (CH₃-2), 23.5 (CH₂-2'), 22.2 (CH₂-4). HRMS (ESI) *m/z* calculated for C₂₇H₃₁NO₂ [M + H]⁺ 402.2428, found: 402.2417.

2-(2-(6,7-Dimethoxy-1,2,3,4-tetrahydroisoquinolin-1-yl)ethyl)-2-methyldihydrobenzopyran-6-ol (7a). ¹H NMR (300 MHz, CDCl₃ + 1 drop CD₃OD) δ 6.51–6.44 (m, 5H, CH-5, CH-7, CH-8, CH-2'', CH-5''), 4.10–4.01 (m, 1H, CH-3'), 3.75 (s, 6H, 2xOCH₃), 3.28–3.20 and 3.02–2.88 (2 m, 2H, CH₂- α), 2.85–2.55 (m, 4H, CH₂-4, CH₂- β), 1.97–1.93 (m, 1H, CH₂-3), 1.72–1.63 (m, 4H, CH₂-1', CH₂-2'), 1.19 (s, 3H, CH₃-2). ¹³C NMR (75 MHz, CDCl₃ + 1 drop CD₃OD) δ 149.8 (C-6), 148.1 (C-8a), 147.7 (C-3'', C-4''), 127.1 (C-1'', C-6''), 121.8 (C-4a), 117.5 (CH-5), 115.4 (CH-7), 114.5 (CH-8), 111.6 and 109.1 (CH-2'', CH-5''), 75.2 (C-2), 55.9 (CH-3'), 55.2 and 55.1 (2xOCH₃), 40.1 (CH₂- α), 35.0 (CH₂-1'), 31.3 (CH₂-3), 29.5 (CH₂- β), 28.6 (CH₂-2'), 23.6 (CH₃-2), 22.1 (CH₂-4). HRMS (ESI) *m/z* calculated for C₂₃H₂₉NO₄ [M + H]⁺ 384.2169, found: 384.2169.

General procedure for synthesis of N-methylated amines 5b, 6b, and 7b. A mixture of **5** (50 mg, 0.11 mmol), **6** (56 mg, 0.11 mmol), and **7** (54 mg, 0.11 mmol), formaldehyde (1 mL), and formic acid (two drops) was dissolved in MeOH (10 mL). The reaction was refluxed under N₂ for 1 hour. The reaction mixture was stirred for an additional 30 minutes at room temperature. Then, sodium borohydride (50 mg, 1.3 mmol) was added, and the reaction mixture was stirred for 45 minutes, and then basified by Et₃N. Water was added (10 mL), and the mixture was extracted with EtOAc (3 \times 10 mL). The combined organic layers were dried over anhydrous Na₂SO₄ and evaporated to dryness. The residue was purified by

silica gel column chromatography (CH₂Cl₂/MeOH, 98:2) to afford 40 mg, 46 mg, and 47.9 mg of **5b**, **6b**, and **7b**, respectively, (76–86% yield) as colorless oils.

3-(6-(p-Fluorobenzyloxy)-2-methyldihydrobenzopyran-2-yl)-N-(p-methoxyphenethyl)-N-methylpropanamine (5b). ¹H NMR (300 MHz, CDCl₃) δ 7.41–7.36 (m, 2H, CH-2'', CH-6''), 7.12–7.03 (m, 4H, CH-3'', CH-5'', CH-2'', CH-5''), 6.85–6.81 (m, 2H, CH-3'', CH-5''), 6.74–6.66 (m, 3H, CH-5, CH-7, CH-8), 4.94 (s, 2H, OCH₂Ph-*p*-F), 3.80 (s, 3H, OCH₃), 2.78–2.73 (m, 4H, CH₂-3', CH₂- β), 2.71–2.70 (m, 2H, CH₂-4), 2.67–2.59 (m, 2H, CH₂- α), 2.34 (s, 3H, NCH₃), 1.82–1.55 (m, 6H, CH₂-3, CH₂-1', CH₂-2'), 1.26 (s, 3H, CH₃-2). ¹³C NMR (75 MHz, CDCl₃) δ 162.6 (d, *J*_{CF} = 244 Hz, C-4''), 158.0 (C-4''), 151.9 (C-6), 148.2 (C-8a), 133.2 (d, *J*_{CF} = 3 Hz, C-1''), 132.0 (C-1''), 129.6 (CH-2'', CH-6''), 129.3 (d, *J*_{CF} = 8 Hz, CH-2'', CH-6''), 121.7 (C-4a), 117.7 (CH-5), 115.4 (d, *J*_{CF} = 21 Hz, CH-3'', CH-5''), 115.2 (CH-7), 114.4 (CH-8), 113.8 (CH-3'', CH-5''), 75.6 (C-2), 70.0 (OCH₂Ph-*p*-F), 59.5 (CH₂-3'), 57.7 (CH₂- α), 55.2 (OCH₃), 41.9 (NCH₃), 37.1 (CH₂-1'), 32.5 (CH₂-3), 31.0 (CH₂- β), 24.0 (CH₃-2), 22.4 (CH₂-4), 21.0 (CH₂-2'). HRMS (ESI) *m/z* calculated for C₃₀H₃₆FNO₃ [M + H]⁺ 478.2752, found: 478.2744.

N-(2,2-Diphenylethyl)-3-(6-(p-fluorobenzyloxy)-2-methyldihydrobenzopyran-2-yl)-N-methylpropan-1-amine (6b). ¹H NMR (300 MHz, CDCl₃) δ 7.43–7.39 (m, 2H, CH-2'', CH-6''), 7.29–7.15 (m, 10H, 2xPh), 7.10–7.05 (m, 2H, CH-3'', CH-5''), 6.75–6.68 (m, 3H, CH-5, CH-7, CH-8), 4.96 (s, 2H, OCH₂Ph-*p*-F), 4.16 (t, *J* = 7.0 Hz, 1H, CH- β), 2.98 (d, *J* = 7.0 Hz, 2H, CH₂- α), 2.65–2.64 (m, 2H, CH₂-4), 2.42–2.38 (m, 2H, CH₂-3'), 2.25 (s, 3H, NCH₃), 1.82–1.65 (m, 2H, CH₂-3), 1.56–1.41 (m, 4H, CH₂-1', CH₂-2'), 1.23 (s, 3H, CH₃-2). ¹³C NMR (75 MHz, CDCl₃) δ 162.0 (d, *J*_{CF} = 244 Hz, C-4''), 151.9 (C-6), 148.3 (C-8a), 143.8 (C-Ph), 133.2 (d, *J*_{CF} = 2 Hz, CH-1''), 129.3 (d, *J*_{CF} = 8 Hz, CH-2'', CH-6''), 128.3 and 126.2 (CH-Ph), 121.8 (C-4a), 117.8 (CH-5), 115.2 (d, *J*_{CF} = 21 Hz, CH-3'', CH-5''), 115.2 (CH-7), 114.4 (CH-8), 75.7 (C-2), 70.1 (OCH₂Ph-*p*-F), 62.7 (CH₂- α), 58.4 (CH₂-3'), 49.5 (CH- β), 42.5 (NCH₃), 37.1 (CH₂-1'), 31.0 (CH₂-3), 24.1 (CH₃-2), 22.5 (CH₂-4), 21.0 (CH₂-2'). HRMS (ESI) *m/z* calculated for C₃₅H₃₈FNO₂ [M + H]⁺ 524.2959, found: 524.2945.

1-(2-(6-(p-Fluorobenzyloxy)-2-methyldihydrobenzopyran-2-yl)ethyl)-6,7-dimethoxy-2-methyl-1,2,3,4-tetrahydroisoquinoline (7b). ¹H NMR (300 MHz, CDCl₃) δ 7.41–7.36 (m, 2H, CH-2'', CH-6''), 7.08–7.03 (m, 2H, CH-3'', CH-5''), 6.73–6.61 (m, 3H, CH-5, CH-7, CH-8), 6.55 and 6.54 (2 s, 2H, CH-2'', CH-5''), 4.93 (s, 2H, OCH₂Ph-*p*-F), 3.84 and 3.83 (m, 6H, 2xOCH₃), 3.58–3.51 (m, 1H, CH-3'), 3.43–3.37 and 3.12–3.06 (2 m, 2H, CH₂- α), 2.73–2.64 (m, 4H, CH₂-4, CH₂- β), 2.40 (s, 3H, NCH₃), 1.95–1.90 (m, 2H, CH₂-3), 1.82–1.56 (m, 4H, CH₂-1', CH₂-2'), 1.26 (s, CH₃-2). ¹³C NMR (75 MHz, CDCl₃) δ 162 (d, *J*_{CF} = 244 Hz, C-4''), 151.9 (C-6), 148.3 (C-8a), 147.3 (C-3'', C-4''), 133.3 (d, *J*_{CF} = 3 Hz, C-1''), 129.4 (d, *J*_{CF} = 8 Hz, CH-2'', CH-6''), 126.9 (C-1'', C-6''), 121.8 (C-4a), 117.7 (CH-5), 115.4 (d, *J*_{CF} = 21 Hz, CH-3'', CH-5''), 115.2 (CH-7), 114.4 (CH-8), 111.3 (CH-2''), 109.8 (CH-5''), 75.8 (C-2), 70.0 (OCH₂Ph-*p*-F), 63.4 (CH-3'), 55.9 and 55.8 (OCH₃), 49.1 (CH₂- α), 42.8 (NCH₃), 34.7 (CH₂-1'), 30.9 (CH₂-3), 29.7 (CH₂-2'), 27.8 (CH₂- β), 24.2 (CH₃-2),



22.5 (CH₂-4). HRMS (ESI) *m/z* calculated for C₃₁H₃₆FNO₄ [M + H]⁺ 506.2701, found: 506.2705.

General procedure for synthesis of *N*-dimethylated amines 5c, 6c, and 7c. A mixture of 5 (50 mg, 0.11 mmol), 6 (56 mg, 0.11 mmol), 7 (54 mg, 0.11 mmol), and methyl iodide (1.5 mL) was dissolved in dimethylformamide (8 mL) and refluxed under N₂ for 30 minutes to 1 hour. Reaction mixtures were extracted with EtOAc (3 × 10 mL). The organic layer was extracted with water and brine, dried with anhydrous Na₂SO₄, filtered, and evaporated to dryness. The residue obtained was subjected to silica gel column chromatography (CH₂Cl₂/MeOH, 95:5) to afford 42.8 mg, 47.4 mg, and 55 mg of the respective compounds 5c, 6c, and 7c (79–96% yield) as brown oils.

3-(6-(*p*-Fluorobenzyloxy)-2-methyldihydrobenzopyran-2-yl)-*N*-(*p*-methoxyphenethyl)-*N,N*-dimethylpropan-1-aminium (5c). ¹H NMR (300 MHz, CDCl₃) δ 7.41–7.36 (m, 2H, CH-2'', CH-6''), 7.25–7.18 (m, 2H, H-2'', H-6''), 7.10–7.01 (m, 2H, CH-3'', CH-5''), 6.91–6.87 (m, 2H, CH-3''', CH-5'''), 6.73–6.67 (m, 3H, CH-5, CH-7, CH-8), 4.94 (s, 2H, OCH₂Ph-*p*-F), 3.78 (s, 3H, OCH₃), 3.59–3.45 (m, 4H, CH₂-α, CH₂-3'), 3.26 (s, N(CH₃)₂), 3.09–3.03 (m, 2H, CH₂-β), 2.80–2.76 (m, 2H, CH₂-4), 2.17–1.68 (m, 6H, CH₂-3, CH₂-1', CH₂-2'), 1.32 (s, 3H, CH₃-2). ¹³C NMR (75 MHz, CDCl₃) δ 162.4 (d, *J*_{CF} = 245 Hz, C-4''), 159.2 (C-4'''), 152.4 (C-6), 147.5 (C-8a), 133.1 (d, *J*_{CF} = 3 Hz, C-1''), 130.2 (CH-2''', CH-6'''), 129.3 (d, *J*_{CF} = 9 Hz, CH-2'', CH-6''), 129.3 (C-1'''), 121.7 (C-4a), 117.6 (CH-5), 115.4 (d, *J*_{CF} = 21 Hz, CH-3'', CH-5''), 115.4 (CH-7), 114.9 (CH-3''', CH-5'''), 114.7 (CH-8), 75.0 (C-2), 70.0 (OCH₂-Ph-*p*-F), 65.8 (CH₂-α), 65.5 (CH₂-3'), 55.4 (OCH₃), 52.3 (N(CH₃)₂), 36.0 (CH₂-1'), 31.9 (CH₂-3), 30.9 (CH₂-β), 23.9 (CH₃-2), 22.7 (CH₂-4), 17.4 (CH₂-2'). HRMS (ESI) *m/z* calculated for C₃₁H₃₈FNO₃ [M + H]⁺ 492.2908, found: 492.2895.

***N*-(2,2-Diphenylethyl)-3-(6-(*p*-fluorobenzyloxy)-2-methyldihydrobenzopyran-2-yl)-*N,N*-dimethylpropan-1-aminium (6c).** ¹H NMR (300 MHz, CDCl₃) δ 7.48–7.40 (m, 2H, CH-2'', CH-6''), 7.39–7.21 (m, 10H, 2xPh), 7.08–7.01 (m, 2H, CH-3'', CH-5''), 6.75–6.58 (m, 3H, CH-5, CH-7, CH-8), 4.94 (s, 2H, OCH₂Ph-*p*-F), 4.52–4.47 (m, 1H, CH-β), 4.26–4.24 (m, 2H, CH₂-α), 3.57–3.59 (m, 2H, CH₂-3'), 3.23 (s, N(CH₃)₂), 2.95–2.68 (m, 2H, CH₂-4), 2.06–1.53 (m, 6H, CH₂-3, CH₂-1', CH₂-2'), 1.30 (s, 3H, CH₃-2). ¹³C NMR (75 MHz, CDCl₃) δ 162.0 (d, *J* = 244 Hz, C-4''), 152.3 (C-6), 147.6 (C-8a), 139.9 (C-Ph), 129.4 (d, *J*_{CF} = 8 Hz, CH-2'', CH-6''), 128.0 and 127.7 (CH-Ph), 121.7 (C-4a), 117.6 (CH-5), 115.5 (d, *J*_{CF} = 22 Hz, CH-3'', CH-5''), 114.7 and 114.5 (CH-7, CH-8), 74.9 (C-2), 70.0 (OCH₂Ph-*p*-F), 67.7 (CH-β), 65.1 (CH₂-α), 53.0 (N(CH₃)₂), 46.7 (CH₂-3'), 36.0 (CH₂-1'), 31.2 (CH₂-3), 24.8 (CH₂-2'), 23.7 (CH₃-2), 22.0 (CH₂-4). HRMS (ESI) *m/z* calculated for C₃₆H₄₀FNO₂ [M + H]⁺ 538.3116, found: 538.3107.

1-(2-(6-(*p*-Fluorobenzyloxy)-2-methyldihydrobenzopyran-2-yl)ethyl)-6,7-dimethoxy-2,2-dimethyl-1,2,3,4-tetrahydroisoquinolin-2-ium (7c). ¹H NMR (300 MHz, CDCl₃) δ 7.41–7.36 (m, 2H, CH-2'', CH-6''), 7.09–7.03 (m, 2H, CH-3'', CH-5''), 6.73–6.65 (m, 5H, CH-5, CH-7, CH-8, CH-2'', CH-5'''), 4.93 (s, 2H, OCH₂Ph-*p*-F), 4.75–4.70 (m, 1H, CH-3'), 4.02–4.01 (m, 2H, CH₂-α), 3.89 and 3.78 (2 s, 6H,

2x OCH₃), 3.50 and 3.30 (2 s, 2xNCH₃), 2.82–2.72 (m, 2H, CH₂-4), 2.36–1.40 (m, 8H, CH₂-3, CH₂-1', CH₂-2', CH₂-β), 1.31 (s, CH₃-2). ¹³C NMR (75 MHz, CDCl₃) δ 162 (C-4''), 152.5 (C-6), 148.4 (C-8a), 147.3 (C-3''', C-4'''), 129.4 (d, *J*_{CF} = 8 Hz, CH-2'', CH-6''), 122.0 (C-1''', C-6'''), 121.6 (C-4a), 117.7 (CH-5), 115.4 (d, *J*_{CF} = 10 Hz, CH-3'', CH-5''), 115.3 (CH-7), 114.7 (CH-8), 111.0 and 109.0 (CH-2''', CH-5'''), 75.2 (C-2), 70.02 (OCH₂Ph-*p*-F), 66.0 (CH-3'), 56.5 (CH₂-α), 56.2 (OCH₃), 52.0 (NCH₃), 33.8 (CH₂-1'), 31.9 (CH₂-β), 30.9 (CH₂-3), 27.1 (CH₂-2'), 24.7 (CH₃-2), 22.7 (CH₂-4). HRMS (ESI) *m/z* calculated for C₃₂H₃₈FNO₄ [M + H]⁺ 520.2858, found: 520.2844.

General procedure for synthesis of urea benzopyrans 5d, 6d, and 7d. A mixture of 5 (50 mg, 0.11 mmol), 6 (56 mg, 0.11 mmol), 7 (54 mg, 0.11 mmol), 4-chlorophenyl isocyanate (49 mg, 0.32 mmol), and a few drops of Et₃N was dissolved in dry dichloromethane (5 mL) and incubated at room temperature and under N₂ overnight. HCl (15 mL) was added, and the mixture was extracted with dichloromethane (3 × 15 mL) and washed with water and brine. The organic layers were dried over anhydrous Na₂SO₄ and evaporated under reduced pressure. The residue was purified by column chromatography (hexane/EtOAc, 8:2, 9:1, and 6:4 respectively) to yield 46 mg, 67 mg, and 65 mg of compound 5d, 6d, and 7d (68–92% yield), respectively, as colorless oils.

3-(*p*-Chlorophenyl)-*N*-(3-(6-(*p*-fluorobenzyloxy)-2-methyldihydrobenzopyran-2-yl)propyl)-*N*-(*p*-methoxyphenethyl)urea (5d). ¹H NMR (300 MHz, CDCl₃) δ 7.42–7.04 (m, 10H, CH-2'', CH-5'', CH-2''', CH-6''', CH-3''', CH-5''', CH-8''', CH-12''', CH-9'', CH-11''), 6.89–6.85 (m, 2H, CH-3'', CH-5''), 6.70–6.67 (m, 3H, CH-5, CH-7, CH-8), 4.94 (s, 2H, OCH₂Ph-*p*-F), 3.78 (s, 3H, OCH₃), 3.53–3.48 (m, 2H, CH₂-α), 3.30–3.24 (m, 2H, CH₂-3'), 2.86–2.73 (m, 4H, CH₂-4, CH₂-β), 1.82–1.72 (m, 4H, CH₂-1', CH₂-2'), 1.69–1.60 (m, 2H, CH₂-3), 1.28 (s, CH₃-2). ¹³C NMR (75 MHz, CDCl₃ + 1 drop CD₃OD) δ 162.1 (d, *J*_{CF} = 244 Hz, C-4''), 158.2 (C-4'''), 155.5 (C=O), 152.0 (C-6), 147.6 (C-8a), 137.5 (C-7''), 132.9 (d, *J* = 3 Hz, C-1''), 130.9 (C-10''), 129.7 (C-1'''), 129.2 (d, *J*_{CF} = 8 Hz, CH-2'', CH-6''), 128.6 (CH-2''', CH-6'''), 121.7 (C-4a), 121.3 (CH-9'', CH-11''), 120.0 (CH-8'', CH-12''), 117.4 (CH-5), 115.2 (CH-7), 115.2 (d, *J*_{CF} = 21 Hz, CH-3'', CH-5''), 114.4 (CH-8), 114.1 (CH-3''', CH-5'''), 75.8 (C-2), 69.9 (OCH₂Ph-*p*-F), 55.1 (OCH₃), 49.7 (CH₂-α), 47.7 (CH₂-3'), 36.0 (CH₂-1'), 33.8 (CH₂-β), 31.0 (CH₂-3), 23.6 (CH₃-2), 22.2 (CH₂-2'), 22.1 (CH₂-4). HRMS (ESI) *m/z* calculated for C₃₆H₃₈ClFN₂O₄ [M]⁺ 617.2575, found: 617.2576.

3-(*p*-Chlorophenyl)-*N*-(2,2-diphenylethyl)-*N*-(3-(6-(*p*-fluorobenzyloxy)-2-methyldihydrobenzopyran-2-yl)propyl)urea (6d). ¹H NMR (300 MHz, CDCl₃) δ 7.46 (d, *J* = 8.8 Hz, 2H, CH-2'', CH-6''), 7.43–6.97 (m, 16H, 2xPh, CH-8''', CH-11'', CH-9'', CH-12'', CH-3'', CH-5''), 6.71–6.21 (m, 3H, CH-5, CH-7, CH-8), 4.93 (s, 2H, OCH₂Ph-*p*-F), 4.35 (t, *J* = 7.4 Hz, 1H, CH-β), 3.95 (d, *J* = 7.4 Hz, 2H, CH₂-α), 3.19–3.12 (m, 2H, CH₂-3'), 2.76–2.70 (m, 2H, CH₂-4), 1.80–1.70 (m, 2H, CH₂-3), 1.55–1.50 (m, 4H, CH₂-1', CH₂-2'), 1.25 (s, 3H, CH₃-2). ¹³C NMR (75 MHz, CDCl₃) δ 162.0 (d, *J*_{CF} = 244 Hz, C-4''), 155.4 (C=O), 152.2 (C-6), 147.8 (C-8a), 142.0 (d, *J* = 2



Hz, C-Ph), 137.8 (C-1^{'''}), 133.1 (d, J_{CF} = 3 Hz, C-1^{'''}), 129.8 (C-4^{'''}), 129.4 (d, J_{CF} = 8 Hz, CH-2^{''}, CH-6^{''}), 128.6 and 127.5 (CH-Ph), 127.1 (CH-9^{'''}, CH-11^{'''}), 121.7 (C-4a), 121.0 (CH-8^{'''}, CH-12^{'''}), 117.7 (CH-5), 115.6 (d, J_{CF} = 19 Hz, CH-3^{''}, CH-5^{''}), 115.3 (CH-7), 114.5 (CH-8), 75.9 (C-2), 70.0 (OCH₂Ph-*p*-F), 53.8 (CH₂-α), 49.9 (CH-β), 48.2 (CH₂-3[']), 36.3 (CH₂-1[']), 31.2 (CH₂-3), 24.0 (CH₃-2), 22.4 (CH₂-2[']), 22.1 (CH₂-4). HRMS (ESI) m/z calculated for C₄₁H₄₀ClFN₂O₃ [M]⁺ 663.2784, found: 663.2764.

N-(*p*-Chlorophenyl)-1-(2-(6-((*p*-fluorobenzyl)oxy)-2-methyldihydrobenzopyran-2-yl)ethyl)-6,7-dimethoxy-3,4-dihydroisoquinoline-2(1H)-carboxamide (7d). ¹H NMR (300 MHz, CDCl₃ + 1 drop CD₃OD) δ 7.37–7.1 (m, 6H, CH-2^{''}, CH-6^{''}, CH-8^{'''}, CH-12^{'''}, CH-9^{'''}, CH-11^{'''}), 7.08–6.89 (m, 2H, CH-3^{''}, CH-5^{''}), 6.68–6.58 (m, 5H, CH-5, CH-7, CH-8, CH-2^{'''}, CH-5^{'''}), 4.87 (s, 2H, OCH₂Ph-*p*-F), 4.08–4.03 (m, 1H, CH-3[']), 3.79 and 3.77 (2s, 6H, 2xOCH₃), 3.19 and 2.91 (2m, 2H, CH₂-α), 2.74–2.67 (m, 4H, CH₂-4, CH₂-β), 1.93–1.65 (m, 6H, CH₂-3, CH₂-1['], CH₂-2[']), 1.31 (s, 3H, CH₃-2). ¹³C NMR (75 MHz, CDCl₃ + 1 drop CD₃OD) δ 162.1 (C-4^{'''}), 155.2 (C=O), 152.3 (C-6), 148.1 (C-8a), 147.5 (C-3^{'''}, C-4^{'''}), 138.0 (C-7^{'''}), 133.2 (C-1^{'''}), 131.2 (C-10^{'''}), 131.0 (CH-2^{''}, CH-6^{''}), 127.1 (C-1^{'''}, C-6^{'''}), 121.6 (CH-9^{'''}, CH-11^{'''}), 120.3 (CH-8^{'''}, CH-12^{'''}), 117.7 (CH-5), 115.5 (CH-3^{''}, CH-5^{''}), 115.2 (CH-7), 114.4 (CH-8), 111.9 and 109.2 (CH-2^{'''}, CH-5^{'''}), 75.6 (C-2), 70.0 (OCH₂Ph-*p*-F), 57.0 (CH-3[']), 55.8 and 55.7 (OCH₃), 32.1 (CH₂-1[']), 31.4 (CH₂-3), 30.4 (CH₂-2[']), 28.1 (CH₂-α), 24.0 (CH₃-2), 23.1 (CH₂-4, CH₂-β). HRMS (ESI) m/z calculated for C₃₇H₃₈ClFN₂O₂ [M]⁺ 645.2526, found: 645.2512.

4.2. Pharmacology

Cell culture. Human TNBC (MDA-MB-231 and MDA-MB-436) and normal breast epithelial (MCF10A) cell lines were obtained from the American Type Culture Collection (ATCC) (LGC Standards, S.L.U. Barcelona, Spain) and cultured in a humidified air incubator at 37 °C and 5% CO₂. Cells were grown in Dulbecco's modified Eagle's medium (DMEM) with nutrient mixture Ham's F-12 (DMEM/F12) supplemented with 10% (v/v) fetal bovine serum (FBS), 2% penicillin/streptomycin, and 1% glutamine.

Cell viability. The cytotoxic effects of the different compounds in the TNBC cells were determined using a water-soluble tetrazolium dye (WST-1) assay kit (K304-2500, Deltaclon, Madrid, Spain). Cells were seeded at 6×10^3 cells per well in 96-well plates. After 24 hours, the cells were treated with different doses of compounds (2.5 μM to 100 μM) or DMSO for negative control groups (0.1%). WST-1 solution at 7% in DMEM-F12 without phenol red was added for 3 hours. The absorbance was then measured at 450 nm and background corrected at 650 nm using Spectra Max Plus (Thermo Fisher Scientific, Waltham, MA, USA). The percentage of viable cells was calculated by setting the negative control group cells to 100%.

Apoptosis/necrosis assay. Apoptosis/necrosis cell death was studied using an Annexin V-FITC/PI dual staining assay. MDA-MB-231 and MDA-MB-436 cells (3×10^4 cells per well) were seeded in 24-well plates and allowed to grow overnight.

The medium was then replaced with the different compounds at their IC₅₀ values or DMSO for negative control groups (0.1%) in complete medium. Then, all cells were processed with the Annexin V-assay kit (ANXCKF7, Immunostep, Salamanca, Spain) according to the manufacturer's instructions. A Becton Dickinson LSR Fortessa cytometer (BD Biosciences, Franklin Lakes, NJ, USA) was used for samples, and cell analyses were performed using BD FACSDiva X20 software.

ROS measurement. MDA-MB-231 and MDA-MB-436 cells were seeded at 2.5×10^4 cells per well in 8-well slides. The following day, the cells were treated with compounds at their IC₂₅ values, DMSO for negative control groups (0.05%), or TBHP at 100 μM for 48 hours. The medium was then replaced with DCFDA at 10 μM (ab113851 DCFDA/H2DCFDA – Cellular ROS Assay Kit, Abcam, Cambridge, UK) in complete medium, and the cells were then incubated for 45 minutes at room temperature in the dark. The fluorescence intensity from each sample was captured by LEICA DMI8 fluorescence microscopy, and images analysis was performed using ImageJ software.

Cell cycle. Cell cycle analysis was carried out to estimate the distribution of the cell population in the different phases of the cell cycle. First, 1.5×10^5 cells per well were seeded in 6-well plates and allowed to grow overnight. The medium was then replaced with the different compounds at their IC₅₀ values or DMSO for negative control groups (0.1%) in complete medium. After 48 hours, untreated and treated cells were harvested, washed with phosphate-buffered saline (PBS), and fixed in ice-cold 70% ethanol for at least 1 hour at –20 °C. Cells were then stained with PI/RNASE solution (PI/RNASE, Immunostep, Salamanca, Spain) and incubated for 24 hours at 4 °C. A BD LSR Fortessa cytometer (BD Biosciences, Franklin Lakes, NJ, USA) was used for samples, and cell analyses were performed using ModFit 4.1 software.

Determination of mRNA expression by quantitative RT-PCR. TNBC cells (1×10^6 cells per well) were seeded in 6-well plates and allowed to grow overnight. The medium was then replaced with the different compounds at their IC₂₅ values or DMSO for negative control groups (0.05%) in complete medium. Total RNA was extracted from mice WAT and liver samples by homogenization using TRIzol RNA Isolation Reagent (Life Technologies, Thermo Fisher Scientific, Waltham, MA) and purified by standard methods. Reverse transcription was performed on 1000 ng of total RNA with a high-capacity cDNA reverse transcription kit (Applied Biosystems, Thermo Fisher Scientific, Waltham, MA). Relative quantification of *Bcl-2*, *CCND1*, and *CCNE2* was determined with the 2^{–ΔΔCt} method using *Gapdh* (Applied Biosystems) as an endogenous control and normalized to the vehicle group.

Statistical analysis. The data are presented as the mean ± SD or ± SEM. Statistical analyses were carried out by one-way or two-way ANOVA, followed by Tukey's or Dunnett's multiple comparisons test (GraphPad Prism 9). Differences with a *p*-value < 0.05 were considered statistically different.



Conflicts of interest

The authors declare that they have no known competing financial interests or personal relationships that could have appeared to influence the work reported in this paper.

Acknowledgements

This work was supported by the Carlos III Health Institute (ISCIII) and the European Regional Development Fund (FEDER) by grant numbers PI21/02045 and PI21/01351, and the Generalitat Valenciana (GVA) by grant numbers AICO/2021/081 and APOTIP/2020/011. Nuria Cabedo was funded by the ISCIII Miguel Servet programme (CPII20/00010), co-funded by the European Social Fund. Carlos Villarroya-Vicente was funded by the ISCIII (PFIS – FI19/00153), Ainhua García by the GVA (AICO/2021/081), and Sandra Torres-Ruiz by a pre-doctoral grant (ACIF/2019/119).

References

- H. Şenol, P. Tulay, M. Ç. Ergören, A. Hanoğlu, İ. Çalış and G. Mocan, Cytotoxic effects of verbascoside on MCF-7 and MDA-MB-231, *Turk. J. Pharm. Sci.*, 2020, **18**, 637–644, DOI: [10.4274/tjps.galenos.2021.36599](#).
- K. R. Senwar, T. S. Reddy, D. Thummuri, P. Sharma, V. G. Naidu, G. Srinivasulu and N. Shankaraiah, Design, synthesis and apoptosis inducing effect of novel (Z)-3-(3'-methoxy-4'-(2-amino-2-oxoethoxy)-benzylidene)indolin-2-ones as potential antitumor agents, *Eur. J. Med. Chem.*, 2026, **118**, 34–36, DOI: [10.1016/j.ejmech.2016.04.025](#).
- R. L. Siegel, K. D. Miller and A. Jemal, Cancer statistics, 2015, *Ca-Cancer J. Clin.*, 2015, **65**, 5–29, DOI: [10.3322/caac.21254](#).
- I. Ahmad and W. Shagufta, Recent developments in steroidal and nonsteroidal aromatase inhibitors for the chemoprevention of estrogen-dependent breast cancer, *Eur. J. Med. Chem.*, 2015, **102**, 375–386, DOI: [10.1016/j.ejmech.2015.08.010](#).
- A. G. Waks and E. P. Winer, Breast cancer treatment: a review, *JAMA, J. Am. Med. Assoc.*, 2019, **321**, 288–300, DOI: [10.1001/jama.2018.19323](#).
- O. A. Bamodu, W. C. Huang, D. T. Tzeng, A. Wu, L. S. Wang, C. T. Yeh and T. Y. Chao, Ovatodiolide sensitizes aggressive breast cancer cells to doxorubicin, eliminates their cancer stem cell-like phenotype, and reduces doxorubicin-associated toxicity, *Cancer Lett.*, 2015, **364**, 125–134, DOI: [10.1016/j.canlet.2015.05.006](#).
- M. Gallorini, A. Cataldi and A. di Giacomo, Cyclin-dependent kinase modulators and cancer therapy, *BioDrugs*, 2012, **26**, 377–391, DOI: [10.1007/BF03261895](#).
- D. Nandini, A. Jennifer and D. Pradip, Therapeutic strategies for metastatic triple-negative breast cancers: from negative to positive, *Pharmaceuticals*, 2021, **14**, 455–472, DOI: [10.3390/ph14050455](#).
- M. Brown, A. Tsodikov, K. R. Bauer, C. A. Parise and V. Caggiano, The role of human epidermal growth factor receptor 2 in the survival of women with estrogen and progesterone receptor-negative, invasive breast cancer, The California Cancer Registry, 1999–2004, *Cancer*, 2008, **112**, 737–747, DOI: [10.1002/cncr.23243](#).
- M. Liao, J. Zhang, G. Wang, L. Wang, J. Liu, L. Ouyang and B. Liu, Small-molecule drug discovery in triple negative breast cancer: current situation and future directions, *J. Med. Chem.*, 2021, **64**, 2382–2418, DOI: [10.1021/acs.jmedchem.0c01180](#).
- O. Gluz, C. Liedtke, N. Gottschalk, L. Pusztail, U. Nitz and N. Harbeck, Triple-negative breast cancer – current status and future directions, *Ann. Oncol.*, 2009, **20**, 1913–1927, DOI: [10.1093/annonc/mdp492](#).
- Y. Li, S. Li, X. Meng, R. Y. Gan, J. J. Zhang and H. B. Li, Dietary natural products for prevention and treatment of breast cancer, *Nutrients*, 2017, **9**, 728, DOI: [10.3390/nu9070728](#).
- Q. Zhao, M. Zhao, A. B. Parriss, Y. Xing and X. Yang, Genistein targets the cancerous inhibitor of PP2A to induce growth inhibition and apoptosis in breast cancer cells, *Int. J. Oncol.*, 2016, **49**, 1203–1210, DOI: [10.3892/ijo.2016.3588](#).
- J. Chen, Y. Duan, X. Zhang, Y. Ye, B. Ge and J. Chen, Genistein induces apoptosis by the inactivation of the IGF-1R/p-Akt signaling pathway in MCF-7 human breast cancer cells, *Food Funct.*, 2015, **6**, 995–1000, DOI: [10.1039/c4fo01141d](#).
- S. S. Bhat, S. K. Prasad, C. Shivamallu, K. S. Prasad, A. Syed, P. Reddy, C. A. Cull and R. G. Amachawadi, Genistein: a potent anti-breast cancer agent, *Curr. Issues Mol. Biol.*, 2021, **43**, 1502–1517, DOI: [10.3390/cimb43030106](#).
- Y. Safdari, M. Khalili, M. A. Ebrahimzadeh, Y. Yazdani and S. Farajnia, Natural inhibitors of PI3K/AKT signaling in breast cancer: emphasis on newly-discovered molecular mechanisms of action, *Pharmacol. Res.*, 2015, **93**, 1–10, DOI: [10.1016/j.phrs.2014.12.004](#).
- A. A. Abd El-Hafeez, H. O. Khalifa, E. A. M. Mahdy, V. Sharma, T. Hosoi, P. Ghosh, K. Ozawa, M. M. Montano, T. Fujimura, A. R. N. Ibrahim, M. A. A. Abdelhamid, S. P. Pack, S. A. Shouman and S. Kawamoto, Anticancer effect of nor-wogonin (5, 7, 8-trihydroxyflavone) on human triple-negative breast cancer cells via downregulation of TAK1, NF-κB, and STAT3, *Pharmacol. Rep.*, 2019, **71**, 289–298, DOI: [10.1016/j.pharep.2019.01.001](#).
- S. Sordon, J. Popłoński, M. Milczarek, M. Stachowicz, T. Tronina, A. Z. Kucharska, J. Wietrzyk and E. Huszcza, Structure-antioxidant-antiproliferative activity relationships of natural C7 and C7-C8 hydroxylated flavones and flavanones, *Antioxidants*, 2019, **8**, 210, DOI: [10.3390/antiox8070210](#).
- K. M. Yap, M. Sekar, Y. S. Wu, S. H. Gan, N. N. I. M. Rani, L. J. Seow, V. Subramaniam, N. K. Fuloria, S. Fuloria and P. T. Lum, Hesperidin and its aglycone hesperetin in breast cancer therapy: A review of recent developments and future prospects, *Saudi J. Biol. Sci.*, 2021, **28**, 6730–6747, DOI: [10.1016/j.sjbs.2021.07.046](#).
- S. Rani, K. Raheja, V. Luxami and K. Paul, A review on diverse heterocyclic compounds as the privileged scaffolds in non-steroidal aromatase inhibitors, *Bioorg. Chem.*, 2021, **113**, 105017, DOI: [10.1016/j.bioorg.2021.105017](#).
- C. Zhang, Z. Wang, Y. Shi, B. Yu and Y. Song, Recent advances of LSD1/KDM1A inhibitors for disease therapy, *Bioorg. Chem.*, 2023, **134**, 106443, DOI: [10.1016/j.bioorg.2023.106443](#).



- 22 M. C. Gonzalez, A. Serrano, M. C. Zafra-Polo, D. Cortes and K. S. Rao, Polycerasoidin and polycerasoidol, two new prenylated benzopyran derivatives from *Polyalthia cerasoides*, *J. Nat. Prod.*, 1995, **58**, 1278–1284, DOI: [10.1021/np50122a022](https://doi.org/10.1021/np50122a022).
- 23 M. C. Zafra-Polo, M. C. González, J. R. Tormo, E. Estornell and D. Cortes, Polyalthidin: new prenylated benzopyran inhibitor of the mammalian mitochondrial respiratory chain, *J. Nat. Prod.*, 1996, **59**, 913–916, DOI: [10.1021/np960492m](https://doi.org/10.1021/np960492m).
- 24 A. Bermejo, A. Collado, I. Barrachina, P. Marqués, N. El Aouad, X. Franck, F. Garibotto, C. Dacquet, D. H. Caignard, F. D. Suvire, R. D. Enriz, L. Piqueras, B. Figadère, M. J. Sanz, N. Cabedo and D. Cortes, Polycerasoidol, a natural prenylated benzopyran with a dual PPAR α /PPAR γ agonist activity and anti-inflammatory effect, *J. Nat. Prod.*, 2019, **82**, 1802–1812, DOI: [10.1021/acs.jnatprod.9b00003](https://doi.org/10.1021/acs.jnatprod.9b00003).
- 25 P. Marques, C. Villarroel-Vicente, A. Collado, A. García, L. Vila, I. Duplan, N. Hennuyer, F. Garibotto, R. D. Enriz, C. Dacquet, B. Staels, L. Piqueras, D. Cortes, M. J. Sanz and N. Cabedo, Anti-inflammatory effects and improved metabolic derangements in ob/ob mice by a newly synthesized prenylated benzopyran with pan-PPAR activity, *Pharmacol. Res.*, 2023, **187**, 106638, DOI: [10.1016/j.phrs.2022.106638](https://doi.org/10.1016/j.phrs.2022.106638).
- 26 H. Taha, C. Y. Looi, A. Arya, W. F. Wong, L. F. Yap, M. Hasanpourghadi, M. A. Mohd, I. C. Paterson and H. Mohd Ali, (6E,10E) Isopolycerasoidol and (6E,10E) isopolycerasoidol methyl ester, prenylated benzopyran derivatives from pseuduvaria monticola induce mitochondrial-mediated apoptosis in human breast adenocarcinoma cells, *PLoS One*, 2015, **10**, e0126126, DOI: [10.1371/journal.pone.0126126](https://doi.org/10.1371/journal.pone.0126126).
- 27 B. C. Pearce, R. A. Parker, M. E. Deason, D. D. Dischino, E. Gillespie, A. A. Qureshi, K. Volk and J. J. Wright, Inhibitors of cholesterol biosynthesis. 2. Hypocholesterolemic and antioxidant activities of benzopyran and tetrahydronaphthalene analogues of the tocotrienols, *J. Med. Chem.*, 1994, **37**, 526–541, DOI: [10.1021/jm00030a012](https://doi.org/10.1021/jm00030a012).
- 28 A. Bermejo, I. Barrachina, N. El Aouad, X. Franck, N. Chahboune, I. Andreu, B. Figadère, L. Vila, N. Hennuyer, B. Staels, C. Dacquet, D. H. Caignard, M. J. Sanz, D. Cortes and N. Cabedo, Synthesis of benzopyran derivatives as PPAR α and/or PPAR γ activators, *Bioorg. Med. Chem.*, 2019, **27**, 115162, DOI: [10.1016/j.bmc.2019.115162](https://doi.org/10.1016/j.bmc.2019.115162).
- 29 A. García, L. Vila, P. Marín, Á Bernabeu, C. Villarroel-Vicente, N. Hennuyer, B. Staels, X. Franck, B. Figadère, N. Cabedo and D. Cortes, Synthesis of 2-prenylated alkoxyated benzopyrans by horner-wadsworth-emmons olefination with PPAR α / γ agonist activity, *ACS Med. Chem. Lett.*, 2021, **12**, 1783–1786, DOI: [10.1021/acsmedchemlett.1c00400](https://doi.org/10.1021/acsmedchemlett.1c00400).
- 30 L. Vila, N. Cabedo, C. Villarroel-Vicente, A. García, Á Bernabeu, N. Hennuyer, B. Staels, X. Franck, B. Figadère, M. J. Sanz and D. Cortes, Synthesis and biological studies of “Polycerasoidol” and “trans- δ -Tocotrienolic acid” derivatives as PPAR α and/or PPAR γ agonists, *Bioorg. Med. Chem.*, 2022, **53**, 116532, DOI: [10.1016/j.bmc.2021.116532](https://doi.org/10.1016/j.bmc.2021.116532).
- 31 A. K. Ghosh and M. Brindisi, Urea derivatives in modern drug discovery and medicinal chemistry, *J. Med. Chem.*, 2020, **63**, 2751–2788, DOI: [10.1021/acs.jmedchem.9b01541](https://doi.org/10.1021/acs.jmedchem.9b01541).
- 32 M. Redza-Dutordoir and D. A. Averill-Bates, Activation of apoptosis signalling pathways by reactive oxygen species, *Biochim. Biophys. Acta*, 2016, **1863**, 2977–2992, DOI: [10.1016/j.bbamer.2016.09.012](https://doi.org/10.1016/j.bbamer.2016.09.012).
- 33 J. M. Adams and S. Cory, The BCL-2 arbiters of apoptosis and their growing role as cancer targets, *Cell Death Differ.*, 2018, **25**, 27–36, DOI: [10.1038/cdd.2017.161](https://doi.org/10.1038/cdd.2017.161).
- 34 J. C. Martinou and R. J. Youle, Mitochondria in apoptosis: Bcl-2 family members and mitochondrial dynamics, *Dev. Cell*, 2011, **21**, 92–101, DOI: [10.1016/j.devcel.2011.06.017](https://doi.org/10.1016/j.devcel.2011.06.017).
- 35 S. Cory and J. M. Adams, The Bcl2 family: Regulators of the cellular life-or-death switch, *Nat. Rev. Cancer*, 2002, **2**, 647–656, DOI: [10.1038/nrc883](https://doi.org/10.1038/nrc883).
- 36 H. Guo, H. Cui, X. Peng, J. Fang, Z. Zuo, J. Deng, X. Wang, B. Wu, K. Chen and J. Deng, Modulation of the PI3K/Akt Pathway and Bcl-2 Family Proteins Involved in Chicken's Tubular Apoptosis Induced by Nickel Chloride (NiCl₂), *Int. J. Mol. Sci.*, 2015, **16**, 22989–23011, DOI: [10.3390/ijms160922989](https://doi.org/10.3390/ijms160922989).
- 37 I. Neganova and M. Lako, G1 to S phase cell cycle transition in somatic and embryonic stem cells, *J. Anat.*, 2008, **213**, 30–44, DOI: [10.1111/j.1469-7580.2008.00931.x](https://doi.org/10.1111/j.1469-7580.2008.00931.x).
- 38 B. Stecca and E. Rovida, Impact of ERK5 on the Hallmarks of Cancer, *Int. J. Mol. Sci.*, 2019, **20**, 1426, DOI: [10.3390/ijms20061426](https://doi.org/10.3390/ijms20061426).
- 39 R. Paudel, L. Fusi and M. Schmidt, The MEK5/ERK5 Pathway in Health and Disease, *Int. J. Mol. Sci.*, 2021, **22**, 7594, DOI: [10.3390/ijms22147594](https://doi.org/10.3390/ijms22147594).
- 40 W. Song, L. Tang, Y. Xu, J. Xu, W. Zhang, H. Xie, S. Wang and X. Guan, PARP inhibitor increases chemosensitivity by upregulating miR-664b-5p in BRCA1-mutated triple-negative breast cancer, *Sci. Rep.*, 2017, **7**, 42319, DOI: [10.1038/srep42319](https://doi.org/10.1038/srep42319).
- 41 W. Song, L. Tang, Y. Xu, J. Xu, W. Zhang, H. Xie, S. Wang and X. Guan, PARP inhibitor increases chemosensitivity by upregulating miR-664b-5p in BRCA1-mutated triple-negative breast cancer, *Sci. Rep.*, 2017, **7**, 42319, DOI: [10.1038/srep42319](https://doi.org/10.1038/srep42319).



References

-
- [1] V. Amico. Marine Brown algae of family Cystoseiraceae: chemistry and chemotaxonomy, *Phytochemistry*, 39 (1995) 1257.
- [2] P. Máximo, L.M. Ferreira, P. Branco, P. Lima, A. Lourenço, Secondary metabolites and biological activity of invasive macroalgae of southern europe, *Marine drugs*, 16 (2018) 265.
- [3] J.P. Baz, L.M. Cañedo, D. Tapiolas, A new tetraprenylhydroquinone derivative with an acetic acid unit from the marine sponge *Ircinia muscarum*, *J. Nat. Prod.* 59 (1996) 960.
- [4] G. Bifulco, I. Bruno, L. Minale, C. Debitus, G. Bourdy, A. Vassas, J. Lavayre, Bioactive prenylhydroquinone sulfates and a novel C₃₁ furanoterpene alcohol sulfate from the marine sponge, *Ircina* sp, *J. Nat. Prod.* 58 (1995) 1444.
- [5] G.J. Hooper, M.T. Davies-Coleman, Sesquiterpene hydroquinones from the south African soft coral *Alcyonium fauri*, *Tetrahedron Lett.* 36 (1995) 3265.
- [6] A. Sato, T. Shindo, N. Kasanuki, K. Hasegawa, Antioxidant metabolites from the tunicate *Amaroucium multiplicatum*, *J. Nat. Prod.* 52 (1989) 975.
- [7] F.D. Monache, M. Marta, M.M. Mac-Quhae, M. Nicoletti, Two new tocotrienoloic acids from the fruits of *Clusia grandiflora* splith, *Gazz. Chim. Ital.* 114 (1984) 135.
- [8] W.N. Setzer, T.J. Green, R.O. Lawton, D.M. Moriarity, R.B. Bates, S. Caldera, W.A. Haber, An antibacterial vitamin E derivative from *Toovomitopsis psychotriifolia*. *Planta Med.* 61 (1995) 275.
- [9] B. Muckensturm, F. Diyani, J.P. Reduron, M. Hildenbrand, 7-Demethylplastocholesterol-2 and 2-Demethylplastoquinone-3 from *Seseli farreynii*, *Phytochemistry*, 45 (1997) 549.
- [10] P.A. Runeberg, Y. Brusentsev, S.M.K. Rendon, P.C. Eklund, Oxidative transformations of lignans, *Molecules (Basel)*, 24 (2019) 300.
- [11] M.C. Gonzalez, A. Serrano, M.C. Zafra-Polo, D. Cortes, K.S. Rao, Polycerasoidin and polycerasoidol, two new prenylated benzopyran derivatives from *Polyalthia cerasoides*, *J. Nat. Prod.* 58 (1995) 1278.
- [12] M.C. Zafra-Polo, M.C. González, J.R. Tormo, E. Estornell, D. Cortes, Polyalthidin: new prenylated benzopyran inhibitor of the mammalian mitochondrial respiratory chain, *J. Nat. Prod.* 59 (1996) 913.
- [13] S.M. Tang, X.T. Deng, J. Zhou, Q.P. Li, X.X. Ge, L. Miao, Pharmacological basis and new insights of quercetin action in respect to its anti-cancer effects, *Biomed. Pharmacother.* 121 (2020) 109604.

-
- [14] G. Gong, Y.Y. Guan, Z.L. Zhang, K. Rahman, S.J. Wang, S. Zhou, X. Luan, H. Zhang, Isorhamnetin: A review of pharmacological effects, *Biomed. Pharmacother.* 128 (2020).
- [15] R. Shafabakhsh, Z. Asemi, Quercetin: a natural compound for ovarian cancer treatment, *J. Ovarian. Res.* 12 (2019) 55.
- [16] J.M. Al-Khayri, G.R. Sahana, P. Nagella, B.V. Joseph, F.M. Alessa, M.Q. Al-Mssallem, Flavonoids as potential anti-inflammatory molecules: A review, *Molecules (Basel)*, 27 (2022) 2901.
- [17] B. Mandal, C.R. Maity, Hypoglycemic action of karanjin, *Acta. Physiol. Pharmacol. Bulg.* 12 (1986) 42.
- [18] D.J. Den Hartogh, E. Tsiani, Antidiabetic properties of naringenin: A citrus fruit polyphenol, *Biomolecules*, 9 (2019) 99.
- [19] D. Barreca, G. Gattuso, E. Bellocchio, A. Calderaro, D. Trombetta, A. Smeriglio, G. Laganà, M. Daglia, S. Meneghini, S. M. Nabavi, Flavanones: Citrus phytochemical with health-promoting properties, *BioFactors*, 43 (2017) 495.
- [20] E. Sozen, T. Demirel, N.K. Ozer, Vitamin E: Regulatory role in the cardiovascular system, *IUBMB Life*, 71 (2019) 507.
- [21] R. Brigelius-Flohé, Vitamin E research: Past, now and future, *Free Radic. Biol. Med.* 177 (2021) 381.
- [22] N. Ruiz Mostacero, M.V. Castelli, A.C. Cutró, A. Hollmann, J.M. Batista, M.Jr. Furlan, J. Valles, C.L. Fulgueira, S.N. López, Antibacterial activity of prenylated benzopyrans from *Peperomia obtusifolia* (Piperaceae), *Nat. Prod. Res.* 35 (2021) 1706.
- [23] A. Kurek, A.M. Grudniak, A. Kraczkiewicz-Dowjat, K.I. Wolska, New antibacterial therapeutics and strategies, *Pol. J. Microbiol.* 60 (2011) 3.
- [24] A.P. Li, Y.H. He, S.Y. Zhang, Y.P. Shi, Antibacterial activity and action mechanism of flavonoids against phytopathogenic bacteria, *Pestic. Biochem. Physiol.* 188 (2022).
- [25] M. Adak, P. Kumar, Herbal anthelmintic agents: a narrative review, *J. Tradit. Chin. Med.* 42 (2022) 641.
- [26] G. Maciel Diogo, J.S. Andrade, P.A. Sales Junior, S. Maria Fonseca Murta, V.M.R. Dos Santos, J.G. Taylor, Trypanocidal activity of flavanone derivatives, *Molecules*, 25 (2020) 397.
- [27] S.L. Badshah, S. Faisal, A. Muhammad, B.G. Poulson, A.H. Emwas, M. Jaremko, Antiviral activities of flavonoids, *Biomed. Pharmacother.* 140 (2021) 111596.
- [28] J. Xu, Z. Xu, W. Zheng, A Review of the antiviral role of green tea catechins, *Molecules*, 22 (2017) 1337.

- [29] G. Simonetti, E. Brasili, G. Pasqua, Antifungal activity of phenolic and polyphenolic compounds from different matrices of *Vitis vinifera* L. against human pathogens, *Molecules*, 25 (2020) 3748.
- [30] L. Pan, X. Li, H. Jin, X. Yang, B. Qin, Antifungal activity of umbelliferone derivatives: Synthesis and structure-activity relationships, *Microb. Pathog.* 104 (2017) 110.
- [31] T.R. Helgren, R.J. Sciotti, P. Lee, S. Duffy, V.M. Avery, O. Igbinoba, M. Akoto, T.J. Hagen, The synthesis, antimalarial activity and CoMFA analysis of novel aminoalkylated quercetin analogs, *Bioorg. Med. Chem. Lett.* 25 (2015) 327.
- [32] R. Devakaram, D.S. Black, K.T. Andrews, G.M. Fisher, R.A. Davis, N. Kumar, Synthesis and antimalarial evaluation of novel benzopyrano[4,3-b]benzopyran derivatives, *Bioorg. Med. Chem.* 19 (2011) 5199.
- [33] H.J Kabbe, H. Heitzer, A new synthesis of 3,4-Dehydro-tocotrienol and Vitamin E, *Synthesis*, 12 (1978) 888.
- [34] B.C. Pearce, R.A. Parker, M.E. Deason, D.D. Dischino, E. Gillespie, A.A. Qureshi, K. Volk, J.J. Wright, Inhibitors of cholesterol biosynthesis. 2. Hypocholesterolemic and antioxidant activities of benzopyran and tetrahydronaphthalene analogues of the tocotrienols, *J. Med. Chem.* 37 (1994) 526.
- [35] D.T. Witiak, E.S. Stratford, R. Nazareth, G. Wagner, D.R. Feller, 6-Chlorochroman-2-carboxylic acids. Synthesis and biological evaluation as antagonists for cholesterol biosynthesis and lipolysis in vitro, *J. Med. Chem.* 14 (1971) 758.
- [36] A. Sato, T. Shindo, N. Kasanuki, K. Hasegawa, Antioxidant metabolites from the tunicate *Amaroucium multiplicatum*, *J. Nat. Prod.* 52 (1989) 975.
- [37] A. Bermejo, I. Barrachina, N. El Aouad, X. Franck, N. Chahboune, I. Andreu, B. Figadère, L. Vila, N. Hennuyer, B. Staels, C. Dacquet, D.H. Caignard, M.J. Sanz, D. Cortes, N. Cabedo, Synthesis of benzopyran derivatives as PPAR α and/or PPAR γ activators. *Bioorg. Med. Chem.* 27 (2019) 115162.
- [38] Q. Wang, M.G. Finn, 2H-Chromenes from salicylaldehydes by a catalytic petasis reaction, *Org. Lett.* 2 (2000) 4063.
- [39] M. Jiang, M. Shi, Lewis acid catalyzed cycloaddition of methylenecyclopropanes with salicylaldehydes, *Org. Lett.* 12 (2010) 2606.
- [40] L. Daniela, R. Ornelio, C. Massimo, A solvent-free protocol for the synthesis of 3-formyl-2H-chromenes via domino oxa Michael/aldol reaction, *Tetrahedron Letters*, 55 (2014) 1752.

- [41] C.R. Lenka, S.K. Nandigama, N.M. Harshadas, An efficient and chemoselective Knoevenagel/Hemiketalization process for the synthesis of new 2H-chromenes in a one-pot three-component reaction, *Helv. Chim. Acta.* 98 (2015) 978.
- [42] T. Kenta, S. Mayumi, S. Yosuke, H. Yujiro, H. Kiyoshi, Highly regioselective synthesis of 2,3-disubstituted 2H-1-benzopyrans: Brønsted acid catalyzed [4+2] cycloaddition reaction with a variety of arylalkynes via *ortho*-quinone methides, *Tetrahedron*, 73 (2017) 6456.
- [43] B.C. Pearce, R.A. Parker, M.E. Deason, A.A. Qureshi, J.J. Wright, Hypocholesterolemic activity of synthetic and natural tocotrienols, *J. Med. Chem.* 35 (1992) 3595.
- [44] J. Cossy, C. Menciau, H. Rakotoarisoa, P.H. Kahn, J.R. Desmurs, A short synthesis of troglitazone: an antidiabetic drug for treating insulin resistance, *Bioorg. Med. Chem. Lett.* 9 (1999) 3439.
- [45] H. Zong, H. Huang, J. Liu, G. Bian, L. Song, Added-metal-free catalytic nucleophilic addition of Grignard reagents to ketones, *J. Org. Chem.* 77 (2012) 4645.
- [46] M. Bilska-Markowska, M. Kazmierczak, Horner–Wadsworth–Emmons reaction as an excellent tool in the synthesis of fluoro-containing biologically important compounds, *Org. Biomolec. Chem.* 21 (2023) 1095.
- [47] R.J. Ouellette, J.D. Rawn, Aldehydes and Ketones: Nucleophilic Addition Reactions, *Organic Chemistry*, 20 (2018) 595.
- [48] C. Villarroel-Vicente, S. Gutiérrez-Palomo, J. Ferri, D. Cortes, N. Cabedo, Natural products and analogs as preventive agents for metabolic syndrome via peroxisome proliferator-activated receptors: An overview, *Eur. J. Med. Chem.* 221 (2021) 113535.
- [49] B. Gross, M. Pawlak, P. Lefebvre, B. Staels, PPARs in obesity-induced T2DM, dyslipidaemia and NAFLD, *Nat. Rev. Endocrinol.* 13 (2017) 36.
- [50] M. Pawlak, P. Lefebvre, B. Staels, Molecular mechanism of PPAR α action and its impact on lipid metabolism, inflammation and fibrosis in non-alcoholic fatty liver disease, *J. Hepatol.* 62 (2015) 720.
- [51] S. K. Ramakrishnan, L. Russo, S. S. Ghanem, P. R. Patel, A. M. Oyarce, G. Heinrich, S. M. Najjar, Fenofibrate decreases insulin clearance and insulin secretion to maintain insulin sensitivity, *J. Biol. Chem.* 291 (2016) 23915.
- [52] F. Lalloyer, B. Vandewalle, F. Percevault, G. Torpier, J. Kerr-Conte, M. Oosterveer, R. Paumelle, J. C. Fruchart, F. Kuipers, F. Pattou, C. Fiévet, B. Staels, B. Peroxisome

- proliferator-activated receptor alpha improves pancreatic adaptation to insulin resistance in obese mice and reduces lipotoxicity in human islets, *Diabetes*, 55 (2006) 1605.
- [53] X. Palomer, E. Barroso, J. Pizarro-Delgado, L. Peña, G. Botteri, M. Zarei, D. Aguilar, M. Montori-Grau, M. Vázquez-Carrera, PPAR β/δ : A key therapeutic target in metabolic disorders, *Int. J. Mol. Sci.* 19 (2018) 913.
- [54] A. Mannan, N. Garg, T.G. Singh, H.K. Kang, Peroxisome Proliferator-Activated Receptor-Gamma (PPAR- γ): Molecular effects and its importance as a novel therapeutic target for cerebral ischemic injury, *Neurochem. Res.* 46 (2021) 2800.
- [55] M. Schupp, M.A. Lazar, Endogenous ligands for nuclear receptors: Digging deeper, *J. Biol. Chem.* 285 (2010) 40409.
- [56] L. Wang, B. Waltenberger, E.M. Pferschy-Wenzig, M. Blunder, X. Liu, C. Malainer, T. Blazevic, S. Schwaiger, J.M. Rollinger, E.H. Heiss, D. Schuster, B. Kopp, R. Bauer, H. Stuppner, V.M. Dirsch, A.G. Atanasov, Natural product agonists of peroxisome proliferator-activated receptor gamma (PPAR γ): a review. *Biochem. pharmacol.* 92 (2014) 73.
- [57] T.M. Willson, P.J. Brown, D.D. Sternbach, B.R. Henke, The PPARs: from orphan receptors to drug discovery, *J. Med. Chem.* 43 (2000) 527.
- [58] D. Toobian, P. Ghosh, G.D. Katkar, Parsing the role of PPARs in macrophage processes, *Front. Immunol.* 12 (2021) 783780.
- [59] C.M. Freitag, R.J. Miller, Peroxisome proliferator-activated receptor agonists modulate neuropathic pain: a link to chemokines?, *Front. Cell. Neurosci.* 8 (2014) 238.
- [60] F. Song, Y.J. Mao, Y. Hu, S.S. Zhao, R. Wang, W.Y. Wu, G.R. Li, Y. Wang, G. Li, Acacetin attenuates diabetes-induced cardiomyopathy by inhibiting oxidative stress and energy metabolism via PPAR- α /AMPK pathway, *Eur. J. Pharmacol.* 922 (2022) 174916.
- [61] Q. Jia, H. Cao, D. Shen, S. Li, L. Yan, C. Chen, S. Xing, F. Dou, Quercetin protects against atherosclerosis by regulating the expression of PCSK9, CD36, PPAR γ , LXRA and ABCA1, *Int. J. Mol. Med.* 44 (2019) 893.
- [62] B. Zhang, Z. Hao, W. Zhou, S. Zhang, M. Sun, H. Li, N. Hou, C. Jing, M. Zhao, Formononetin protects against ox-LDL-induced endothelial dysfunction by activating PPAR- γ signaling based on network pharmacology and experimental validation, *Bioengineered*, 12 (2021) 4887.
- [63] L. Feng, H. Luo, Z. Xu, Z. Yang, G. Du, Y. Zhang, L. Yu, K. Hu, W. Zhu, Q. Tong, K. Chen, F. Guo, C. Huang, Y. Li, Bavachinin, as a novel natural pan-PPAR agonist, exhibits

- unique synergistic effects with synthetic PPAR- γ and PPAR- α agonists on carbohydrate and lipid metabolism in db/db and diet-induced obese mice. *Diabetologia*, 59 (2016) 1276.
- [64] A. Bermejo, A. Collado, I. Barrachina, P. Marqués, N. El Aouad, X. Franck, F. Garibotto, C. Dacquet, D.H. Caignard, F.D. Suvire, R.D. Enriz, L. Piqueras, B. Figadère, M.J. Sanz, N. Cabedo, D. Cortes, Polycerasoidol, a natural prenylated benzopyran with a dual PPAR α /PPAR γ agonist activity and anti-inflammatory effect, *J. Nat. Prod.* 82 (2019) 1802.
- [65] P. Marques, C. Villarroel-Vicente, A. Collado, A. García, L. Vila, I. Duplan, N. Hennuyer, F. Garibotto, R.D. Enriz, C. Dacquet, B. Staels, L. Piqueras, D. Cortes, M.J. Sanz, N. Cabedo, Anti-inflammatory effects and improved metabolic derangements in ob/ob mice by a newly synthesized prenylated benzopyran with pan-PPAR activity, *Pharmacol. Res.* 187 (2023) 106638.
- [66] Y. Sun, Y. Liu, X. Ma, H. Hu, The Influence of cell cycle regulation on chemotherapy, *Int. J. Mol. Sci.* 22 (2021) 6923.
- [67] E.S. Wenzel, A.T.K. Singh, Cell-cycle checkpoints and aneuploidy on the path to cancer, *In Vivo*, 32 (2018) 1.
- [68] R.S. Wong, Apoptosis in cancer: from pathogenesis to treatment, *J. Exp. Clin. Cancer Res.* 30 (2011) 87.
- [69] L.J. Su, J.H. Zhang, H. Gomez, R. Murugan, X. Hong, D. Xu, F. Jiang, Z.Y. Peng, Reactive oxygen species-induced lipid peroxidation in apoptosis, autophagy, and ferroptosis, *Oxid. Med. Cell. Longev.* (2019) 5080843.
- [70] H. Şenol, P. Tulay, M.Ç. Ergören, A. Hanoğlu, İ. Çalış, G. Mocan, Cytotoxic effects of verbascoside on MCF-7 and MDA-MB-231, *Turk. J. Pharm. Sci.* 18 (2021) 637.
- [71] K.R. Senwar, T.S. Reddy, D. Thummuri, P. Sharma, V.G. Naidu, G. Srinivasulu, N. Shankaraiah, Design, synthesis and apoptosis inducing effect of novel (Z)-3-(3'-methoxy-4'-(2-amino-2-oxoethoxy)-benzylidene)indolin-2-ones as potential antitumor agents, *Eur. J. Med. Chem.* 118 (2016) 34.
- [72] R.L. Siegel, K.D. Miller, A. Jemal, Cancer statistics, 2015, *CA. Cancer J. Clin.* 65 (2015) 5.
- [73] I. Ahmad, Shagufta, Recent developments in steroidal and nonsteroidal aromatase inhibitors for the chemoprevention of estrogen-dependent breast cancer, *Eur. J. Med. Chem.* 102 (2015) 375.
- [74] A.G. Waks, E.P. Winer, Breast cancer treatment: a review, *JAMA*, 321 (2019) 288.

- [75]. O.A. Bamodu, W.C. Huang, D.T. Tzeng, A. Wu, L.S.Wang, C.T. Yeh, T.Y. Chao, Ovatodiolide sensitizes aggressive breast cancer cells to doxorubicin, eliminates their cancer stem cell-like phenotype, and reduces doxorubicin-associated toxicity. *Cancer lett.* 364 (2015) 125.
- [76]. M. Gallorini, A. Cataldi, V. di Giacomo, Cyclin-dependent kinase modulators and cancer therapy, *BioDrugs*, 26 (2012) 377.
- [77]. O. Gluz, C. Liedtke, N. Gottschalk, L. Pusztail, U. Nitz, N. Harbeck, Triple-negative breast cancer – current status and future directions, *Ann. Oncol.* 20 (2009) 1913–1927.
- [78]. M. Liao, J. Zhang, G. Wang, L. Wang, J. Liu, L. Ouyang, B. Liu, Small-molecule drug discovery in triple negative breast cancer: current situation and future directions, *J. Med. Chem.* 64 (2021) 2382.
- [79]. Y. Li, S. Li, X. Meng, R.Y. Gan, J.J. Zhang, B.B. Li, Dietary natural products for prevention and treatment of breast cancer, *Nutrients*, 9 (2017) 728.
- [80]. Q. Zhao, M. Zhao, A.B. Parris, Y. Xing, X. Yang, Genistein targets the cancerous inhibitor of PP2A to induce growth inhibition and apoptosis in breast cancer cells, *Int. J. Oncol.* 49 (2016) 1203.
- [81]. J. Chen, Y. Duan, X. Zhang, Y. Ye, B. Ge, J. Chen, Genistein induces apoptosis by the inactivation of the IGF-1R/p-Akt signaling pathway in MCF-7 human breast cancer cells, *Food. Funct.* 6 (2015) 995.
- [82]. S.S. Bhat, S.K. Prasad, C. Shivamallu, K.S. Prasad, A. Syed, P. Reddy, C.A. Cull, R.G. Amachawadi, Genistein: a potent anti-breast cancer agent, *Curr. Issues. Mol. Biol.* 43 (2021) 1502.
- [83]. Y. Safdari, M. Khalili, M.A. Ebrahimzadeh, Y. Yazdani, S. Farajnia, Natural inhibitors of PI3K/AKT signaling in breast cancer: emphasis on newly-discovered molecular mechanisms of action, *Pharmacol. Res.* 93 (2015) 1.
- [84]. A.A. Abd El-Hafeez, H.O. Khalifa, E.A.M. Mahdy V. Sharma, T. Hosoi, P. Ghosh, K. Ozawa, M.M. Montano, T. Fujimura, A.R.N. Ibrahim, M.A.A. Abdelhamid, S.P. Pack, S.A. Shouman, S. Kawamoto, Anticancer effect of nor-wogonin (5, 7, 8-trihydroxyflavone) on human triple-negative breast cancer cells via downregulation of TAK1, NF- κ B, and STAT3, *Pharmacol. Rep.* 71 (2019) 289.
- [85]. S. Sordon, J. Popłoński, M. Milczarek, M. Stachowicz, T. Tronina, A.Z. Kucharska, J. Wietrzyk, E. Huszcza, Structure-antioxidant-antiproliferative activity relationships of natural C7 and C7-C8 hydroxylated flavones and flavanones, *Antioxidants (Basel)*, 8 (2019) 210.

-
- [86] K.M. Yap, M. Sekar, Y.S. Wu, S.H. Gan, N.I.M. Rani, L.J. Seow, V. Subramaniyan, N.K. Fuloria, S. Fuloria, P.T. Lum, Hesperidin and its aglycone hesperetin in breast cancer therapy: A review of recent developments and future prospects, *Saudi J. Biol. Sci.* 28 (2021) 6730.
- [87] S. Rani, K. Raheja, V. Luxami, K. Paul, A review on diverse heterocyclic compounds as the privileged scaffolds in non-steroidal aromatase inhibitors, *Bioorg. Chem.* 113 (2021) 105017.
- [88] C. Zhang, Z. Wang, Y. Shi, B. Yu, Y. Song, Recent advances of LSD1/KDM1A inhibitors for disease therapy, *Bioorg. Chem.* 134 (2023) 106443.
- [89] H. Taha, C.Y. Looi, A. Arya, W.F. Wong, L.F. Yap, M. Hasanpourghadi, M.A. Mohd, I.C. Paterson, H. Mohd Ali, (6E,10E) Isopolycerasoidol and (6E,10E) isopolycerasoidol methyl ester, prenylated benzopyran derivatives from *pseuduvaria monticola* induce mitochondrial-mediated apoptosis in human breast adenocarcinoma cells, *PloS one*, 10 (2015) e0126126.

Conclusions

1. New series of 2-prenylated alkoxyated benzopyran possessing the α -alkoxy- α,β -unsaturated moiety on the prenylated chain have been synthesised via the Grignard reaction followed by the Horner–Wadsworth–Emmons reaction. Synthetic derivatives were efficient in activating both hPPAR α and hPPAR γ as dual PPAR α/γ agonists. The elongation of the side chain from five to nine carbons was beneficial to activate hPPAR γ .

(Article 1)

2. Three series of prenylated benzopyrans were efficiently prepared with a sequence of reactions including Grignard reaction followed by Witting olefination with (carbethoxyethylidene) triphenylphosphorane to introduce one, two or three prenylated moieties in the side chain. Transactivation activity demonstrated that seven-carbon synthetic derivatives displayed selectivity for hPPAR α and nine-carbon derivatives showed high efficacy to activate hPPAR γ . **(Article 2)**

3. Two series of 2-alkyl hydrazones with three-carbon or seven-carbon side chain at 2-position of benzopyran nucleus were synthesised. Synthesised compounds showed partial hPPAR α/γ or hPPAR α/β agonism activity and attenuated inflammatory markers such as *IL-6* and *MCP-1* in THP-1 cells via NF- κ B pathway activation. The side chain at the 2-position in the benzopyran nucleus required the C=N double bond in the hydrazone function to activate the PPAR isoforms. **(Article 3)**

4. Three series of 2-aminopropyl derivatives containing a benzopyran nucleus have been synthesised and evaluated in triple-negative breast cancer cell lines being the N-methylated derivatives (tertiary amines) the most potent compounds followed by secondary amine benzopyrans, quaternary amine salts and free phenolic derivatives. Synthesised compounds promoted apoptosis or caused cell cycle arrest by downregulating apoptotic *Bcl-2* or cyclins (*CCND1* and *CCNDE2*), respectively. **(Article 4)**

5. Benzopyran derivatives analogues of polycerasoidol emerge as lead compounds for developing useful candidates to prevent cardiovascular diseases associate with metabolic disorders or useful agents against breast cancer. **(Final conclusion)**

Conclusiones

1. Se han sintetizado nuevas series de benzopiranos alcoxilados 2-prenilados que poseen el éster α -alkoxi- α,β -insaturado en la cadena prenilada mediante la reacción de Grignard seguida de la reacción de Horner–Wadsworth–Emmons. Los derivados sintéticos fueron eficientes activando ambas hPPAR α and hPPAR γ como agonistas duales PPAR α/γ . El alargamiento de la cadena lateral de cinco a nueve carbonos fue beneficioso para activar hPPAR γ . **(Artículo 1)**

2. Se prepararon eficientemente tres series de benzopiranos prenilados con una secuencia de reacciones que incluía la reacción de Grignard seguida de la olefinación de Wittig con (carbetoxtetilidina) trifenilfosforano para introducir uno, dos o tres elementos prenilados en la cadena lateral. La actividad de transactivación demostró que los derivados sintéticos de cadena lateral de siete carbonos mostraron selectividad por hPPAR α y aquellos con cadena lateral de nueve carbonos presentaron alta eficacia para activar hPPAR γ . **(Artículo 2)**

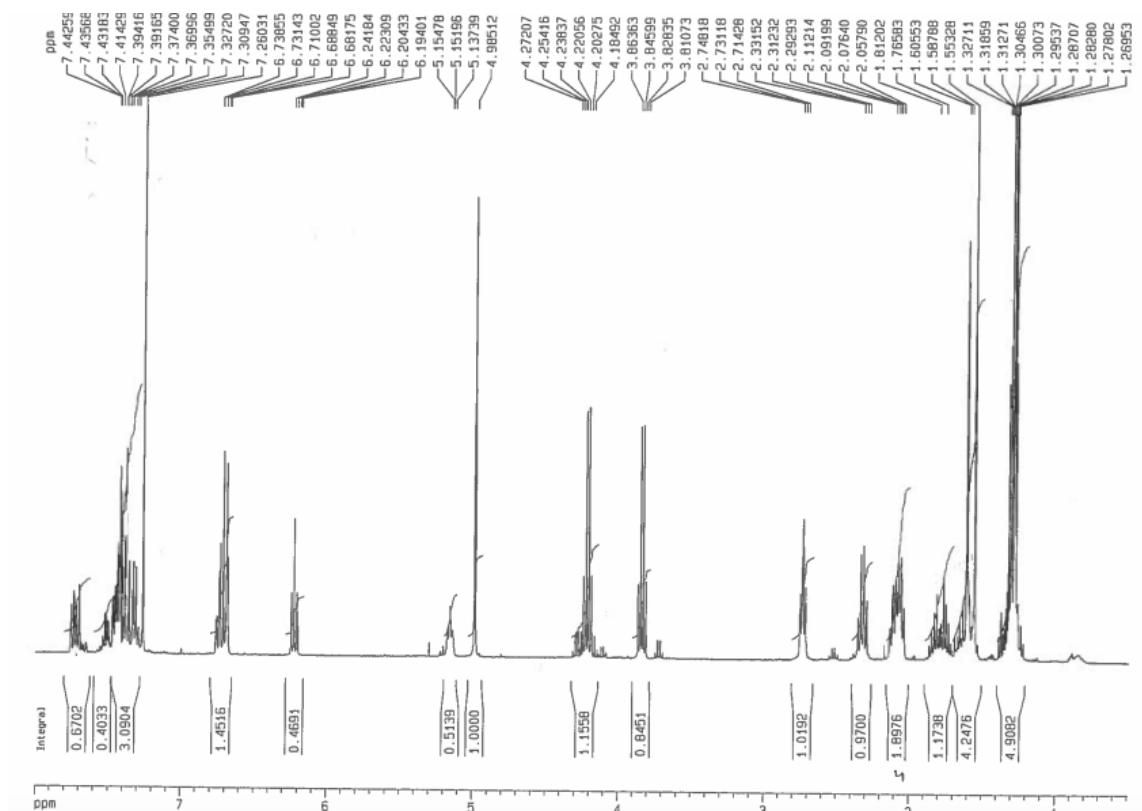
3. Se sintetizaron dos series de 2-alkil hidrazonas con la cadena lateral de tres o siete carbonos en la posición 2 del núcleo de benzopirano. Los compuestos sintetizados mostraron actividad agonista parcial hPPAR α/γ o hPPAR α/β y atenuaron marcadores inflamatorios como *IL-6* y *MCP-1* en células THP-1 mediante la activación de la vía NF- κ B. La cadena lateral en la posición 2 del núcleo del benzopirano requería el doble enlace C=N en la función hidrazona para activar las isoformas PPAR. **(Artículo 3)**

4. Se han sintetizado tres series de derivados 2-aminopropílicos que contienen un núcleo de benzopirano y se han evaluado en líneas celulares de cáncer de mama triple negativo, siendo los derivados *N*-metilados (aminas terciarias) los compuestos más potentes, seguidos de los benzopiranos de aminas secundarias, las sales de aminas cuaternarias y los derivados fenólicos libres. Los compuestos sintetizados promovieron la apoptosis o provocaron la detención del ciclo celular mediante la regulación a la baja de *Bcl-2* o ciclinas apoptóticas (*CCND1* y *CCNDE2*), respectivamente. **(Artículo 4)**

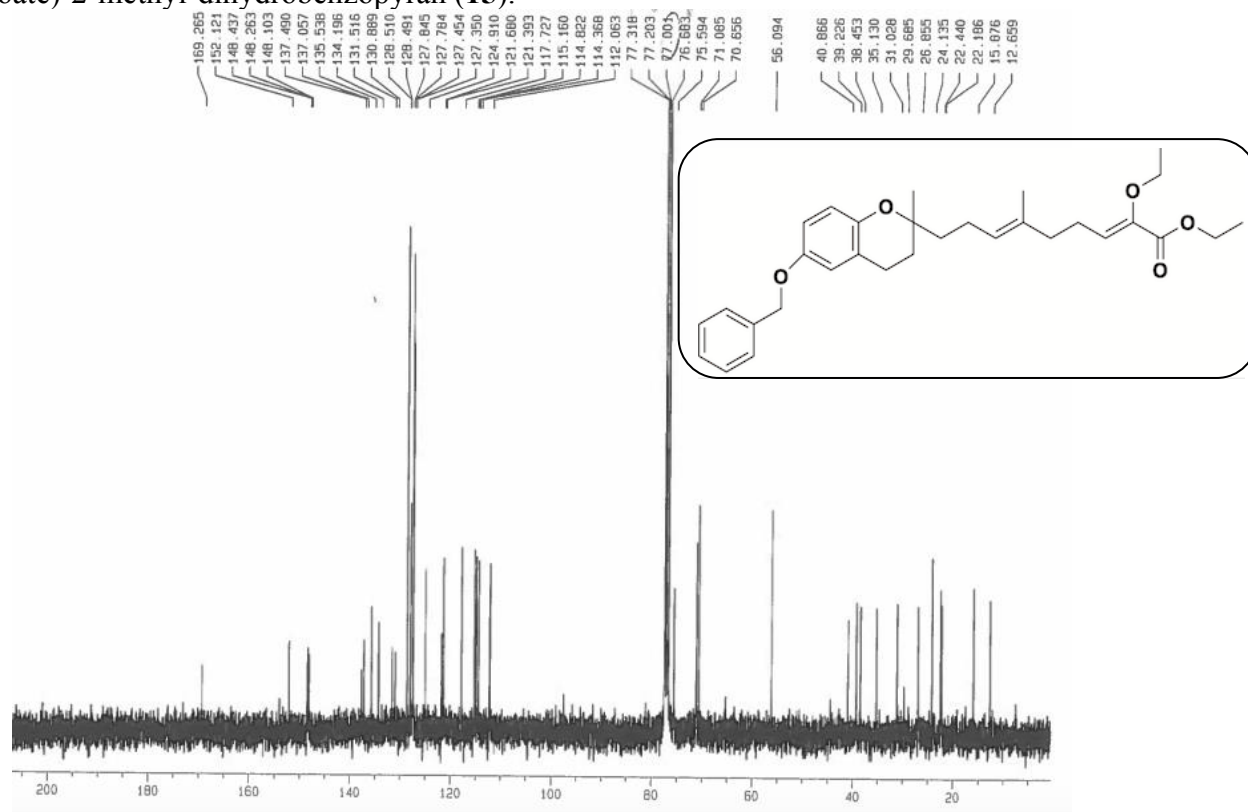
5. Los derivados benzopiranos análogos de polycerasoidol surgen como compuestos líderes para desarrollar candidatos útiles para prevenir enfermedades cardiovasculares asociadas a trastornos metabólicos o agentes útiles contra el cáncer de mama.
(Conclusión final)

Annex

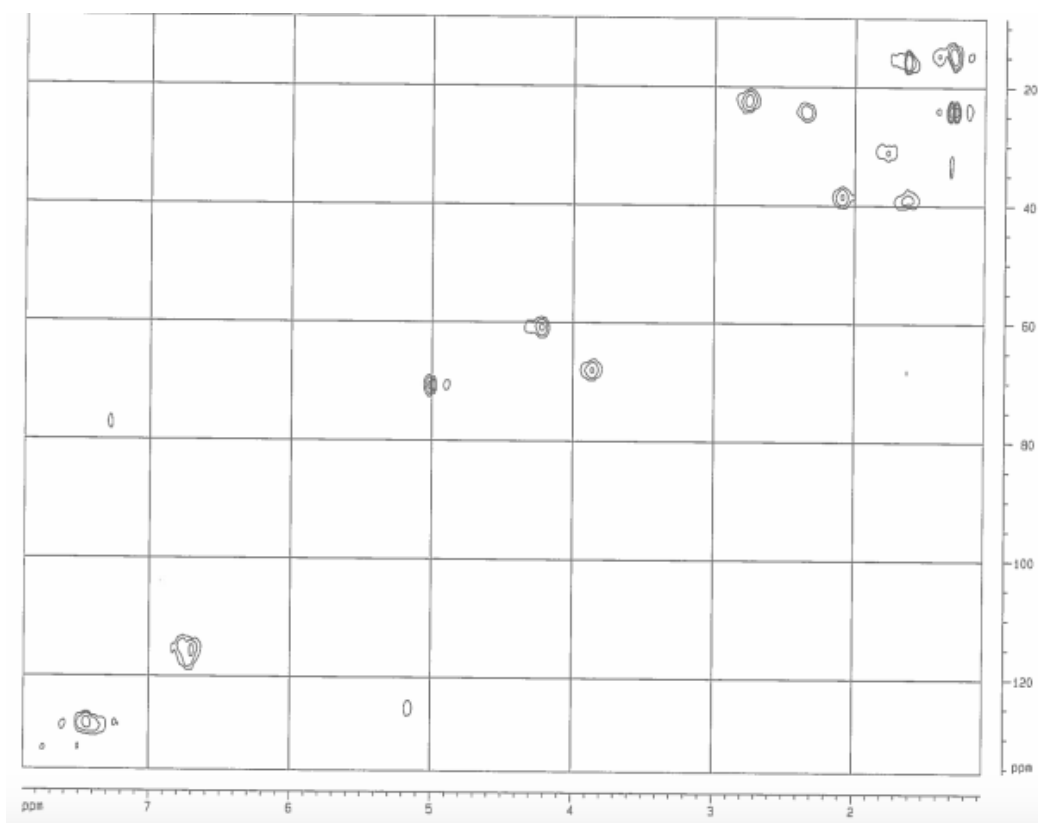
Article 1: Synthesis of 2-prenylated alkoxyated benzopyrans by Horner-Wadsworth–Emmons olefination with PPAR α / γ Agonist Activity, *ACS Medicinal Chemistry Letters*, 12 (2021) 1783-1786.



¹H NMR (300 MHz, CDCl₃) of 6-benzyloxy-2-((8'-ethoxy-4'-methyl)ethylnona-3'E, 7'Z-dienoate)-2-methyl-dihydrobenzopyran (**15**).

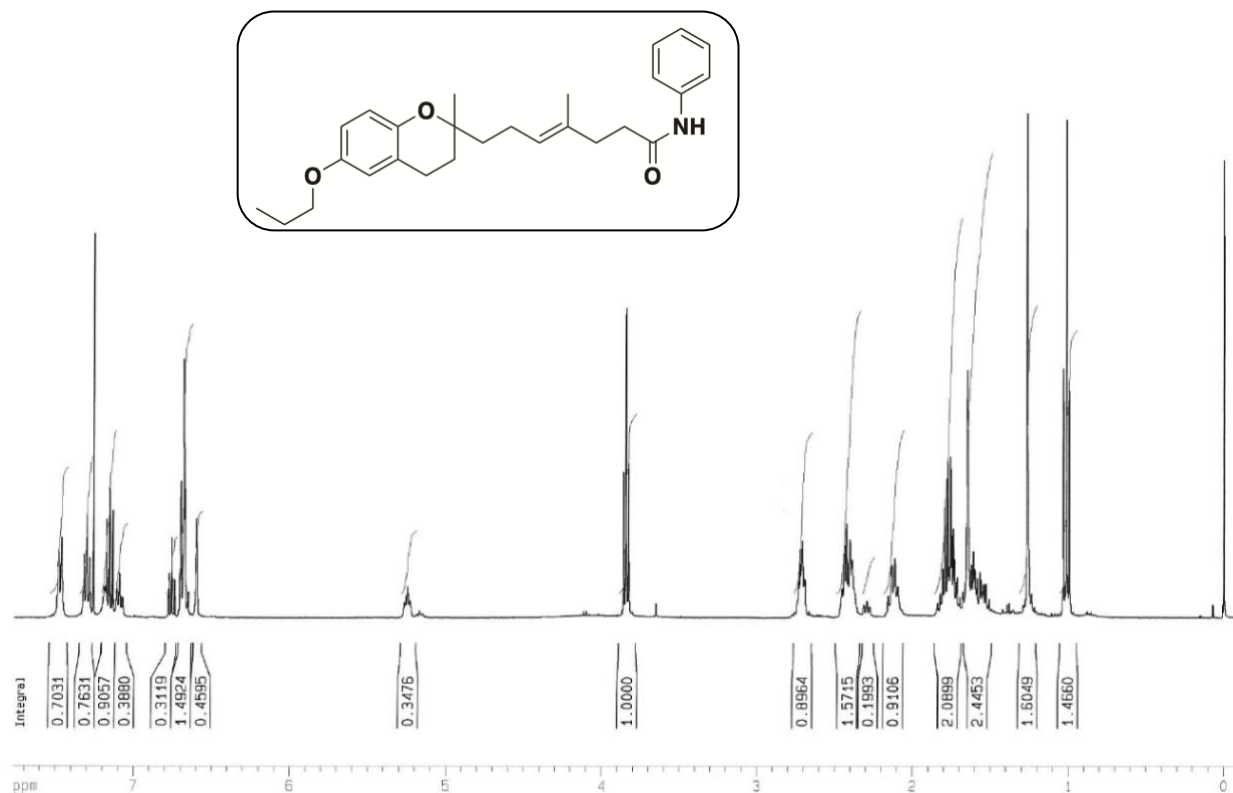


¹³C NMR (75 MHz, CDCl₃) of 6-benzyloxy-2-((8'-ethoxy-4'-methyl)ethylnona-3'E, 7'Z-dienoate)-2-methyl-dihydrobenzopyran (**15**).

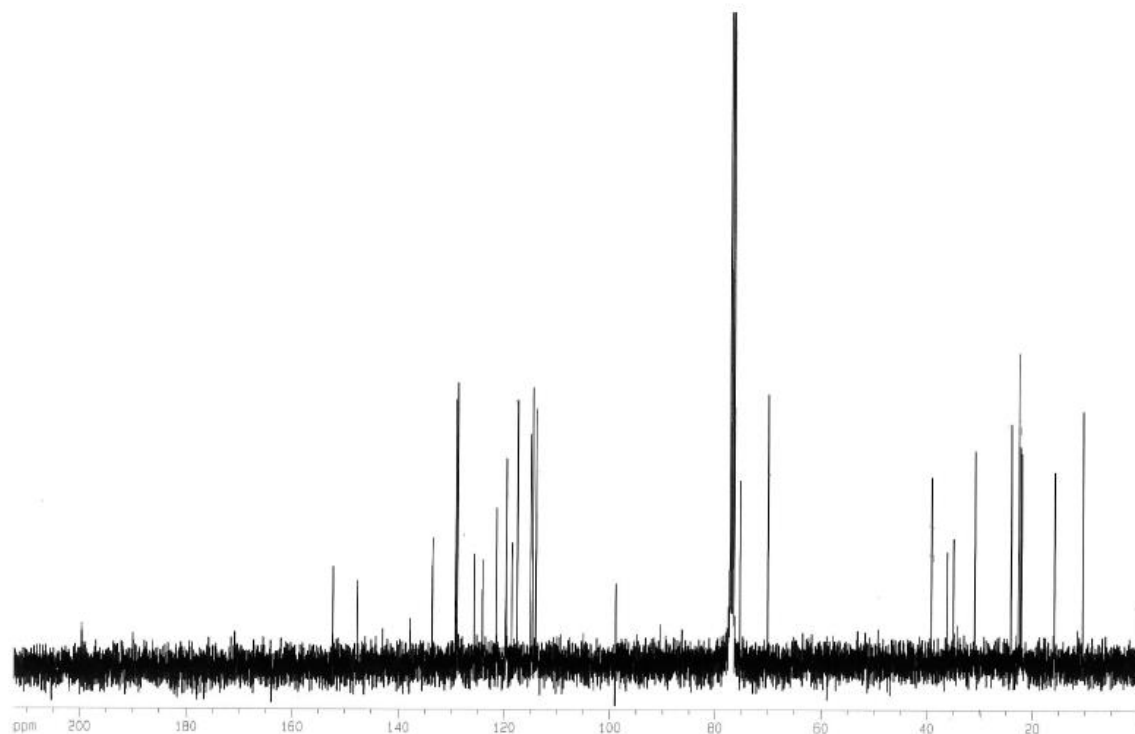


HSQC (300 MHz, CDCl_3) of 6-benzyloxy-2-((8'-ethoxy-4'-methyl)ethynona-3'E, 7'Z-dienoate)-2-methyl-dihydrobenzopyran (**15**).

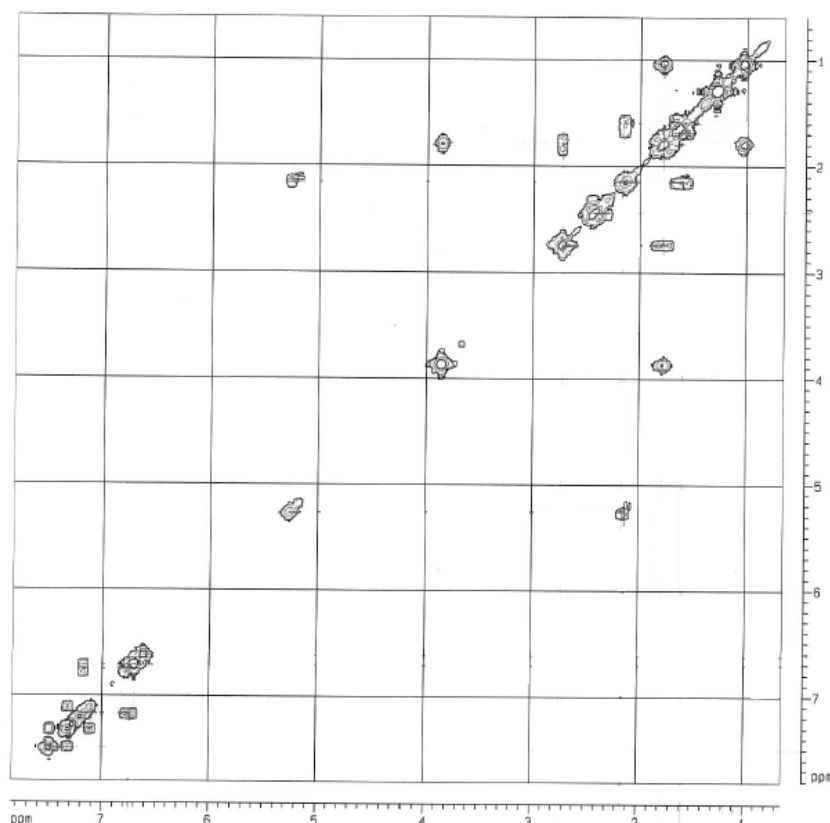
Article 2: Synthesis and biological studies of “Polycerasoidol” and “trans- δ -Tocotrienolic acid” derivatives as PPAR α and/or PPAR γ agonists, *Bioorganic & Medicinal Chemistry*, 53 (2022) 116532.



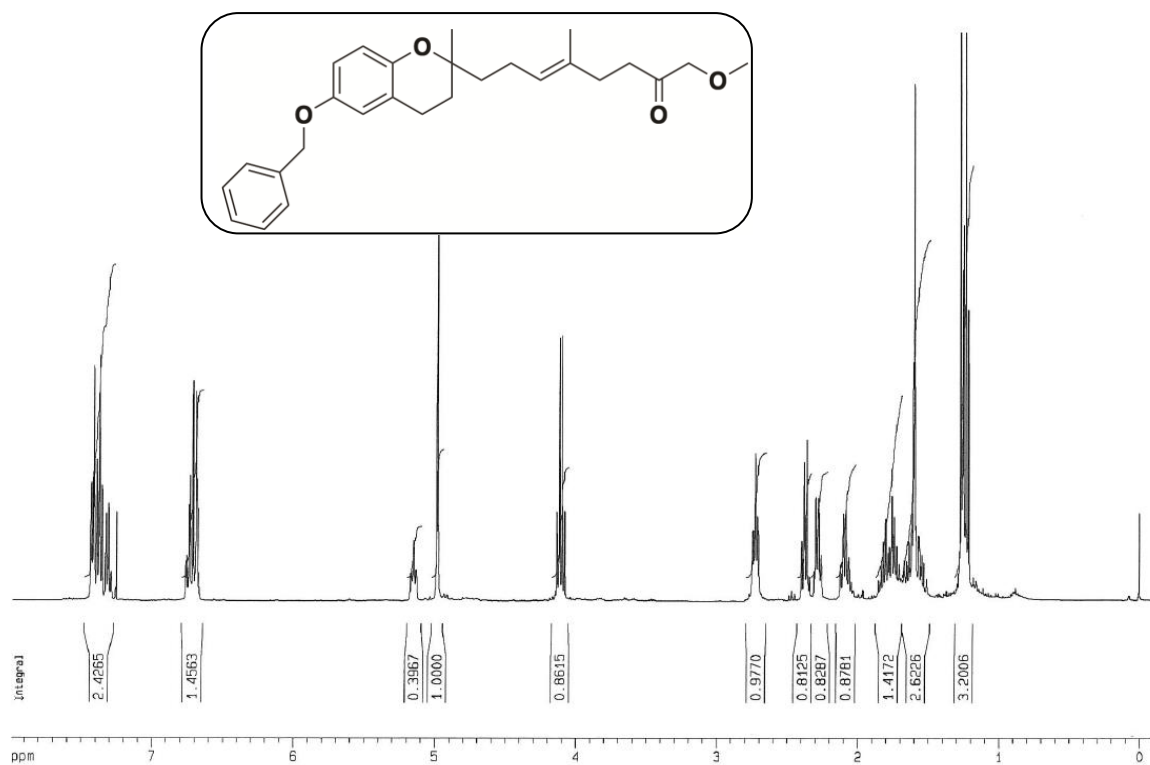
¹H NMR (300 MHz, CDCl₃) of 2-methyl-2-((4'-methyl)-N-phenylhept-3'-enamide)-6-propoxydihydrobenzopyran (**7**).



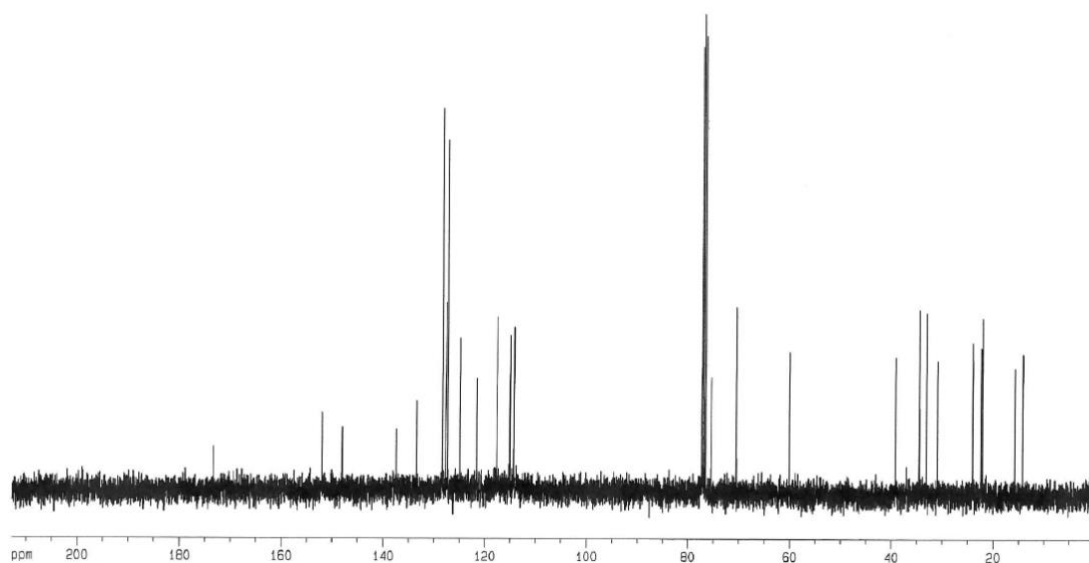
¹³C NMR (75 MHz, CDCl₃) of 2-methyl-2-((4'-methyl)-N-phenylhept-3'-enamide)-6-propoxydihydrobenzopyran (**7**).



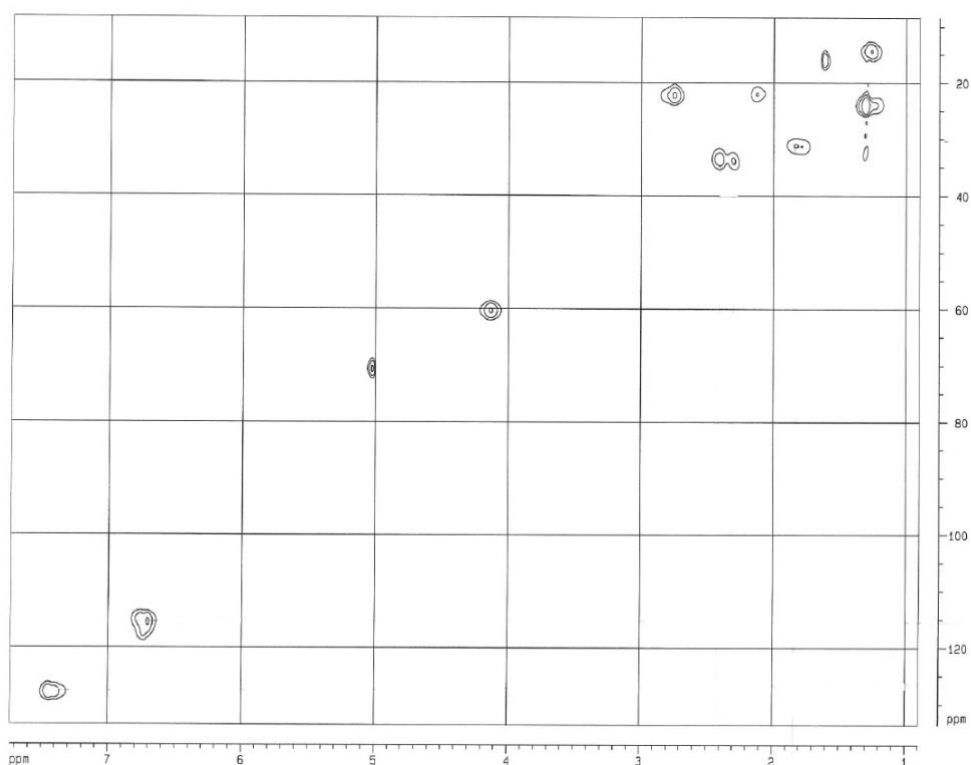
COSY (300 MHz, CDCl_3) of 2-methyl-2-((4'-methyl)-N-phenylhept-3'-enamide)-6-propoxydihydrobenzopyran (**7**).



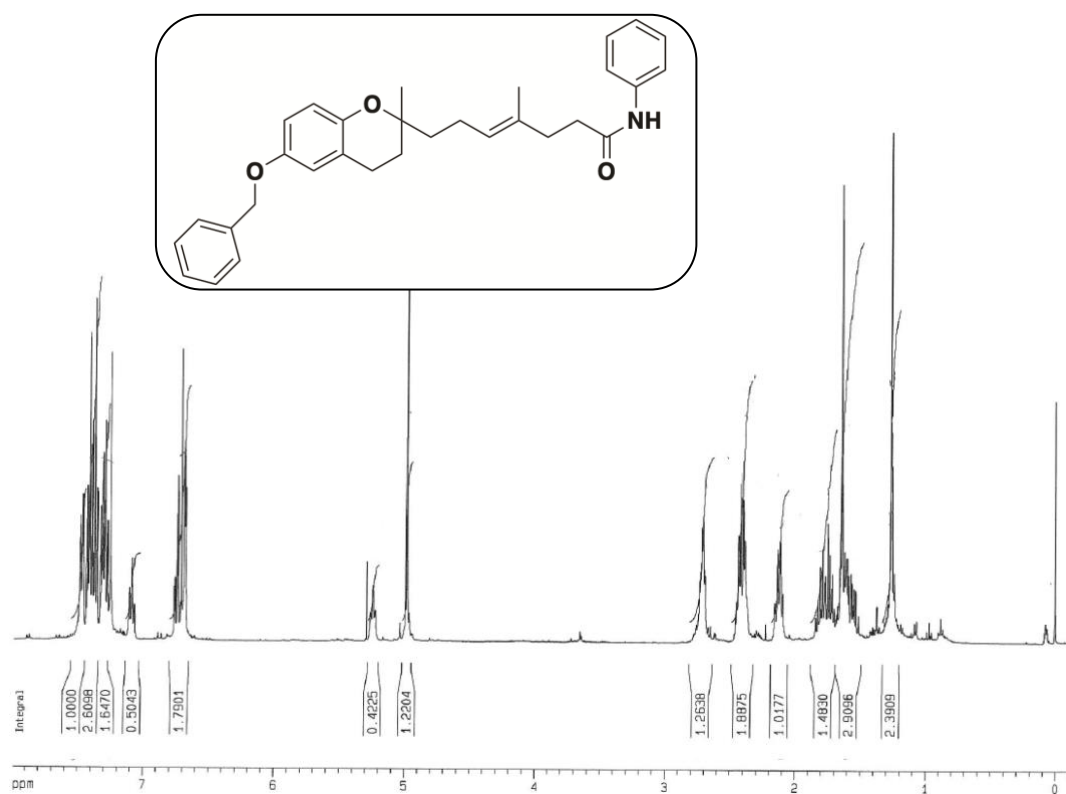
^1H NMR (400 MHz, CDCl_3) of 6-benzyloxy-2-methyl-2-((4'-methyl)ethylhept-3'-enoate)-dihydrobenzopyran (**8**).



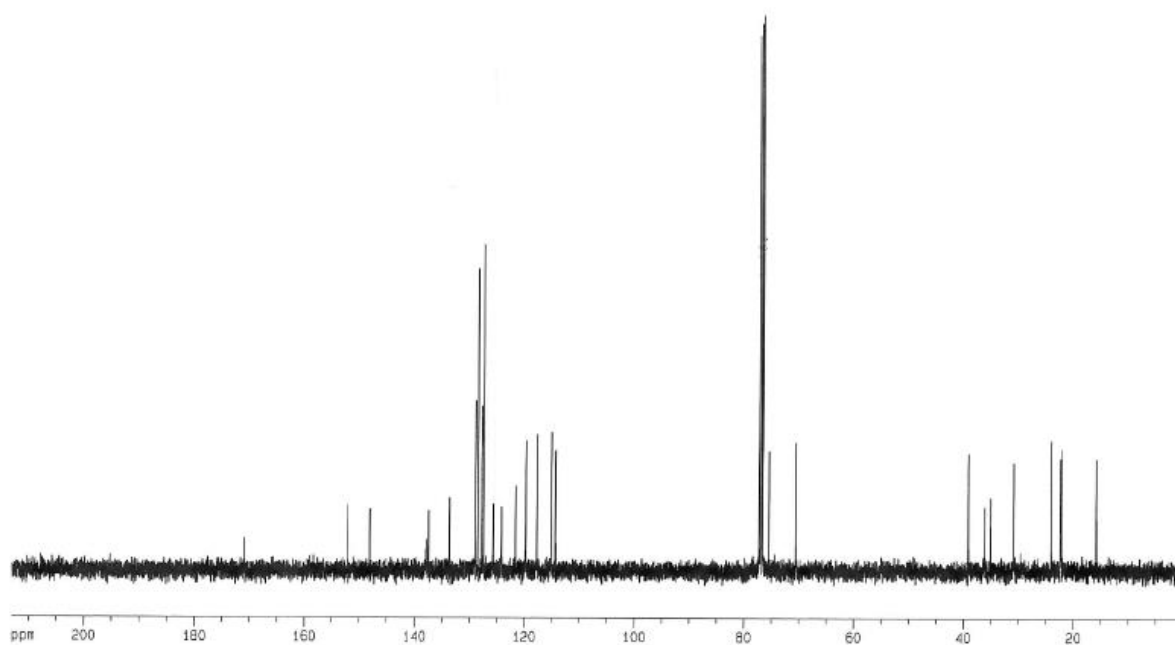
^{13}C NMR (100 MHz, CDCl_3) of 6-benzyloxy-2-methyl-2-((4'-methyl)ethylhept-3'-enoate)-dihydrobenzopyran (**8**).



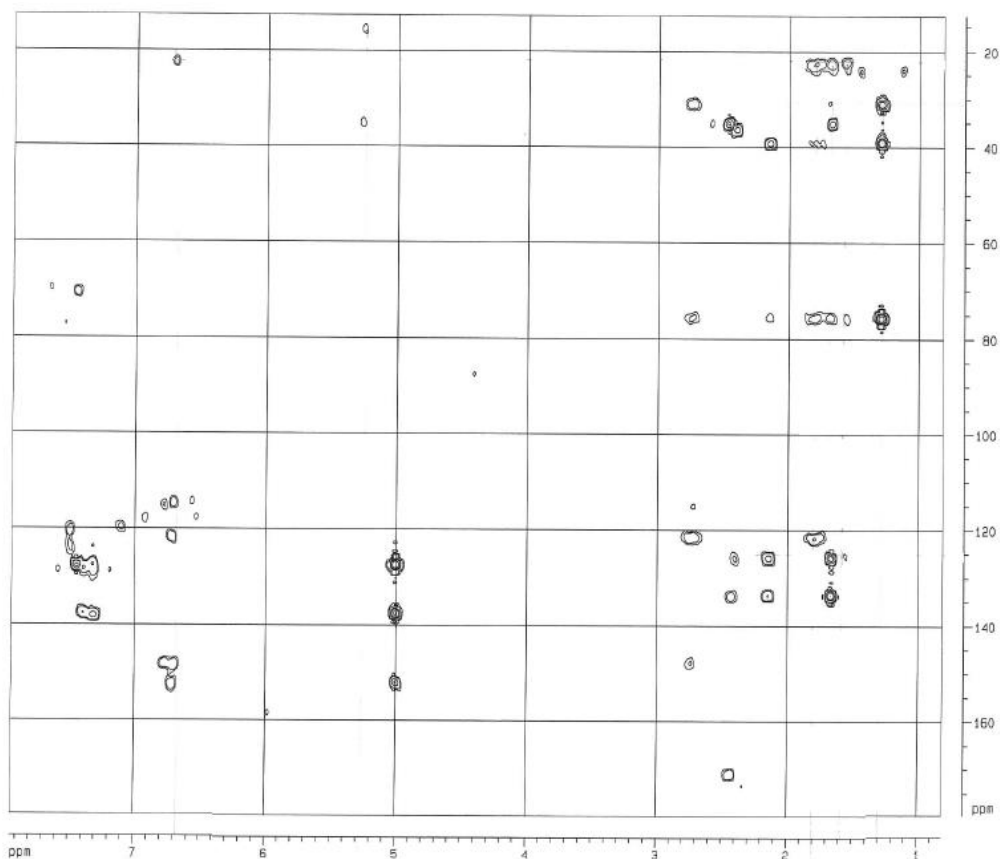
HSQC (400 MHz, CDCl_3) of 6-benzyloxy-2-methyl-2-((4'-methyl)ethylhept-3'-enoate)-dihydrobenzopyran (**8**).



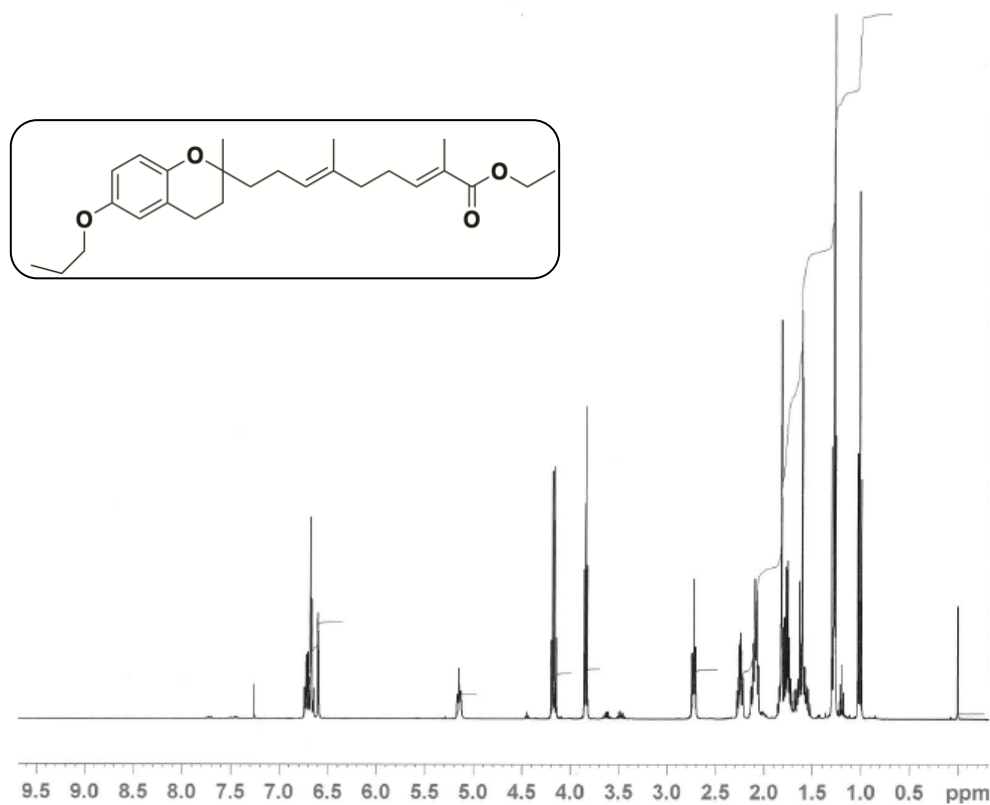
¹H NMR (400 MHz, CDCl₃) of 6-benzyloxy-2-methyl-2-(N-phenyl(4'-methyl)hept-3'-enamide)-dihydrobenzopyran (**9**).



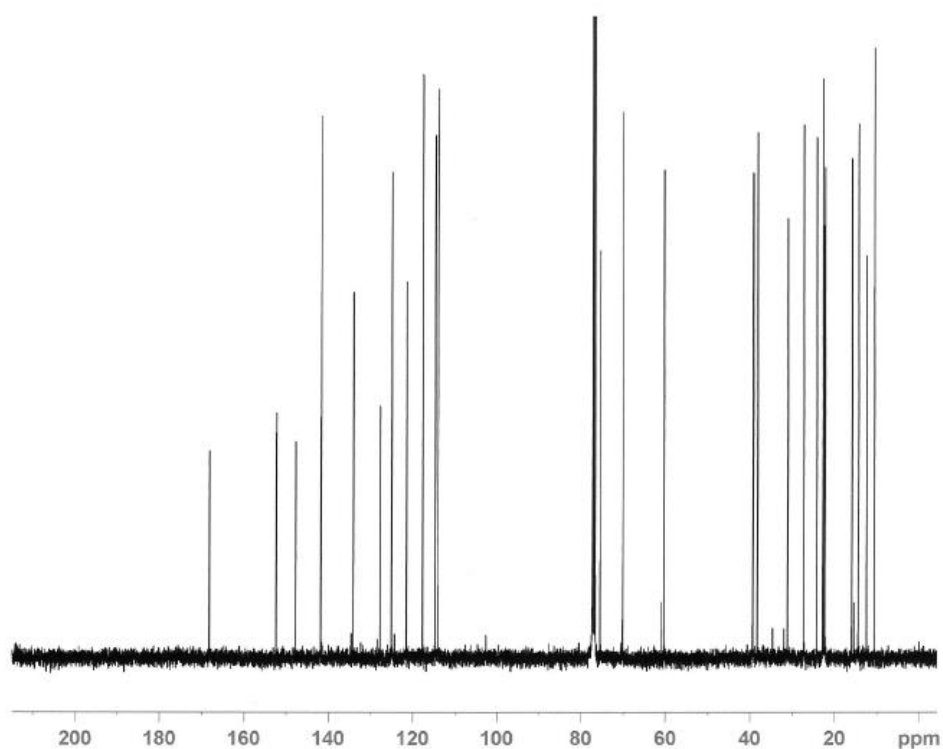
¹³C NMR (100 MHz, CDCl₃) of 6-benzyloxy-2-methyl-2-(N-phenyl(4'-methyl)hept-3'-enamide)-dihydrobenzopyran (**9**).



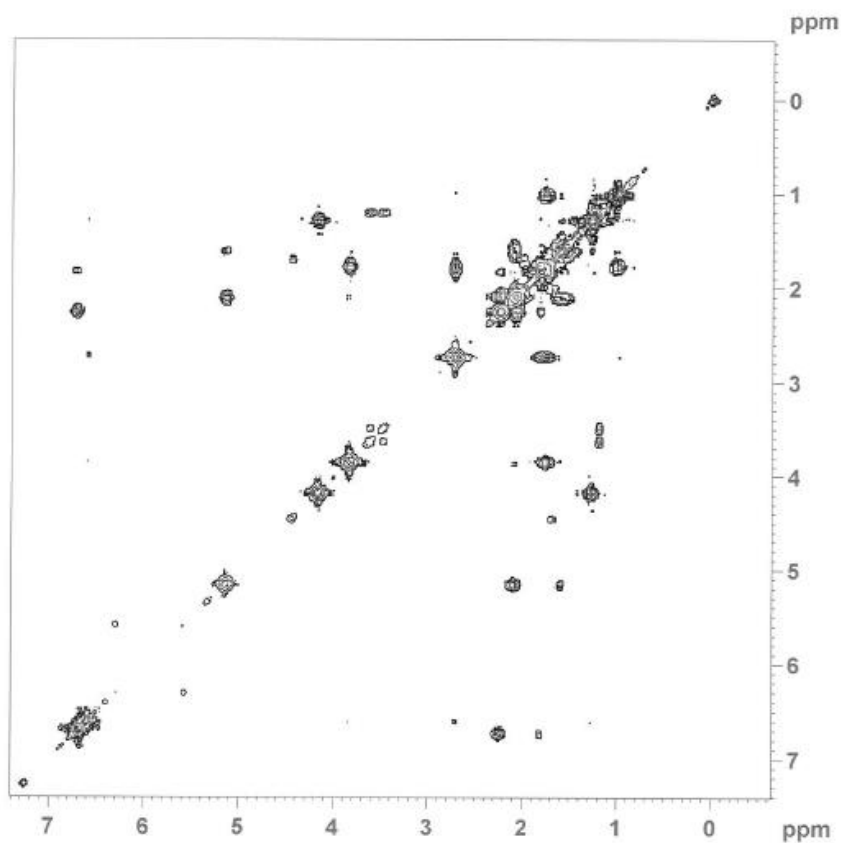
HMBC (400 MHz, CDCl_3) of 6-benzyloxy-2-methyl-2-(N-phenyl(4'-methyl)hept-3'-enamide)-dihydrobenzopyran (**9**).



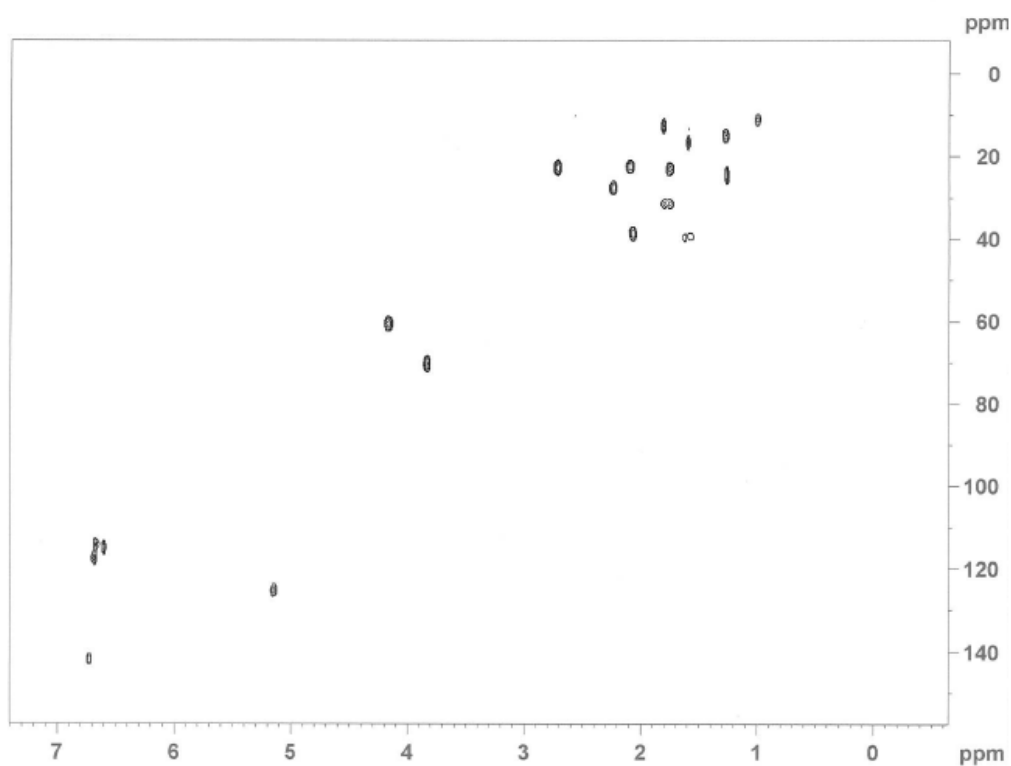
^1H NMR (400 MHz, CDCl_3) of 2-((4',8'-dimethyl)ethylnonan-3',7'-dienoate)-2-methyl-6-propoxydihydro-benzopyran (**12**).



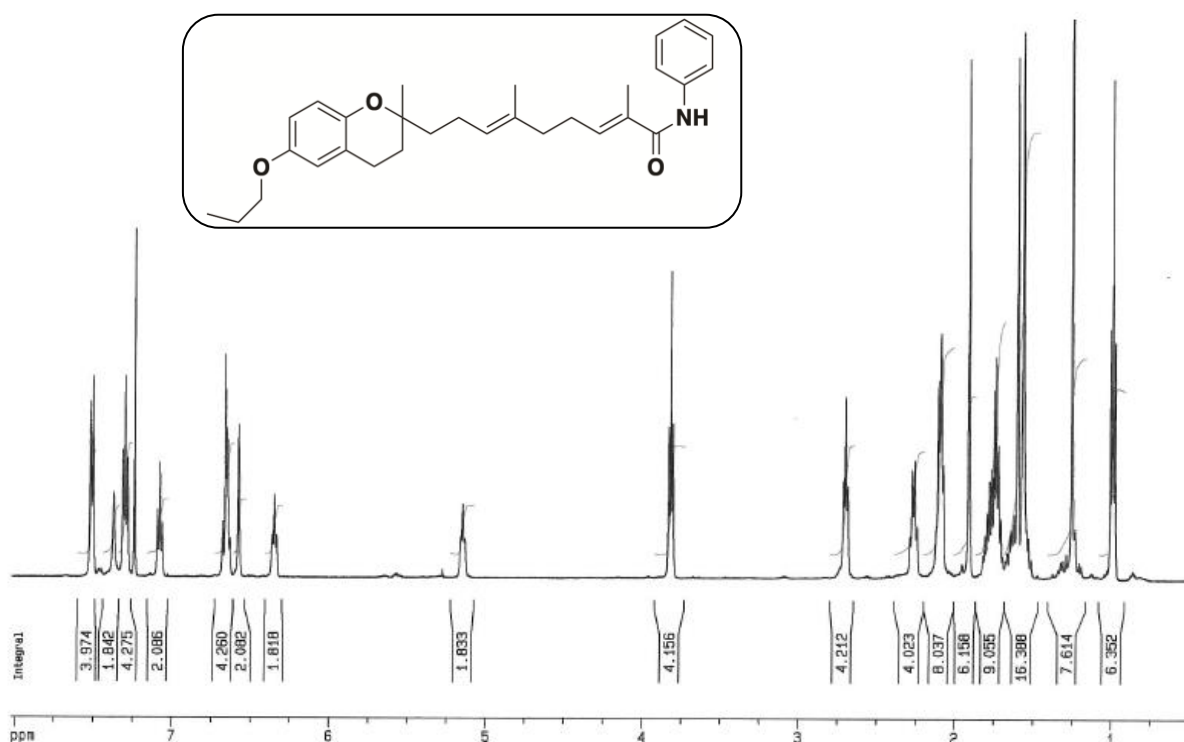
^{13}C NMR (100 MHz, CDCl_3) of 2-((4',8'-dimethyl)ethylnonan-3',7'-dienoate)-2-methyl-6-propoxydihydro-benzopyran (**12**).



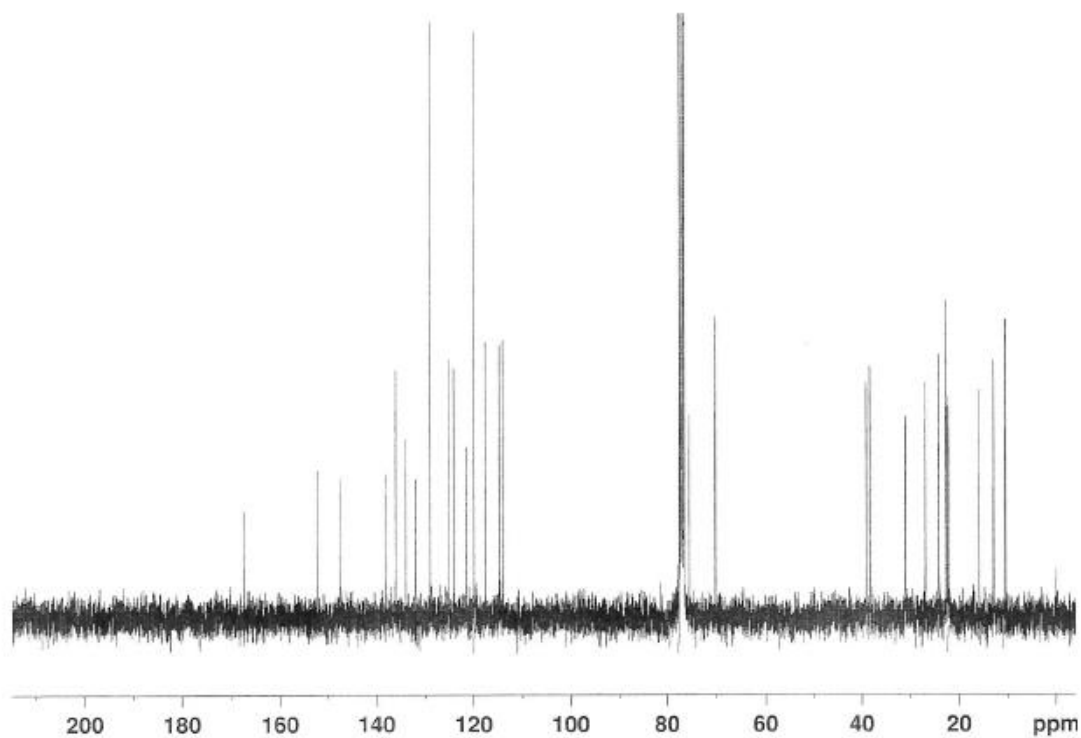
COSY (400 MHz, CDCl_3) of 2-((4',8'-dimethyl)ethylnonan-3',7'-dienoate)-2-methyl-6-propoxydihydro-benzopyran (**12**).



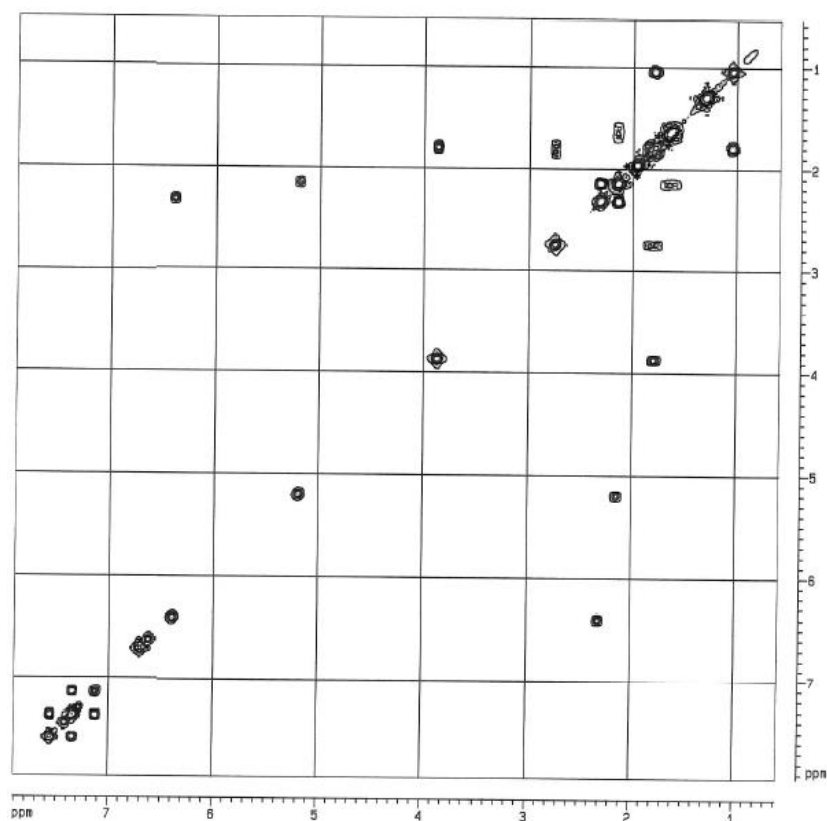
HSQC (400 MHz, CDCl₃) of 2-((4',8'-dimethyl)ethylnonan-3',7'-dienoate)-2-methyl-6-propoxydihydro-benzopyran (**12**).



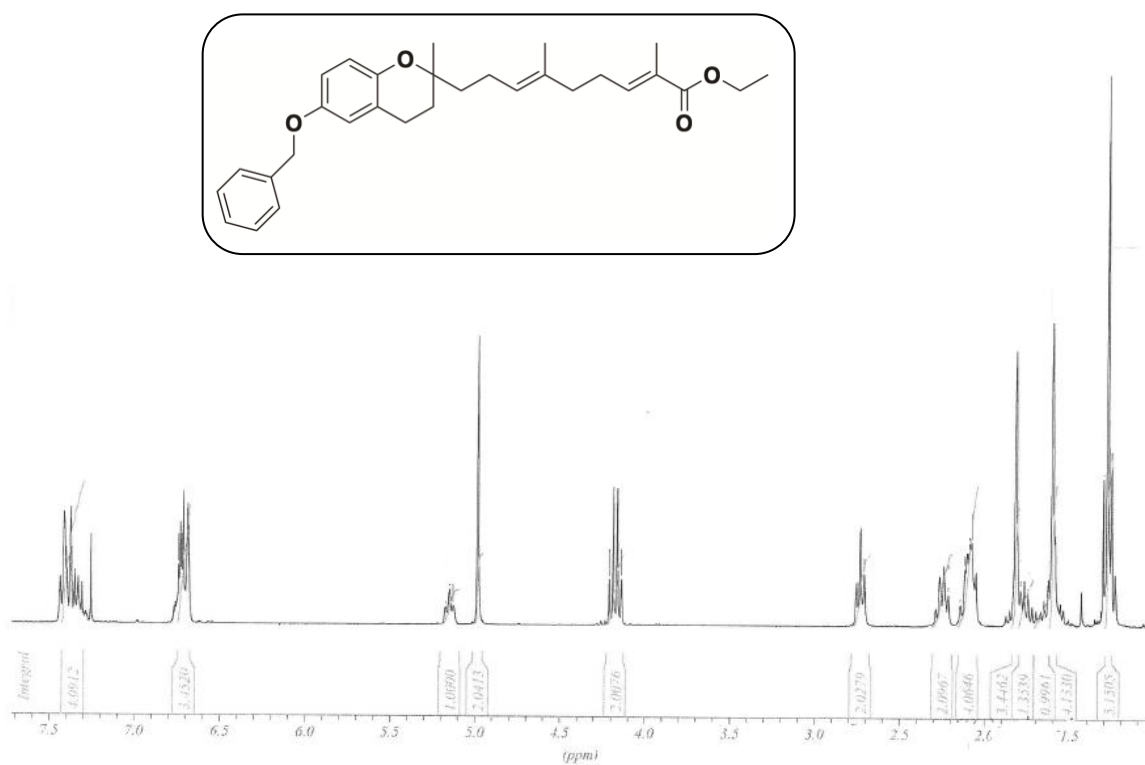
¹H NMR (300 MHz, CDCl₃) of 2-methyl-2-((4',8'-dimethyl)-N-phenylnona-3',7'-dienamide)-6-propoxydihydro-benzopyran (**13**).



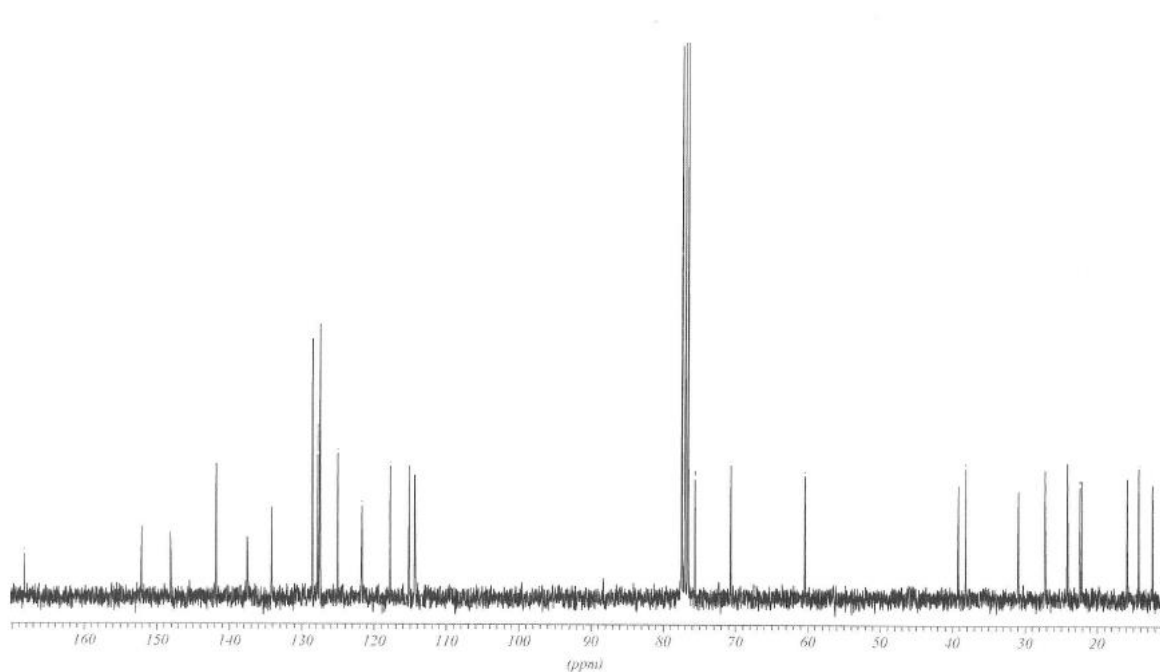
^{13}C NMR (75 MHz, CDCl_3) of 2-methyl-2-((4',8'-dimethyl)-N-phenylnona-3',7'-dienamide)-6-propoxydihydro-benzopyran (**13**).



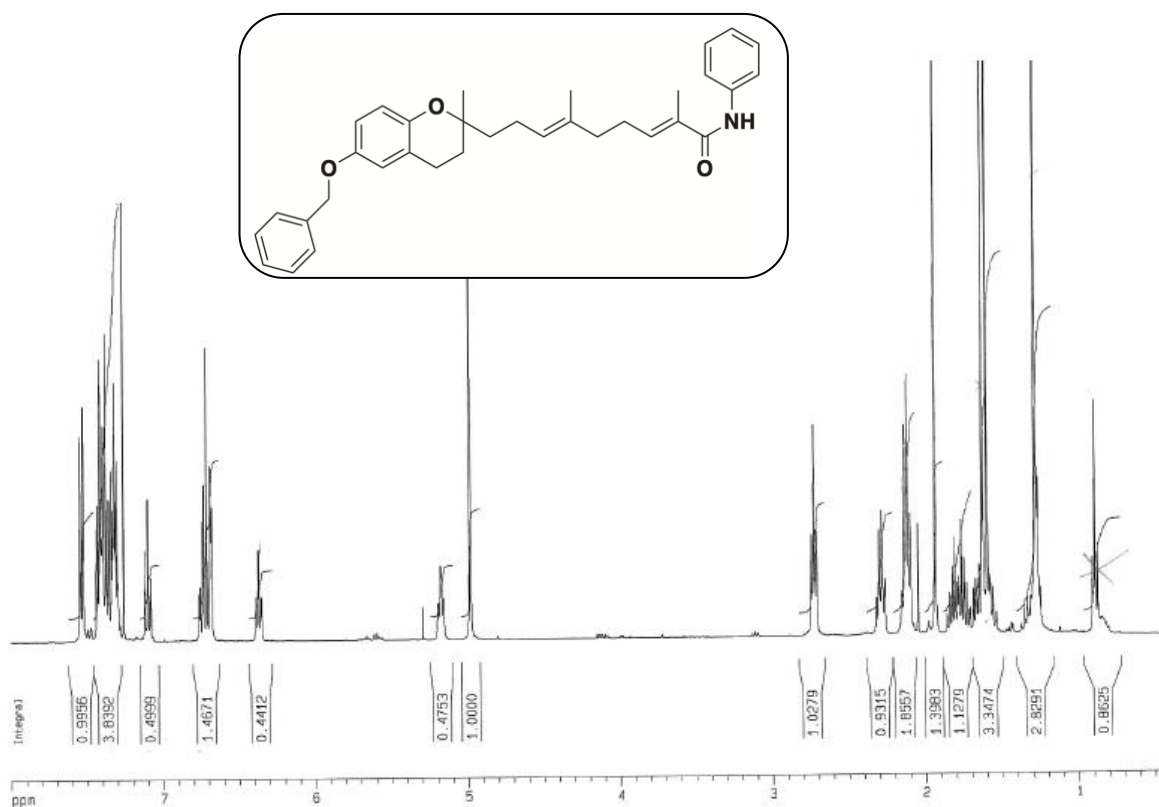
COSY (300 MHz, CDCl_3) of 2-methyl-2-((4',8'-dimethyl)-N-phenylnona-3',7'-dienamide)-6-propoxydihydro-benzopyran (**13**).



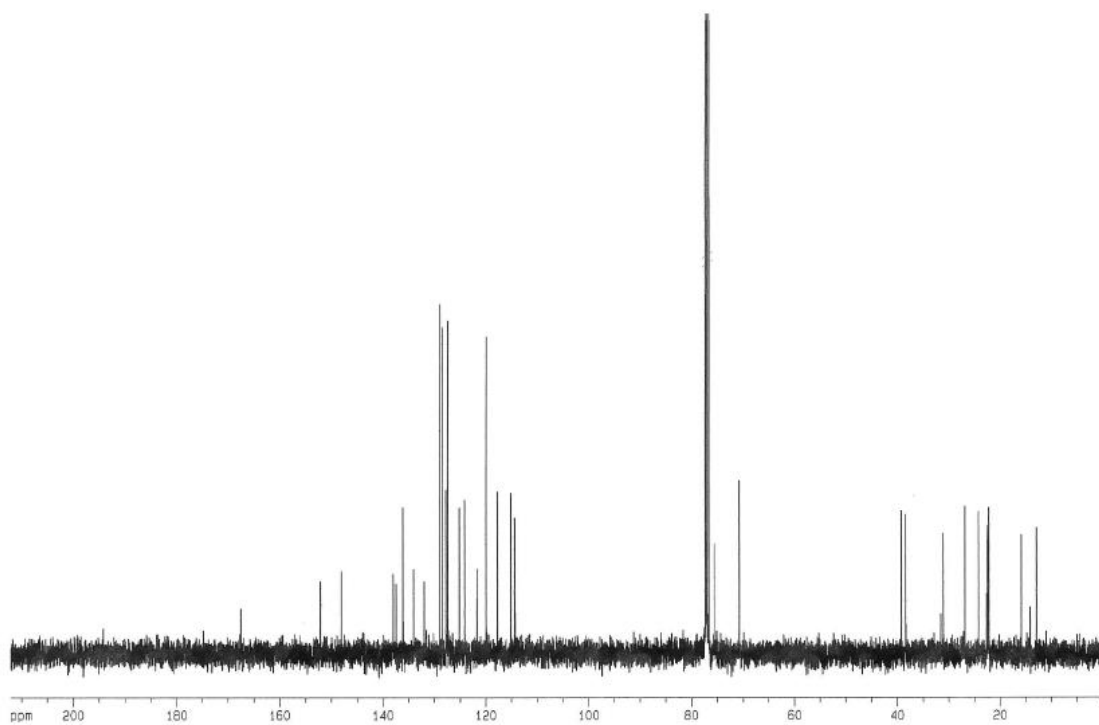
¹H NMR (300 MHz, CDCl₃) of 6-benzyloxy-2-((4',8'-dimethyl)ethylnona-3',7'-dienoate)-2-methyl-dihydro-benzopyran (**14**).



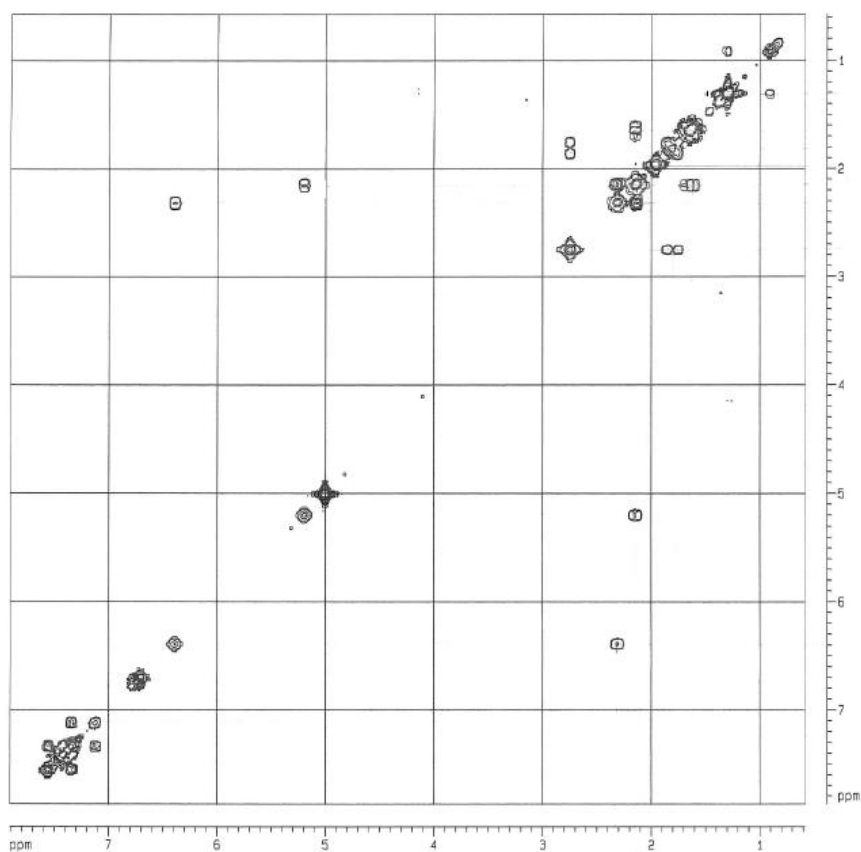
¹³C NMR (75 MHz, CDCl₃) of 6-benzyloxy-2-((4',8'-dimethyl)ethylnona-3',7'-dienoate)-2-methyl-dihydro-benzopyran (**14**).



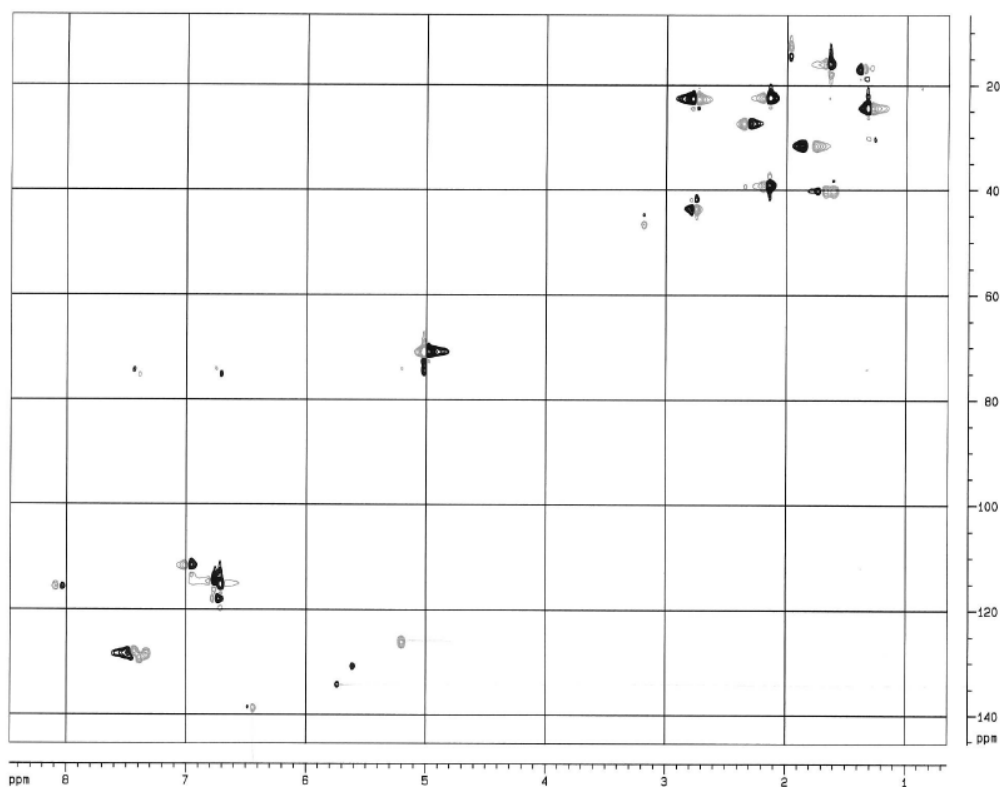
¹H NMR (300 MHz, CDCl₃) of 6-benzyloxy-2-methyl-2-((4',8'-dimethyl)-N-phenylnona-3',7'-dienamide)-dihydro-benzopyran (**15**).



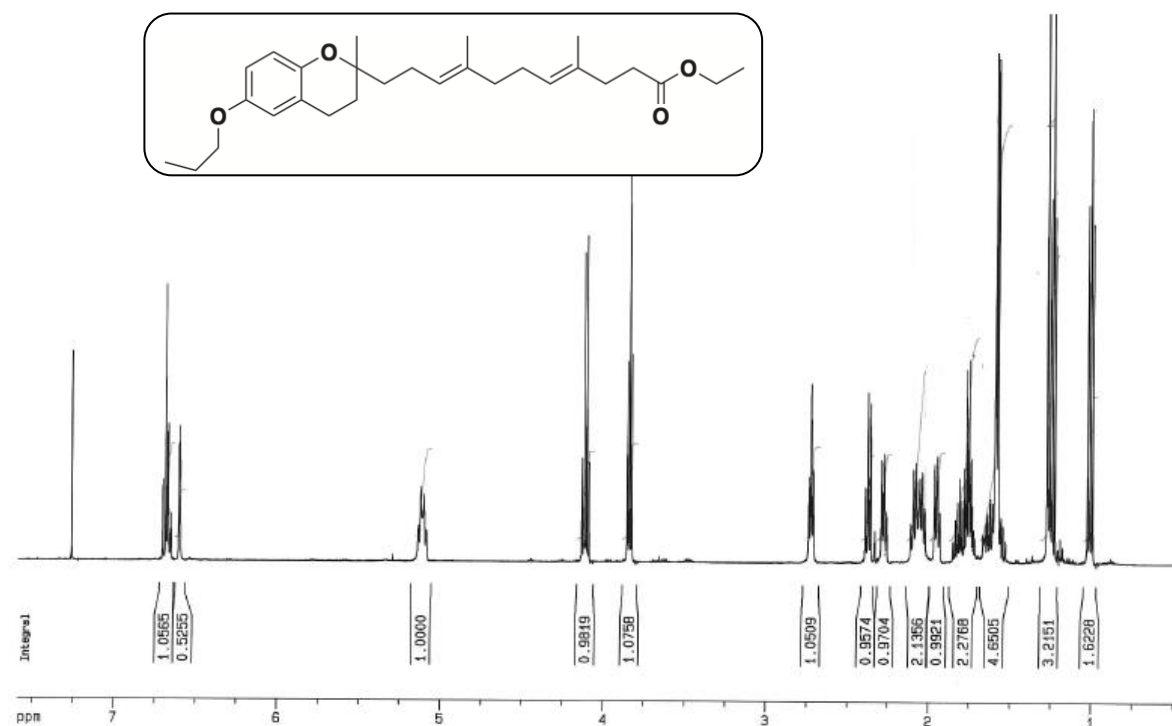
¹³C NMR (75 MHz, CDCl₃) of 6-benzyloxy-2-methyl-2-((4',8'-dimethyl)-N-phenylnona-3',7'-dienamide)-dihydro-benzopyran (**15**).



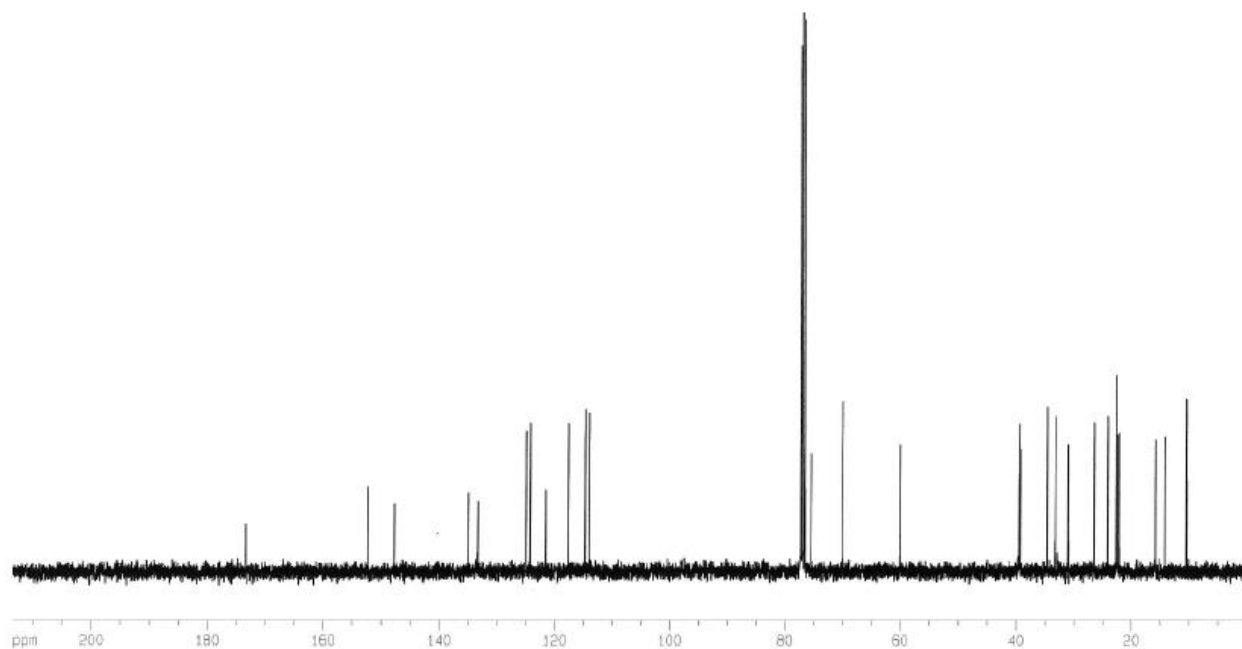
COSY (300 MHz, CDCl₃) of 6-benzyloxy-2-methyl-2-(((4',8'-dimethyl)-N-phenylnona-3',7'-dienamide)-dihydro-benzopyran (**15**).



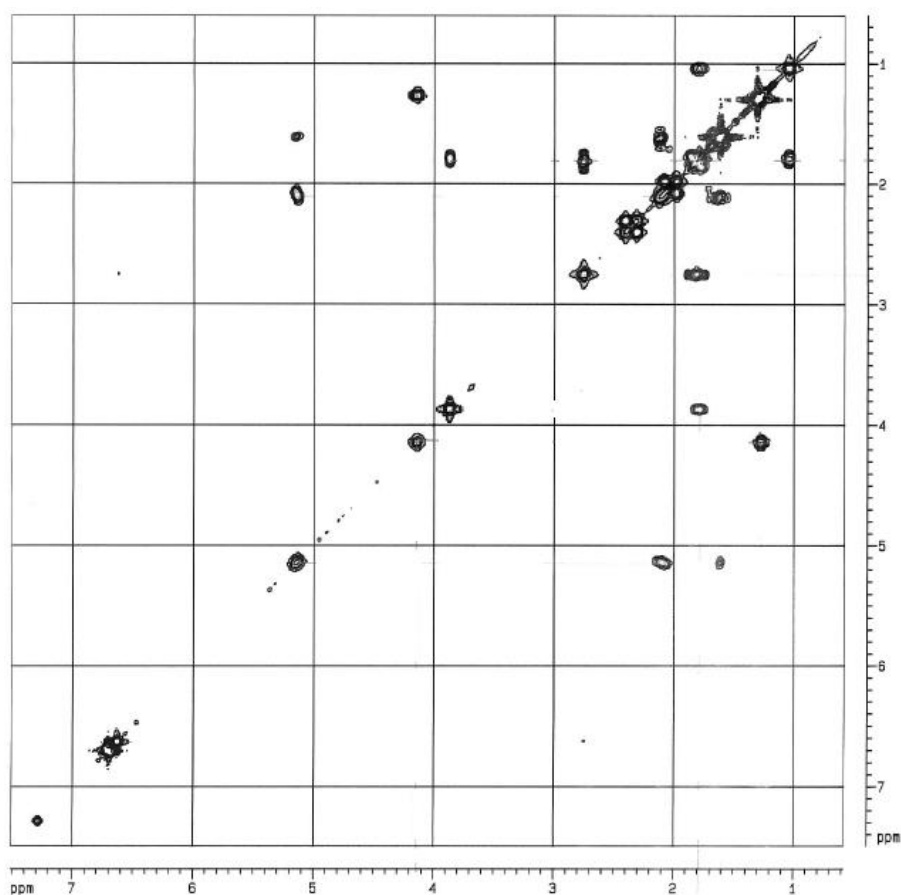
HSQC (300 MHz, CDCl₃) of 6-benzyloxy-2-methyl-2-(((4',8'-dimethyl)-N-phenylnona-3',7'-dienamide)-dihydro-benzopyran (**15**).



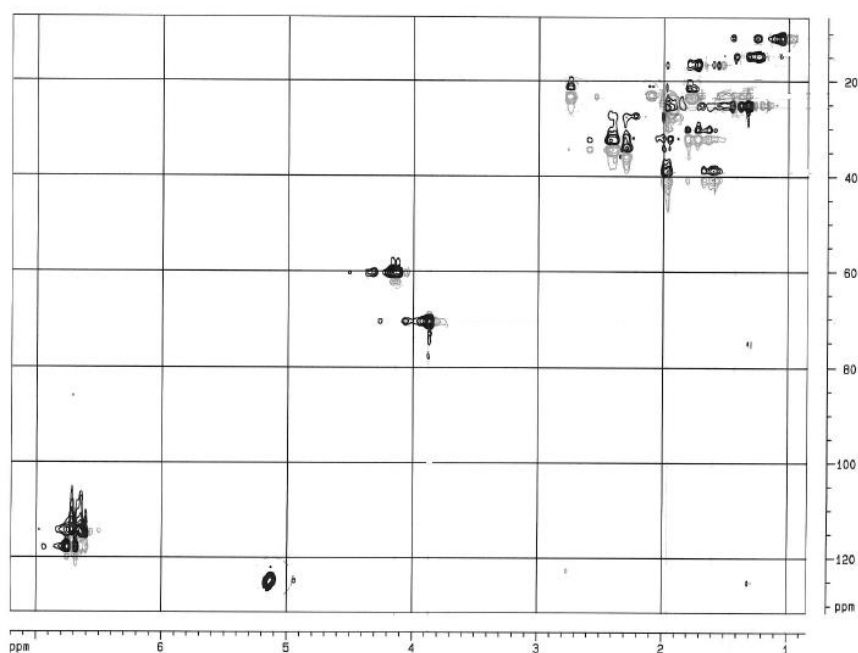
¹H NMR (300 MHz, CDCl₃) of 2-((4',8'-dimethyl)ethylundeca-3',7'-dienoate)-2-methyl-6-propoxydihydro-benzopyran (**17**).



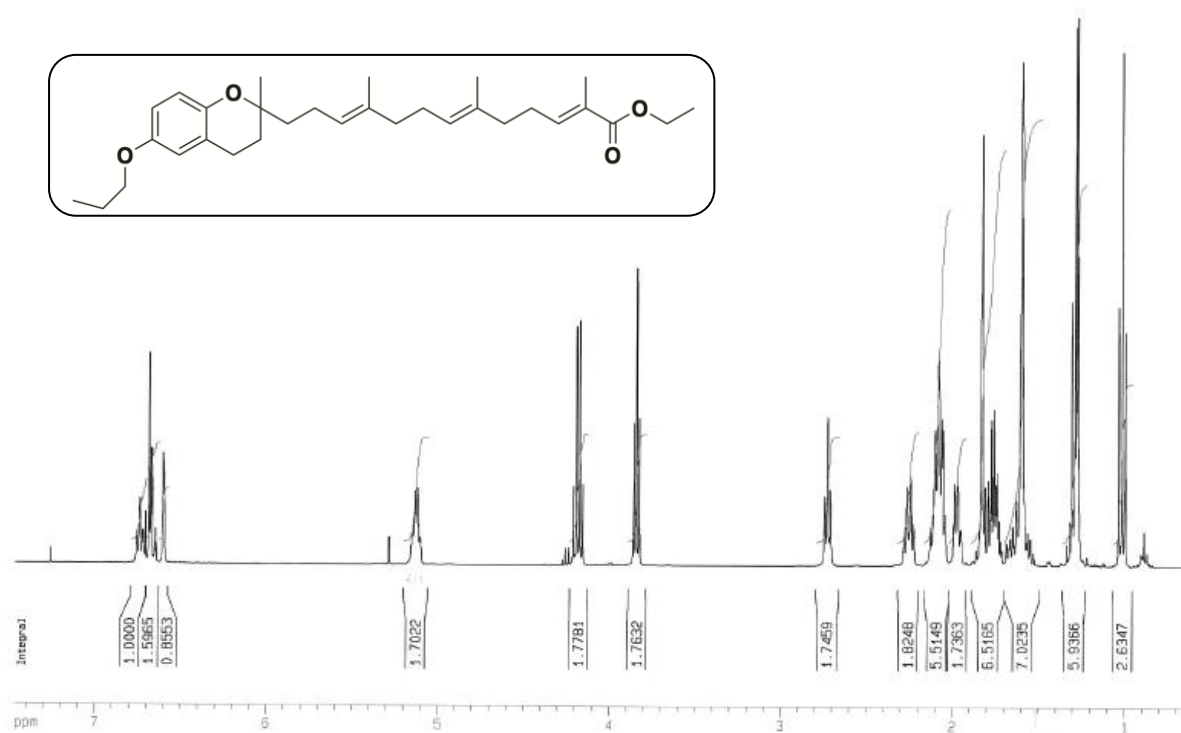
¹³C NMR (75 MHz, CDCl₃) of 2-((4',8'-dimethyl)ethylundeca-3',7'-dienoate)-2-methyl-6-propoxydihydro-benzopyran (**17**).



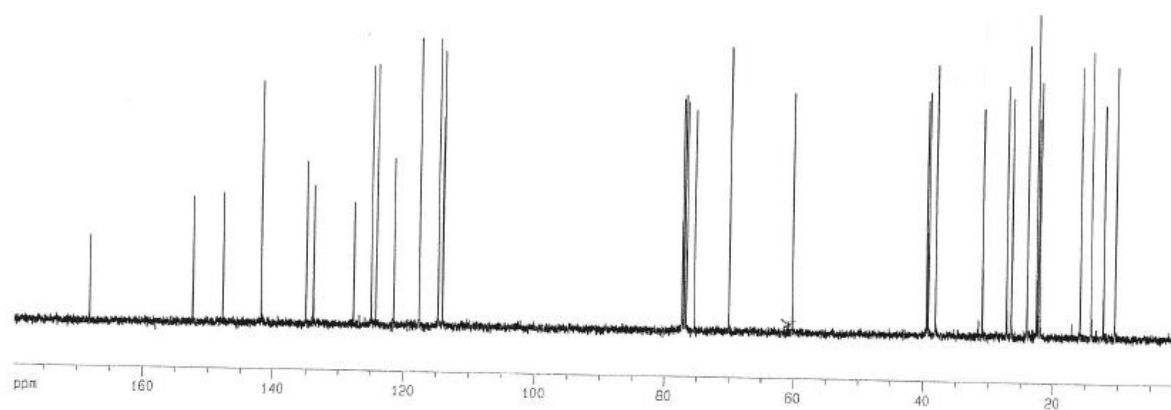
COSY (300 MHz, CDCl₃) of 2-((4',8'-dimethyl)ethylundeca-3',7'-dienoate)-2-methyl-6-propoxydihydro-benzopyran (**17**).



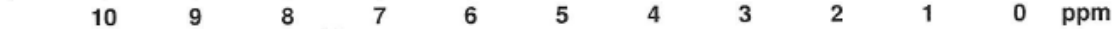
HSQC (300 MHz, CDCl₃) of 2-((4',8'-dimethyl)ethylundeca-3',7'-dienoate)-2-methyl-6-propoxydihydro-benzopyran (**17**).



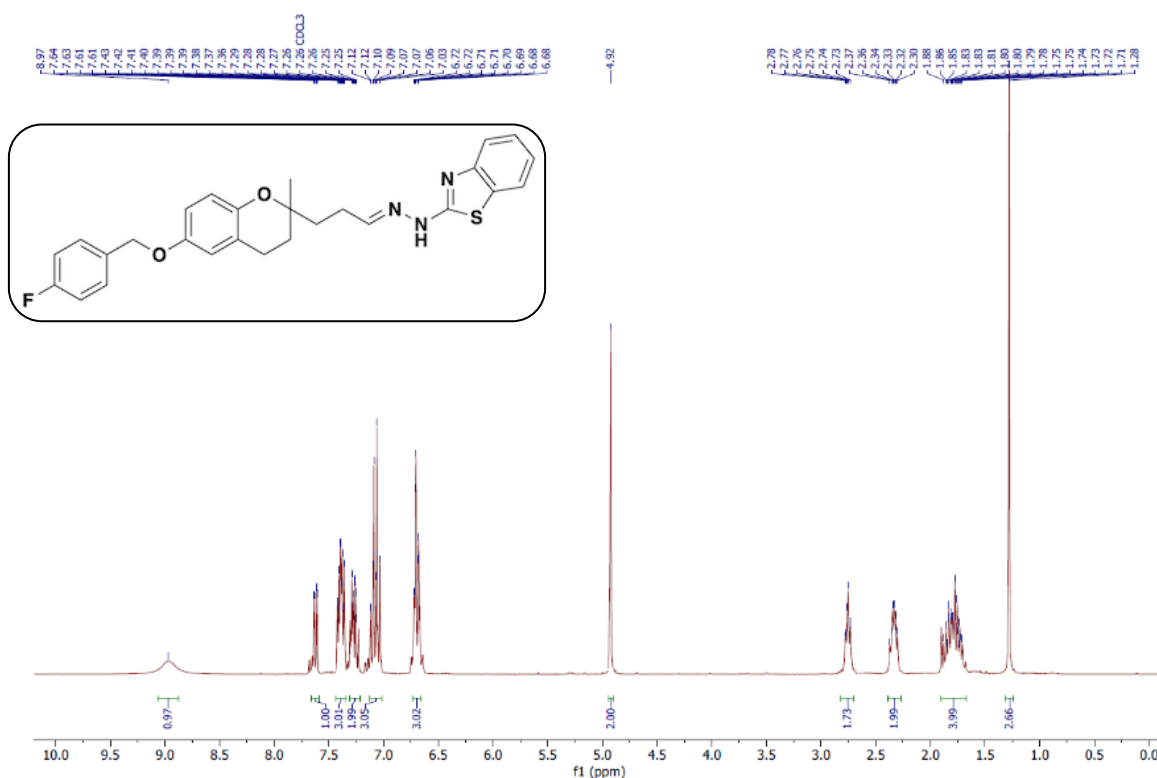
¹H NMR (400 MHz, CDCl₃) of 2-Methyl-6-propoxy-2-((4',8',12'-trimethyl)ethyltrideca-3',7',11'-trienoate)-dihydro-benzopyran (**20**).



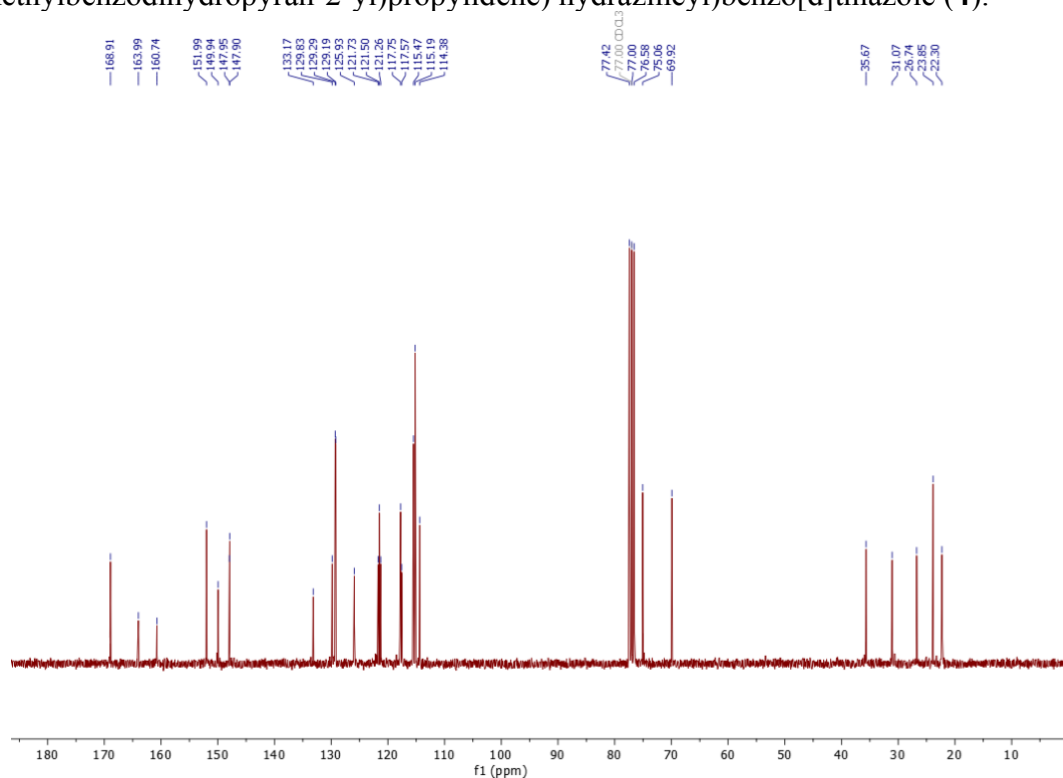
¹³C NMR (100 MHz, CDCl₃) of 2-Methyl-6-propoxy-2-((4',8',12'-trimethyl)ethyltrideca-3',7',11'-trienoate)-dihydro-benzopyran (**20**).



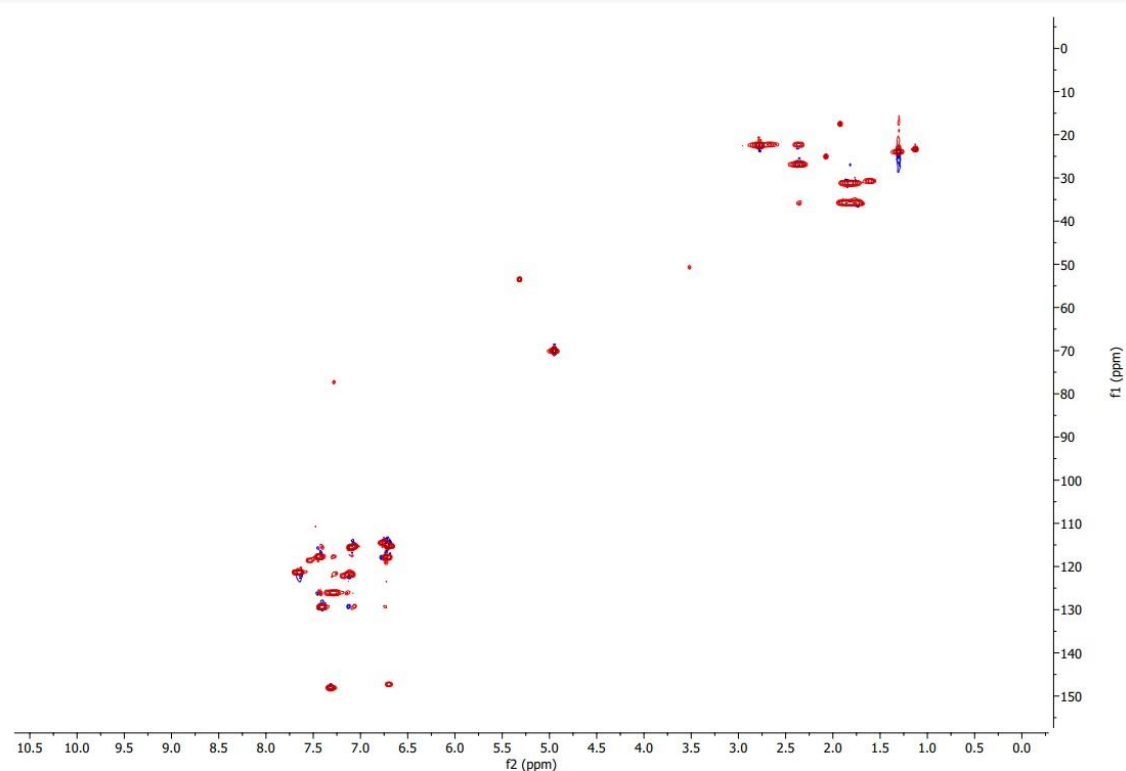
Article 3: Benzopyran hydrazones with dual PPAR α / γ or PPAR α / δ agonism and an anti-inflammatory effect on human THP-1 macrophages, *European Journal of Medicinal Chemistry*, in press.



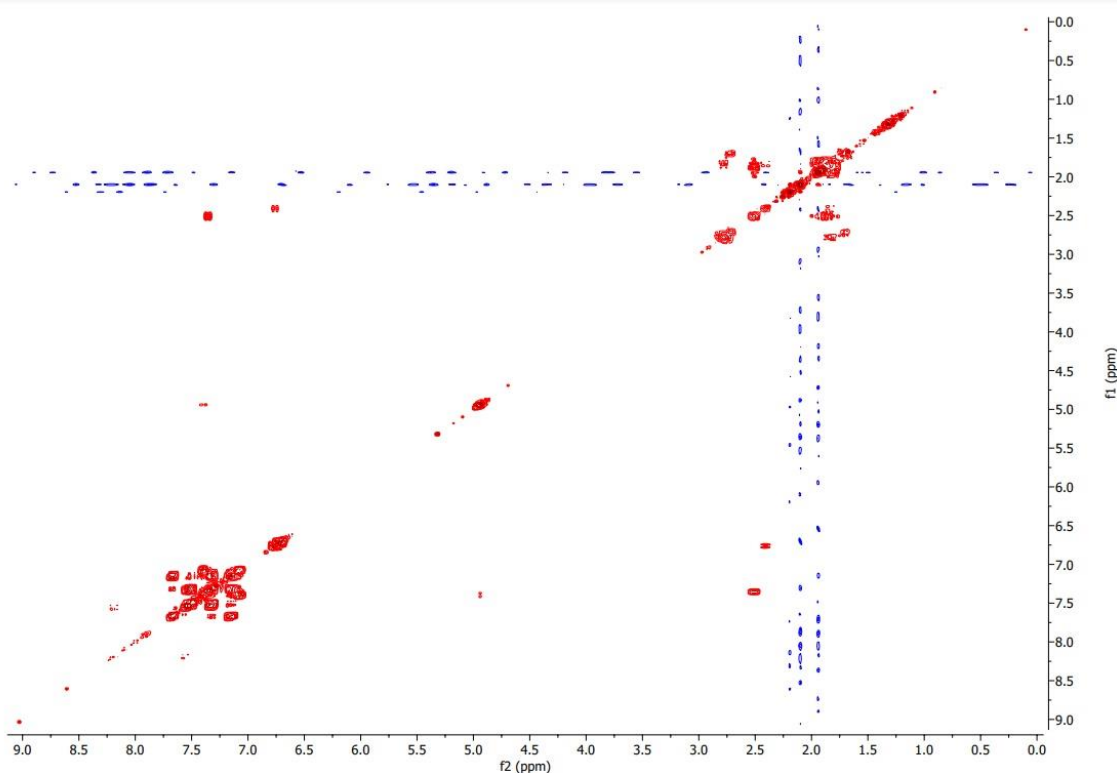
¹H NMR (300 MHz, CDCl₃) of 2-(2-(3-(6-((p-Fluorobenzyl)oxy)-2-methylbenzodihydropyran-2-yl)propylidene) hydrazineyl)benzo[d]thiazole (4).



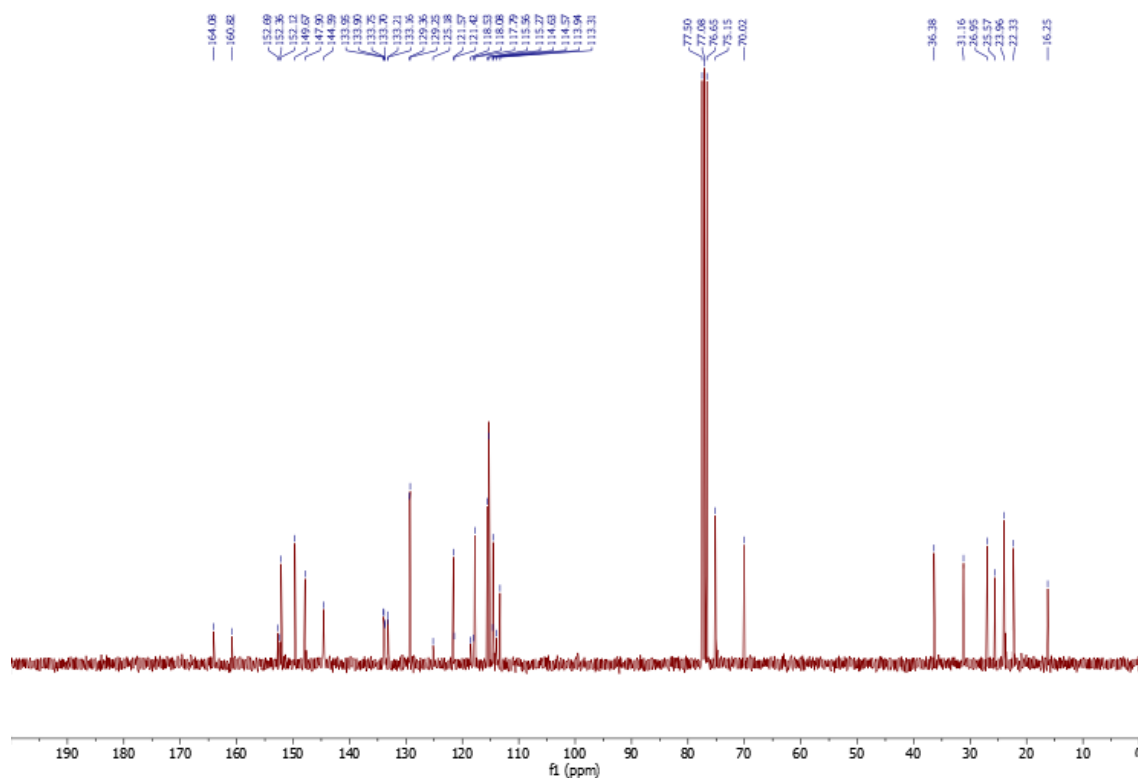
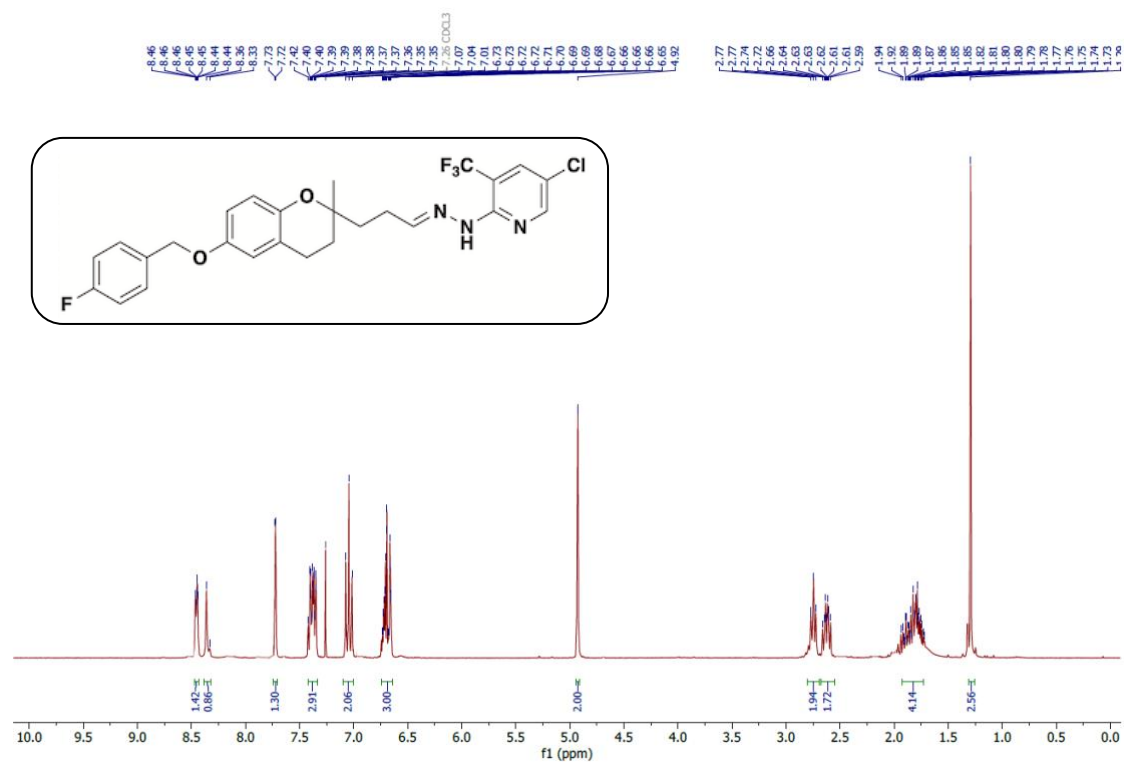
¹³C NMR (75 MHz, CDCl₃) of 2-(2-(3-(6-((p-Fluorobenzyl)oxy)-2-methylbenzodihydropyran-2-yl)propylidene) hydrazineyl)benzo[d]thiazole (4).

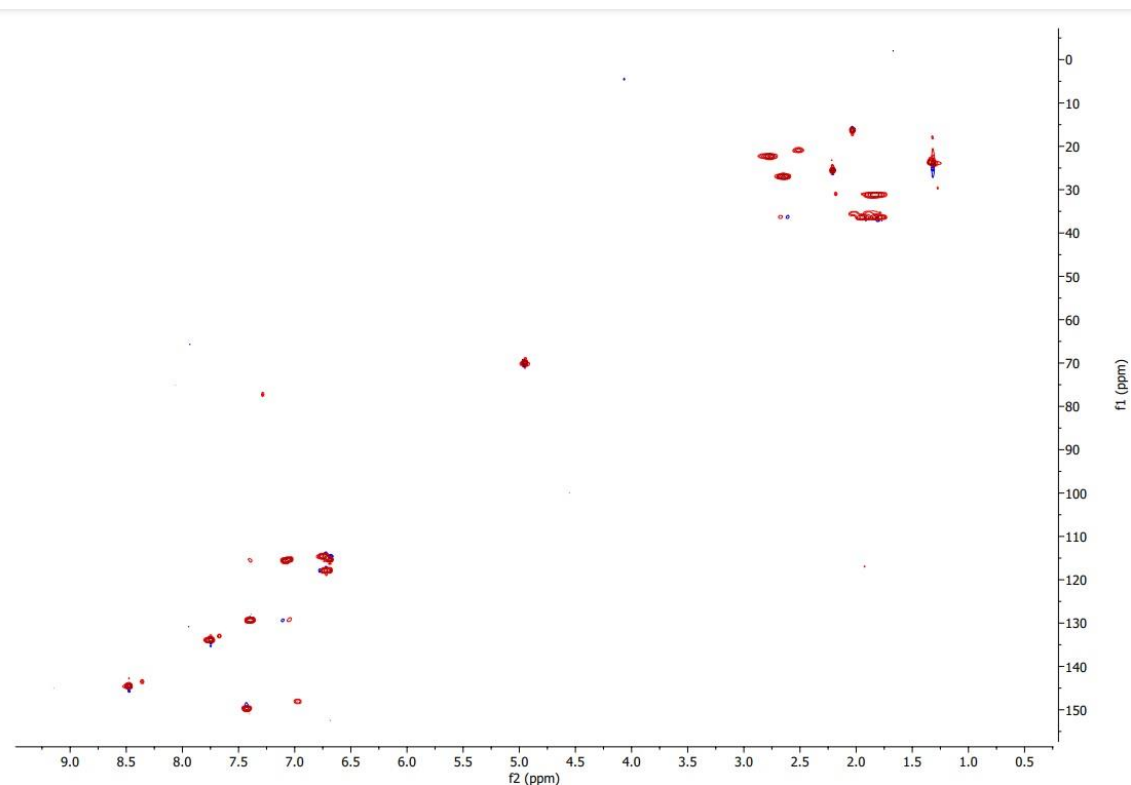


HSQC (300 MHz, CDCl₃) of 2-(2-(3-(6-((*p*-Fluorobenzyl)oxy)-2-methylbenzodihydropyran-2-yl)propylidene) hydrazineyl)benzo[d]thiazole (**4**).

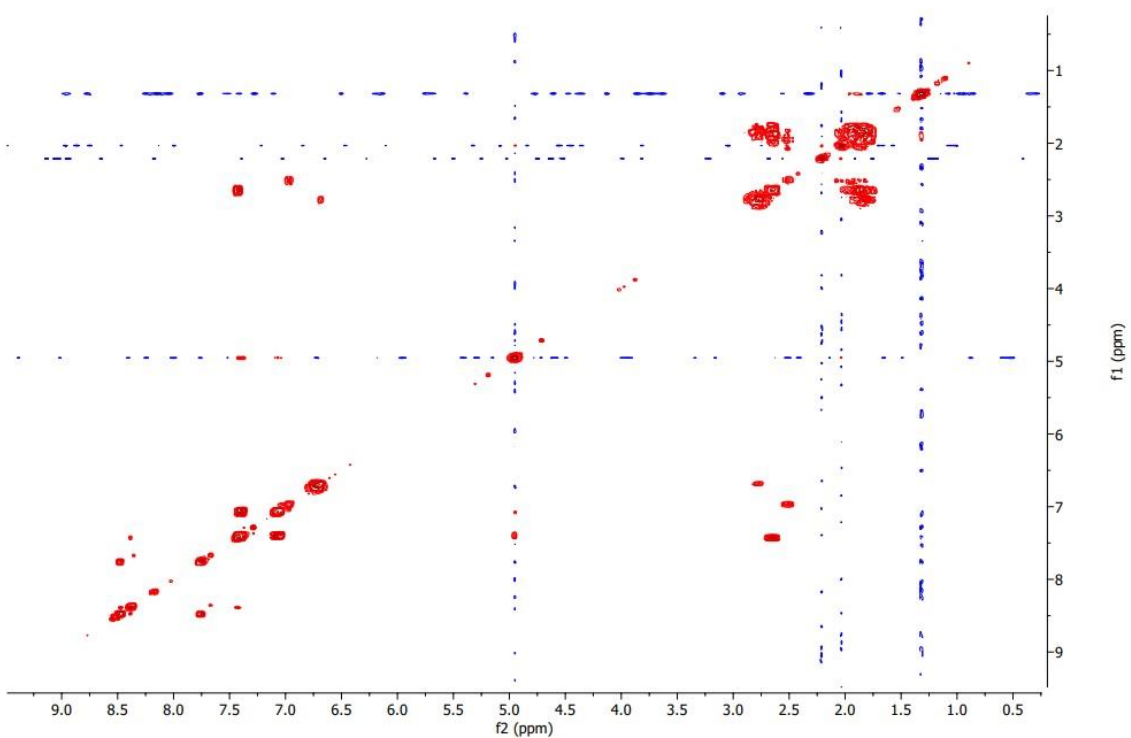


COSY (300 MHz, CDCl₃) of 2-(2-(3-(6-((*p*-Fluorobenzyl)oxy)-2-methylbenzodihydropyran-2-yl)propylidene) hydrazineyl)benzo[d]thiazole (**4**).

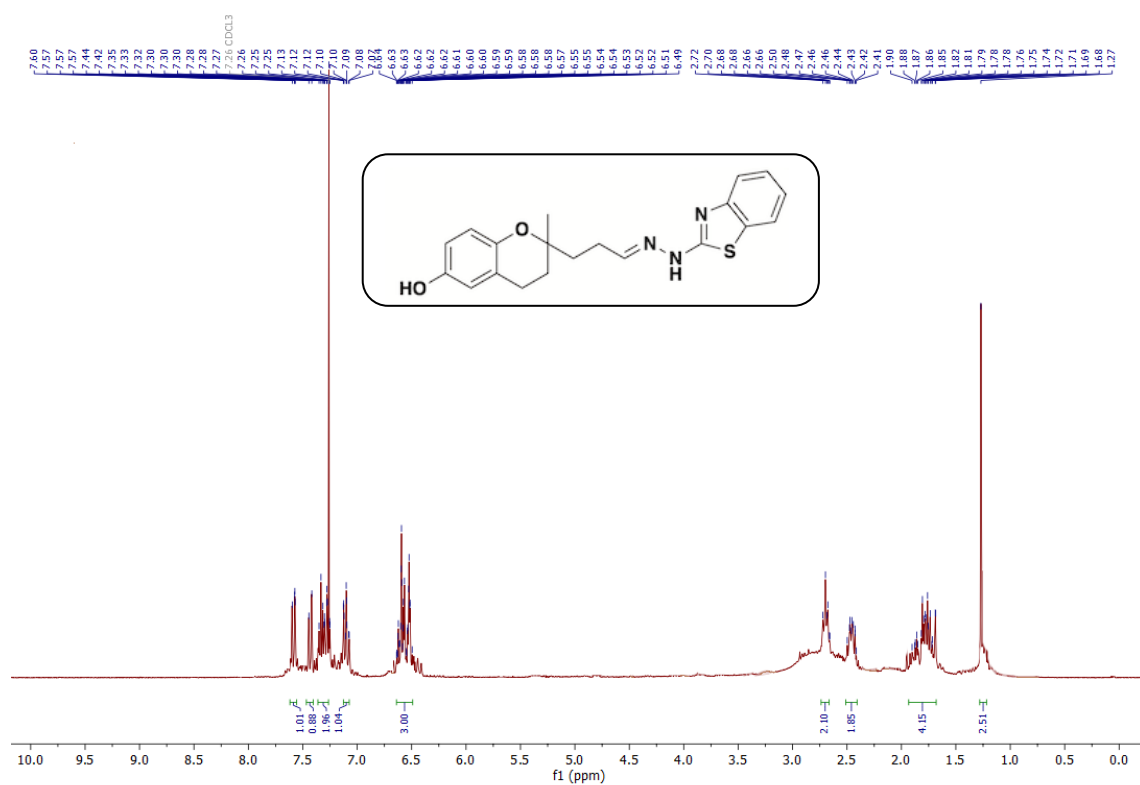




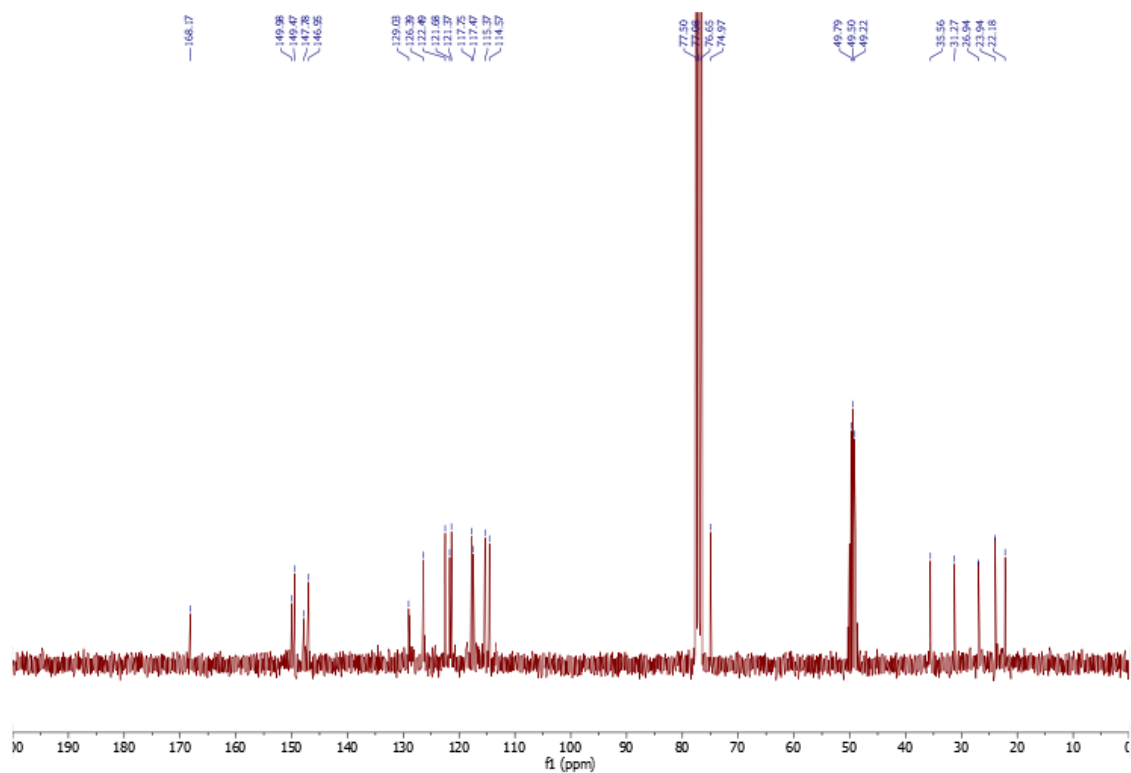
HSQC (300 MHz, CDCl₃) of 5-Chloro-2-(2-(3-(6-((p-fluorobenzyl)oxy)-2-methyl benzodihydropyran-2-yl)propylidene)hydrazineyl)-3-(trifluoromethyl)pyridine (**5**).



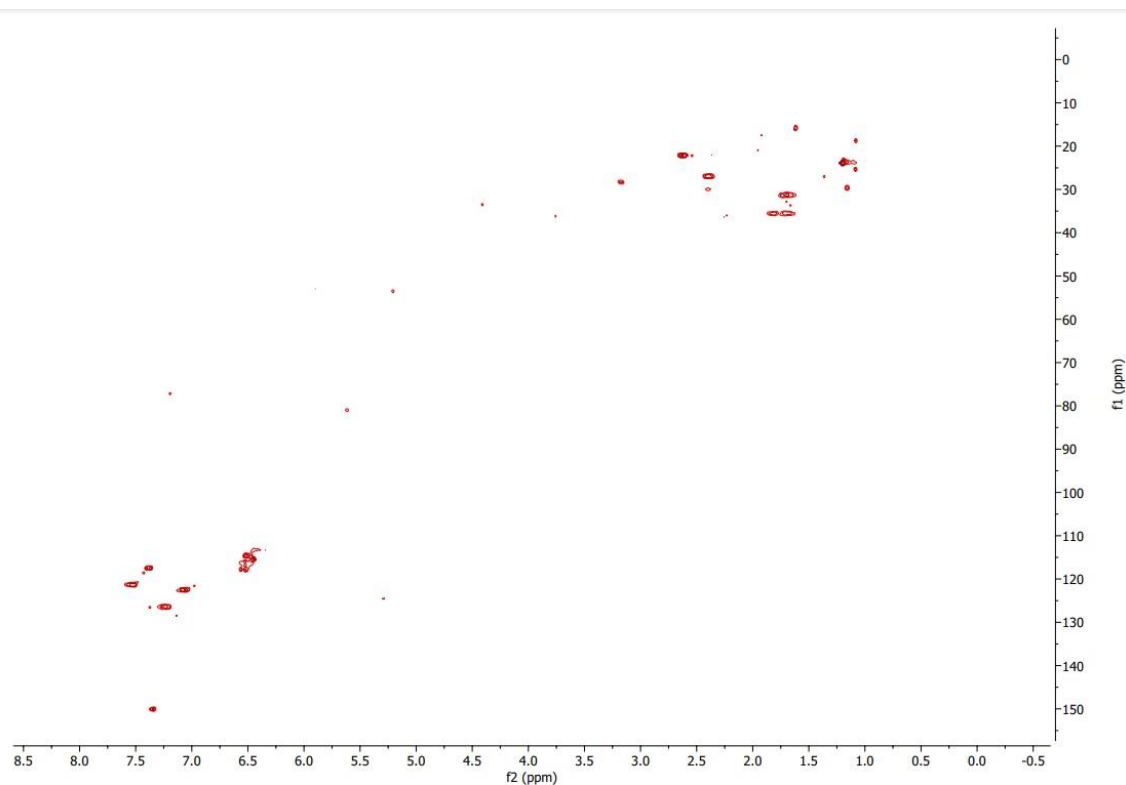
COSY (300 MHz, CDCl₃) of 5-Chloro-2-(2-(3-(6-((p-fluorobenzyl)oxy)-2-methyl benzodihydropyran-2-yl)propylidene)hydrazineyl)-3-(trifluoromethyl)pyridine (**5**).



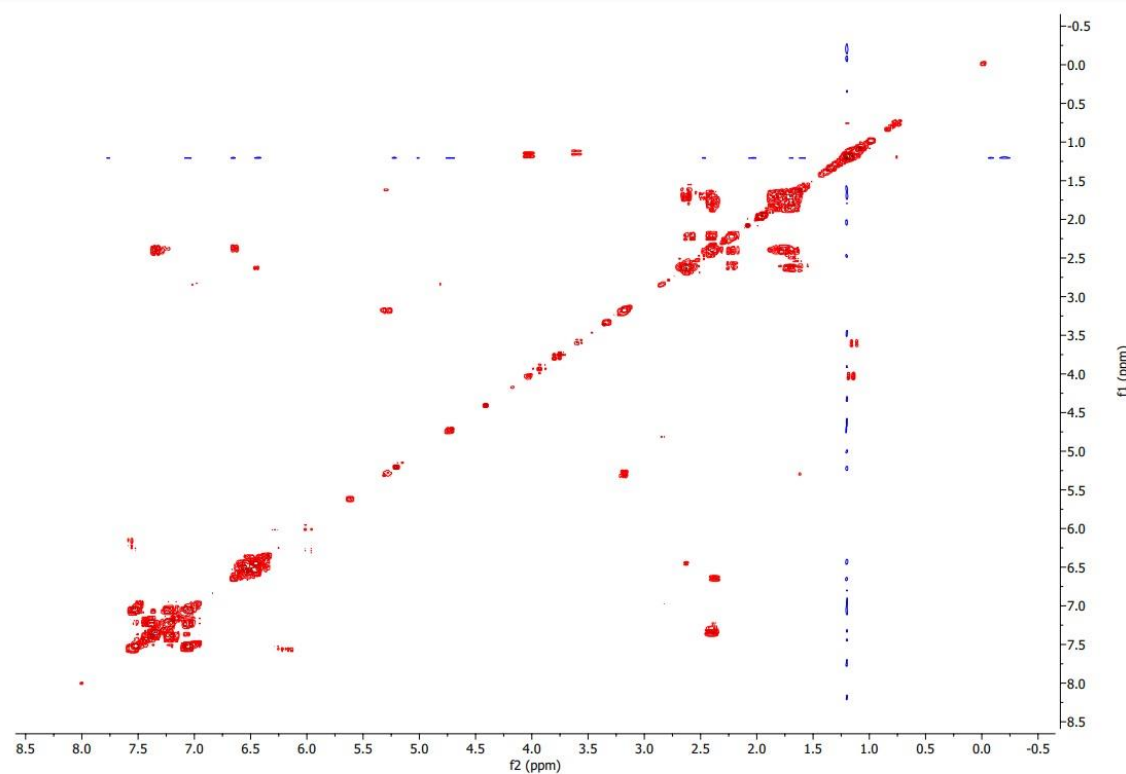
¹H NMR (300 MHz, CDCl₃ + 1 drop CD₃OD) of 2-(3-(2-(Benzo[d]thiazol-2-yl)hydrazineylidene)propyl)-2-methylbenzodihydropyran-6-ol (**6**).



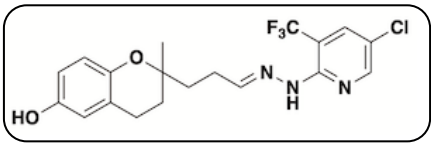
¹³C NMR (75 MHz, CDCl₃ + 1 drop CD₃OD) of 2-(3-(2-(Benzo[d]thiazol-2-yl)hydrazineylidene)propyl)-2-methylbenzodihydropyran-6-ol (**6**).

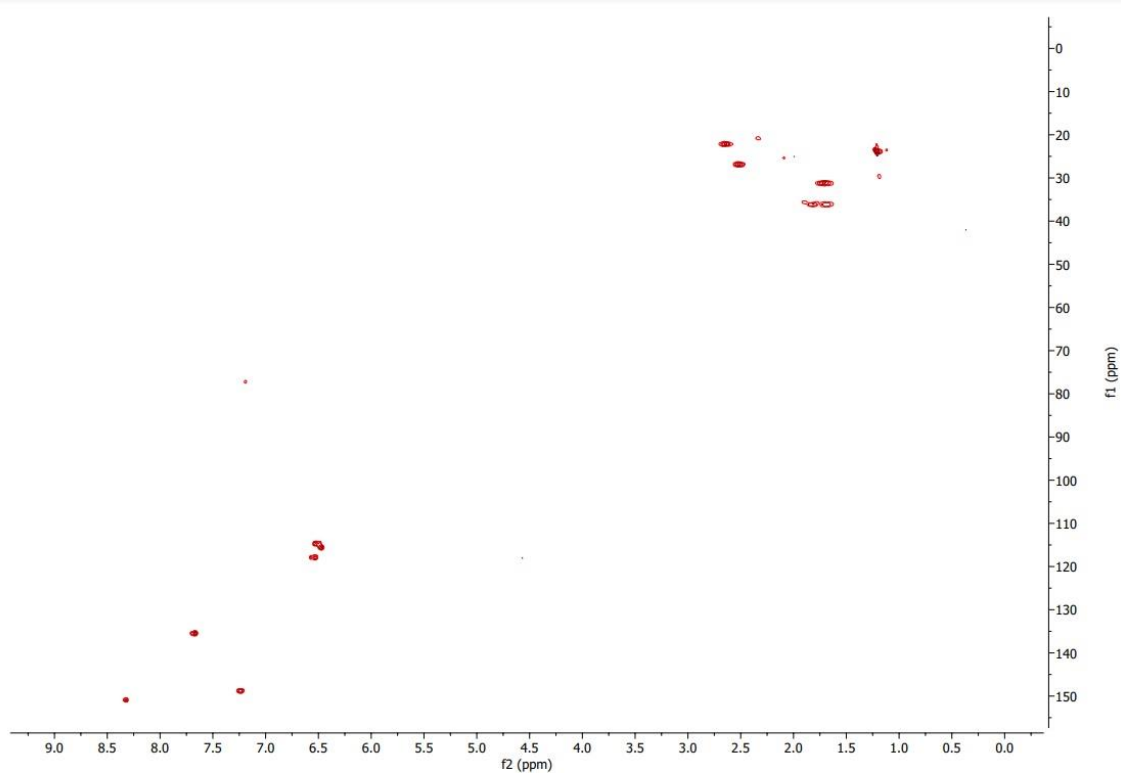


HSQC (300 MHz, CDCl₃) of 2-(3-(2-(Benzo[d]thiazol-2-yl)hydrazineylidene)propyl)-2-methylbenzodihydropyran-6-ol (**6**).

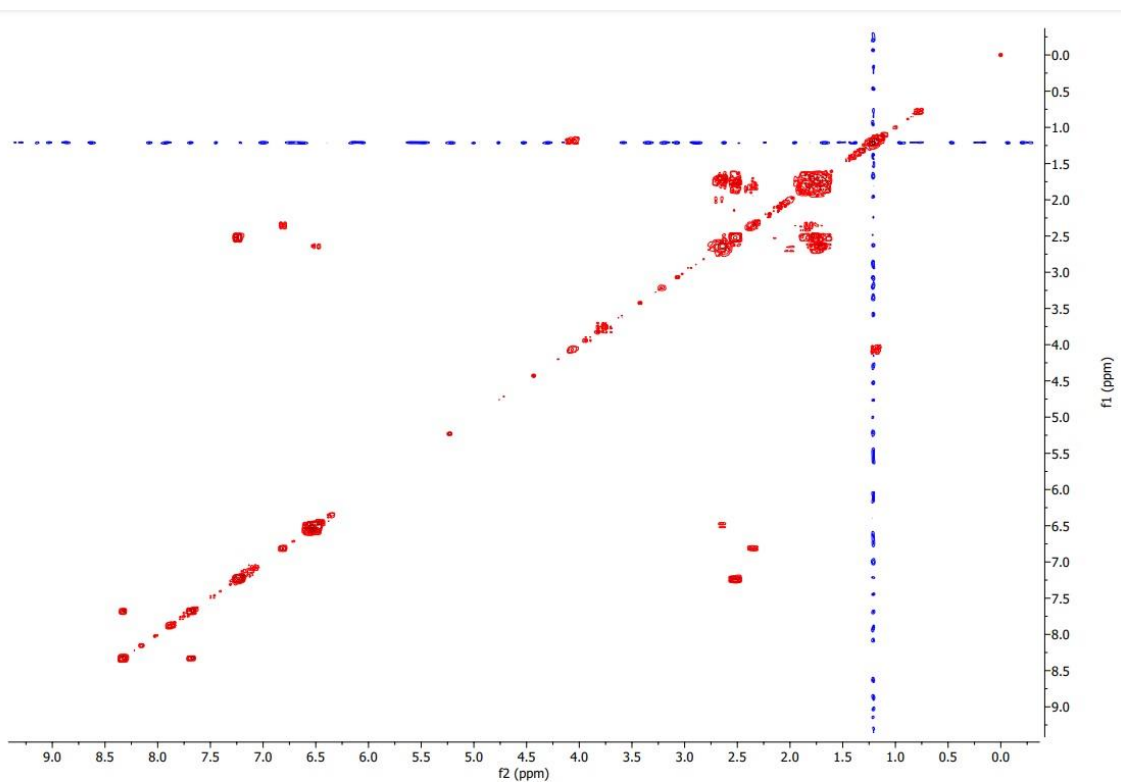


COSY (300 MHz, CDCl₃) of 2-(3-(2-(Benzo[d]thiazol-2-yl)hydrazineylidene)propyl)-2-methylbenzodihydropyran-6-ol (**6**).

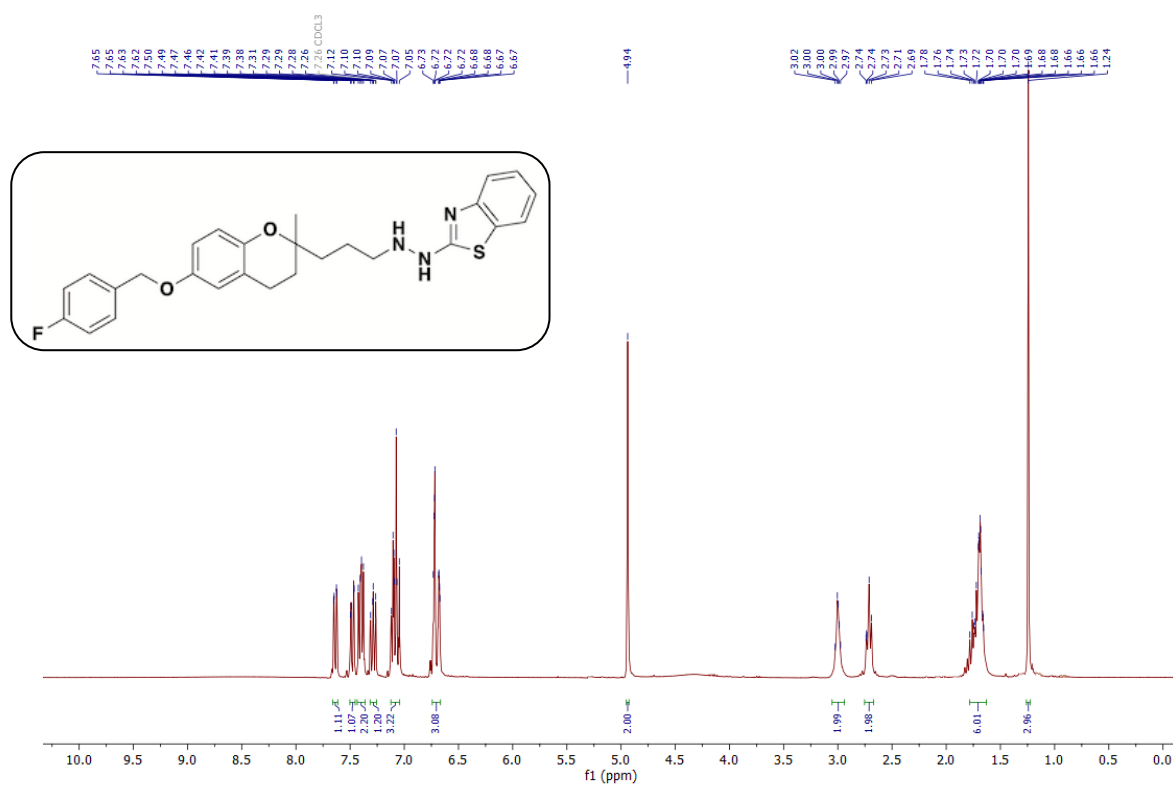




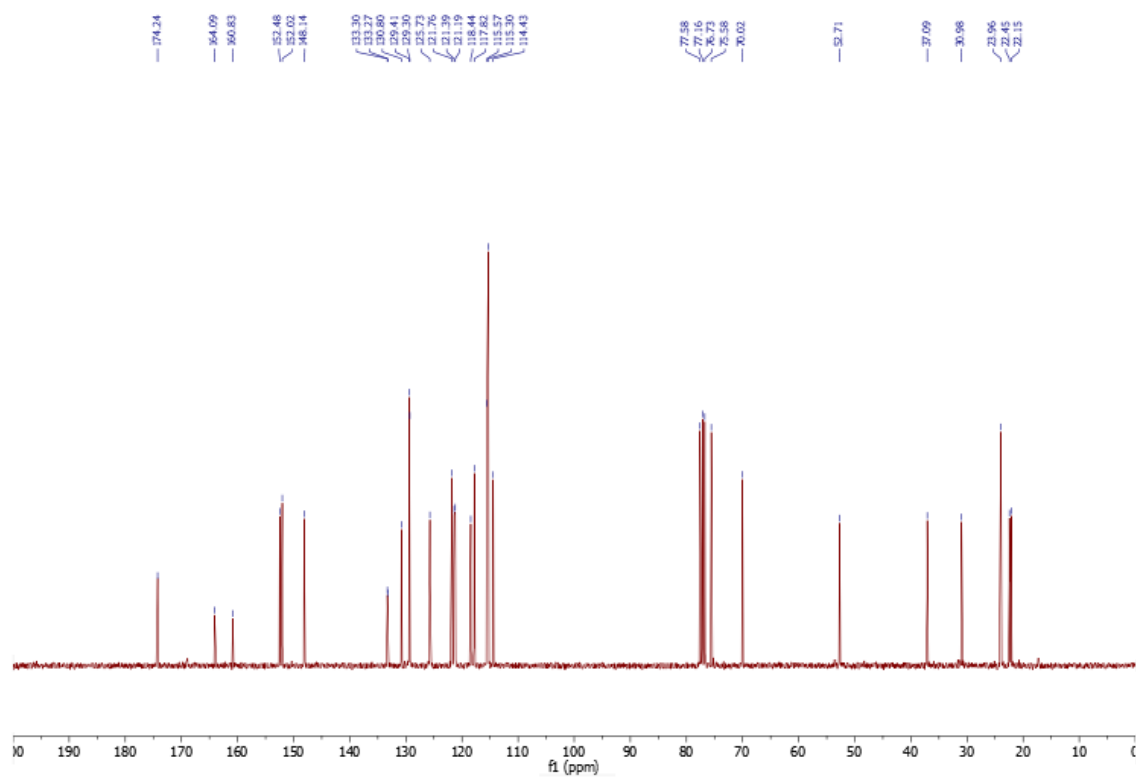
HSQC (300 MHz, CDCl₃) of 2-(3-(2-(5-Chloro-3-(trifluoromethyl)pyridin-2-yl)hydrazineylidene)propyl)-2-methylbenzodihydropyran-6-ol (**7**).



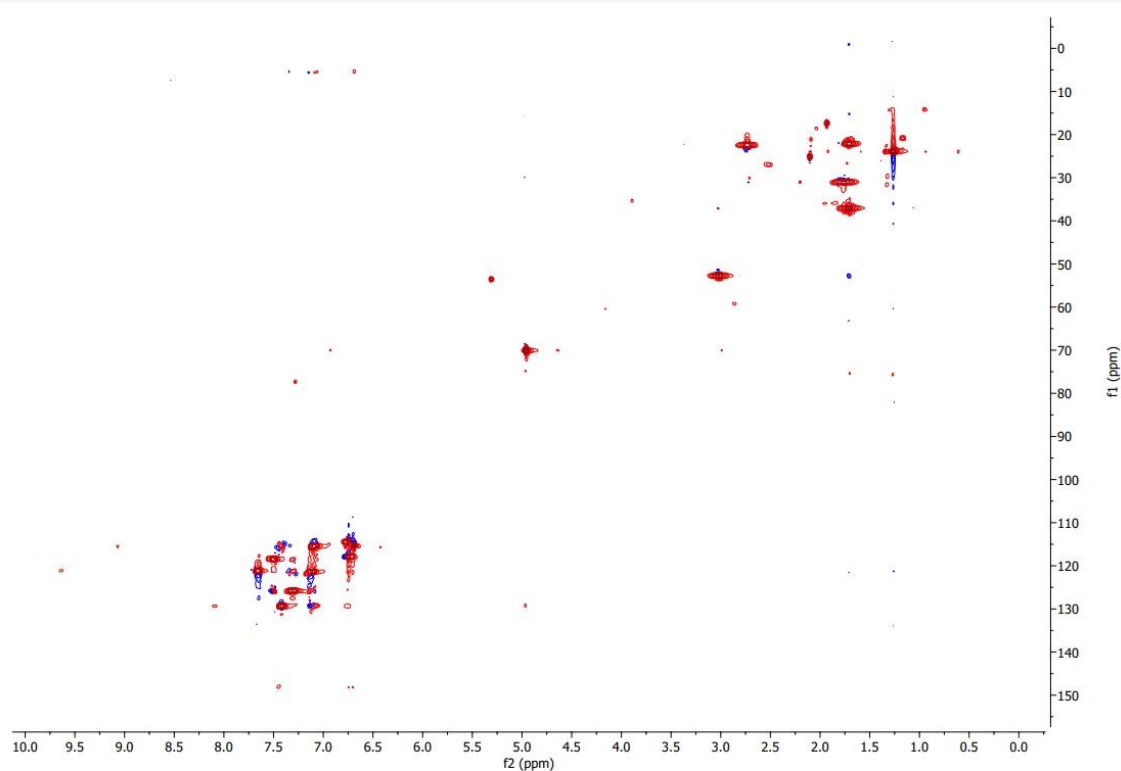
COSY (300 MHz, CDCl₃) of 2-(3-(2-(5-Chloro-3-(trifluoromethyl)pyridin-2-yl)hydrazineylidene)propyl)-2-methylbenzodihydropyran-6-ol (**7**).



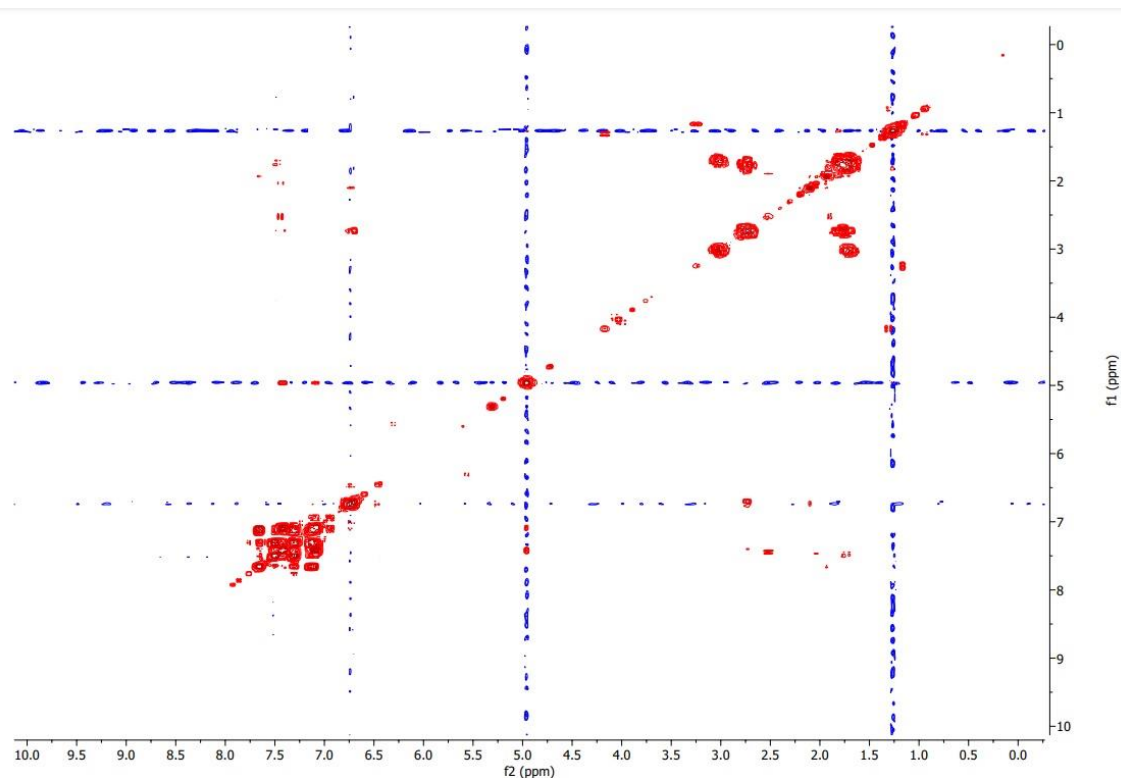
¹H NMR (300 MHz, CDCl₃) of 2-(2-(3-(6-((*p*-Fluorobenzyl)oxy)-2-methylbenzodihydro pyran-2-yl)propyl)hydrazineyl)benzo[d]thiazole (**8**).



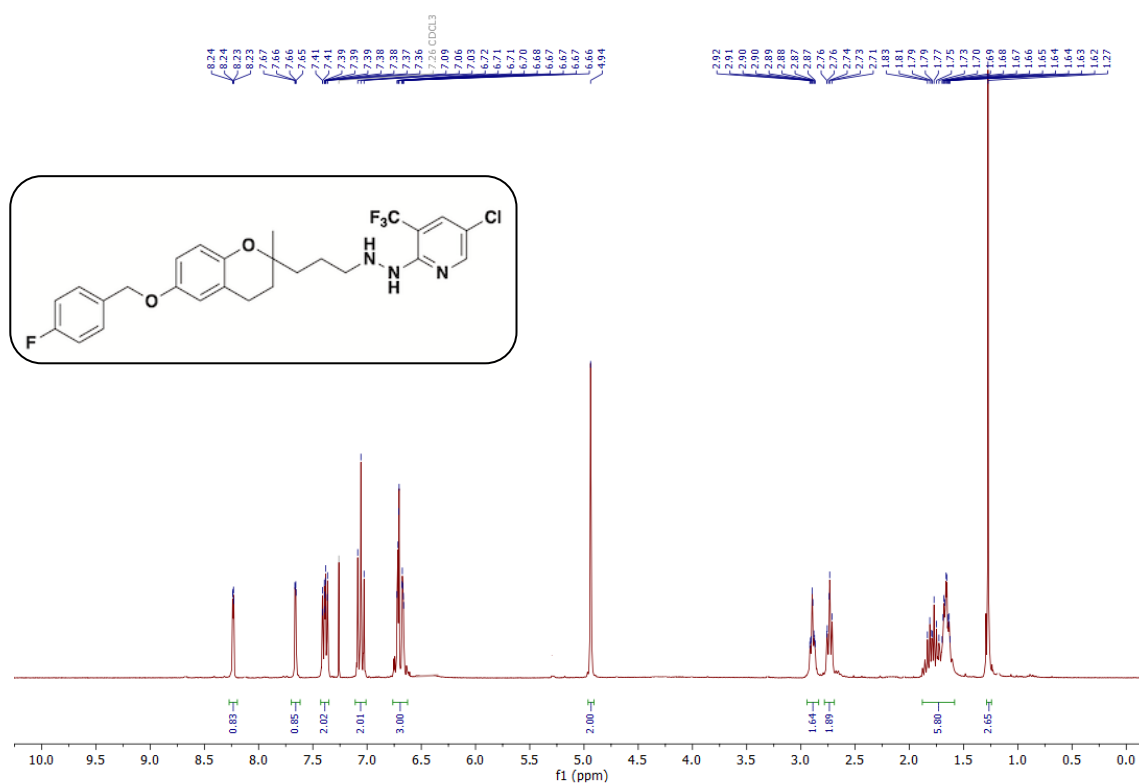
¹³C NMR (75 MHz, CDCl₃) of 2-(2-(3-(6-((*p*-Fluorobenzyl)oxy)-2-methylbenzodihydro pyran-2-yl)propyl)hydrazineyl)benzo[d]thiazole (**8**).



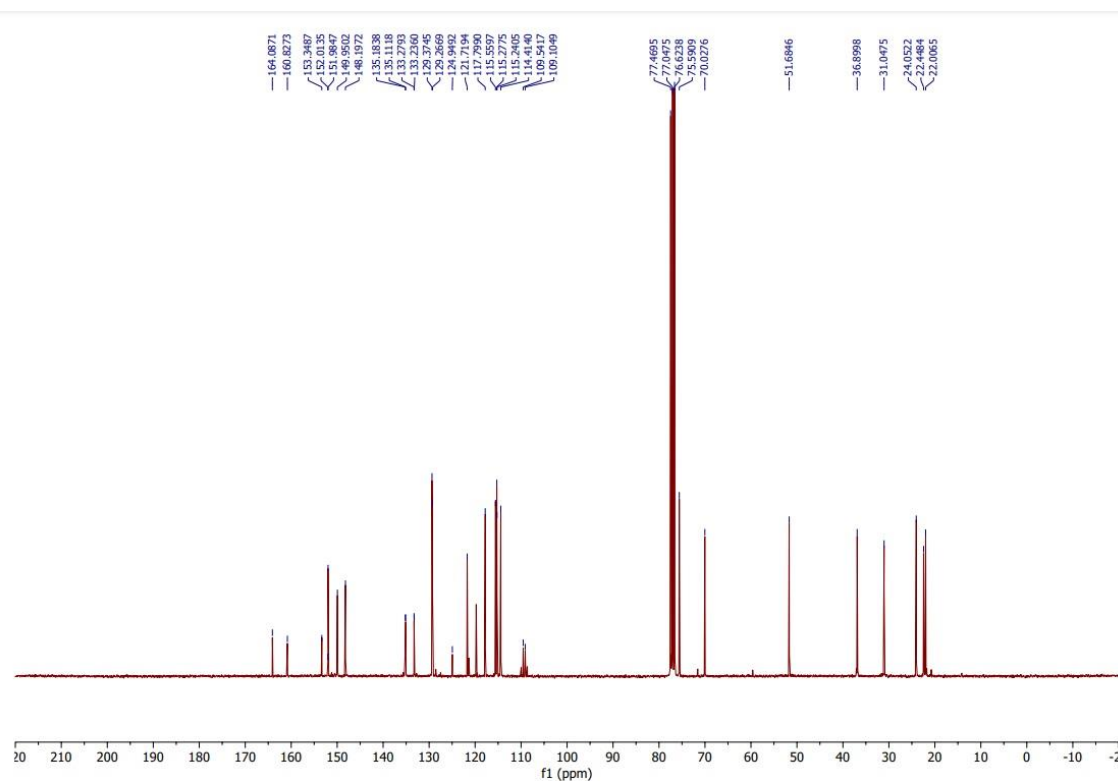
HSQC (300 MHz, CDCl₃) of 2-(2-(3-(6-((*p*-Fluorobenzyl)oxy)-2-methylbenzodihydro pyran-2-yl)propyl)hydrazineyl)benzo[d]thiazole (**8**).



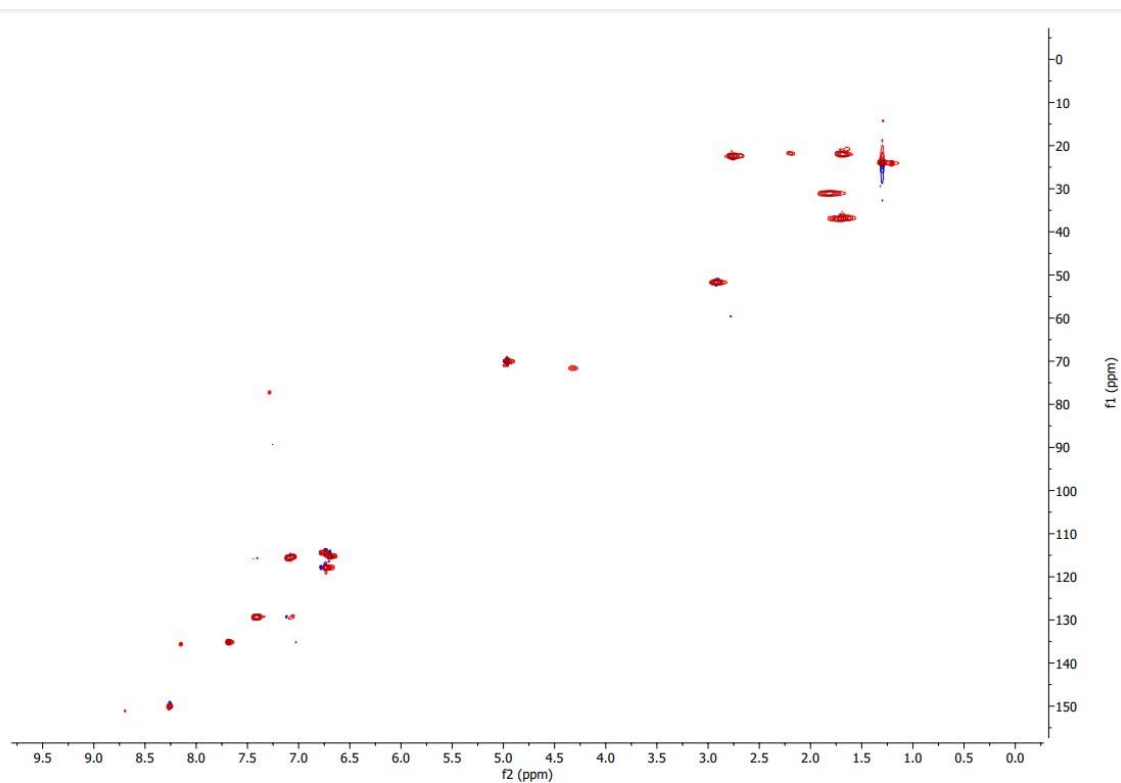
COSY (300 MHz, CDCl₃) of 2-(2-(3-(6-((*p*-Fluorobenzyl)oxy)-2-methylbenzodihydro pyran-2-yl)propyl)hydrazineyl)benzo[d]thiazole (**8**).



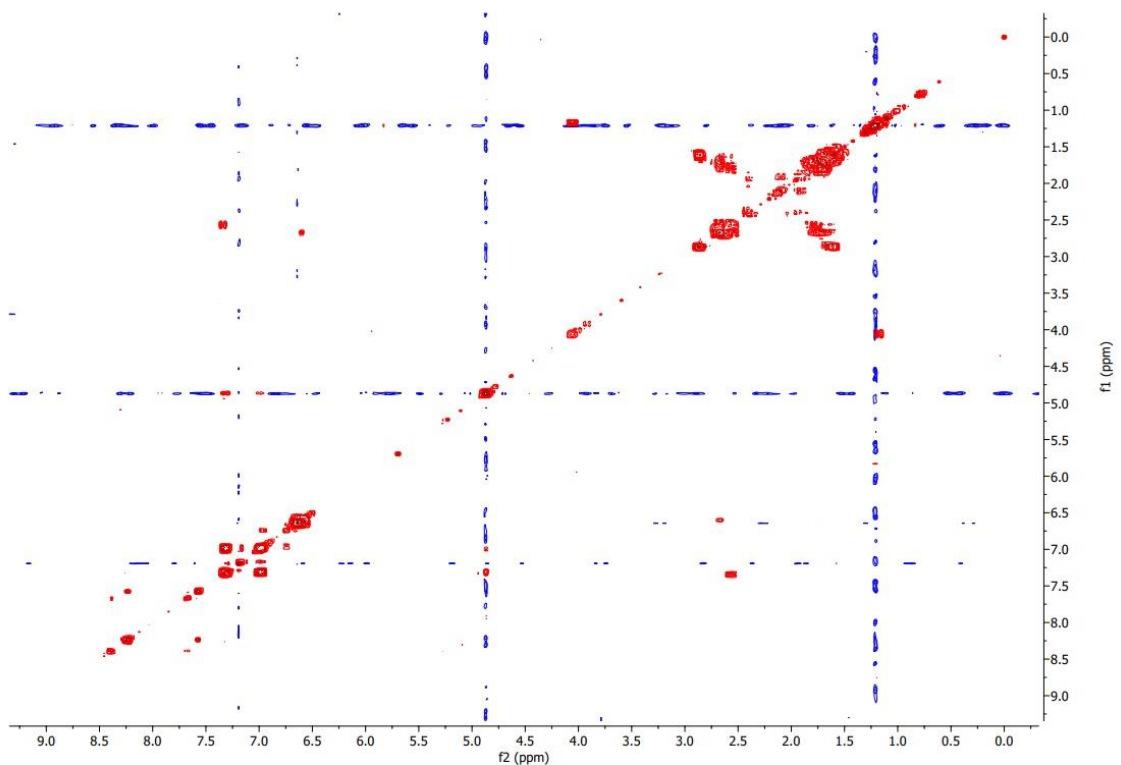
¹H NMR (300 MHz, CDCl₃) of 5-Chloro-2-(2-(3-(6-((p-fluorobenzyl)oxy)-2-methylbenzodihydropyran-2-yl)propyl)hydrazineyl)-3-(trifluoromethyl)pyridine (**9**).



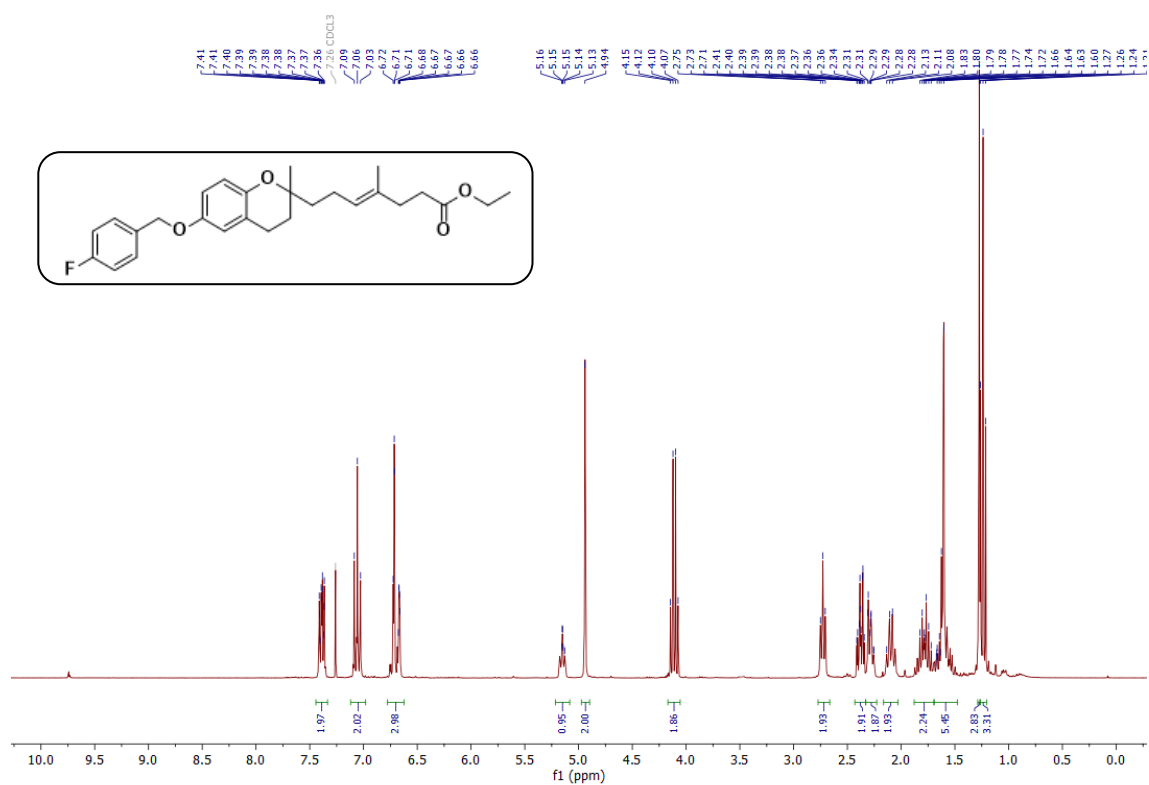
¹³C NMR (75 MHz, CDCl₃) of 5-Chloro-2-(2-(3-(6-((p-fluorobenzyl)oxy)-2-methylbenzodihydropyran-2-yl)propyl)hydrazineyl)-3-(trifluoromethyl)pyridine (**9**).



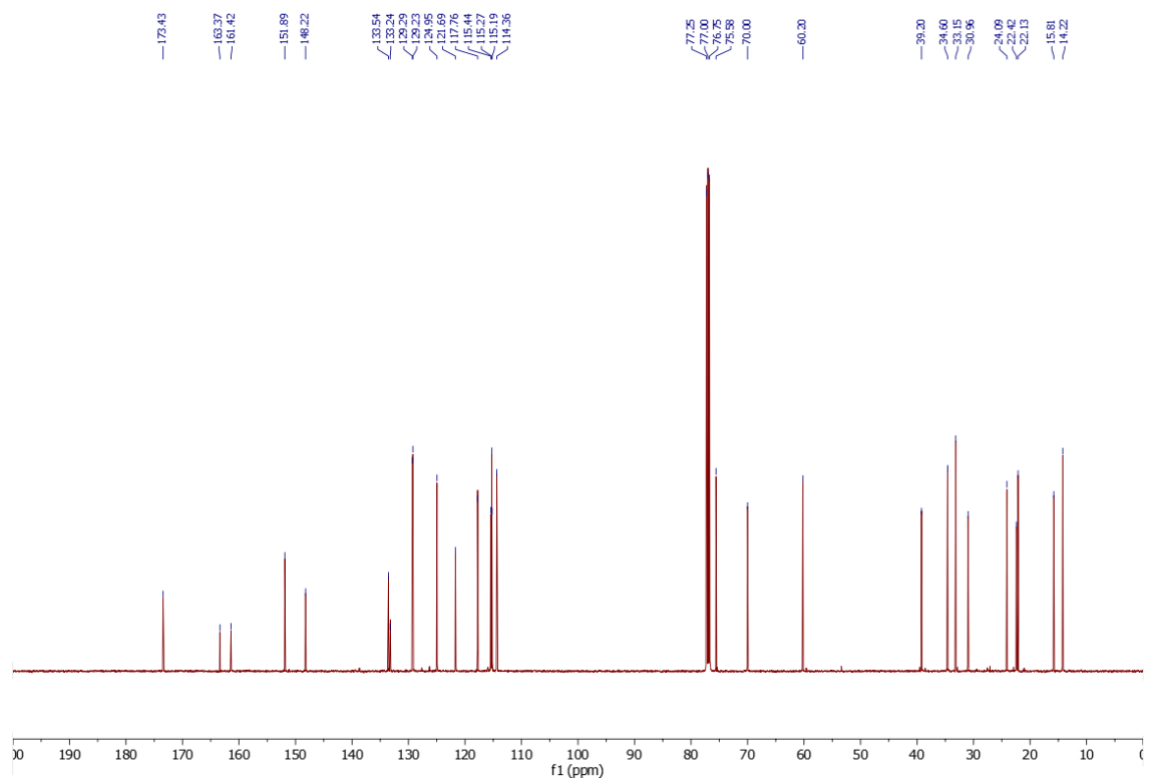
HSQC (300 MHz, CDCl₃) of 5-Chloro-2-(2-(3-(6-((p-fluorobenzyl)oxy)-2-methylbenzodihydropyran-2-yl)propyl)hydrazineyl)-3-(trifluoromethyl)pyridine (**9**).



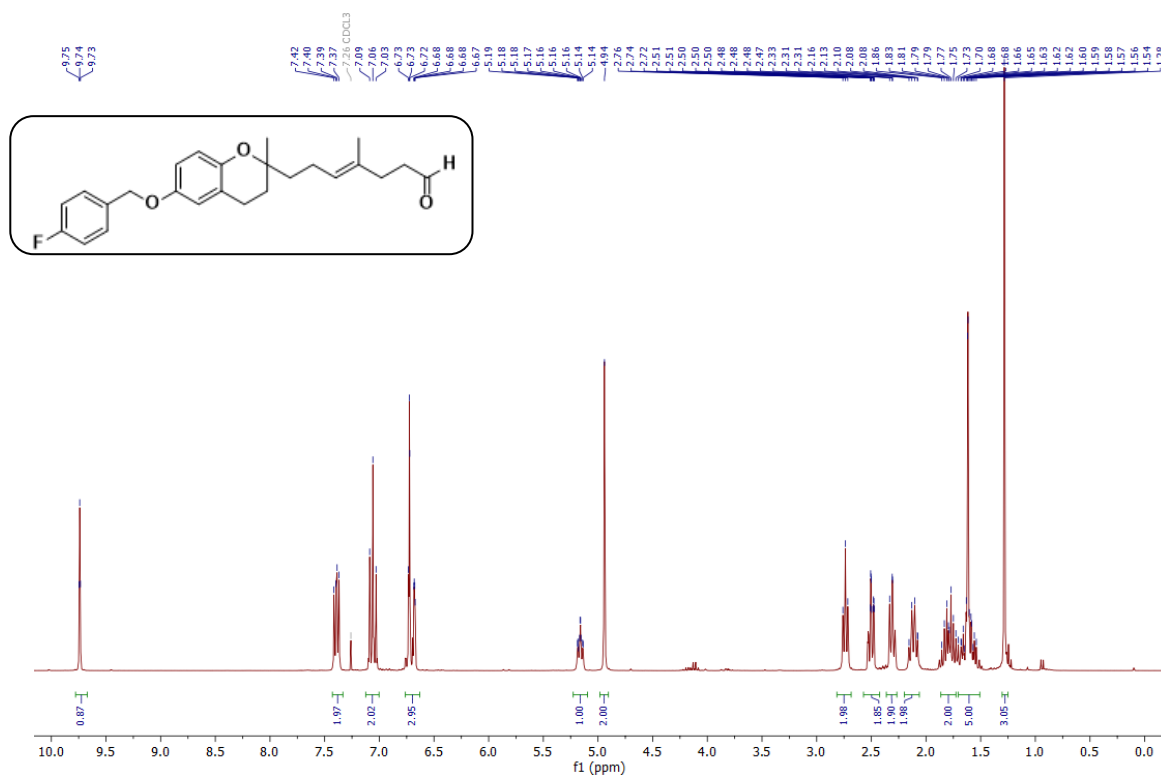
COSY (300 MHz, CDCl₃) of 5-Chloro-2-(2-(3-(6-((p-fluorobenzyl)oxy)-2-methylbenzodihydropyran-2-yl)propyl)hydrazineyl)-3-(trifluoromethyl)pyridine (**9**).



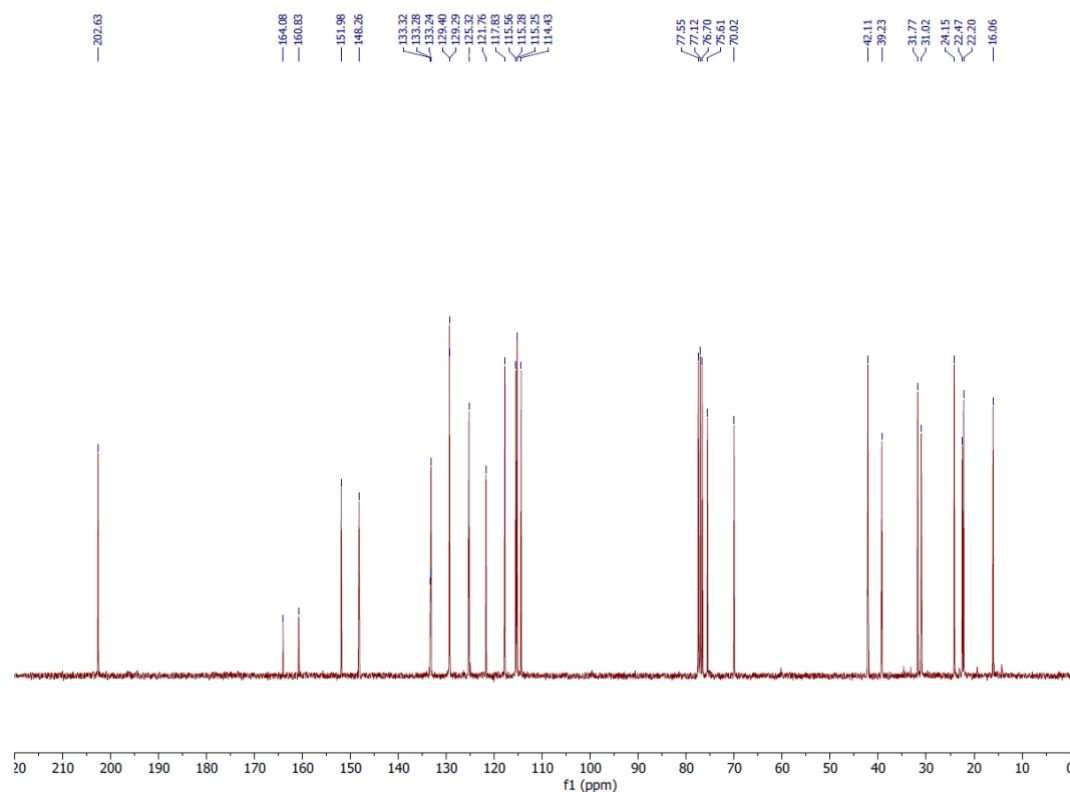
¹H NMR (300 MHz, CDCl₃) of Ethyl 7-(6-((*p*-fluorobenzyl)oxy)-2-methyldihydrobenzopyran-2-yl)-4-methylhept-4-enoate (**11**)



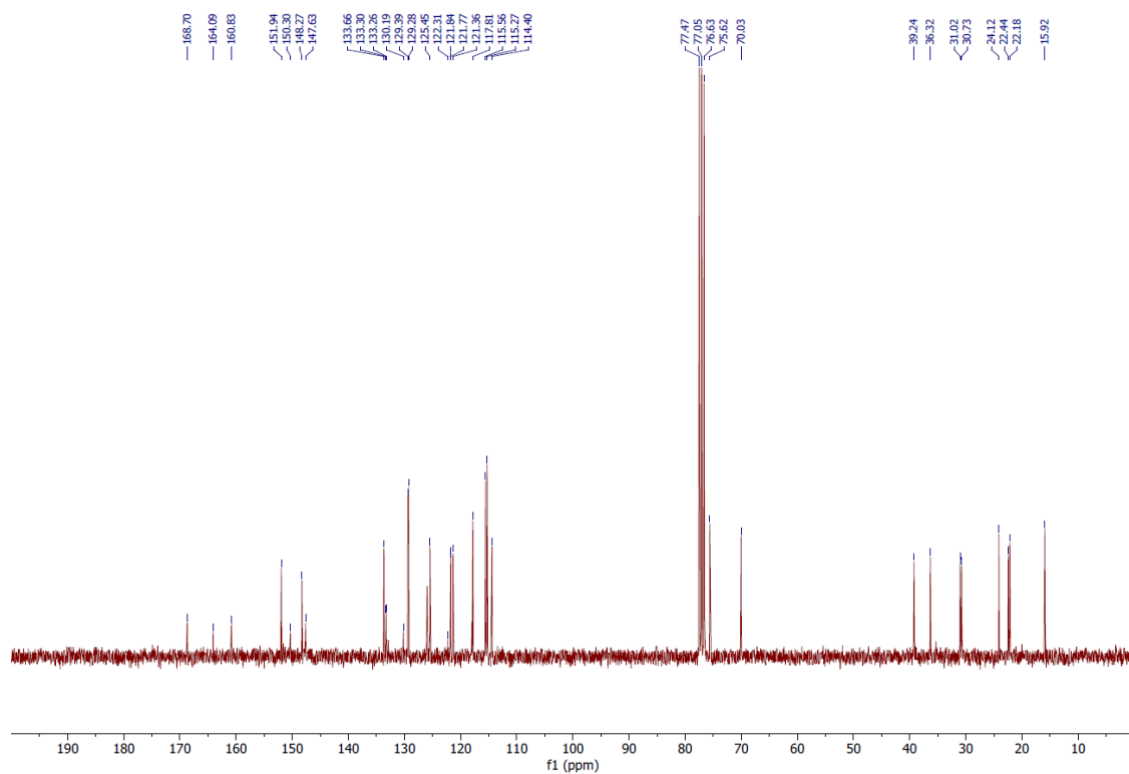
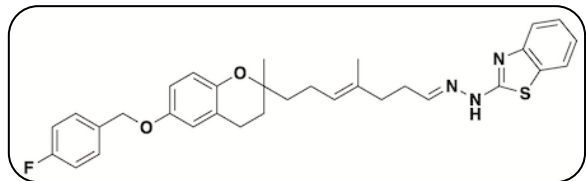
¹³C NMR (75 MHz, CDCl₃) of Ethyl 7-(6-((*p*-fluorobenzyl)oxy)-2-methyldihydrobenzopyran-2-yl)-4-methylhept-4-enoate (**11**)

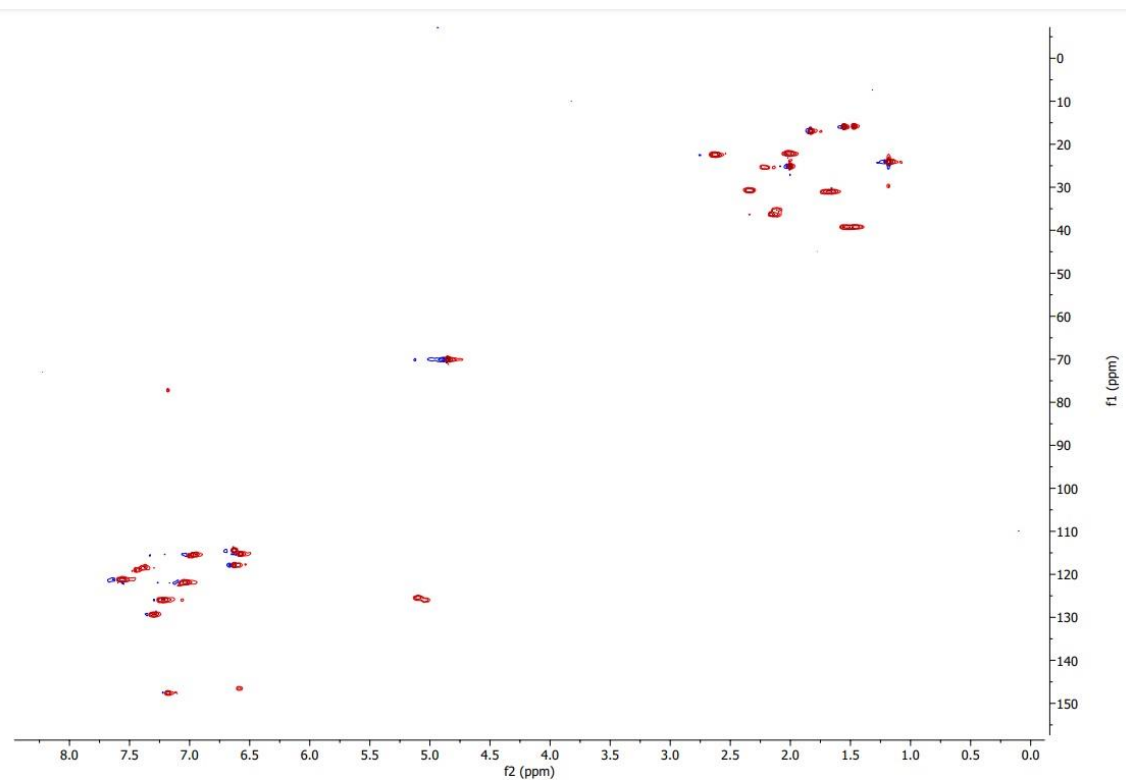


¹H NMR (300 MHz, CDCl₃) of 7-(6-((*p*-Fluorobenzyl)oxy)-2-methyldihydrobenzopyran-2-yl)-4-methylhept-4-enal (**12**)

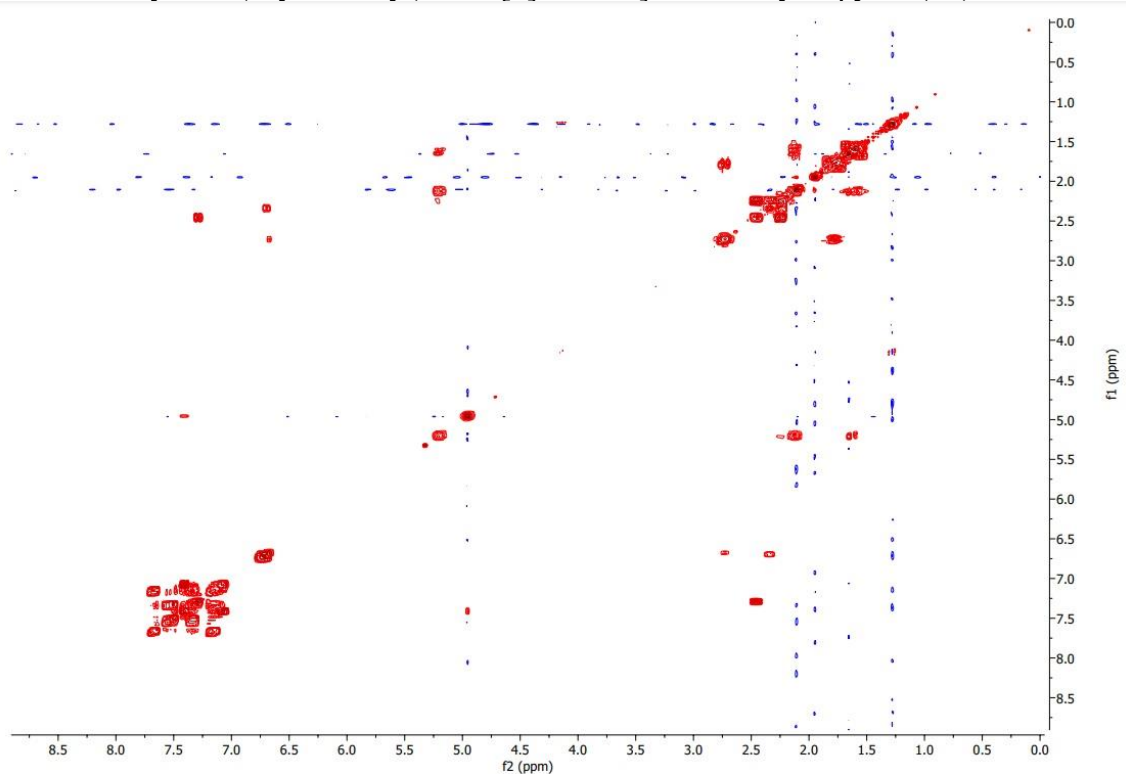


¹³C NMR (75 MHz, CDCl₃) of 7-(6-((*p*-Fluorobenzyl)oxy)-2-methyldihydrobenzopyran-2-yl)-4-methylhept-4-enal (**12**)

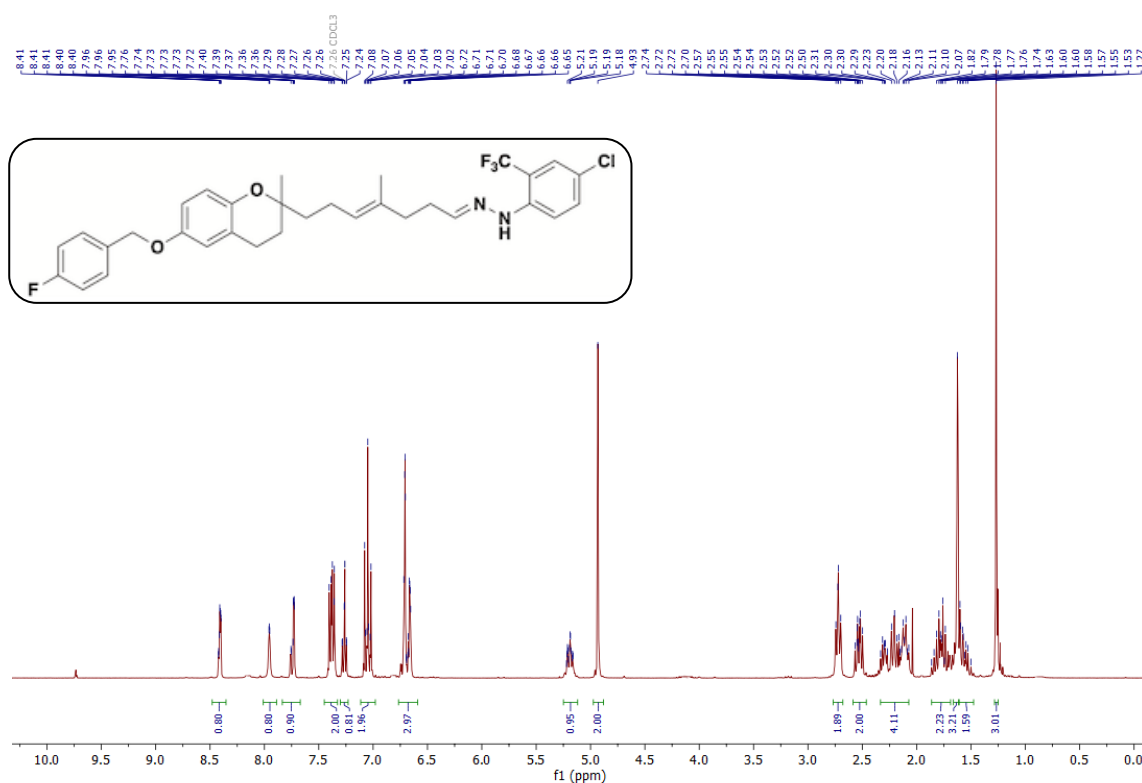




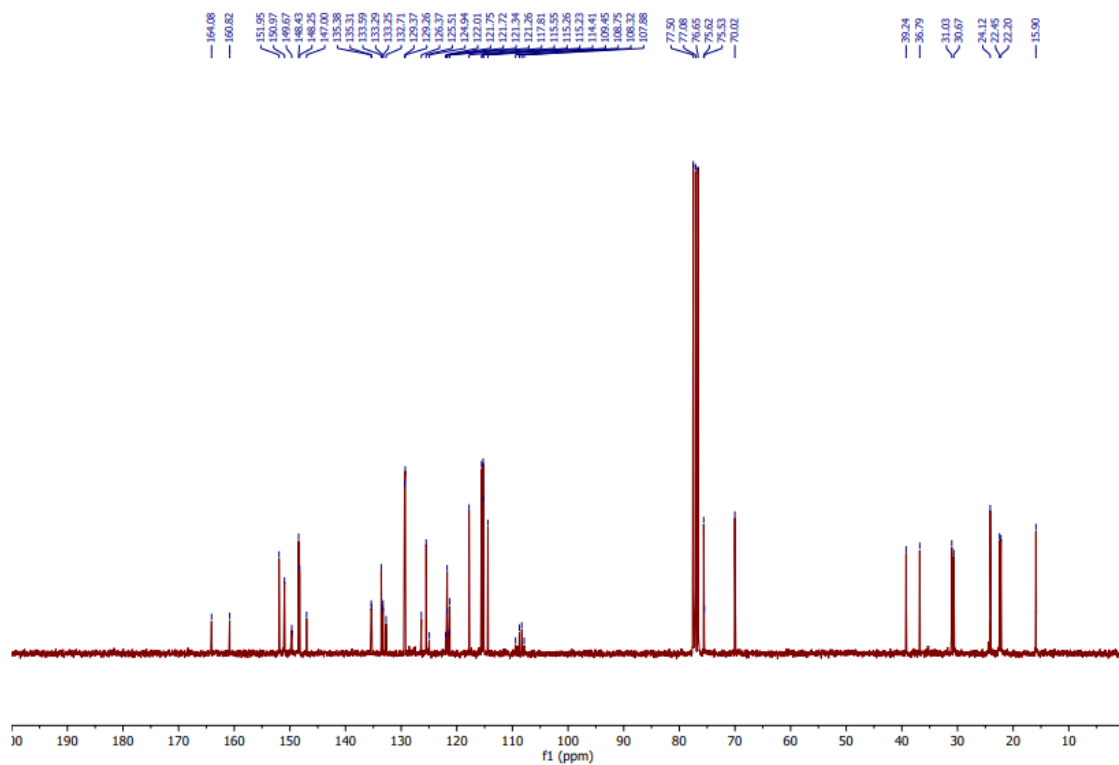
HSQC (300 MHz, CDCl₃) of 6-(*p*-Fluorobenzyloxy)-2-methyl-2-[1-((4-methylhept-4-en-1-ylidene) hydrazineyl)benzo[d]thiazole]-benzodihydropyran (**13**).



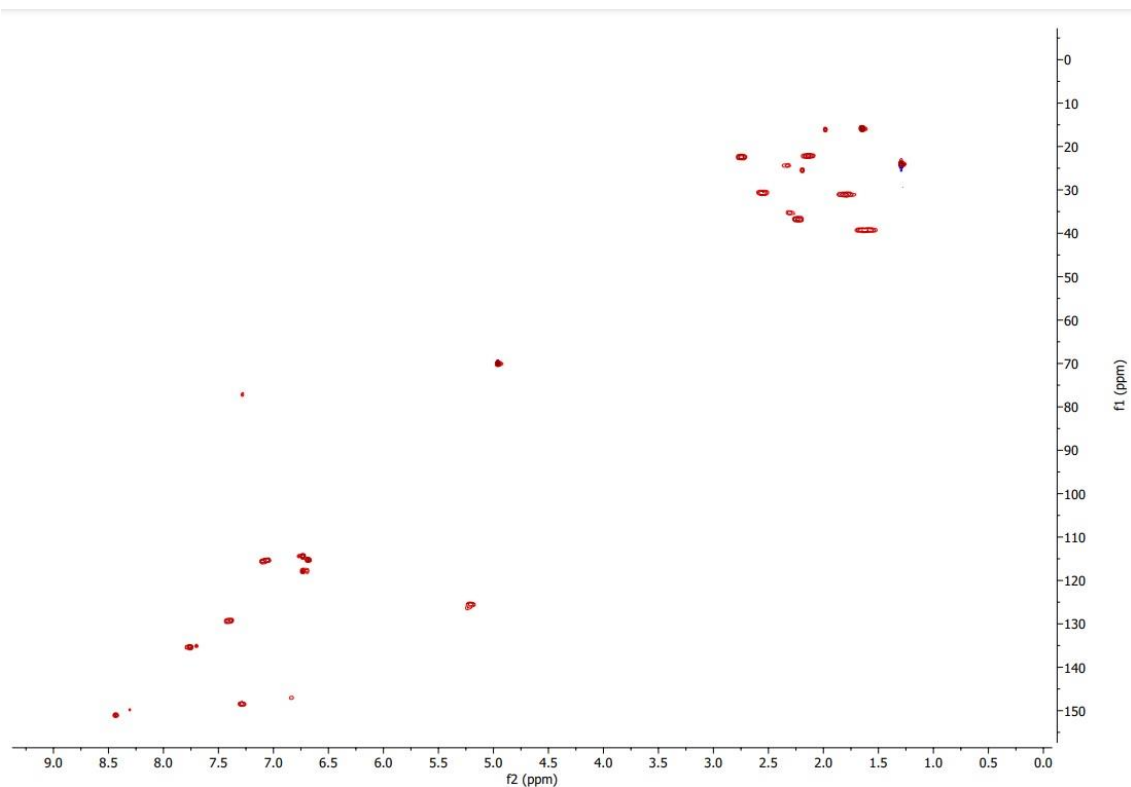
COSY (300 MHz, CDCl₃) of 6-(*p*-Fluorobenzyloxy)-2-methyl-2-[1-((4-methylhept-4-en-1-ylidene) hydrazineyl)benzo[d]thiazole]-benzodihydropyran (**13**).



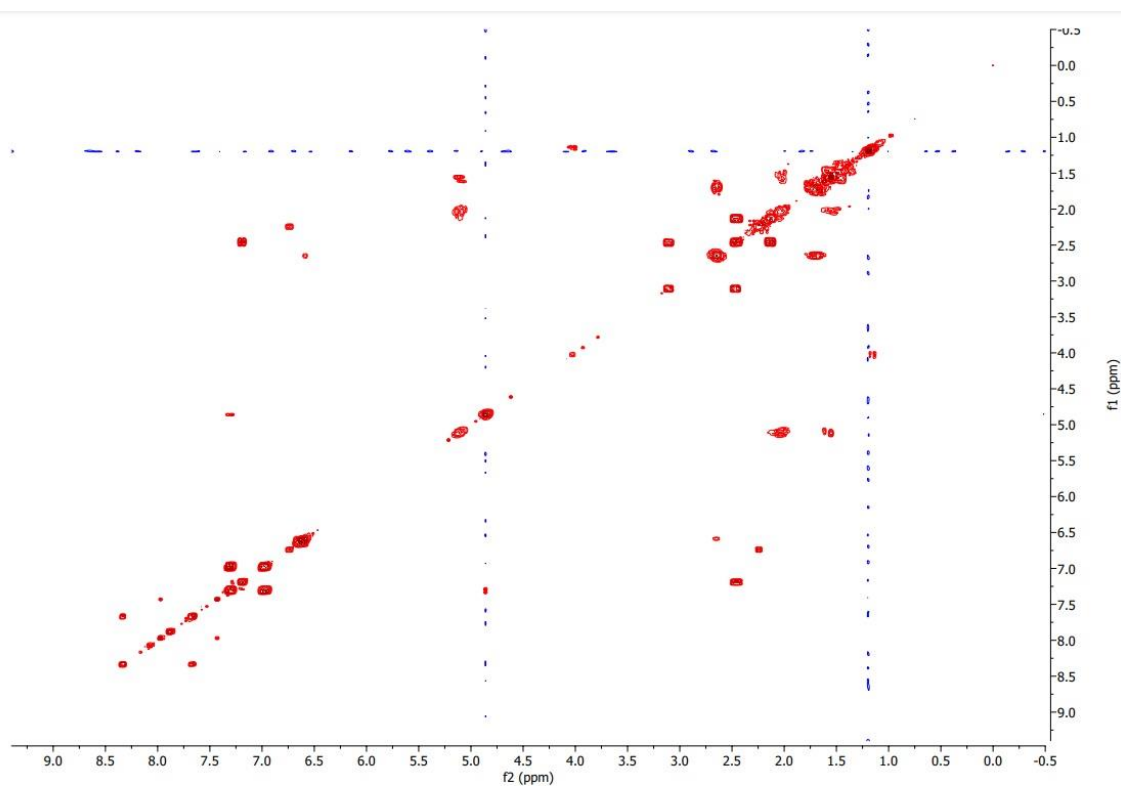
^1H NMR (300 MHz, CDCl_3) of 5-Chloro-2-(2-7-(6-((*p*-fluorobenzyl)oxy)-2-methylbenzodihydropyran-2-yl)-4-methylhept-4-en-1-ylidene)hydrazineyl)-3-(trifluoromethyl)pyridine (**14**).



^{13}C NMR (75 MHz, CDCl_3) of 5-Chloro-2-(2-7-(6-((*p*-fluorobenzyl)oxy)-2-methylbenzodihydropyran-2-yl)-4-methylhept-4-en-1-ylidene)hydrazineyl)-3-(trifluoromethyl)pyridine (**14**).

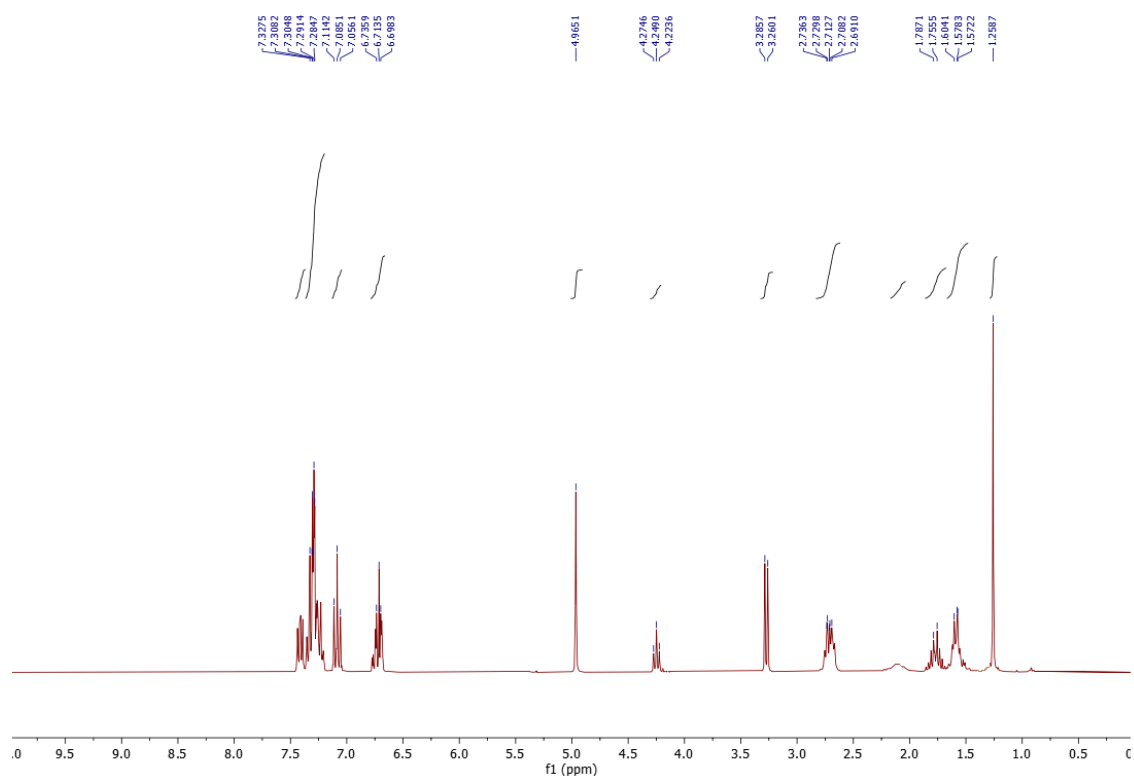


HSQC (300 MHz, CDCl₃) of 5-Chloro-2-(2-7-(6-((*p*-fluorobenzyl)oxy)-2-methylbenzodihydropyran-2-yl)-4-methylhept-4-en-1-ylidene)hydrazineyl)-3-(trifluoromethyl)pyridine (**14**)

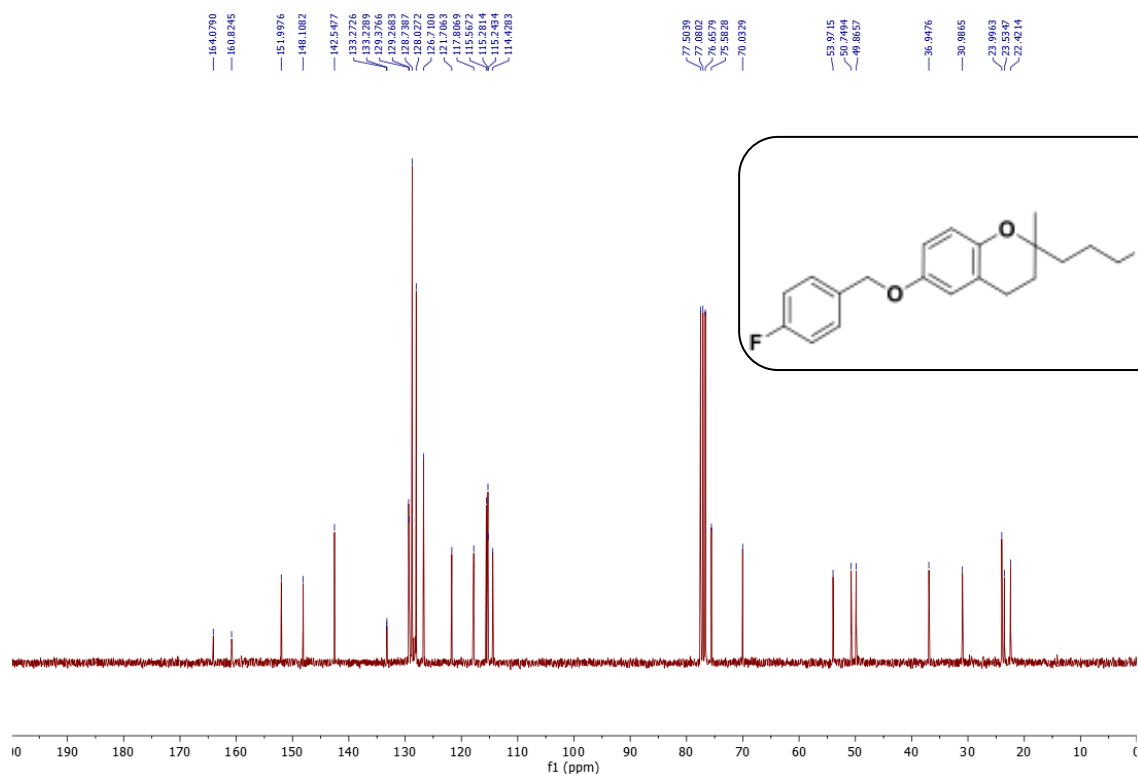


COSY (300 MHz, CDCl₃) of 5-Chloro-2-(2-7-(6-((*p*-fluorobenzyl)oxy)-2-methylbenzodihydropyran-2-yl)-4-methylhept-4-en-1-ylidene)hydrazineyl)-3-(trifluoromethyl)pyridine (**14**)

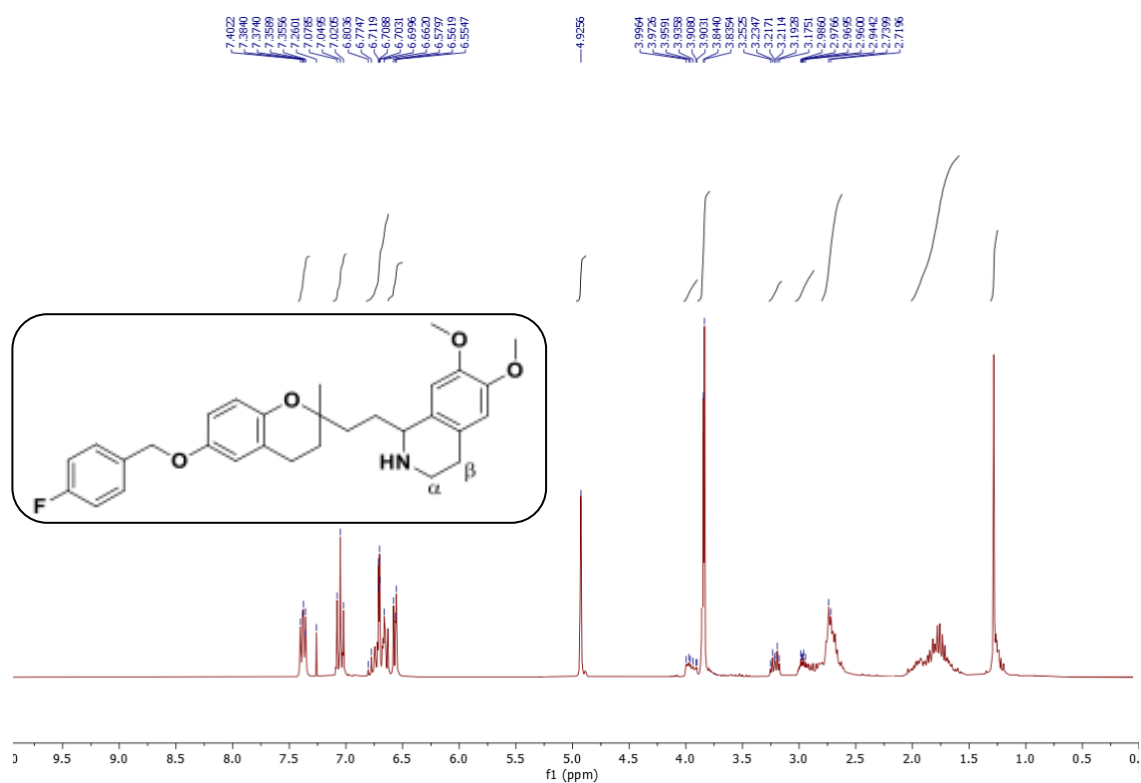
Article 4: Synthesis of 2-Aminopropyl benzopyran derivatives as potential agents against triple negative breast cancer, *RSC Medicinal Chemistry*, 14 (2023) 2327.



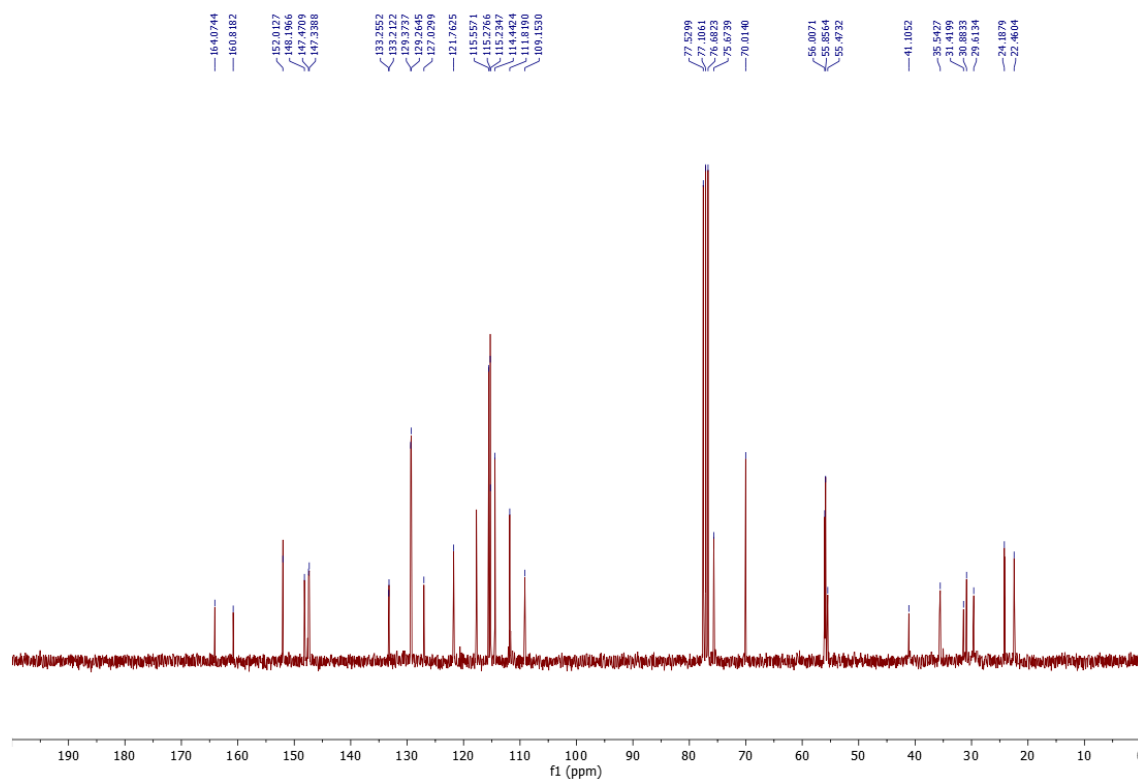
¹H NMR (300 MHz, CDCl₃) of *N*-(2,2-Diphenylethyl)-3-(6-(*p*-fluorobenzyloxy)-2-methyldihydrobenzopyran-2-yl)propanamine (**6**).



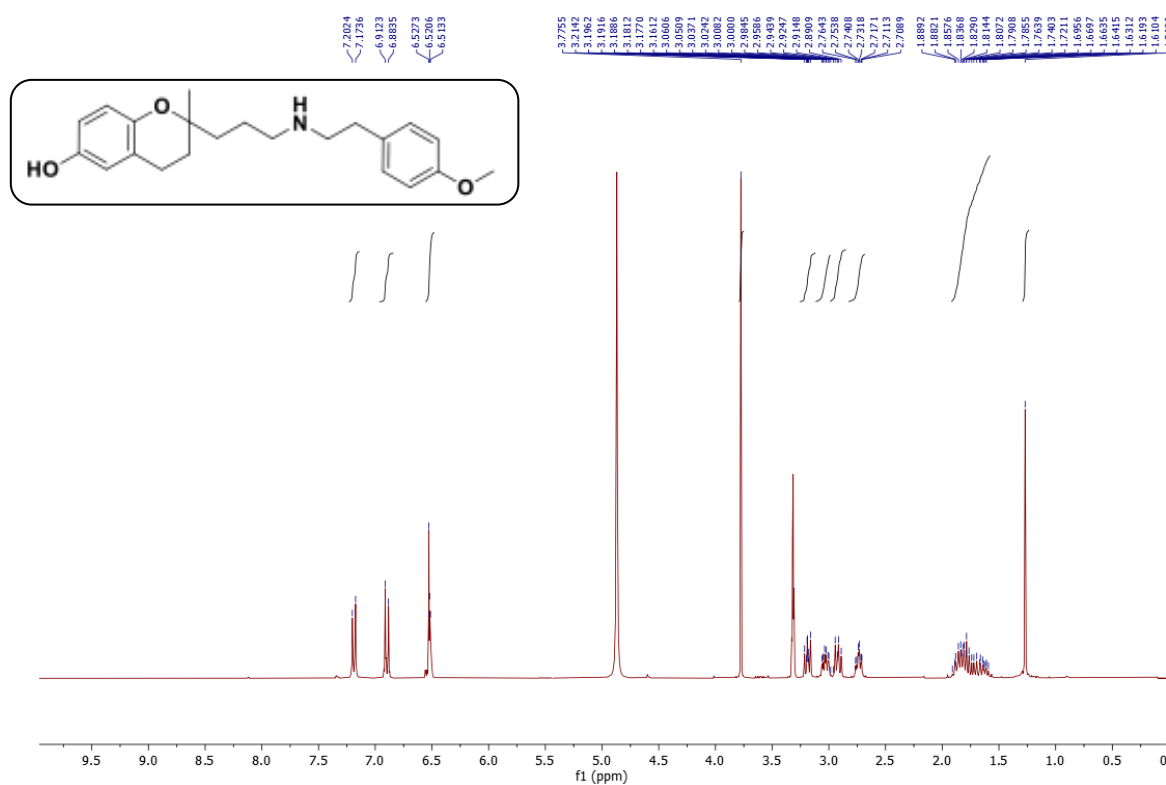
¹³C NMR (75 MHz, CDCl₃) of *N*-(2,2-Diphenylethyl)-3-(6-(*p*-fluorobenzyloxy)-2-methyldihydrobenzopyran-2-yl)propanamine (**6**).



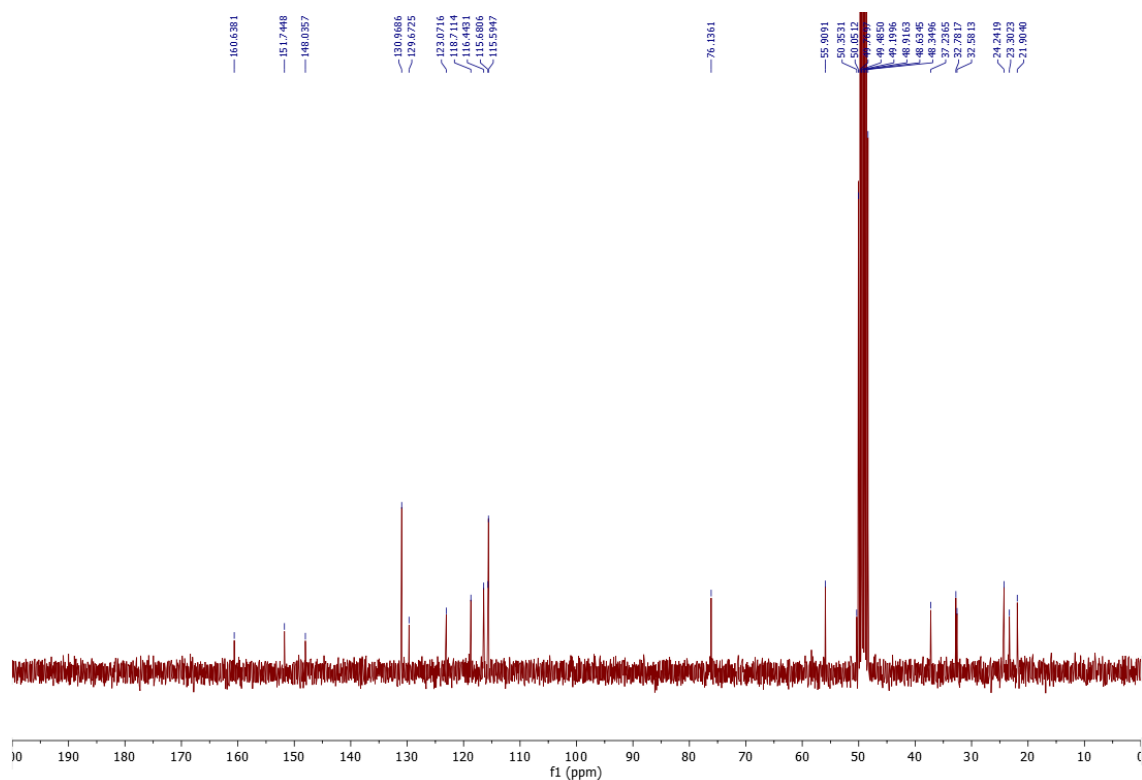
¹H NMR (300 MHz, CDCl₃) of 1-(2-(6-((*p*-Fluorobenzyl)oxy)-2-methyldihydrobenzopyran-2-yl)ethyl)-6,7-dimethoxy-1,2,3,4-tetrahydroisoquinoline (**7**).



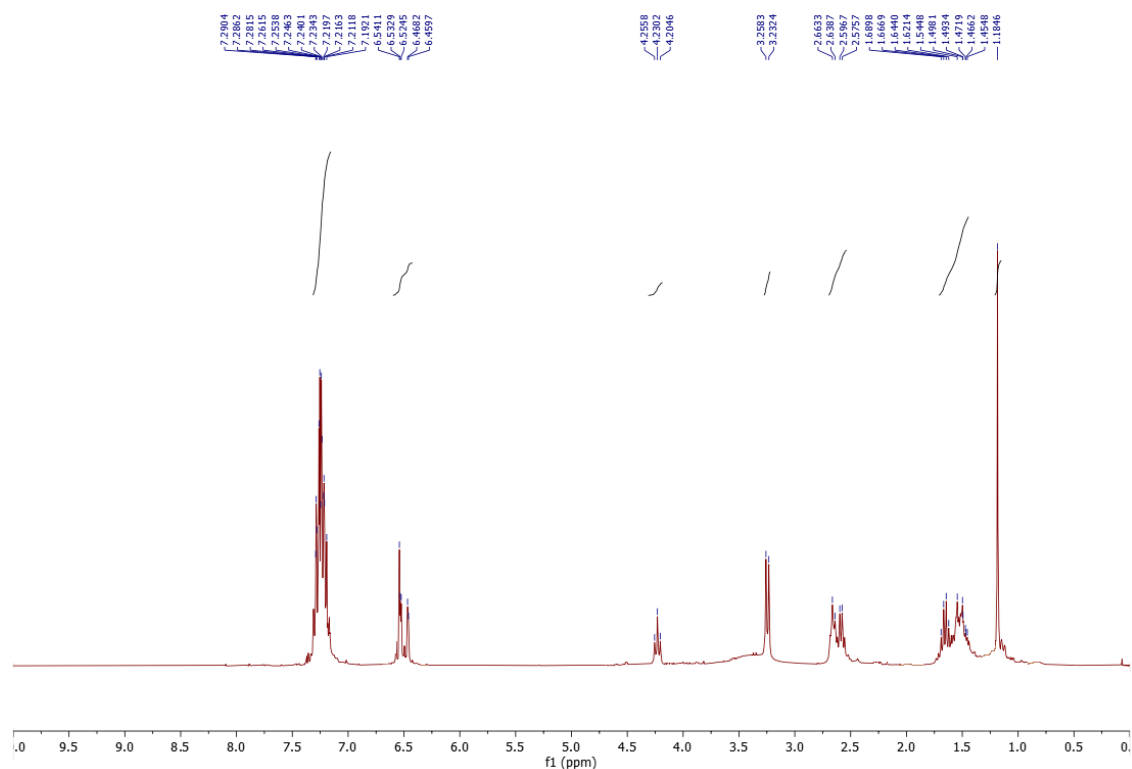
¹³C NMR (75 MHz, CDCl₃) of 1-(2-(6-((*p*-Fluorobenzyl)oxy)-2-methyldihydrobenzopyran-2-yl)ethyl)-6,7-dimethoxy-1,2,3,4-tetrahydroisoquinoline (**7**).



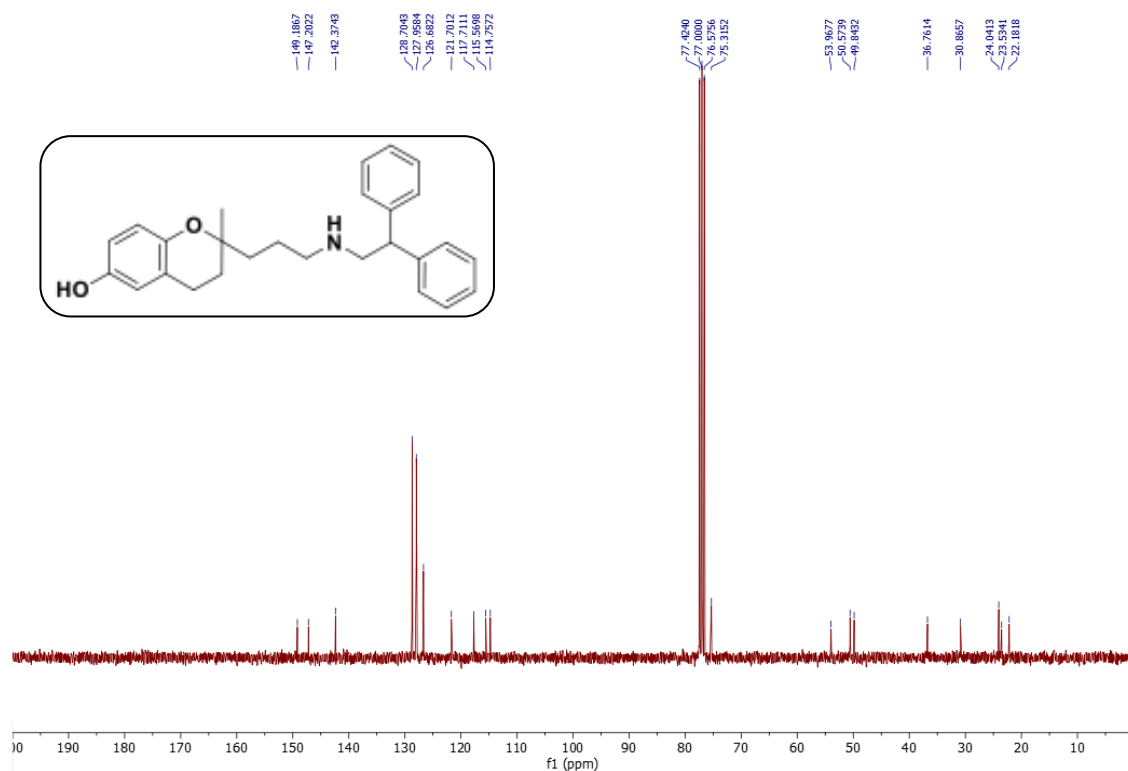
^1H NMR (300 MHz, CD_3OD) of 3-(6-Hydroxy-2-methyldihydrobenzopyran-2-yl)-*N*-(*p*-methoxyphenethyl)propanamine) (**5a**).



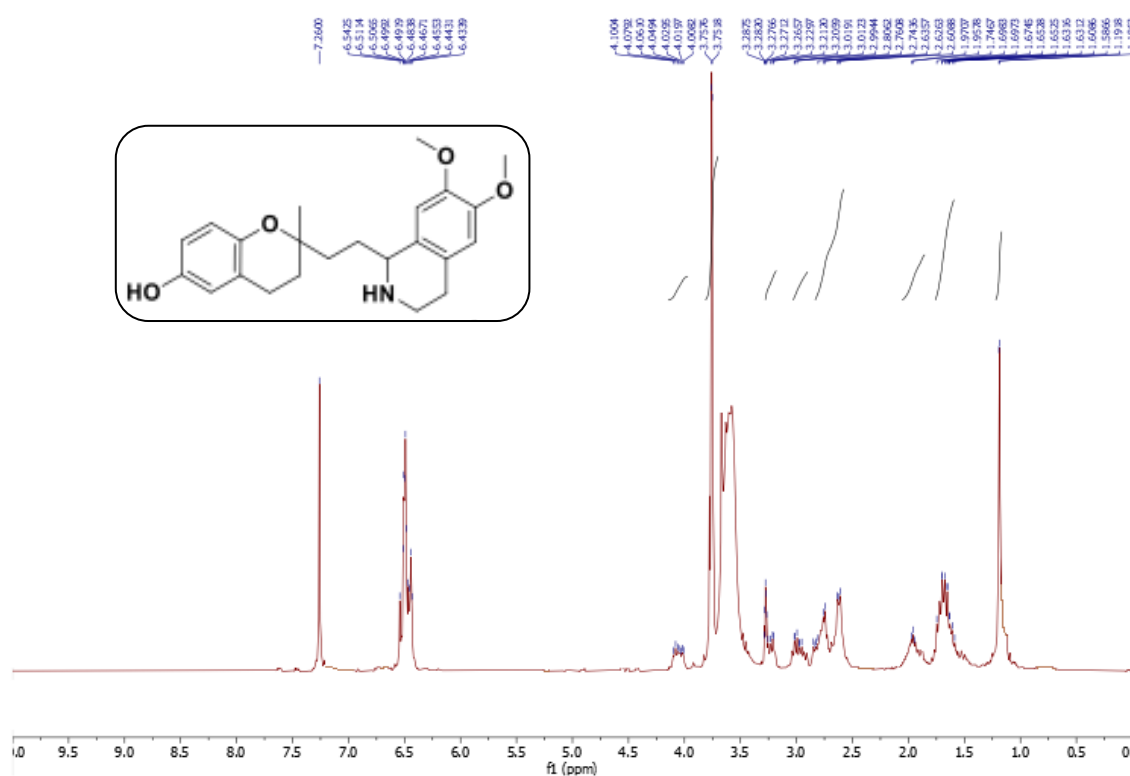
^{13}C NMR (75 MHz, CD_3OD) of 3-(6-Hydroxy-2-methyldihydrobenzopyran-2-yl)-*N*-(*p*-methoxyphenethyl)propanamine) (**5a**).



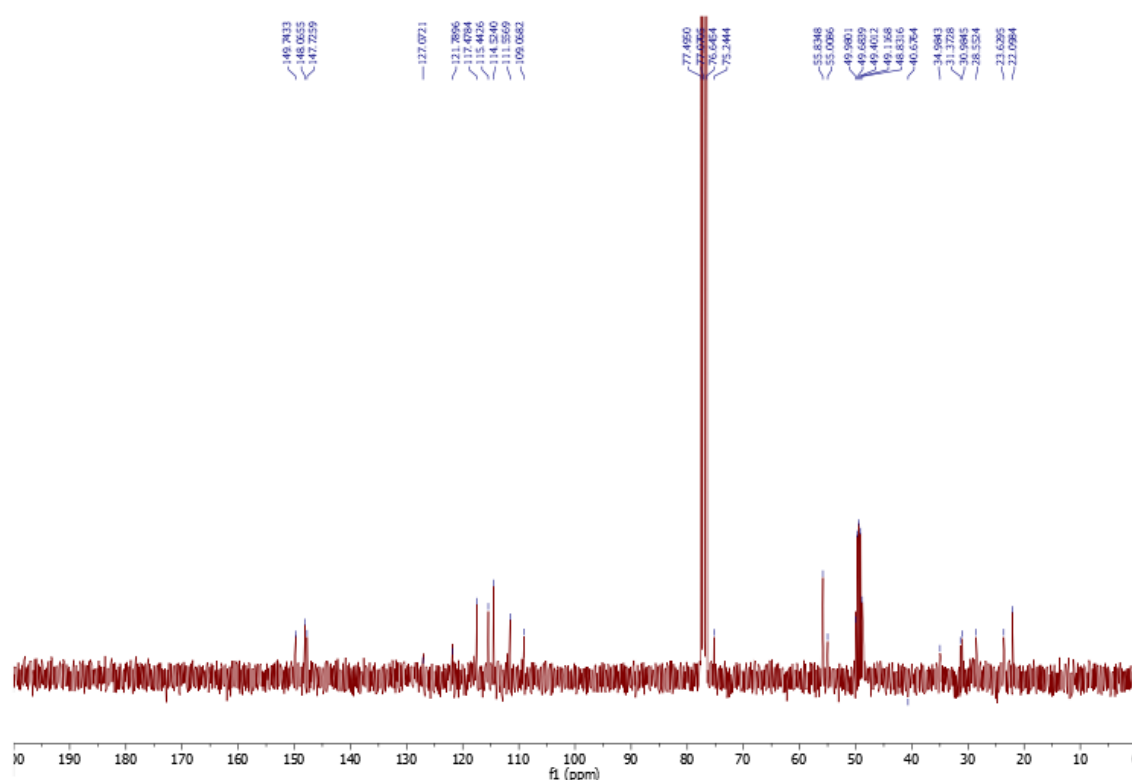
¹H NMR (300 MHz, CDCl₃) of 2-(3-((2,2-Diphenylethyl)amino)propyl)-2-methyl-dihydrobenzopyran-6-ol (**6a**).



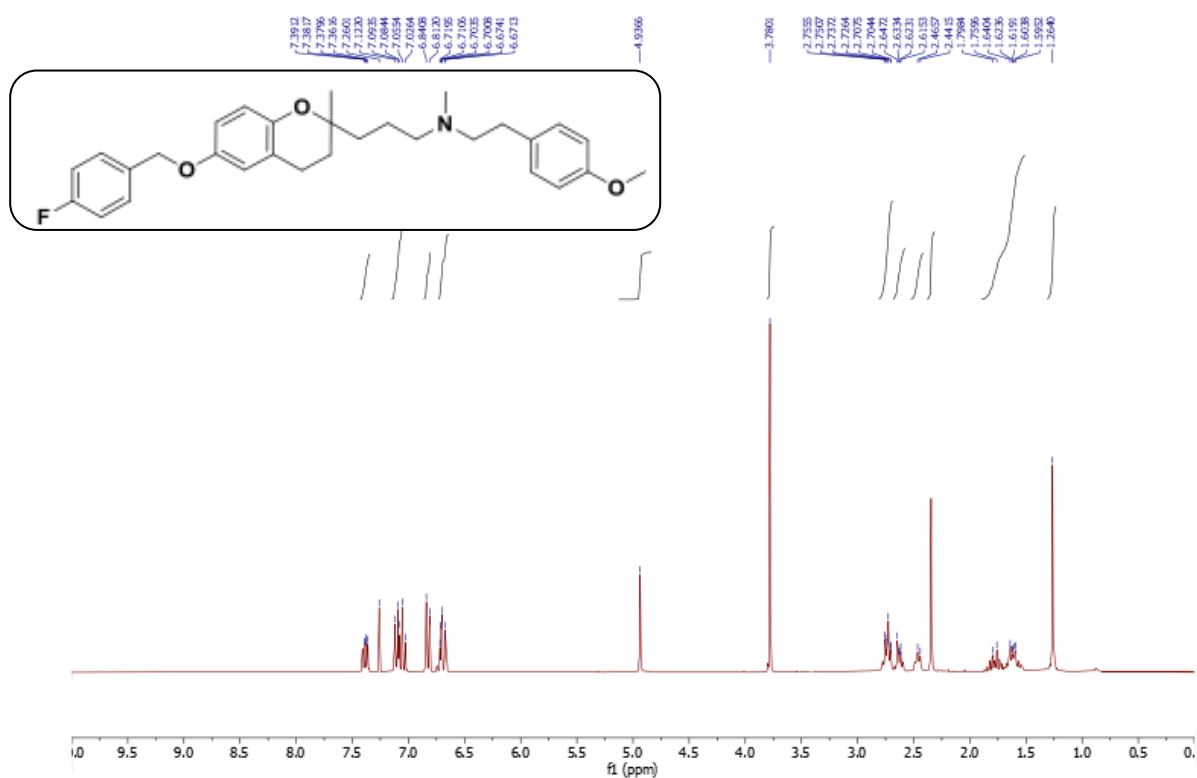
¹³C NMR (75 MHz, CDCl₃) of 2-(3-((2,2-Diphenylethyl)amino)propyl)-2-methyl-dihydrobenzopyran-6-ol (**6a**).



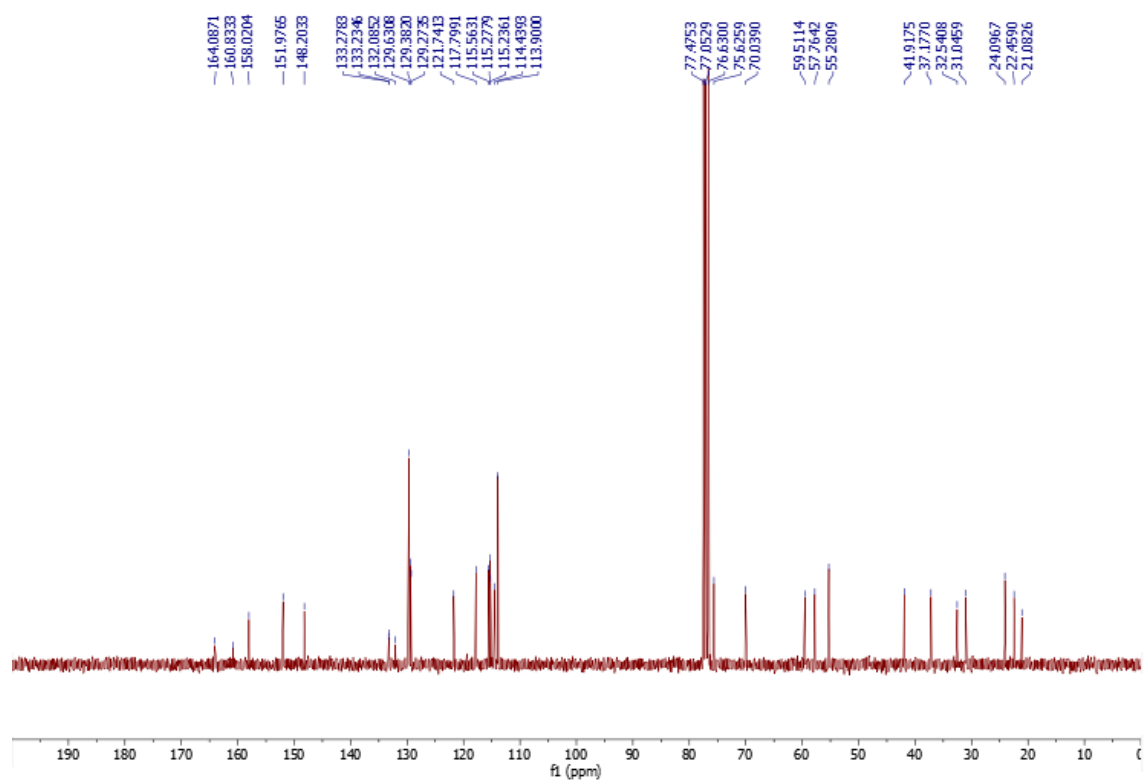
^1H NMR (300 MHz, $\text{CDCl}_3 + 1$ drop CD_3OD) of 2-(2-(6-7-Dimethoxy-1,2,3,4-tetrahydroisoquinolin-1-yl)ethyl)-2-methyldihydrobenzopyran-6-ol (7a).



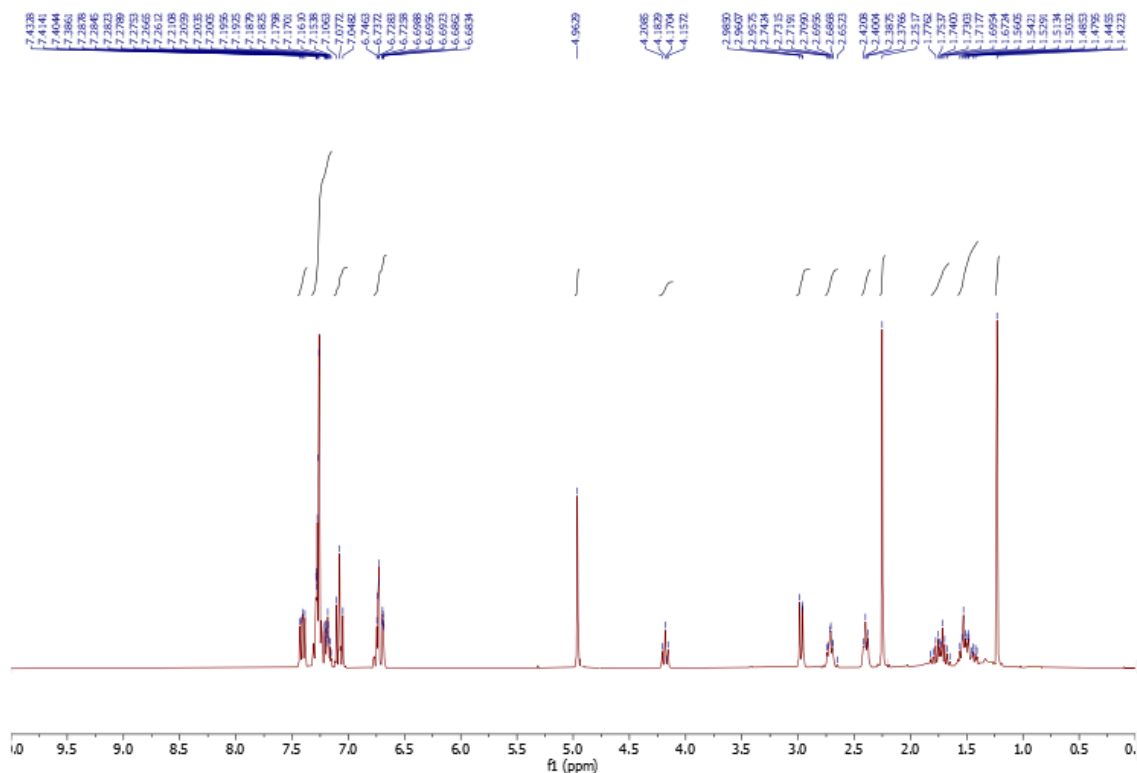
^{13}C NMR (75 MHz, $\text{CDCl}_3 + 1$ drop CD_3OD) of 2-(2-(6-7-Dimethoxy-1,2,3,4-tetrahydroisoquinolin-1-yl)ethyl)-2-methyldihydrobenzopyran-6-ol (7a).



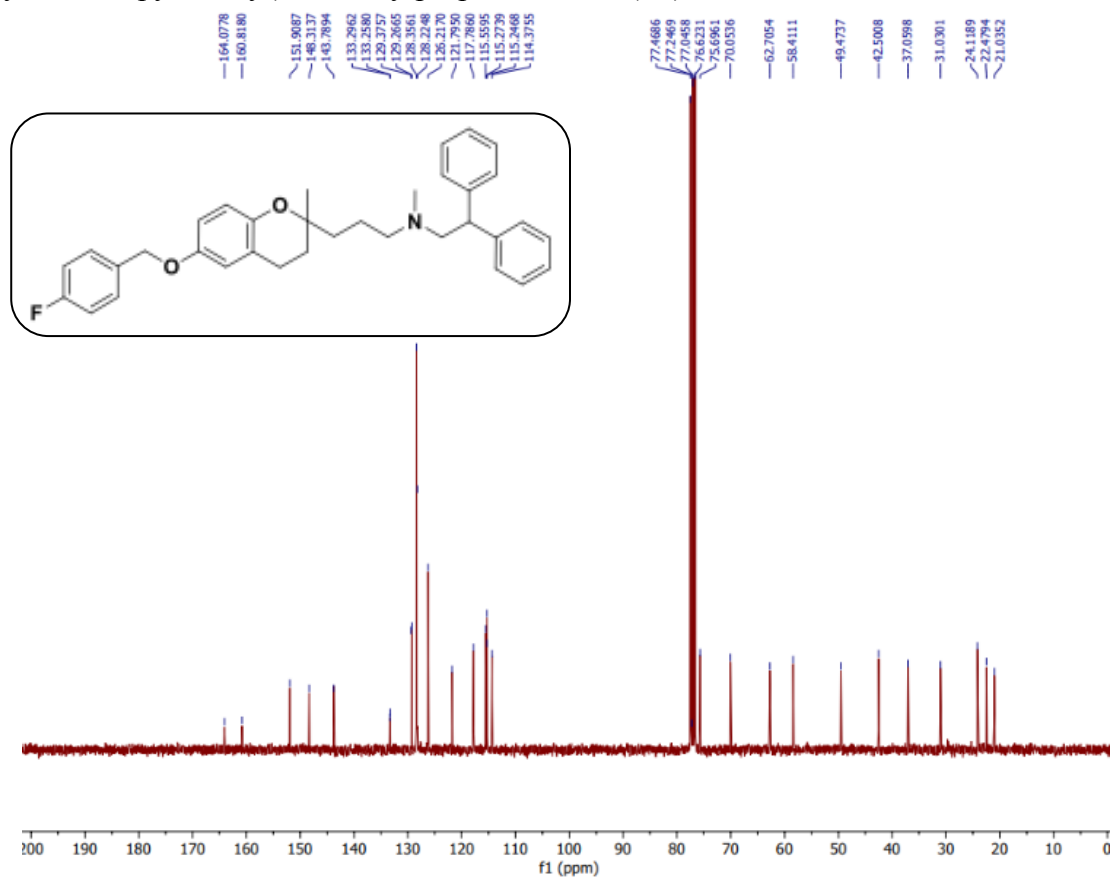
¹H NMR (300 MHz, CDCl₃) of 3-(6-(*p*-Fluorobenzyloxy)-2-methyldihydrobenzopyran-2-yl)-*N*-(*p*-methoxyphenethyl)-*N*-methylpropanamine (**5b**).



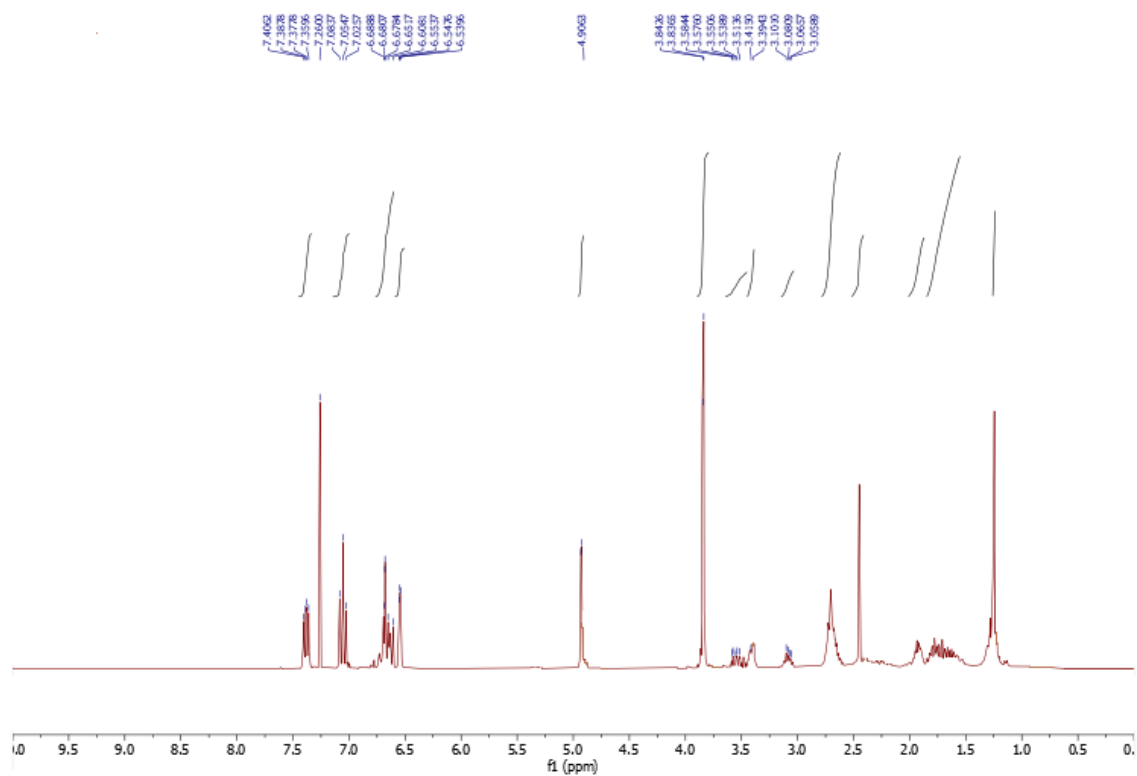
¹³C NMR (75 MHz, CDCl₃) of 3-(6-(*p*-Fluorobenzyloxy)-2-methyldihydrobenzopyran-2-yl)-*N*-(*p*-methoxyphenethyl)-*N*-methylpropanamine (**5b**).



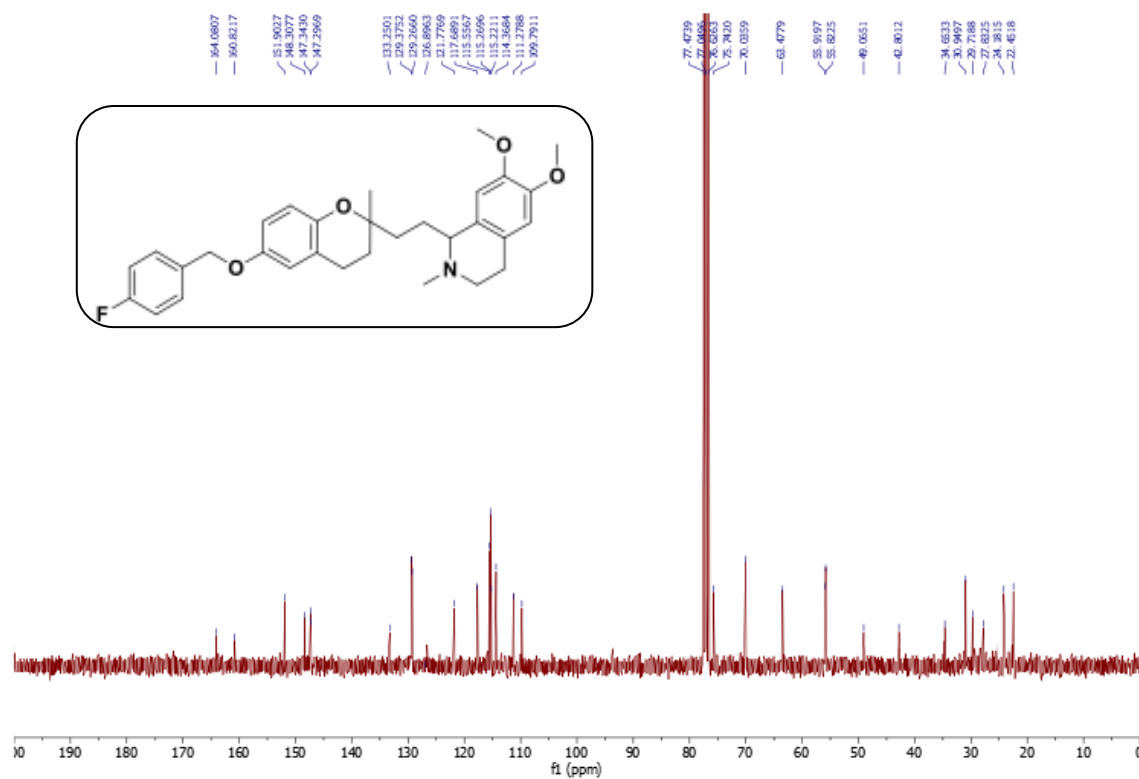
¹H NMR (300 MHz, CDCl₃) of *N*-(2,2-Diphenylethyl)-3-(6-((*p*-fluorobenzyl)oxy)-2-methyl-dihydrobenzopyran-2-yl)-*N*-methylpropan-1-amine (**6b**).



¹³C NMR (75 MHz, CDCl₃) of *N*-(2,2-Diphenylethyl)-3-(6-((*p*-fluorobenzyl)oxy)-2-methyl-dihydrobenzopyran-2-yl)-*N*-methylpropan-1-amine (**6b**).



¹H NMR (300 MHz, CDCl₃) of 1-(2-(6-((*p*-fluorobenzyl)oxy)-2-methyldihydrobenzopyran-2-yl)ethyl)-6,7-dimethoxy-2-methyl-1,2,3,4-THIQ (**7b**).

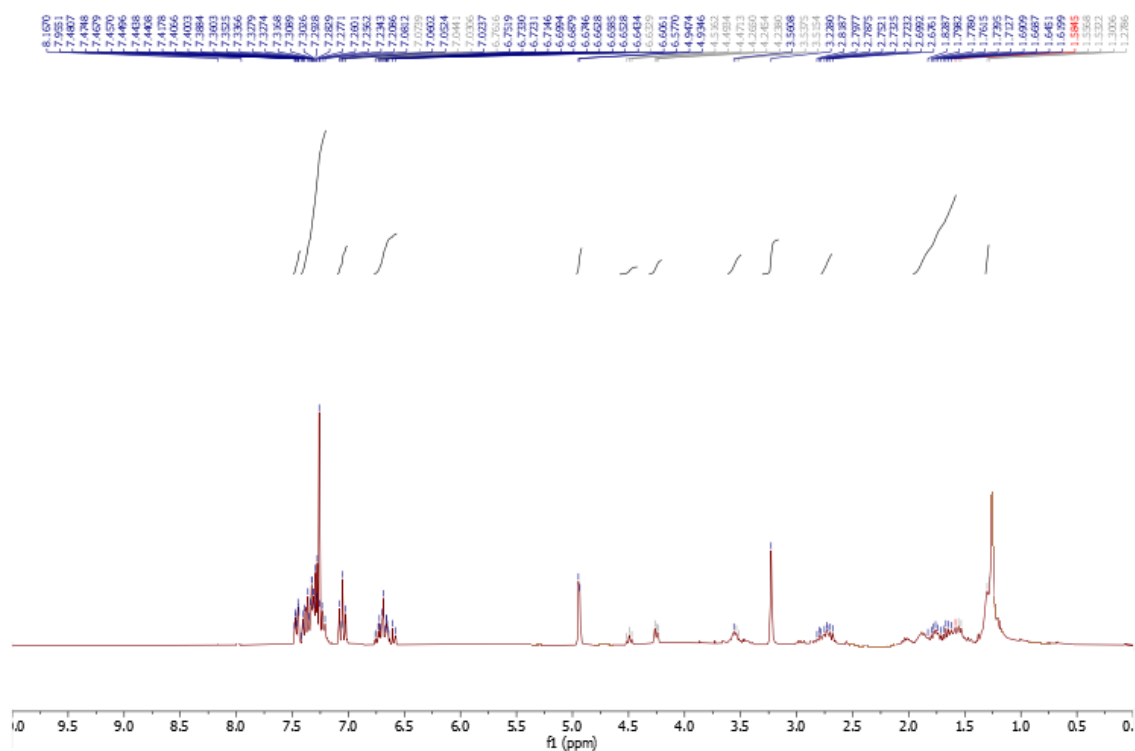


¹³C NMR (75 MHz, CDCl₃) of 1-(2-(6-((*p*-fluorobenzyl)oxy)-2-methyldihydrobenzopyran-2-yl)ethyl)-6,7-dimethoxy-2-methyl-1,2,3,4-THIQ (**7b**).

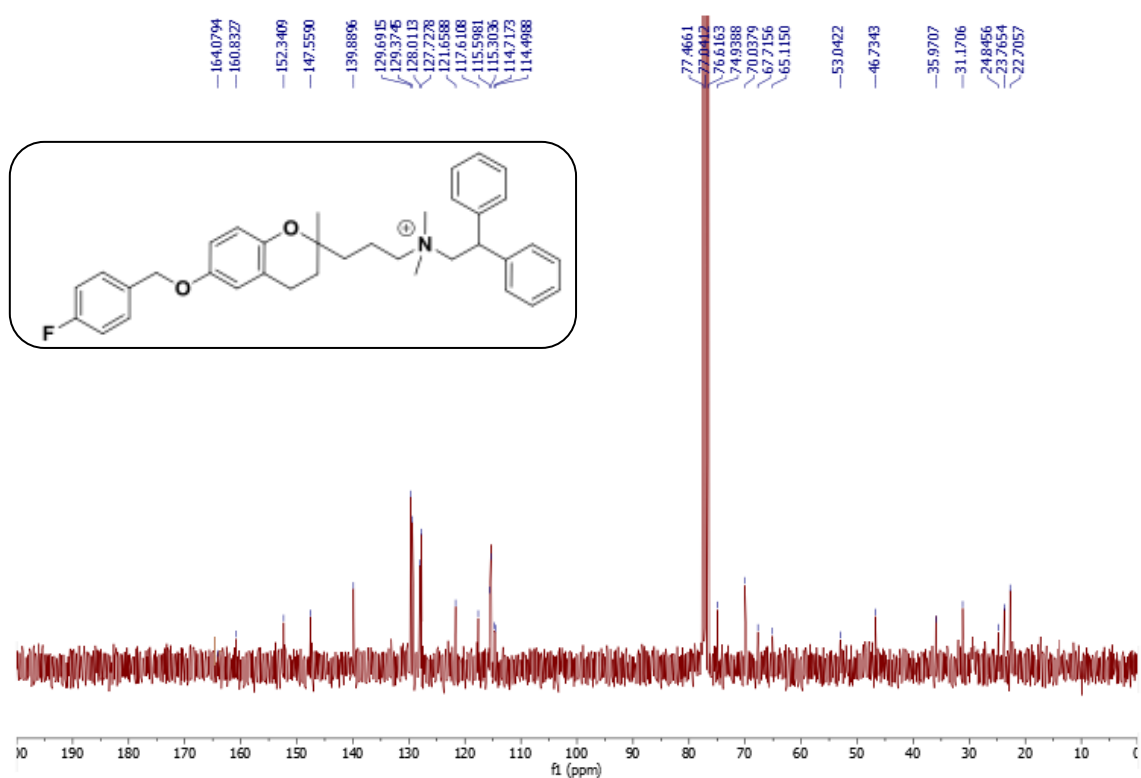
Chemical shifts (ppm) labeled on the spectrum:

- 164.0883
- 160.7612
- 159.2008
- 152.3766
- 147.5372
- 138.0527
- 132.4697
- 129.3684
- 129.2534
- 121.6706
- 117.5888
- 115.5320
- 115.2506
- 115.2466
- 114.8510
- 114.7118
- 77.4340
- 77.2042
- 76.9993
- 76.5742
- 74.9025
- 69.9884
- 65.4705
- 65.5319
- 55.4029
- 52.2821
- 35.9405
- 31.8874
- 30.9131
- 23.8877
- 22.6570
- 17.3678

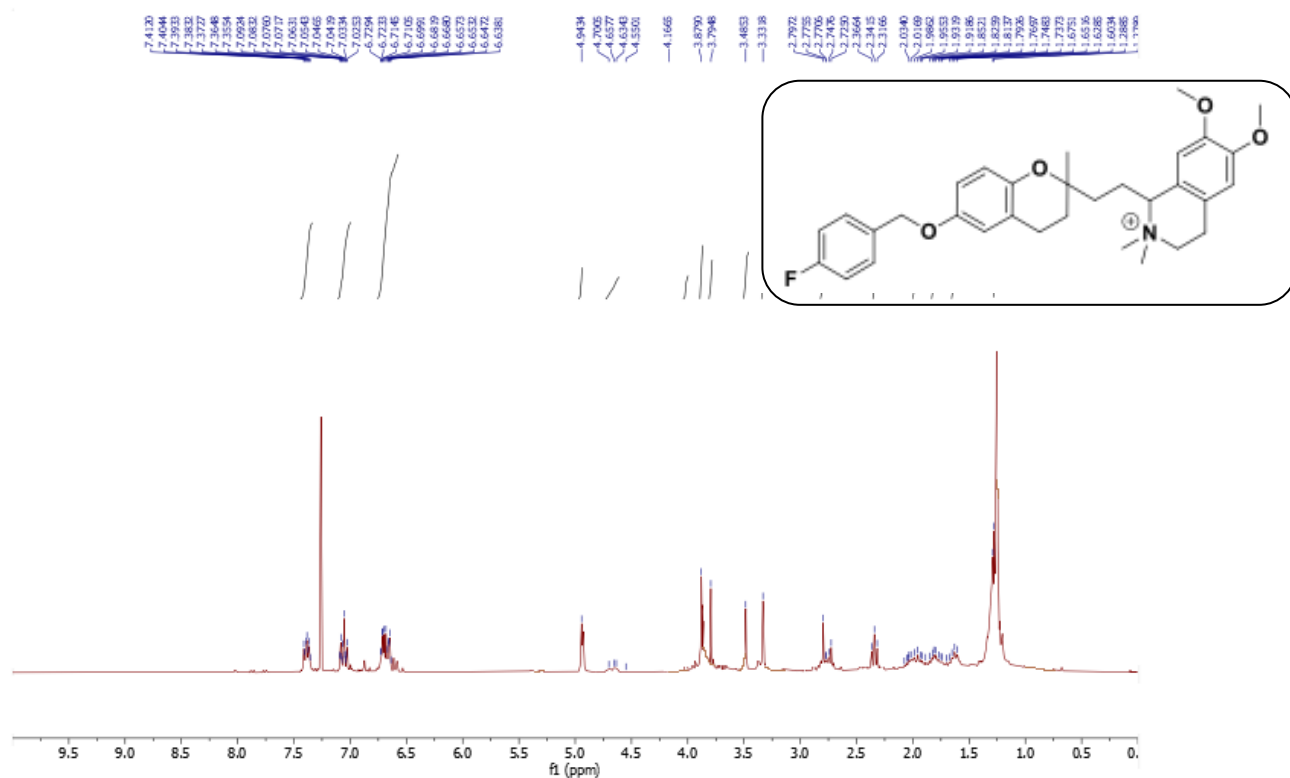
158



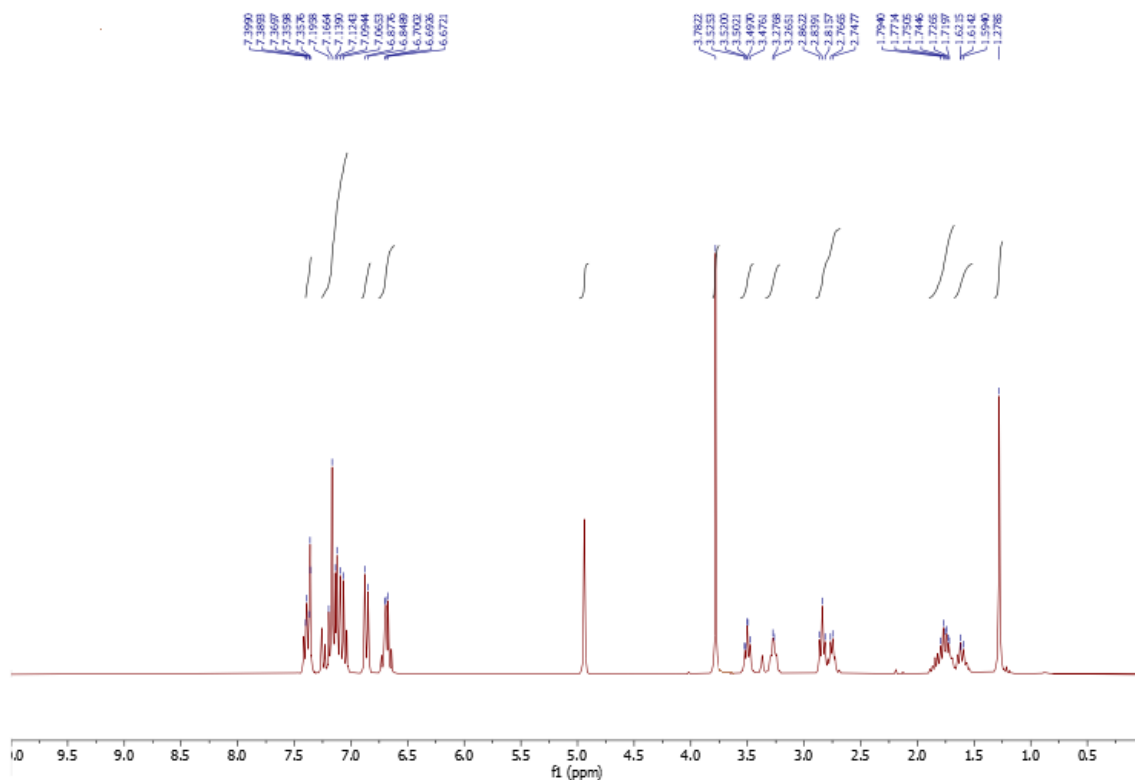
^1H NMR (300 MHz, CDCl_3) of *N*-(2,2-Diphenylethyl)-3-6-((*p*-fluorobenzyl)oxy)-2-methyldihydrobenzopyran-2-yl)-*N,N*-dimethylpropan-1-aminium (**6c**).



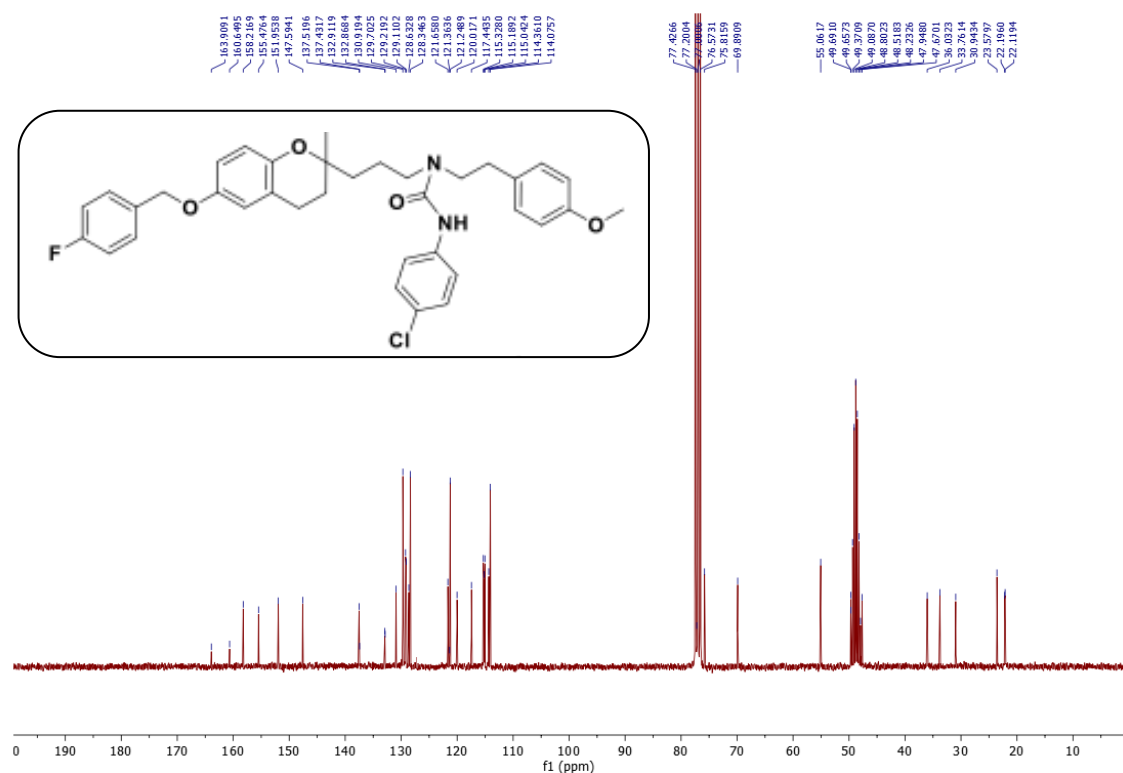
^{13}C NMR (75 MHz, CDCl_3) of *N*-(2,2-Diphenylethyl)-3-6-((*p*-fluorobenzyl)oxy)-2-methyldihydrobenzopyran-2-yl)-*N,N*-dimethylpropan-1-aminium (**6c**).



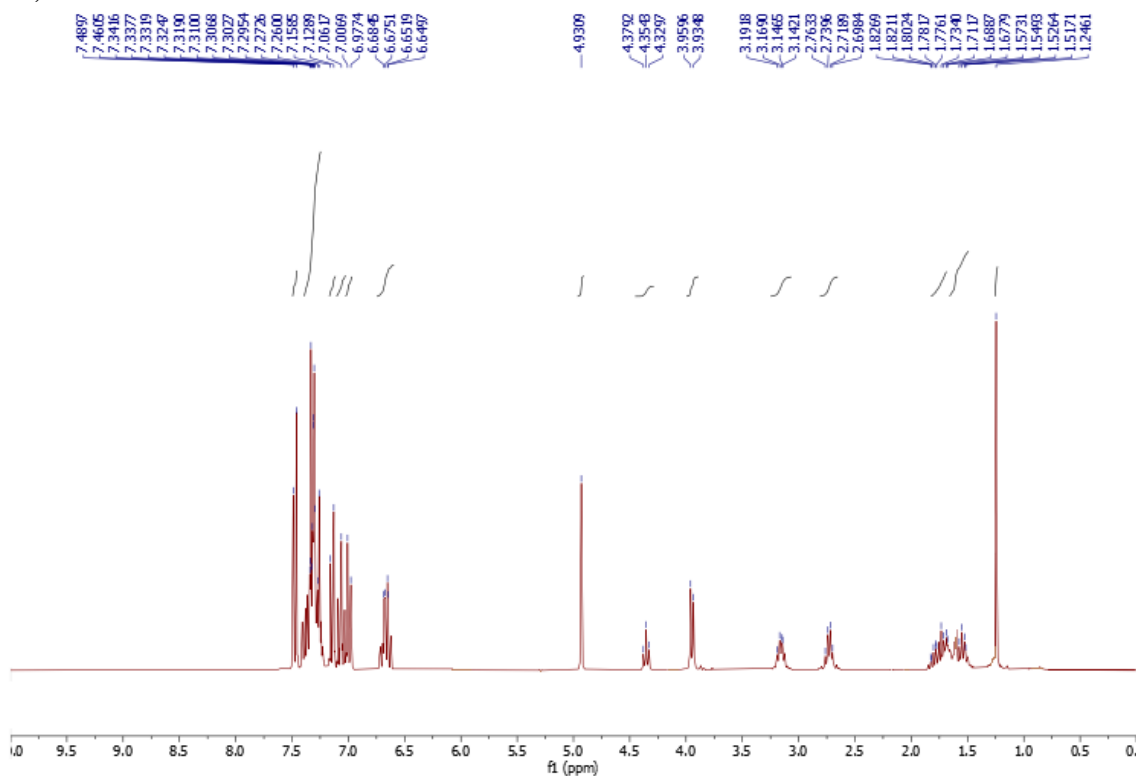
¹H NMR (300 MHz, CDCl₃) of 1-(2-(6-((*p*-Fluorobenzyl)oxy)-2-methyldihydrobenzopyran-2-yl)ethyl)-6,7-dimethoxy-2,2-dimethyl-1,2,3,4-tetrahydroisoquinolin-2-ium (7c).



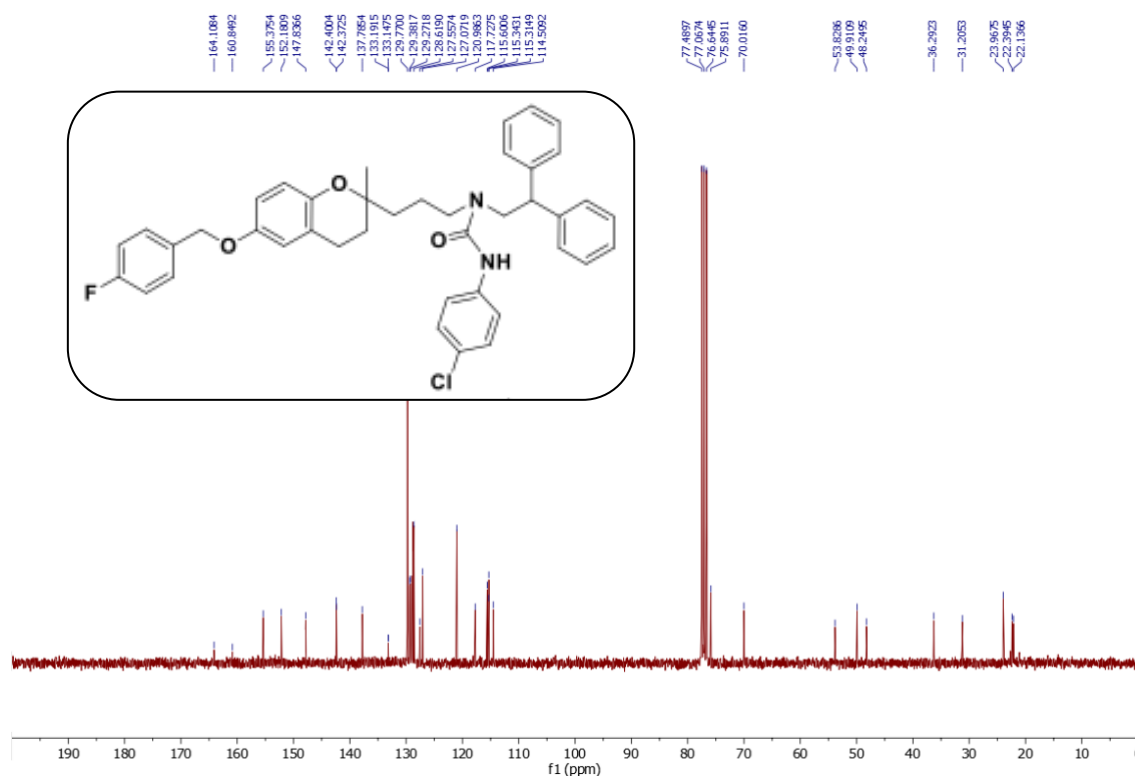
¹H NMR (300 MHz, CDCl₃) of 3-(*p*-Chlorophenyl)-*N*-(3-(6-((*p*-fluorobenzyl)oxy)-2-methyldihydrobenzopyran-2-yl)propyl)-*N*-(*p*-methoxyphenethyl)urea (5d).



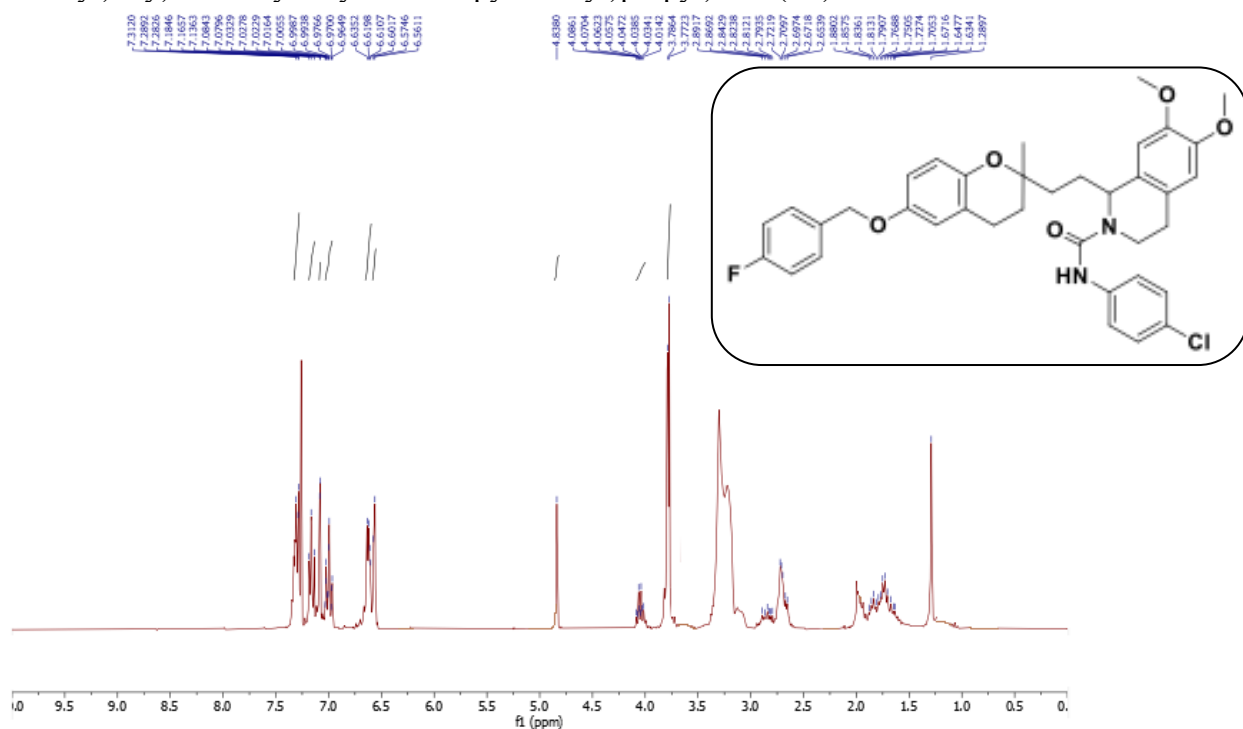
¹³C NMR (75 MHz, CDCl₃ + 1 drop CD₃OD) of 3-(*p*-Chlorophenyl)-*N*-(3-(6-((*p*-fluorobenzyl)oxy)-2-methyldihydrobenzopyran-2-yl)propyl)-*N*-(*p*-methoxyphenethyl)urea (**5d**).



¹H NMR (300 MHz, CDCl₃) of 3-(*p*-Chlorophenyl)-*N*-(2,2-diphenylethyl)-*N*-(3-(6-((*p*-fluorobenzyl)oxy)-2-methyldihydrobenzopyran-2-yl)propyl)urea (**6d**).



¹³C NMR (75 MHz, CDCl₃) 3-(*p*-Chlorophenyl)-*N*-(2,2-diphenylethyl)-*N*-(3-(6-((*p*-fluorobenzyl)oxy)-2-methyldihydrobenzopyran-2-yl)propyl)urea (**6d**).



¹H NMR (300 MHz, CDCl₃ + 1 drop CD₃OD) of *N*-(*p*-Chlorophenyl)-1-(2-(6-((*p*-fluorobenzyl)oxy)-2-methyldihydrobenzopyran-2-yl)ethyl)-6,7-dimethoxy-3,4-dihydroisoquinoline-2(1*H*)-carboxamide (**7d**).